A MOLECULAR STUDY ON SOME GENES KNOWN TO BE RELATED TO DISUSE MUSCLE ATROPHY IN THE AFRICAN LUNGFISH, *PROTOPTERUS ANNECTENS*, DURING THREE PHASES OF AESTIVATION

ONG LI YING JASMINE

(B. Sc. (Hons), NUS)

A THESIS SUBMITTED FOR THE DEGREE OF DOCTOR OF PHILOSOPHY

DEPARTMENT OF BIOLOGICAL SCIENCES

NATIONAL UNIVERSITY OF SINGAPORE

2016

DECLARATION

I hereby declare that the thesis is my original work and it has been written by me in its entirety. I have duly acknowledged all the sources of information which have been used in the thesis.

This thesis has also not been submitted for any degree in any university previously.

Ong Li Ying Jasmine

30th May 2016

Acknowledgements

This PhD journey would not have been possible without the constant help, support and encouragement from those around me.

To Prof Ip, my supervisor, words alone cannot express my gratitude towards you. Thank you for your guidance and teachings, and for being so patient with me. Thank you for the critical feedback so that I can reflect on my mistakes and be a better person and scientist. Thank you for all the opportunities that you have given me to learn thus far. Thank you being such an inspirational teacher.

To Mrs Wong Wai Peng, thank you for always being there. I'm very grateful for your constant support and encouragement.

To my two friends who have walked this entire journey with me, Xiu Ling and You Rong, thank you for everything – the work, the sweat, the tears, the laughter, the fun and most importantly, for being there with me. Thank you for making this journey enjoyable and memorable for me, and for tolerating me.

To my labmates, Biyun and Kum Chew, thank you for your guidance and patience with me, especially when it comes to experiments that I'm not familiar with. To Celine, thank you for bringing back goodies from Malacca, and for your constant encouragement and support. To Mel Veen, thank you for your encouragement and support during tough times. Thank you all for making this learning journey enjoyable, for adding laughter and fun in lab, making seemingly mundane tasks enjoyable.

To my mother and sister, thank you for your understanding and for accommodating me throughout this journey. Thank you for your support and trust in me even though you do not really understand what I'm doing most of the time.

To my friends outside lab, thank you for all the care, concern and support you have shown me thus far.

To NUS, thank you for the research scholarship, without which I would not have embarked on this journey.

Table of contents

Abstract

African lungfishes (*Protopterus* spp) can aestivate without food and water for many years. Disuse muscle atrophy is not prominent during aestivation, and lungfish aroused from aestivation can struggle out of the cocoon. Hence, there could be a tight regulation of genes/proteins involved in muscle formation and muscle degradation, and in oxidative defense as disuse muscle atrophy is partially attributable to oxidative damages, in the aestivating fish. This study aimed to sequence certain genes known to be involved in muscle formation [*peroxisome proliferator-activated receptor-γ coactivator-1α*, *myogenic differentiation 1* (*myod1*), *myogenin*, *mitogen-activated protein kinases 1* and *3*] or muscle degradation [*histone deacetylase 1*, *forkhead box O1* (*foxO1*), *forkhead box O3*, *myostatin* (*mstn*) and *F-box protein 32* (*fbxo32*)] from the skeletal muscle of *Protopterus annectens*, and to determine the effects of aestivation on their mRNA expression levels and protein abundances. Efforts were also made to determine effects of aestivation on (1) the mRNA expression levels and protein abundances of genes/proteins involved in oxidative defense [copper-zinc superoxide dismutase (*CuZnsod*/CuZnSod), manganese superoxide dismutase (*Mnsod*/MnSod), catalase (*cat*/Cat), glutathione peroxidases 1 (*gpx1*/Gpx1) and 4 (*gpx4*/Gpx4)], (2) the specific activities of Sod, Cat, Gpx, Glutathione reductase and Glutathione-S-transferase, and (3) the levels of several oxidative stress markers in the skeletal muscle. During the induction phase of aestivation, probably due to the short period of fasting and incompleteness of muscle disuse, the expressions of various genes/proteins involved in muscle formation and muscle degradation underwent only minor changes, of which only *tp53* and Fbxo32 increased and decreased, respectively.

These results indicate a possible suppression of muscle degradation, which does not support the proposition that tissue reconstruction elsewhere involves the mobilization of proteins/amino acids from the muscle. The increases in Cat protein abundance, Gr activity, [GSSG] and [GSSG]/[GSH], and lack of changes in the levels of oxidative damage products demonstrate the robustness of the antioxidant defense system in the muscle of *P. annectens*. During the maintenance phase of aestivation, despite the aestivating lungfish undergoing severe fasting, the expressions of genes/proteins involved in muscle formation and degradation were maintained at control levels, except for Myod1 which displayed an increase in the protein abundance. Muscle mass preservation was probably achieved by maintaining a certain rate of protein synthesis and suppressing fasting- and/or disuse-induced increase in muscle degradation. An upregulation in the protein abundance of CuZnSod, but not MnSod, suggests that CuZnSod could be the main Sod protecting the muscle from oxidative damage. Increases in the expression of *gpx4*/Gpx4 and [GSH] indicate that the antioxidant capacity in the skeletal muscle of *P. annectens* was up-regulated. During the arousal phase of aestivation, the expression of genes/proteins involved in muscle formation remained unchanged. Muscle degradation was likely suppressed, with decreases in protein abundance of FoxO1, Mstn and Fbxo32, indicating that muscle protein was not mobilized for tissue reconstruction and regenerating. Increases in MnSod activity and protein abundances of CuZnSod, Cat and Gpx1, coupled with decreases in the concentrations of oxidative damage products, indicate that arousal led to increased antioxidant defenses with minimal or no oxidative stress.

List of Tables

List of Figures

Notes on abbreviations

Two different types of abbreviations were adopted in this study for gene and protein symbols. This is because the standard abbreviations of genes/proteins of fishes (http://zfin.org/cgi-bin/webdriver?MIval=aa-ZDB_home.apg) are different from those of frogs and human/non-human primates (http://www.genenames.org).

Specifically, for fishes, gene symbols are italicized, all in lower case, and protein designations are the same as the gene symbol, but not italicized with the first letter in upper case. The advantage and appropriateness of using two types of abbreviations is that it would allow immediate interpretation of the affiliation between the abbreviation with fish or human/non-human primates. All abbreviations were defined at the first time of usage in the text.

1. Literature review

1.1. Lungfishes

Lungfishes belong to a unique clade of sarcopterygian fishes and are considered to be the most closely related living species to the ancestor of tetrapods (Forey, 1986; Meyer and Wilson, 1990; Marshall and Schultze, 1992; Tohyama et al., 2000; Perry et al., 2001; Brinkmann et al., 2004; Amemiya et al., 2013). There are three extant genera of lungfishes, *Protopterus*, *Lepidosiren* and *Neoceratodus*, which are endemic species of Africa, South America and Australia, respectively. These three genera of lungfishes have evolved separately since the beginning of the continental drift which promoted the splitting of big continents (de Almeida-Val et al., 2015). Protopterids share similar morphological characteristics with *Lepidosiren.* Based on this, *Protopterus* and *Lepidosiren* consist of one lineage which is apparently unchanged from the ancestral Dipterus of the Carboniferous Period, and is thus regarded as the mainline of dipnoan evolution (Graham, 1997). However, *Neoceratodus* is a descendant of the fossil form Ceratodus which occurred on all continents from the Triassic to Cretaceous Periods (Graham, 1997).

There are six species of extant lungfishes, namely *Lepidosiren paradoxa* in South America (Fitzinger, 1837), *Neoceratodus forsteri* in Australia (Krefft, 1870) and *Protopterus annectens* (Owen, 1839), *P. amphibius* (Peters, 1844), *P. aethiopicus* (Heckel, 1851) and *P. dolloi* (Boulenger, 1900) in Africa. Commonly found in the Amazon River basin of South America, *L. paradoxa* inhabits stagnant or lentic water systems (Lowe-McConnell, 1987; Planquette et al., 1996). In Australia, *N. forsteri* is restricted to the river channels and tributary streams within Southeast Queensland

(Kind, 2010). The four African lungfishes have a broad geographical distribution in Africa (de Almeida-Val et al., 2015). *Protopterus aethiopicus* is extensively distributed in eastern and central Africa, surrounding Congo, Nile Rivers and Lakes Victoria, Tanganyika, Albert, Edward, George, and Kyoga (de Almeida-Val et al., 2015). *Protopterus amphibius* is distributed in East Africa, while *P. annectens* is found in western Africa and in the Zambezi and Limpopo Rivers of southern Africa (de Almeida-Val et al., 2015). *Protopterus dolloi* is found mainly in the Congo basin (de Almeida-Val et al., 2015). Although sympatric populations of the four African lungfishes are rare considering their natural geographical distribution, they may still co-occur in some places (Mlewa et al., 2010).

The lungfishes (subclass Dipnoi) possess lungs and are able to breathe air, and are described as bimodal breathers. Dipnoans deviate from other sarcopterygians in having a mosaic of bones (Schultze, 2015). However, extant lungfishes show reductions and fusions of the skull roof bones, which demonstrate no homology with the skull roof bones of tetrapods or actinopterygians (de Almeida-Val et al., 2015). The separation of Dipnoi as a discrete group is based mainly on the structure and arrangement of the skull bones, the teeth, and the endoskeleton of the paired fins (de Almeida-Val et al., 2015).

There are two orders of Dipnoi, which are distinguishable based mainly on the number of lungs possessed: Ceratodontiformes which comprises *Neoceratodus*, and Lepidosireniformes which includes both *Protopterus* and *Lepidosiren.* Ceratodontiformes have only one lung, while Lepidosireniformes have two lungs that are fused anteriorly. *Neoceratodus forsteri* has robust flipper-like pectoral and pelvic

fins, larger scales and a more laterally compressed body (Thomson, 1969; Kemp, 1986; Nelson, 2006). In addition, *N. forsteri* is a bimodal air-breather and possesses well-developed gills, which support respiration in well-aerated waters, and a dorsal lung, which is used when oxygen levels are low or in forced exercise. By contrast, *L. paradoxa* and the *Protopterus* spp. exhibit elongated bodies, filamentous pectoral and pelvic fins, and their dorsal caudal and anal fins are fused into one continuous diphycercal tail (Bemis et al., 1987). As their gills do not allow them to breathe exclusively in water, *L. paradoxa* and the *Protopterus* spp. are obligate air-breathers, and they have to gulp atmospheric air to supply their oxygen requirements. The larval stage of *L. paradoxa* and the *Protopterus* spp., but not *N. forsteri,* possesses external gills (de Almeida-Val et al., 2015). Although *L. paradoxa* and the *Protopterus* spp. share morphological similarities, *Protopterus* spp. has an additional gill arch (5 versus 4) and lacks the hyper-vascularised pelvic fins that *L. paradoxa* males develop during the spawning season (Mlewa et al., 2010).

Within *Protopterus*, the body of *P. amphibius* is uniformly blue or slaty-green with small or inconspicuous black spots, whereas the body of *P. annectens* is olive or brown at the dorsal side and lighter at the ventral side, with black and brown spots on the body and fins except on the belly (Trewavas, 1954). Both *P. annectens* and *P. amphibius* have broad membranes on its pectoral fins, and retain three external gills on each side near the operculum for life, with *P. annectens* possessing smaller external gills than *P. amphibius* (Mlewa et al., 2010). The body of *P. dolloi* is brown and relatively slender, whereas the body of *P. aethiopicus* is more cylindrical with a pinkish toned ground colour or yellowish gray colour with dark slate-gray splotches

(Bailey, 1994). This creates a marbling effect over the body and fins of *P. aethiopicus* (Bailey, 1994). The colour pattern of the body of *P. aethiopicus* varies, with a darker dorsal side and a lighter ventral side (Bailey, 1994). External gills is absent in juveniles and adult of *P. dolloi* and *P. aethiopicus* (Greenwood, 1986). The *Protopterus* spp. can also be distinguished by the number of ribs present; *P. amphibius* has 27-30 ribs, *P. annectens* has 32-37 ribs, *P. aethiopicus* has 38-39 ribs, and *P. dolloi* has 47-55 ribs (Poll, 1961).

1.2. Aestivation

Aestivation is a state of torpor that is usually associated with high environmental temperature with absolutely no food and water intake for an extended period of time (Ip and Chew, 2010). From the behavioural point of view, aestivation could be defined as inactivity at high environmental temperature to survive arid conditions (except for aquatic aestivators like sponges and sea cucumbers) in terrestrial animals, especially during summer (Gregory, 1982; Peterson and Stone, 2000). Ultsch (1989) advanced the all-behaviour position and described aestivation as 'a non-mobile fossorialism'. From the physiological point of view, aestivation is often associated with metabolic depression (Storey, 2002), because conservation of metabolic fuels has been regarded as an essential adaptation during long periods of aestivation without food intake. While this association is obviously present in endothermic mammals during aestivation, it remains debatable as to whether it can be universally applied to aestivating ectothermic animals. For instance, in aestivating turtle (Hailey and Loveridge, 1997), metabolic depression has been proposed to decrease both urea production and respiratory water loss, along with conserving metabolic fuels (Storey

and Storey, 1990, Guppy and Withers, 1999). Yet, whether metabolic depression in aestivating turtles is an adaptation to aestivation or simply a response to fasting is still debatable (Belkin, 1965; Sievert et al., 1988). In fact, the decrease in oxygen consumption in laboratory-aestivating yellow mud turtle *Kinosternon flavescens* is identical to that of fully hydrated turtles which are fasted for an equivalent period of time (Seidel, 1978; Hailey and Loveridge, 1997).

While *N. forsteri* does not aestivate (Kemp, 1986), *L. paradoxa* and the *Protopterus* spp. greatly increase their chances of survival during periods of dry seasons by burrowing into the ground and aestivating (Johansen and Lenfant, 1967; Johansen et al., 1976). As lungfishes do not have limbs to facilitate locomotion on land, they would have to passively tolerate desiccation, and aestivation could be the only means for survival under dehydration at high temperature. In their natural environment, *L. paradoxa* and the *Protopterus* spp. inhabit swampy areas which dry out annually and the intensity of dryness varies according to the weather cycle of each year. When most of the water has dried up and only mud remains, *L. paradoxa* burrows in the mud up to 50 cm to avoid drying out (Berra, 2001), leaving two or three holes for breathing purposes. *Lepidosiren paradoxa* excavates the burrows by biting the soil and expelling mud through the gill openings. After finishing the burrow excavation, *L. paradoxa* turns around and remains with its head facing the burrow opening, so that it can obtain oxygen. However, unlike the *Protopterus* spp., *L. paradoxa* does not form a mucous cocoon.

Aestivation in the *Protopterus* spp. covers the time between two wet seasons, which is normally only a fraction of a year (Johnels and Svensson, 1954). However,

the duration of the dry season, and hence the length of aestivation, can vary significantly each year. In certain areas, like Lake Edward (Poll and Damas, 1939) and Lake Victoria (Smith, 1931), *Protopterus* spp. may live for years without being forced into aestivation by drought (Johnels and Svensson 1954). Among the four African lungfishes, *P. annectens* is more reliant on aestivation (Smith, 1931). During desiccation, *P. annectens* excavates a short burrow in mud and secretes mucus that gradually hardens to form a cocoon over itself (Johnels and Svensson, 1954). Yet, cocoon formation rarely occurs in the natural environment for the other three *Protopterus* species (Brien et al., 1959; Greenwood, 1986). It was reported that in Stanley Pool (Congo River), the burrows of *P. dolloi* remained wet in their lower part without cocoon formation (Brien et al., 1959). Moreover, the burrows of *P. aethiopicus* described by Wasawo (1959) resemble the combined dry-season burrow and breeding nest of *P. dolloi* (Greenwood, 1986). Nevertheless, when the lakes dry out, *P. aethiopicus* secretes mucus that gradually hardens to form a cocoon, which may reduce water loss. Hence, there are variations in aestivation behaviour and in burrow conditions (notably with or without a cocoon) among African lungfishes, which is probably dependant on the characteristics of the intensity of the drought and the freshwater environment (Otero, 2011). It is critical to note that, under laboratory conditions, *P. aethiopicus*, *P. amphibius* and *P. dolloi* can be induced to enter aestivation (Smith, 1931; Brien et al., 1959; Janssens, 1964; Greenwood, 1986; Chew et al., 2004; Ip et al., 2005a; Loong et al., 2005; Perry et al., 2008) and they are able to produce cocoons similar to those described for *P. annectens*. Despite the fact that there are altogether six species of extant lungfishes in the world distributed over three

continents (Africa, Australia, and South America), only African lungfishes can aestivate without food and water intake in subterranean mud cocoon for up to 5 years (Smith, 1931), which could be the longest aestivation period known for vertebrates.

Other than aerial respiration, there are a number of physiological adaptations that are required for aestivation to occur successfully. These adaptations include decreased metabolic rate, renal shutdown and mechanisms to limit the negative effects of fat and protein metabolism during fasting without access to water (Fishman et al., 1992). Many of these physiological adaptations respond specifically to the lack of water during aestivation, and thus would not be expected to be observed in lungfishes in water-filled burrows (Mlewa et al., 2010). Nevertheless, when the surrounding water is inadequate for the lungfish to forage, there would still be a prolonged period of seasonal fasting that the lungfish experiences. This fasting period is similar in length to the period of aestivation in the natural habitat of the lungfish. Non-aestivating lungfishes are able to fast for prolonged periods without excessive physiological stress, and this ability enhances their survival in strongly seasonal environments (Mlewa et al., 2010). It has been reported that a specimen of *P. aethiopicus* has survived without food for 3.5 years in an aquarium and appears to be in good condition (El Hakeem, 1979). Fasting in lungfishes, similar to aestivation, is accompanied by a decrease in metabolism and oxygen consumption (Fishman et al., 1992). However, the decrease is less rapid as metabolic wastes can be excreted or diffused to the surrounding water.

Aestivation comprises three phases: induction, maintenance, and arousal. To understand aestivation, it is important to distinguish the mechanisms and processes

involved in the three different phases: induction, maintenance and arousal. Although many features of the maintenance phase of aestivation in African lungfishes have been well characterized, there is still a dearth of information on the induction factors/mechanisms, the maintenance mechanisms and the process/mechanism of arousal from aestivation.

1.2.1. The induction phase

1.2.1.1. Processing of external stimuli and internal cues for aestivation

Several induction factors have been proposed for aestivation in African lungfishes in the past (Fishman et al., 1986). These factors include (1) starvation, resulting in metabolic, circulatory and respiratory changes, (2) dehydration, which leads to metabolic acidosis and oliguria/anuria, (3) air-breathing on land, bringing about respiratory acidosis and CO_2 retention, and (4) stress, affecting thyroid function and/or inducing the release of neurohumoral mediators. It is highly probable that multiple factors are involved in initiating aestivation, and there are synergistic effects between factors.

Ionic composition of the ambient water and salinity changes could be critical signals in initiating aestivation. It was reported that *P. dolloi* exposed to water at salinity 3 for 6 days exhibited consistently lower daily urea excretion rate as compared with the freshwater control (Ip et al., 2005b). Besides, there were decreases in urea contents in various tissues and organs. Ip et al. (2005b) therefore concluded that *P. dolloi* could respond to salinity changes in the external medium as it dried up, suppressing ammonia production in preparation of aestivation. The osmolality of the external medium (90 mosmol kg^{-1}) at salinity 3 was lower than the blood osmolality

(260–280 mosmol kg^{-1}). Moreover, the blood osmolality of experimental fish exposed to salinity 3 was comparable to that of the freshwater control. Thus, the decreases in endogenous ammonia production were unrelated to dehydration. Since the control and experimental fish were fasted for the same period of 6 days, the decreases in endogenous ammonia production were unrelated to fasting. Furthermore, both groups of fish had free access to air, and had comparable blood pH, P_{O_2} and P_{CO_2} at the end of the 6-day period, and hence the results obtained by Ip et al. (2005b) could not be a result of metabolic/respiratory acidosis or CO_2 retention. Therefore, they concluded that salinity and ionic composition changes in the external medium could act as important signals to initiate aestivation in *P. dolloi* during the induction phase as the external medium dried up (Ip et al., 2005b).

At present, there is a dearth of information on the internal cues involved in the initiation of aestivation in African lungfishes. As fasting is known to be one of the inducing factors of aestivation, urea accumulation could be an essential part of the induction mechanism. Ip et al. (2005c) thus undertook a series of experiments to determine whether ammonia (as NH_4Cl) injected intra-peritoneally into *P. dolloi*, would be excreted directly instead of being detoxified to urea, and to examine whether injected urea would be retained in this lungfish, leading to decreases in liver arginine and brain tryptophan levels which were observed during aestivation on land. Despite being ureogenic, *P. dolloi* rapidly excreted the excess ammonia within the subsequent 12 hours after intra-peritoneal injection of NH_4Cl. By contrast, only a small percentage (34%) of urea was excreted during the subsequent 24 hours when urea was injected intra-peritoneally into *P. dolloi*. At hour 24, significant quantities of

urea were retained in various tissues of *P. dolloi*. Intra-peritoneal injection of urea led to decreases in endogenous ammonia production, hepatic arginine and brain tryptophan contents in *P. dolloi,* all of which had been observed in aestivating *P. dolloi* (Chew et al., 2004). Hence, it was concluded that urea synthesis and accumulation could be one of the essential internal cues for initiating and perpetuating aestivation in *P. dolloi,* and urea might have a physiological role other than being an accumulating nitrogenous end-product (Ip et al., 2005c).

1.2.1.2. Hyperventilation, metabolic rate and oxidative defense

There can be an increase in metabolic rate in African lungfishes during the induction phase of aestivation. Hyperventilation occurs and the ventilation rate is enhanced two- to five-fold during the first 30 days of aestivation, before returning to the control range (2-10 per hour) within 45 days (DeLaney et al., 1974). During the first 10 days of aestivation, there is an increase in the arterial P_{O_2} from the control range of 25-40 to 50-58 mmHg, which then returns to the control range (DeLaney et al. 1974). The increase in metabolic rate can be a result of the structural and functional modifications of cells and tissues in preparation for the maintenance phase.

With hyperventilation and a possible increase in metabolism, it is highly possible for the African lungfish to be confronted with oxidative stress during the induction phase of aestivation. However, there is little information on the importance of antioxidant molecules and enzymatic oxidative defense in African lungfishes during this period. Ascorbate is renowned for its anti-oxidative and anti-stress properties. Although the majority of tetrapods can synthesize ascorbate from glucose in their kidney and/or liver, only certain fish species can synthesize ascorbate in the

kidney. The activity of L-gulono-γ-lactone oxidase, an enzyme involved in ascorbate synthesis, has been detected in the kidney of *P. aethiopicus* (Touhata et al., 1995) and *P. annectens* (Ching et al., 2014), indicating the capacity for ascorbate synthesis in African lungfishes. Ching et al. (2014) also reported that the expressions of *L-gulono-γ-lactone oxidase*/L-Gulono-γ-lactone oxidase, as well as its enzyme activity, were detectable in not only the kidney but also the brain of *P. annectens*. The expression of *L-gulono-γ-lactone oxidase* in the brain could be necessary for the aestivating lungfish in ensuring a continuous supply of ascorbate to counter oxidative stress when the main site of ascorbate production, the kidney, shuts down. Indeed, transient increases in ascorbate and total ascorbate + dehydroascorbate concentrations were observed in the brain of *P. annectens* after 6 days of aestivation in air (Ching et al., 2014). These increases could be attributed to an increase in oxidative stress resulting from hyperventilation and a possible increase in metabolic rate during the induction phase, thereby leading to increases in ascorbate as an oxidative defense measure.

1.2.1.3. Decreased ammonia production, increased urea synthesis and energy metabolism

Although decreased ammonia production was suspected to occur during aestivation (Janssens and Cohen, 1968), its importance during both the induction and maintenance phases has only been confirmed recently (Chew et al., 2003, 2004, Loong et al., 2005, Ip et al., 2005a). Chew et al. (2003) demonstrated that urea concentrations increased significantly in muscle (8-fold), liver (10.5-fold), and plasma (12.6-fold) of *P. dolloi* exposed to air for 6 days without entering to aestivation. In addition, there was a significant increase in the urea excretion rate in *P.*

dolloi exposed to air for 3 days or more (Chew et al., 2003). Taken together, these results indicate that *P. dolloi* increased the rate of urea synthesis to detoxify ammonia during this period. Besides, there was an increase in the ornithine-urea cycle capacity in the liver, as indicated by the significant increases observed in the activities of carbamoyl phosphate synthetase III (3.8-fold), argininosuccinate synthetase + argininosuccinate lyase (1.8-fold) and glutamine synthetase (2.2-fold) during aerial exposure (Chew et al., 2003). Moreover, the ammonia excretion rate in the experimental fish decreased significantly but there were no significant increases in ammonia contents in the muscle, liver or plasma, signifying that endogenous ammonia production was drastically reduced (Chew et al., 2003). The apparent decrease in ammonia production in *P. dolloi* was associated with significant decreases in concentrations of glutamate, glutamine, lysine and total free amino acid in the liver (Chew et al., 2003). Thus, Chew et al. (2003) interpreted that a decrease in proteolysis and amino acid catabolism could have occurred. However, in retrospect, the reduction in ammonia production during the induction phase of aestivation should not be viewed as an adaptation responding solely to ammonia toxicity and conservation of metabolic fuels (Chew et al., 2003). There could actually be an increase in protein synthesis, which would also lead to decreases in ammonia production and in the total free amino acid content. Since the mucus usually comprises of glycoproteins (Ángeles Esteban, 2012), there could be an increase in the synthesis of certain proteins for increased mucus production during the induction phase. Furthermore, structural modifications cannot occur without increased protein synthesis. Hence, the results obtained by Chew et al. (2003) could be interpreted as

the occurrence of increased protein synthesis and turnover instead of decreased protein degradation during the induction phase of aestivation.

In a separate study, Loong et al. (2005) reported that the rates of urea synthesis in *P. aethiopicus* and *P. annectens* during 6 days of aerial exposure increased only 1.2- and 1.5-fold, respectively, which were smaller than that in *P. dolloi*. However, unlike *P. dolloi*, aerial exposure had no significant effects on the hepatic Cps III activities of *P. aethiopicus* and *P. annectens*. Instead, aerial exposure induced relatively greater degrees of reductions in ammonia production in *P. aethiopicus* (34%) and *P. annectens* (37%) than in *P. dolloi* (28%). Thus, it was concluded that there were subtle differences in responses by various species of African lungfishes to aerial exposure, and it would seem that *P. aethiopicus* and *P. annectens* depended more on a reduction in ammonia production rather than an increase in urea synthesis to ameliorate ammonia toxicity during the induction phase of aestivation (Loong et al., 2005). In addition, there were significant increases in the mRNA expression levels of *carbamoyl phosphate synthetase III* (Loong et al., 2012a), *argininosuccinate synthetase* and *argininosuccinate lyase* (Chng et al., 2014), indicating increased urea synthesis in the liver of *P. annectens* during the induction phase of aestivation. Aestivation in hypoxia or in mud had a delayed effect on the increase in the mRNA expression of *carbamoyl phosphate synthetase III*, which extended beyond the induction phase of aestivation, highlighting the importance of differentiating effects intrinsic to aestivation from those intrinsic to hypoxia (Loong et al., 2012a).

Aestivation-specific gene clusters have been identified through the determination of differential gene expressions in the liver of *P. annectens* after 6 days of aestivation in air (normoxia) using suppression subtractive hybridization PCR (Loong et al., 2012b). Loong et al. (2012b) reported that 6 days of aestivation in normoxia resulted in the upregulation of mRNA expression levels of several genes related to urea synthesis, confirming that urea synthesis, despite being an energy-intensive process, was an essential adaptive response of aestivation. Furthermore, several mRNAs encoding proteins involved in lipoprotein metabolism were upregulated, indicating that there could be an increase in fatty acid synthesis from carbon chains released from amino acid catabolism during the induction phase. Some of the carbon chains from amino acid catabolism could also be channeled into glycogen, and indeed, there were downregulation of some genes related to glycolysis.

1.2.1.4. Structural modifications in preparation for the maintenance phase

Aestivation in African lungfishes has been associated with structural and functional modifications in at least the heart (Icardo et al., 2008), kidney (Ojeda et al., 2008; Amelio et al., 2008), intestine (Icardo et al., 2012a) and spleen (Icardo et al., 2012b). Icardo et al. (2008) reported that in fresh water, the myocytes in the trabeculae associated with the free ventricular wall of *P. dolloi* showed structural signs of low transcriptional and metabolic activity (heterochromatin, mitochondria of the dense type). These signs are partially reversed in aestivating *P. dolloi* (euchromatin, mitochondria with a light matrix), and paradoxically, aestivation appears to trigger an increase in transcriptional and synthetic myocardial activities, especially at the level of the ventricular septum (Icardo et al., 2008). Moreover, Ojeda et al. (2008)

demonstrated structural modifications in all the components of the renal corpuscle of aestivating *P. dolloi*. All these structural changes have to occur during the induction phase to shut off functions of certain tissues or organs and prepare the aestivating lungfish to survive the maintenance phase of aestivation (which can last up to 4 years). As African lungfishes are deprived of food at the start of aestivation, reconstruction and regeneration of cells and tissues would require mobilization of proteins from biological structures of specific functions, leading to a rapid protein turnover with perhaps little nitrogenous waste production (Chew et al., 2015). Although preservation of muscle structure and function is essential for the survival of aestivating African lungfishes when they arouse, the resources required for reconstructing and regenerating cells and tissues may be derived from the mobilization of proteins from the muscle, as the muscle is the largest protein source in African lungfishes. To date, there is a dearth of knowledge as to where aestivating African lungfishes obtain the resources for the required structural and functional modifications to sustain them through aestivation.

1.2.2. The maintenance phase

1.2.2.1. Arrested growth and regeneration

Growth and regeneration is arrested in African lungfishes during aestivation. Conant (1973) reported that when *P. annectens* and *P. aethiopicus* were induced to aestivate after they had regenerated varying amounts of limb and tail tissue, aestivation sharply limited but did not halt further growth if the regenerate was in the latent phase. Short-term aestivation experiments revealed that the bulk of the growth took place during the induction phase preceding dry cocoon formation (Conant, 1973). Therefore,

Conant (1973) concluded that deep aestivation inhibited tissue regeneration, which would imply that the fish must regain the ability of tissue regeneration upon arousal from aestivation. In addition, Conant (1976) reported that prolonged aestivation (> 17 months) in African lungfishes was associated with shrinkage of the body including fins and skeletal elements. The tail tip became noticeably blunter as the axis shortens and all limbs shortened during prolonged aestivation. It was reported that after 28 weeks of aestivation, one fish had lost 57 g out of the original 345 g, was 35 mm shorter than the original 400 mm snout-tail length, and had both pectoral and pelvic limbs shortened (Blanc et al., 1956).

1.2.2.2. Preservation of biological structures

Animals generally go into a protein catabolic state during long periods of fasting, mobilizing amino acids as metabolic fuels and releasing endogenous ammonia (Chew et al., 2015). Nonetheless, unlike lipids and carbohydrates, proteins have to be mobilized from biological structures of specific functions as there is no known protein store in animals. Cardiac, skeletal and smooth muscles are protein structures with contractile properties. However, cardiac muscles must be spared from catabolism until extremely critical moments. Though skeletal muscle is the most prominent protein source that can be mobilized, preservation of muscle structure and strength is required for aestivating African lungfishes in preparation for arousal. This must be achieved despite the lack of locomotor activity and long-term skeletal muscle disuse (Chew et al., 2015). Skeletal muscle disuse can result in decreased protein synthesis and increased proteolysis, leading to muscle atrophy in mammals (Childs, 2003). Yet, a drastic increase in protein degradation, as in the case of fasting alone,

does not occur in aestivating African lungfishes; they can effectively preserve muscle structure and strength by suppressing proteolysis and amino acid catabolism (Chew et al., 2015). Thus, as suggested by Ip and Chew (2010), suppressing proteolysis during the maintenance phase of aestivation should be considered mainly as an adaptive strategy to preserve proteinaeous structures and functions (Hudson et al., 2005; Symonds et al., 2007), and metabolic fuel conservation can at best be regarded as a subsidiary phenomenon.

1.2.2.3. Torpor and muscle disuse

During periods of fasting, African lungfishes conserve energy by reducing locomotor activity. Conant (1973) reported that normally well-fed lungfishes (*P. annectnens* and *P. aethiopicus*) demonstrated limited nocturnal movement, with occasional episodes of swimming alternating with quiet periods. However, all such movements were abolished after 2 months of fasting, and except for respiration, the lungfishes seemed to remain motionless for days at a time. In comparison, African lungfishes remain motionless inside their cocoons in mud (DeLaney et al., 1974; Fishman et al., 1986; Sturla et al., 2002; Loong et al., 2008b) or in air (Chew et al., 2004; Ip et al., 2005a; Loong et al., 2008b) during the maintenance phase of aestivation. Locomotor activity absolutely ceases, although the aestivating lungfish would continue to respond to sensory stimuli with bradycardia and altered breathing. In humans, disuse-induced muscle atrophy occurs as a result of limb immobilization (stemming from bone fractures) or extended bed rest, or as a result of micro-gravity effects during prolonged space travel (Fitts et al., 2000, 2001). Hence, the aestivating African lungfish represents a rare case of a fish being able to suppress muscle atrophy despite

long periods of fasting and inactivity. It has been reported that disuse muscle atrophy in mammals occurs as a result of decreased muscle protein synthesis and increased muscle protein degradation (Booth and Seider, 1979; Thomason et al., 1989). Although it is unclear whether protein synthesis is suppressed during aestivation, the expression of myosin isoforms remains unchanged in the muscle of aestivating *P. annectens* (Chanoine et al., 1994). There could be enhanced protein breakdown, but protease (cathepsin) activities in liver and muscle are the same among unfed, fed and aestivated *Protopterus* (Janssens, 1964). In fact, African lungfishes only lose approximately 9–18% of their original body mass after 250 days of aestivation (Smith et al., 1930). Moreover, disuse muscle atrophy is not overtly noticeable in *P. dolloi* and *P. annectens* even after 1 year of aestivation in air under laboratory conditions, as the lungfishes can struggle out of the mucus cocoon and swim to the water surface to breathe air within 1–2 h upon arousal (Y.K. Ip and S. F. Chew, unpublished observations). This contrasts greatly with human muscles, which undergo rapid atrophy when not in use. Currently, there is little information on how African lungfishes suppress disuse muscle atrophy during aestivation.

1.2.2.4. Nitrogen metabolism

During the maintenance phase of aestivation, there is a complete cessation of feeding in African lungfishes for an extended period. Therefore, they must rely on stored fuel for energy production. Babiker and El Hakeem (1979) suggested that *P. annectens* probably utilized carbohydrate during the initial phase of aestivation only, and it relied almost entirely on protein during the maintenance phase of aestivation. Amino acids can be released from muscles and other tissues through increased protein

catabolism, of which the degradation of amino acids can result in the release of ammonia. However, the aestivating African lungfish would have to preserve its muscle structure and strength so that it can struggle out of the cocoon upon subsequent arousal (Chew et al., 2015), and hence muscle protein should be sparingly catabolized. Anyway, ammonia is toxic (Cooper and Plum, 1987); it acts on the central nervous system of vertebrates, including fish, causing hyperventilation, hyperexcitability, convulsions, coma and death. Therefore, African lungfishes ameliorate ammonia toxicity during emersion or aestivation by increasing urea synthesis and suppressing ammonia production (see Chew and Ip, 2014 for a review).

Despite suppressing ammonia production during the maintenance phase, endogenous ammonia must be detoxified because of the complete impediment of ammonia excretion. By synthesizing and accumulating the moderately less toxic urea, aestivating African lungfishes can carry out protein catabolism for a longer period without being intoxicated by ammonia, and this increases their chances of surviving aestivation. Chew et al. (2004) reported that the rate of urea synthesis in *P. dolloi* increased by 2.4- and 3.8-fold during 6 days and 40 days of aestivation in air, respectively. Although activities of ornithine-urea cycle enzymes in fish aestivated for 6 days remained unchanged, the activities of several ornithine-urea cycle enzymes increased significantly in fish aestivated for 40 days. Previous works by Janssens and Cohen (1968) showed that urea accumulation occurred in *P. aethiopicus* aestivated for 78–129 days in an artificial mud cocoon, but they concluded that urea accumulation did not involve an increase in the rate of urea synthesis, even though the fish appeared to be in continuous gluconeogenesis throughout aestivation.

Subsequently, Ip et al. (2005a) undertook a study to test the hypothesis that the urea synthesis rate in *P. aethiopicus* was up-regulated to detoxify ammonia during the initial period of aestivation (day 0 to day 12), and that a profound suppression of ammonia production occurred at a later period of aestivation (day 34 to day 46) which eliminated the need to sustain the increased rate of urea synthesis. Contrary to the report of Janssens and Cohen (1968), Ip et al. (2005a) demonstrated a drastic increase in urea synthesis (3-fold) in *P. aethiopicus* during the initial 12 days of aestivation, although the magnitude of the increase in urea synthesis decreased over the next 34 days. Between day 34 and day 46 (12 days), the urea synthesis rate decreased to 42% of the day 0 control value instead (Ip et al., 2005a). There were significant increases in tissue urea contents and activities of some ornithine-urea cycle enzymes in the liver (Ip et al., 2005a). Since there was a meagre 20% decrease in the rate of ammonia production in *P. aethiopicus* during the initial 12 days, as compared to a 96% decrease during the final 12 days of aestivation (day 34 to day 46), Ip et al. (2005a) concluded that *P. aethiopicus* depended mainly on increased urea synthesis to ameliorate ammonia toxicity during the initial period of aestivation, but it suppressed ammonia production profoundly during prolonged aestivation, eliminating the need to increase urea synthesis which is energy intensive.

1.2.2.5. Increased oxidative defense

Page et al. (2010) reported that most of the major intracellular antioxidant enzymes, including copper-zinc superoxide dismutase (CuZnSod), manganese Sod (MnSod), catalase (Cat), glutathione peroxidase (Gpx) and glutathione reductase (Gr), were upregulated in the brain of *P. dolloi* after 60 days of aestivation. Activities of several

of these enzymes also increased in the heart during aestivation (Page et al., 2010). These increases were unrelated to fasting as similar phenomena were not observed in a group of fish which were deprived of food but maintained in water for the same period of time. Products of oxidative protein damage and lipid peroxidation were similar in control and aestivating lungfishes, but protein nitrotyrosine levels were elevated in the brain of aestivators. Hence, Page et al. (2010) concluded that aestivating *P. dolloi* experienced little oxidative damage in the brain and heart due to increased oxidative stress resistance in these organs resulting from increases in intracellular antioxidant capacity.

It was reported that ascorbate levels decreased 99.9%, and dehydroascorbate increased 48.5% in the kidney of *P. annectens* after 6 months of aestivation in air (Ching et al., 2014). These changes were accompanied with significant decreases in the mRNA expression level and protein abundance of L-Gulono-γ-lactone oxidase in the kidney (Ching et al., 2014). These changes could be related to the shut-down of renal function (DeLaney et al., 1974) and change in renal corpuscle structure during the maintenance phase of aestivation (Ojeda et al., 2008). As kidney is the major site of ascorbate synthesis in lungfishes, the decline of L-Gulono-γ-lactone oxidase activity and hence ascorbate production could expose the lungfish to possible oxidative stress during aestivation. However, there was only a minor decrease in ascorbate levels in the brain of *P. annectens* after 6 months of aestivation, which could be attributed to the expression of *L-gulono-γ-lactone oxidase* and the presence of L-Gulono-γ-lactone oxidase enzyme activity in the brain of *P. annectens* (Ching et

al., 2014). To date, there is no information on oxidative defenses in the muscle of aestivating lungfishes.

1.2.3. The arousal phase

1.2.3.1. Tissue regeneration and feeding

During arousal, blood flow and heart beat rate recovers. Ojeda et al. (2008) reported that all the modifications which rendered the kidney non-functional during the maintenance phase of aestivation were partially reversed during the first few days of arousal with the return of water. In addition, Garofalo et al. (2015) reported that the protein abundance of nitric oxide synthase (Nos) and v-AKT murine thymoma viral oncogene homolog (Akt) were down-regulated in the gills during the maintenance phase and up-regulated during the arousal phase, while the opposite trend was observed in the lungs of *P. annectens*. This occurred in parallel with organ readjustment in the gills and lungs of *P. annectens* during aestivation and arousal. Since the Nos/NO system is often associated with Akt in amplifying and integrating extracellular signals for redox balance, cell survival and osomoregulatory signal transduction (Amelio et al., 2013), Garofalo et al. (2015) proposed that Nos and Akt could play a role in morpho-functional readjusting processes in the gills and lungs of *P. annectens*. However, the exact mechanism for tissue regeneration in African lungfishes during the arousal phase is still not known.

African lungfishes would start feeding only after 7-10 days of arousal from aestivation. This indicates that some restructuring of the intestinal epithelium is a prerequisite to feeding. Icardo et al. (2012) reported that cell phenotypes in the digestive tract of *P. annectens* were restored in about 6 days after arousal from 6

months of aestivation. However, full structural recovery is not attained during the experimental period (15 days post-aestivation; Icardo et al., 2012). Therefore, the initial recovery of the intestinal epithelium was independent of food intake. Since structural modifications for tissue regeneration would require increased syntheses of certain proteins, and since they occurred before re-feeding, it would imply the mobilization of amino acids of endogenous origin. However, at present, there is a dearth of knowledge on protein degradation and synthesis, especially in the skeletal muscle, during the arousal phase of aestivation. Moreover, there is no information on postprandial nitrogen metabolism and excretion in African lungfishes upon arousal from aestivation.

1.2.3.2. Excretion of accumulated urea

Upon arousal in water, African lungfishes can efficiently excrete the excess urea accumulated in the body during the maintenance phase of aestivation (Smith, 1930; Janssens, 1964). Chew et al. (2003) reported that the urea excretion rate increased by 22-fold in *P. dolloi* during re-immersion after 6 days of terrestrial exposure as compared to the control fish. This is the greatest increase in urea excretion reported for fishes during emersion-immersion transition, and suggests that *P. dolloi* possesses transporters which facilitate the urea excretion upon arousal. Subsequently, Wood et al. (2005) reported that after 21-30 days of aestivation in air or exposure to air without aestivation, the urea excretion rate increased, reaching 2000-6000 μmol-N h^{-1} kg^{-1} at 10-24 hours, in *P. dolloi* during re-immersion. During arousal, increased urea excretion in *P. dolloi* occurred in pulses (Wood et al., 2005). Ip and Chew (2010) proposed that it can be an adaptation to assure complete rehydration, which is

dependent on tissue urea content, and to minimize instantaneous osmotic shock to cells, upon arousal. Through the injection of NH_4Cl + urea, Ip et al. (2005c) concluded that excretion of accumulated urea in *P. dolloi* was regulated by the level of internal ammonia. Hence, it is possible that an increase in ammonia production occurred through increased amino acid catabolism upon arousal, and the increased production of endogenous ammonia act as a signal to enhance urea excretion. However, it is not known whether the increased amino acid catabolism occurs through increased mobilization of muscle protein.

1.2.3.3. Increased metabolic rate, energy metabolism and oxidative stress

There is no available information on the metabolic rate of African lungfishes after arousal from long periods of aestivation. However, it would be logical to deduce that arousal leads to an increase in the metabolic rate for structural and functional of cells and tissues. Furthermore, increases in oxygen consumption and metabolism could lead to increased oxidative stress, although how the African lungfish defends itself against oxidative stress remains unclear. Aroused fish would only start to feed after 7–10 days, and the origins of fuel for ATP production to support locomotor activity and tissue reconstruction/regeneration remain unclear. It is possible that there could be increased mobilization of muscle protein during the arousal phase of aestivation, but this aspect has not been investigated yet.

1.3. Genes/proteins involved in muscle formation

1.3.1. Ppargc-1α

Peroxisome proliferator-activated receptor-γ coactivator-1α (PPARGC-1α) is an important transcriptional coactivator involved in the regulation of fibre type

composition, metabolic function, mitochondrial biogenesis, and antioxidant gene expression (St-Pierre et al., 2006; Scarpulla, 2008). PPARGC-1α binds to and coactivates multiple transcription factors including many nuclear receptors (Lindholm et al., 2012). As PPARGC-1α plays an important role in cell metabolism, it is tightly regulated. Signaling pathways which control *PPARGC-1α* gene expression includes calcium signaling (Wu et al., 2002b), calcineurin A (Handschin et al., 2003) and cyclic AMP (Yoon et al., 2001). When these pathways are activated, different transcription factors are mobilized to *PPARGC-1α* gene regulatory regions depending on the context and tissue. PPARGC-1α activity can be regulated by various post-translational modifications, including phosphorylation, acetylation and ubiquitylation. PPARGC-1α can undergo phosphorylation by various kinases, including p38 mitogen-activated protein kinase (MAPK) (Fan et al., 2004), AMP-activated protein kinase (AMPK) (Jäger et al., 2007), AKT/protein kinase B (Li et al., 2007), and glycogen synthase kinase 3β (Olson et al., 2008), thereby affecting PPARGC-1α activity in different ways. PPARGC-1α can also be acetylated by acetyltransferases such as the histone acetyltransferase GCN5 (Lerin et al., 2006) and be deacetylated by sirtuin 1 (Gerhart-Hines et al., 2007; Cantó et al., 2009). Furthermore, PPARGC-1α protein stability is regulated by specific E3 ligases (Olson et al., 2008; Wei et al., 2012; Trausch-Azar et al., 2015).

PPARGC-1α is strongly expressed in skeletal muscle, and its expression is enhanced by multiple signals including exercise (Pilegaard et al., 2003; Terada and Tabata, 2004; Akimoto et al., 2005) and β-adrenergic signaling (Miura et al., 2007; Chinsomboon et al., 2009). PPARGC-1α has a protective effect on muscle,

preventing it from atrophying by reducing proteolysis without affecting protein synthesis (Brault et al., 2010; Geng et al., 2011; Bonaldo and Sandri, 2013). Transgenic mice expressing PPARGC-1α are protected from denervation-induced atrophy (Sandri et al., 2006), muscle dystrophy (Handschin et al., 2007a) and sarcopenia (Wenz et al., 2009). In addition, PPARGC-1α has anti-inflammatory effects in skeletal muscle. PPARGC-1α is involved in the regulation of several antioxidant genes in various tissues, and a lack of PPARGC-1α leads to increased ROS levels (St-Pierre et al., 2006). The mRNA levels of pro-inflammatory cytokines (tumour necrosis factor α and interleukin 6) and ROS levels increased in the skeletal muscle of PPARGC-1α-knockout mice (Handschin et al., 2007b). Life-long PPARGC-1α overexpression suppresses pro-inflammatory cytokine expression in aged mice (Wenz et al., 2009). A dramatic decrease in PPARGC-1α protein expression observed in mouse tibialas anterior muscle after 14 days of immobilization and 5 days of remobilization indicated that the down-regulation of PPARGC-1α is a key cellular mechanism, which leads to the deterioration of muscle phenotypic changes following immobilization-remobilization (Kang and Ji, 2013). Overexpression of PPARGC-1α by transfection in the same mice models used by Kang and Ji (2013) can protect the tibialas anterior muscle from immobilization-induced metabolic and antioxidant disturbances (Kang et al., 2015). Furthermore, transgenic induction of PPARGC-1α extends the maintenance of skeletal muscle function in the CuZnSOD mouse model of amyotrophic lateral sclerosis (Da Cruz et al., 2012). PPARGC-1α also protects the skeletal muscle of hibernators from atrophy (Eddy and Storey, 2003; Eddy et al., 2005a; Xu et al., 2013), and could thus play a

similarly important role in aestivating lungfishes, especially since it is heavily regulated.

1.3.2. Myod1

Myogenic differentiation 1 (MYOD1) belongs to a family of vertebrate proteins which are potent transcription factors for muscle genes (Pownall et al., 2002). As one of the four myogenic regulatory factors (Weintraub et al., 1991; Rudnicki and Jaenisch, 1995), MYOD1 possesses the conserved basic helix-loop-helix (bHLH) domain, which makes it such a potent transcription factor. The bHLH domain mediates DNA binding and is necessary for heterodimerization with E proteins which facilitate the recognition of genomic E-boxes (Massari and Murre, 2000). These genomic E-boxes are found in the promoter region of many muscle-specific genes (Massari and Murre, 2000). Furthermore, there is a conserved set of amino acids in the basic region of MYOD1 and other myogenic bHLH proteins which alter the transcriptional activity of the bound MYOD1 (Brennan et al., 1991; Davis et al., 1990). This conserved set of amino acids, also known as the myogenic code, is thought to function by interacting with cofactors such as myocyte enhancer factor 2 (Molkentin et al., 1995) to alter the conformation of the bound MYOD1 in a manner which allows for cofactor interactions at other regions (Bengal et al., 1994; Ma et al., 1994). MYOD1 is known to promote specification and proliferation along with myogenic factors 5 and 6 (Olson, 1992; Megeney and Rudnicki, 1995; Seale et al., 2000; Hawke and Garry, 2001; Kitzmann and Fernandez, 2001).

Although null mutation in MYOD1 results in roughly normal muscle development in mice embryos, there is a delay in early limb and branchial arch

muscle development (Arnold and Winter, 1998). In mice, null mutations in MYOD1 and myogenic factor 5 result in a complete absence of skeletal myocytes or myofibres (Arnold and Winter, 1998). This implies that either MYOD1 or myogenic factor 5 is necessary for the formation and/or survival of myoblasts (Arnold and Winter, 1998). MYOD1 is negatively regulated by myostatin (MSTN) (McFarlane et al., 2006) and can be degraded by F-box protein32 (FBXO32) (Tintignac et al., 2005).

1.3.3. Myog

Myogenin (MYOG), similar to MYOD1, is one of the four myogenic regulatory factors (Weintraub et al., 1991; Rudnicki and Jaenisch, 1995). However, unlike MYOD1, MYOG promotes and maintains the terminal differentiation of muscle along with myogenic factor 6 (Olson, 1992; Megeney and Rudnicki, 1995; Hawke and Garry, 2001). MYOG apparently functions downstream of MYOD1 and myogenic factor 5 to activate muscle gene expression (Tapscott, 2005). The importance of MYOG expression has been highlighted by the failure of MYOG-knockout mice to form myofibres (Hasty et al., 1993; Venuti et al., 1995) due to interference with differentiation of already determined myogenic cells. This is consistent with studies in cultured cell systems demonstrating that while MYOG is not expressed in myoblasts during proliferation, it is regulated in the terminal differentiation process as it is essential in turning on the muscle gene expression program (Cusella-De Angelis et al., 1992). The expression of MYOG is induced in regenerating adult myofibres after muscle damage (Zhao et al., 2002). However, conditional knockout in adult muscle does not negatively affect regeneration,

indicating that MYOG seems to be less essential in the differentiation process in regenerating muscle (Meadows et al., 2011).

In MYOG-knockout mice, the expression of several differentiation markers including myosin heavy chain and myogenic factor 6 decreased, while MYOD1 expression is normal (Hasty et al., 1993), suggesting that MYOD1 expression is unaffected by MYOG. There is increasing evidence demonstrating that MYOG is associated with muscle atrophy induced by disuse, such as denervation (Moresi et al., 2010; Macpherson et al., 2011) and hindlimb suspension (Modziak et al., 1999; Alway et al., 2001). MYOG expression increases in these mammalian disuse models and it appears to be positively related to disuse muscle atrophy. This is attributed to the decrease in the expression of atrogenes and myogenic regulatory factors in the skeletal muscle of MYOG-null mice (Moresi et al., 2010). It would thus be interesting to note how the expression of Myog and Myod1 changes in the skeletal muscle of *P. annectens* during three phases of aestivation.

1.3.4. Mapk1/3

MAPK1/3 is also known as extracellular signal-regulated kinases 2 and 1, respectively. MAPK1/3 belong to a family of protein phosphorylating enzymes (Lawan et al., 2013) which includes p38 MAPK, c-Jun NH2-terminal kinases 1, 2 and 3, and extracellular signal-regulated kinase 5 (Bogoyevitch and Court, 2004; Zarubin and Han, 2005; Bogoyevitch, 2006; Whitmarsh, 2006). MAPKs are involved in the regulation of multiple cellular responses in immunology, neurobiology, physiology and energy metabolism (Wancket et al., 2012). MAPKs regulate cellular activities such as proliferation, apoptosis, differentiation and motility (Pearson et al., 2001;

Cuevas et al., 2007) through transcriptional activation as well as posttranslational modification on downstream targets. Furthermore, MAPKs play an important role in energy metabolism through the modulation of lipid metabolism (Wu et al., 2006; Roth et al., 2009; Flach et al., 2011) and skeletal muscle growth and fibre type (Wancket et al., 2012). The fundamental role of MAPKs in a wide range of biological processes indicates that MAPKs are tightly regulated. In fact, MAPK activation occurs through a three-tiered phosphorylation relay which transmits signals from the surface of the cell into biochemical responses (Dhanasekaran et al., 2007; Turjanski et al., 2007). This relay involves the phosphorylation and activation of MAPKs by upstream MAPK kinases (MKKs), and the phosphorylation and activation of MKKs by upstream MKK kinases (MKKKs) (Dhanasekaran et al., 2007; Turjanski et al., 2007). The regulation of MAPKs is extremely complex as there are multiple kinases within each tier of the phosphorylation relay (Geisler et al., 2013).

There is increasing evidence for the importance of the MAPK pathway in muscle atrophy. MAPK phosphatase 1 is a negative regulator of MAPKs; it dephosphorylates and inactivates MAPKs (Lawan et al., 2013). Overexpression of MAPK phosphatase 1 induces profound muscle fibre atrophy, probably via the ubiquitin-proteasome pathway (Shi et al., 2009). This atrophic effect can be conferred through the MAPK1/3 signaling pathway. MAPK1/3 is associated with the increase in muscle mass and the decrease in the expression of muscle RING-finger protein-1 (MuRF1), an E3-ubiquitin ligase implicated in muscle atrophy (Shi et al., 2009). Hence, MAPK1/3 is involved in protecting skeletal muscle from atrophy. This proposition is further supported by the findings that the MAPK1/3 pathway enhances

protein synthesis by controlling ribosomal RNA gene expression, thereby counteracting muscle wasting (Stefanovsky et al., 2006). Moreover, the MAPK1/3 pathway also prevents muscle wasting induced by oxidative stress (Yang et al., 2010). Besides, MAPK1 expression increases in the skeletal muscles of Richardson's ground squirrels during hibernation (MacDonald and Storey, 2005), further supporting the proposition that MAPK1/3 protects skeletal muscle against atrophy. Thus, Mapk1/3 might play an important role in protecting the skeletal muscle of *P. annectens* against atrophy, especially during the maintenance phase of aestivation.

1.3.5. General changes in expression of *ppargc-1α*/Ppargc-1α, *myod1*/Myod1, *myog*/Myog and *mapk*/Mapk, which are involved in muscle formation, during fasting or muscle disuse

PPARGC-1α: PPARGC-1α is a critical cofactor for mitochondrial biogenesis (Pérez-Shindler and Handschin, 2013). The mRNA levels of *PPARGC-1α* decrease in response to muscle atrophy due to fasting, disuse or denervation (Sandri et al., 2006; Sacheck et al., 2007). The maintenance of high levels of PPARGC-1α during catabolic conditions, whether by transfecting adult myofibres or in transgenic mice, spares muscle mass during fasting, denervation, aging, heart failure and sarcopenia (Sandri et al., 2006; Wenz et al., 2009; Geng et al., 2011). Overexpression of PPARGC-1α in adult muscle fibres inhibits muscle mass loss induced by food deprivation and FOXO3 overexpression (Sandri et al., 2006). Moreover, PPARGC-1α overexpression in the muscle of transgenic mice was reported to extend lifespan and prevent muscle wasting that is characteristic of ageing mice (Wenz et al., 2009). PPARGC-1α overexpression in mice glycolytic muscles led to not only inactivation

of forkhead transcription factor signaling via increased Akt/protein kinase B expression, but also increased expression of both inducible and endothelial nitric oxide synthases, SODs and CAT, production of nitric oxide, and reduced oxidative stress (Geng et al., 2011). The beneficial effect that PPARGC-1α has on muscle mass is due to reduced protein breakdown via inhibition of autophagy-lysosome and ubiquitin-proteasome degradation systems (Brault et al., 2010; Bonaldo and Sandri, 2013). PPARGC-1α inhibits FoxO3 transcriptional activity (Sandri et al., 2006) but does not affect protein synthesis. Hence, PPARGC-1α protects muscle from atrophy by 1) preventing the excessive activation of protein degradation systems through the inhibition of FOXO, a pro-atrophy transcription factor, without perturbing the translational machinery; and 2) enhancing nitric oxide antioxidant defenses and inactivation of the forkhead transcription factor signaling pathways (Geng et al., 2011).

MYOD1 and MYOG: MYOD1 promotes specification and proliferation of skeletal muscle, while MYOG promotes myoblast differentiation (Olson, 1992; Megeney and Rudnicki, 1995; Seale et al., 2000; Hawke and Garry, 2001; Kitzmann and Fernandez, 2001). MYOD1 has been implicated in muscle atrophy induced by fasting (Lagirand-Cantaloube et al., 2009) and disuse (Mozdziak et al., 1999; Alway et al., 2001; Moresi et al., 2010). Overexpressing a MYOD1 mutant lacking FBXO32-mediated ubiquitination decreases muscle atrophy induced by food deprivation in mice (Lagirand-Cantaloube et al., 2009), implying that MYOD1 protects skeletal muscle against atrophy. On the other hand, expression of MYOD1 and MYOG increase during hindlimb suspension (Mozdziak et al., 1999; Alway et

al., 2001) and after denervation (Moresi et al., 2010). Denervated muscle induces MYOG, which contributes to muscle atrophy by regulating the expression of atrogenes (Macpherson et al., 2011). In muscles of MYOG-null mice which undergo denervation to induce atrophy, expression of myogenic regulatory factors and atrogenes are greatly reduced (Moresi et al., 2010). However, Smith et al. (2014) have recently demonstrated that increases in expression of MYOD1 and MYOG occurred much later than the increases in those of atrogenes in the muscle of mice during hindlimb suspension. Hence, it has been postulated that increased MYOD1 and MYOG expression during hindlimb suspension offer protection to myofibres instead (Smith et al., 2014).

MAPK1/3: MAPK1/3 is involved in the regulation of protein synthesis and the enhancement of genes involved in glyconeogenesis, angiogenesis and glucose transport (Murgia et al., 2000; Koulmann and Bigard, 2006). MAPK1/3 promotes cell survival by reducing proteasome activity, myonuclear apoptosis and mitochondrial breakdown (Powers et al., 2007). MAPK1/3 has also been implicated in the increase in muscle mass and the decrease in MuRF1 expression (Shi et al., 2009). Furthermore, inhibition of MAPK1/3 in both slow and fast muscles induces profound atrophy (Shi et al., 2009). The MAPK1/3 pathway is preferentially activated in fast skeletal muscles (Shi et al., 2007, 2008), and protects skeletal muscle from oxidative stress-mediated wasting (Yang et al., 2010). MAPK1/3 pathway was reported to counteract muscle atrophy through increased protein synthesis by controlling ribosomal RNA gene expression (Stefanovsky et al., 2006). However, there is little information on how MAPK1/3 responds to muscle atrophy induced by fasting or disuse.

1.4. Genes/proteins involved in muscle degradation

1.4.1. Hdac1

Histone deacetylases (HDACs) are generally associated with repression of gene expression (Ito et al., 2000; Forsberg and Bresnick, 2001; Wade, 2001). There are four classes of HDACs (Gallinari et al., 2007). Class I and class II HDACs are evolutionarily related and share a common enzymatic mechanism – the hydrolysis of the acetyl-lysine amide bond catalyzed by zinc (Gallinari et al., 2007). The class I HDACs consists of HDAC1, 2, 3 and 8, and is most closely related to the transcriptional regulator RPD3 in yeast (de Ruijter et al., 2003). Class II HDACs, which comprises HDAC4, 5, 6, 7, 9 and 10, possess similar domains to HDA1, which is another deacetylase found in yeast (Bjerling et al., 2002). Higher organisms also express another Zn-dependent HDAC, HDAC11 (Gao et al., 2002). However, HDAC11 is phylogenetically different from both class I and II HDACs and is classified as a separate class under class IV. Class III HDACs are not evolutionarily related to the other three classes of HDACs, and they catalyze the transfer of the acetyl group onto the sugar moiety of NAD (Blander and Guarente, 2004).

Of the class I HDACs, HDAC1 and HDAC2 share the highest similarity (de Ruijter et al., 2003). For both enzymes, the catalytic domain is on the N terminus, and this domain forms the major part of the proteins (Kao et al., 2000; Cress and Seto, 2001; Wade, 2001; Li et al., 2002). However, cofactors are required for HDAC activity to occur as both HDAC1 and HDAC2 are inactive when they are produced using recombinant techniques (de Ruijter et al., 2003). Both enzymes are found exclusively in the nucleus, as they lack a nuclear export signal (NES) (Johnstone,

2002). Due to their similarity, both HDAC1 and HDAC2 are regulated in a similar manner. The activities of both enzymes are regulated by the availability of co-repressors and phosphorylation (de Ruijter et al., 2003). Mutation of crucial phosphorylation sites in HDAC1 leads to a decrease in its activity (Pflum et al., 2001; Galasinski et al., 2002).

1.4.2. FoxO1/3

FOXO proteins belong to a subclass of Forkhead transcription factors, which are characterized by a winged helix DNA-binding domain, the Forkhead box (Kaestner et al., 2000). FOXO proteins are transcription factors involved in numerous physiological and pathological processes, such as aging, neurological diseases and cancer (Greer and Brunet, 2008; Maiese et al., 2008). Invertebrates possess one FoxO factor while four FOXO family members, FOXO1, FOXO3, FOXO4 and FOXO6 are expressed in mammals. FOXO family members recognized and bind to the conserved consensus core motif TTGTTTAC (Furuyama et al., 2000; Xuan and Zhang, 2005). They are potent transcriptional activators which promote cell cycle arrest, ROS detoxification, damaged DNA repair, apoptosis and autophagy by upregulating specific genes (Brunet et al., 1999; Dijkers et al., 2000; Medema et al., 2000; Kops et al., 2002; Nemoto and Finkel, 2002; Tran et al., 2002; Lee et al., 2003; Murphy et al., 2003; Mammucari et al., 2007; Zhao et al., 2007). FOXO proteins are also involved in the regulation of cell differentiation in blood, adipose tissue and muscle (Hribal et al., 2003; Nakae et al., 2003; Bakker et al., 2004; Miyamoto et al., 2007; Tothova et al., 2007). With such diverse cellular functions, it is unsurprising that FOXO proteins are regulated by a broad spectrum of external stimuli, including insulin, growth

factors, nutrients, cytokines and oxidative stress, through changes in post-translational modifications (Calnan and Brunet, 2008). These post-translational modifications include phosphorylation, acetylation, and ubiquitination, which affect the subcellular localization of FOXO proteins (see review by Calnan and Brunet, 2008).

Out of the four FOXO family members, FOXO1 and FOXO3 have been associated with muscle atrophy. The mRNA expression of *FoxO1* and *FoxO3* increases in the muscle of rats after fasting or caloric restriction for 48 h (Furuyama et al., 2002; Imae et al., 2003), indicating that nutrient deprivation can induce a signaling cascade to elicit the transcription of FOXO factor genes. In various models of muscle atrophy, reduced activity of the AKT pathway results in decreased levels of phosphorylated FOXO in the cytoplasm and a profound increase of nuclear FOXO (Brunet et al., 1999; Sandri et al., 2004; Latres et al., 2005). The translocation and activity of FOXO proteins is necessary for upregulating FBXO32, and it has been shown that FOXO3, when transfected into skeletal muscles *in vivo*, is sufficient to promote FBXO32 expression and muscle atrophy (Sandri et al., 2004). Furthermore, deacetylation of FOXO3a by HDAC1 promotes FBXO32 and MuRF1 expression (Beharry et al., 2014). In addition, significantly reduced muscle mass and fibre atrophy are observed in FOXO1 transgenic mice, implying that FOXO members are sufficient to promote muscle loss (Kamei et al., 2004; Southgate et al., 2007).

FOXO family members have also been associated with MSTN (McFarlane et al., 2006; Allen and Unterman, 2007). MSTN was reported to upregulate essential atrophy ubiquitin ligases in muscle cell cultures in a FOXO-dependent manner, as

MSTN treatment blocks the IGF1-PI3K-AKT pathway, activating FOXO1 in the process and hence increasing FBXO32 expression (McFarlane et al., 2006). Conserved sequences sharing multiple binding sites for FOXO proteins have been identified in the *Mstn* promoter from various organisms (Allen and Unterman, 2007; Allen and Du, 2008; Dall'Olio et al., 2010). Moreover, some of these binding sites were demonstrated to be essential for FOXO1 binding and *Mstn* expression (Allen and Unterman, 2007; Allen and Du, 2008). It is thus believed that MSTN expression is controlled by FOXO1, and this supports the view that the MSTN pathway synergizes with the AKT-FOXO signaling pathway (Allen and Unterman, 2007).

1.4.3. Tp53

Tumour protein 53 (TP53) is known for its tumor suppressor role and is an essential regulator of cellular responses to a number of stress signals (Varquez et al., 2008; Riley et al., 2008), which include DNA damage and oncogene activation. The activation of TP53 by various stress signals leads to either apoptosis or cell-cycle arrest in cells (Riley et al., 2008), and the final outcome of the cell is determined by the level of TP53. Higher levels of TP53 results in apoptosis while low TP53 levels favours cell cycle arrest (Laptenko and Prives, 2006).

Signal transduction-activated TP53 has two modes of action (Norbury and Zhitovsky, 2004; Varquez et al., 2008). TP53 binds to DNA as a tetramer in a sequence specific manner (Norbury and Zhitovsky, 2004; Varquez et al., 2008), functioning as either a transcriptional activator or transcriptional repressor (Riley et al., 2008). This means that TP53 regulates the expression of a large number of target genes (Horn and Vousden, 2007; Riley et al., 2008). TP53-induced apoptosis occurs

by upregulating pro-apoptotic genes and repressing anti-apoptotic genes (Chakraborty et al., 2003; Norbury and Zhitovsky, 2004; Horn and Vousden, 2007), thereby promoting apoptosis, which accounts for its tumour suppressor role. However, TP53 also leads to cell cycle arrest (Alberts et al., 2008) when it transcriptionally activates cyclin dependent kinase inhibitor $p21^{Waf1/Cip1}$ (Horn and Vousden, 2007). This inhibits a number of cyclin-dependent kinases regulating cell cycle, thereby arresting the cell cycle in the G_1 phase (Sherr and Roberts, 1995).

TP53 can also be activated by nutrient deprivation and oxidative stress (Bieging et al., 2014), both processes which may occur in the African lungfish during aestivation. Nutrient deprivation activates AMPK, which in turn activates TP53, consequently inhibiting proliferation and leading to decreased cell growth (Bieging et al., 2014) to facilitate cell survival. Oxidative stress can either induce DNA damage which in turn activates TP53, or activate TP53 by affecting the redox state (Méplan et al., 2000) and oxidation of TP53 (Augustyn et al., 2007). Mitochondrial ROS, which has been implicated in muscle disuse atrophy (Muller et al., 2007; Kavazis et al., 2009; Min et al., 2011; Powers et al., 2011; Talbert et al., 2013), has been demonstrated to be a key component of stress-induced TP53 activation (Karawajew et al., 2005). There is increasing evidence that skeletal muscle atrophy is promoted by TP53. Transgenic mice expressing an activated TP53 construct age prematurely and undergo severe muscle atrophy (Schwarzkopf et al., 2008). On the other hand, a global loss of TP53 expression in mice makes them more prone to cancer, but increases their resistance to cancer-induced skeletal muscle atrophy (Schwarzkopf et al., 2006). Furthermore, various muscle atrophy stimuli such as denervation, aging,

unloading, immobilization and Huntington's disease enhance the expression of TP53 and TP53 target genes in skeletal muscle, indicating that TP53 plays a critical role in muscle wasting under these conditions (Stevenson et al., 2003; Welle et al., 2003, 2004; Siu and Alway, 2005a, b; Edwards et al., 2007; Ehrnhoefer et al., 2013; Fox et al., 2014). It would be of great interest to note the changes in the expression of *tp53*/Tp53 in the skeletal muscle of *P. annectens* during three phases of aestivation.

1.4.4. Mstn

MSTN, also known as growth differentiation factor 8, is part of the transforming growth factor (TGF) β superfamily, where members of this superfamily are involved in the regulation of a range of cellular processes mediating growth processes in vertebrates. MSTN negatively regulates muscle growth (Matsakas and Diel, 2005; Joulia-Ekaza and Cabello, 2006; Allen and Unterman, 2007; Ji et al., 2008; Li et al., 2008). Deleting MSTN in mice results in a significant and widespread increase in skeletal muscle mass through muscle hypertrophy and hyperplasia (McPherron et al., 1997; Lin et al., 2002; Zimmers et al., 2002). Mutations in *Mstn* of some cattle and sheep breeds cause a double-muscling phenotype in these animals (Kambadur et al., 1997; McPherron and Lee, 1997; Hadjipavlou et al., 2008). Hence, the most critical function of MSTN is to regulate skeletal muscle growth.

Muscle mass preservation is tightly regulated by the delicate balance between protein synthesis and muscle degradation. There is increasing evidence that MSTN may decrease muscle mass by reducing protein synthesis (Taylor et al., 2001; Suryawan et al., 2006; Welle et al., 2006, 2009). MSTN can inhibit protein synthesis in both myoblasts and myotubes *in vitro* (Taylor et al., 2001). Mice with constitutive

MSTN deficiency have increased rate of myofibrillar protein synthesis, as compared to normal mice (Welle et al., 2006, 2009). Furthermore, follistatin, which inhibits MSTN, stimulates protein synthesis in the skeletal muscle of neonatal rats (Suryawan et al., 2006). Follistatin overexpression results in increased muscle mass in animals (Lee and McPherron, 2001; Haidet et al., 2008). Consistent with MSTN's inhibitory effect on protein synthesis, MSTN negatively regulates the AKT/mammalian target of rapamycin signaling pathway, which plays a critical role in regulating protein synthesis (Sarbassov et al., 2005; Amirouche et al., 2009; Trendelenburg et al., 2009; Sartori et al., 2009; Lipina et al., 2010). In these studies, muscle proteolysis does not seem to be affected by MSTN. However, it has been demonstrated the MSTN upregulates the ubiquitin-proteasome pathway via FOXO (section 1.4.2), leading to increased proteolysis in the muscle (McFarlane et al., 2006).

MSTN also inhibits both myoblast proliferation and differentiation. MSTN inhibits myoblast proliferation by enhancing cyclin D1 protein degradation to arrest cell cycle at the G_1-phase (Yang et al., 2007). Furthermore, MSTN inhibits myoblast differentiation by downregulating the expression of genes involved in muscle differentiation, which include *Myod1* and *Myog* (Langley et al., 2002; Ríos et al., 2002; Joulia et al., 2003). Instead of promoting differentiation or apoptosis of myoblasts (McFarlane et al., 2008), MSTN stimulates quiescence by inhibiting MYOD1 activity (Langley et al., 2002; McCroskery et al., 2003; Amthor et al., 2006; Manceau et al., 2008). MSTN is involved in muscle atrophy; its expression is enhanced in muscle atrophy induced by glucocorticoid (Ma et al., 2003; Allen et al., 2010) and in skeletal muscle degeneration-related diseases, including HIV infection

(Gonzalez-Cadavid et al., 1998) and chronic illnesses (Reardon et al., 2001). Increased MSTN expression is observed in the skeletal muscle of mice after hindlimb suspension (Carlson et al., 1999), sciatic nerve resection (Shao et al., 2007), spaceflight (Allen et al., 2009), and unilateral lower limb suspension (Gustafsson et al., 2010). Moreover, in humans, MSTN expression is enhanced after chronic disuse (Reardon et al., 2001), and after 5 days of immobilization (Dirks et al., 2014). MSTN expression has been demonstrated to remain unchanged in the skeletal muscle of hibernating thirteen-lined ground squirrels (Brooks et al., 2011). To date, however, there is little information on the expression of MSTN in the skeletal muscle of naturally torpid animals, and how the changes in the expression of MSTN, if any, facilitate muscle mass preservation in these animals. Since HDAC1 is a regulator of FOXO, and since FOXO controls MSTN expression, it is therefore important to study the changes in the expression of these three genes/proteins as changes in any of them might favour muscle degradation in the skeletal muscle of *P. annectens* especially during the maintenance phase.

1.4.5. Fbxo32

FBXO32, commonly known as atrogin-1, is an E3 ubiquitin ligase that is selectively expressed in muscles at a relatively low level under normal conditions (Bodine, 2013). The function of E3 ubiquitin ligases is to transfer ubiquitin molecules to a substrate protein (d'Azzo et al., 2005). This inactivates and marks the substrate protein for proteasomal degradation (d'Azzo et al., 2005). FBXO32 can be upregulated in skeletal muscle atrophy caused by disuse or denervation (Bodine et al., 2001; Sacheck et al., 2007; Suzuki et al., 2007; Kim et al., 2008), sepsis (Frost et al., 2007),

glucocorticoid treatment (Tobimatsu et al., 2009), and food deprivation in mammals (Jagoe et al., 2002; Lecker et al., 2004), birds (Nakashima et al., 2006) and fish (Rescan et al., 2007; Cleveland et al., 2009; Bower et al., 2010). Although it has been more than a decade since FBXO32 was found to correlate with muscle atrophy, the exact mechanism(s) of how FBXO32 leads to muscle atrophy remains unclear. It has been proposed that FBXO32 controls protein synthesis by regulating the translation initiation factor, eIF3f (Lagirand-Cantaloube et al., 2008). Nonetheless, skeletal muscles of mice with a null deletion of FBXO32 are not larger in size as compared to control mice, and eIF3f expression does not increase in FBXO32 null mice (Bodine, 2013).

FBXO32 expression is regulated by multiple transcription factors. These include the glucocorticoid receptor, FOXO1 and FOXO3 (section 1.4.2) (Sandri et al., 2004; Sacheck et al., 2007). Glucocorticoid levels increase during fasting (Lecker et al., 1999; Braun et al., 2011), and have been demonstrated to upregulate the expression FBXO32 (Tomas et al., 1979; Goldberg et al., 1980; Löfberg et al., 2002). However, glucocorticoids are unlikely to be responsible for the increase in FBXO32 expression in mammalian disuse models (Tischler, 1994; Watson et al., 2012).

FBXO32 deletion spares muscle mass following denervation (Bodine et al., 2001). Increases in the mRNA expression level of *Fbxo32* in the skeletal muscles of non-hibernators under conditions of inactivity and unloading have been reported to facilitate the ubiquitination of muscle proteins, thereby increasing proteolytic degradation by proteasome (Bodine et al., 2001; Sandri et al., 2004; Clarke et al., 2007; Cohen et al., 2009). By contrast, the stable *Fbxo32* mRNA expression and the

suppression of proteolytic degradation by proteasome in the skeletal muscles are apparently associated with the protection of hibernators from disuse muscle atrophy (Velickovska et al., 2005; Velickovska and van Breukelen, 2007; Lee et al., 2010; Andres-Mateos et al., 2013; Dang et al., 2016). Since FBXO32 is one of the main enzymes determining muscle degradation, it is of interest to investigate the changes in the expression of *fbxo32*/Fbxo32 in the muscle of *P. annectens* during three phases of aestivation.

1.4.6. General changes in expression of *hdac1*/Hdac1, *foxo*/FoxO, *tp53*/TP53, *mstn*/Mstn and *fbxo32*/Fbxo32, which are involved in muscle degradation, during fasting or muscle disuse

HDAC1: Class I HDACs are key regulators of FOXO and the muscle-atrophy program during both fasting and skeletal muscle disuse (Beharry et al., 2014). HDAC1 alone is adequate and required to activate FOXO and induce muscle fibre atrophy *in vivo*, and is required for contractile dysfunction and muscle atrophy associated with muscle disuse (Beharry et al., 2014). Furthermore, HDAC1 can interact with the bHLH domain of MYOD1 to silence MYOD1-dependent transcription of muscle-specific genes by keeping MYOD1 in a deacetylated and transcriptionally repressed form (Mal et al., 2001). The deacetylase activity of HDAC1 is necessary for muscle atrophy to occur, and has been linked to the HDAC1-induction of several atrophy genes, including FBXO32, which requires the deacetylation of FOXO3a (Beharry et al., 2014). It was discovered that HDAC1 was essential for maintaining normal skeletal muscle structure and function (Moresi et al., 2012). This was associated with the regulation of autophagic flux and HDAC1-

dependent induction of several genes associated with autophagy, such as *Atg5*, *Gabarap11*, *Lc3* and *p62* (Moresi et al., 2012). Autophagic flux is necessary for cellular homeostasis under normal circumstances, but increased autophagic flux during catabolism promotes muscle atrophy (Mammucari et al., 2007; Masiero and Sandri, 2010). However, autophagy inhibition does not prevent skeletal muscle atrophy during denervation and fasting; instead it promotes greater muscle loss (Masiero and Sandri, 2010).

FOXO: The translocation and activity of FOXO family members are necessary for the upregulation of *Fbxo32*. AKT phosphorylation of FOXO proteins promotes their nuclear export to the cytoplasm. Decreased activity of the AKT pathway observed in various models of muscle atrophy leads to reduced levels of phosphorylated FOXO in the cytoplasm and a significant increase of nuclear FOXO (see review by Calnan and Brunet, 2008). FOXO3 has been demonstrated to be necessary for the upregulation of *Fbxo32* in muscle atrophy induced by fasting (Mammucari et al., 2007) and denervation (Sandri et al., 2004). Furthermore, FOXO1 transgenic mice demonstrate significantly reduced muscle mass and fibre atrophy, indicating that FOXO members are sufficient to promote muscle loss (Kamei et al., 2004; Southgate et al., 2007). FOXO is induced during disuse muscle atrophy, and FOXO signaling is required to cause muscle wasting (Senf et al., 2010). FOXO knockdown by RNAi blocks the upregulation of *Fbxo32* expression during muscle atrophy and muscle loss (Sandri et al., 2004; Liu et al., 2007).

TP53: TP53 is a nuclear phosphoprotein and a key regulator of cell survival and proliferation. Increases in TP53 activity have been correlated with skeletal

muscle atrophy *in vivo* under conditions of stress like inflammation, aging and chronic exposure to double-stranded DNA breaks (Schwarzkopf et al., 2006; Edwards et al., 2007; Rodier et al., 2007; Schwarzkopf et al., 2008; Didier et al., 2012). However, it is unclear if TP53 contributes to muscle atrophy induced by fasting. A recent study reported an enhanced TP53-independent *p21* expression in the skeletal muscle during fasting (Tinkum et al., 2013), indicating that TP53 might not contribute towards fasting-induced muscle atrophy. TP53 may also contribute to apoptosis-mediated muscle wasting since its expression in the muscle is increased after 14 days of space-flight (Ohnishi et al., 1999), and after 7 or 14 days of unloading (Siu and Alway, 2005a). Recently, TP53 was identified as an essential mediator of immobilization-induced muscle atrophy (Fox et al., 2014).

MSTN: The mRNA expression of *Mstn* increased dramatically in the fast-twitch tibialis anterior muscle of mice deprived of food for 2 days (Allen et al., 2010). Levels of *Mstn*/MSTN increased in the muscle of rodents after hindlimb suspension (Carlson et al., 1999), after denervation (Shao et al., 2007), and after 11 days of spaceflight (Allen et al., 2009). Similar increases in *MSTN*/MSTN expression were also reported in humans after chronic disuse (Reardon et al., 2001) and after unilateral lower limb suspension (Gustafsson et al., 2010).

FBXO32: Fbxo32 is a E3-ubiquitin ligase involved in the ubiquitination and proteolysis of muscle proteins (Glass, 2003; Sacheck et al., 2004; Bodine et al., 2013). The mRNA levels of *Fbxo32* increases rapidly in various models of atrophy and is thought to play a role in initiating the atrophy process in the muscle (Bodine et al., 2001; Foletta et al., 2011). Fasted mice were reported to have an increase in the

mRNA expression of *Fbxo32* (Gomes et al., 2001; Sandri et al., 2004). Similarly, an upregulation of *Fbxo32*/FBXO32 was reported in the muscle of mice following denervation (Bodine et al., 2001). Similar results were also observed after immobilization (Jones et al., 2004; Abadi et al., 2009), after spaceflight in rodents (Allen et al., 2009), and after 3 days of unilateral lower limb immobilization in humans (Gustafsson et al., 2010). Up-regulation in the mRNA expression level of *Fbxo32* in the skeletal muscles of non-hibernators under conditions of inactivity and unloading facilitate the ubiquitination of muscle proteins, thereby increasing proteolytic degradation by proteasome (Bodine et al., 2001; Sandri et al., 2004; Clarke et al., 2007; Cohen et al., 2009).

1.5. Genes/proteins involved in oxidative defense

1.5.1. Sod

SOD is an antioxidant enzyme that catalyzes the disproportionation of O_2^- to H_2O_2 and water (Fridovich, 1986; Fridovich, 1995). As SODs are metalloenzymes, they are classified according to the metal ion cofactor required for their activity: the copper/zinc type (CuZnSOD), the manganese type (MnSOD), the iron type (FeSOD), and the nickel type (NiSOD) (Youn et al., 1996). In eukaryotes, cytosolic CuZnSOD, glycosylated extracellular CuZnSOD, and mitochondrial MnSOD have been found (Fridovich, 1995), and overexpression of mitochondrial MnSOD or cytosolic CuZnSOD increase oxidative stress resistance (Murakami et al., 1997; Shan et al., 2007; Jang et al., 2009). CuZnSOD can be found abundantly in the cytoplasm (Halliwell and Gutteridge, 1989), but it has also been observed in endosomes and the mitochondrial intermembrane space (Saito et al., 1989; Kawamata and Manfredi,

2010). On the other hand, mitochondrial MnSOD is encoded by the nuclear gene, and it is synthesized and translocated into the mitochondrial matrix with mature enzyme activity (Wispé et al., 1989). The presence of MnSOD within the mitochondria indicates that the superoxide produced in the mitochondria does not cross membranes readily, and because of its negative effects on biomolecules, superoxide must be dismutated immediately by SOD, preferably at the production site of superoxide. It is henceforth thought that MnSOD is a major scavenger of ROS in the mitochondrial matrix among the aerobic organisms (Cadenas and Davies, 2000). Furthermore, MnSOD is essential for survival – *MnSod* gene knockout in mice (Williams et al., 1998) and fruit flies (Duttaroy et al., 2003) is lethal.

Mitochondrial ROS has been implicated in skeletal muscle disuse, as inactivity-induced ROS is produced mainly in the mitochondria (Muller et al., 2007; Kavazis et al., 2009; Min et al., 2011; Powers et al., 2011; Talbert et al., 2013). Although it would be logical to assume that mitochondria ROS is scavenged by MnSod, it is possible that CuZnSOD could scavenge mitochondrial ROS, as there is increasing evidence of CuZnSOD being located in the mitochondrial inter-membrane space (Saito et al., 1989; Kawamata and Manfredi, 2010). CuZnSOD exists as a functional homodimer. The dimerization of each monomer requires disulphide bond formation, protein folding, Cu and Zn loading and dimer formation (Hitchler and Domann, 2014). It was thought that CuZnSOD processing affects its subcellular localization (Hitchler and Domann, 2014). CuZnSOD is imported as a catalytically inactive enzyme into the intermembrane space during mitochondrial import, and is processed by the copper chaperone for CuZnSOD (CCS) into the active enzyme, and

stays trapped in the mitochondria (Leitch et al., 2009; Kawamata and Manfredi, 2010). The import of CuZnSOD and CCS occurs via a disulphide relay system involving the import receptor Mia40 (Reddehase et al., 2009; Kawamata and Manfredi, 2010). In addition, stress signals can affect the subcellular localization of CuZnSOD. Increased stress can lead to the import of CuZnSOD from the cytosol into the nucleus (Zlatković and Filipović, 2011).

Increases in CuZnSOD activity have been reported in the muscle of aestivating snails (Hermes-Lima and Storey, 1995; Salway et al., 2010) and spadefoot toads (Grundy and Storey, 1998). It is clear that CuZnSOD plays an important role in protecting the skeletal muscle from oxidative damage due to mitochondrial ROS in these aestivators.

1.5.2. Cat

CAT is an extremely active catalyst produced naturally which degrades H_2O_2 without the consumption of cellular reducing equivalents, thus utilising energy efficiently (Ścibior, and Czeczot, 2006). There is a net gain of reducing equivalents, and hence, cellular energy. It is therefore not surprising that all aerobic organisms contain CAT. It is usually found in peroxisomes of all aerobic organisms, as there are many H_2O_2-producing enzymes within peroxisomes (Ścibior, and Czeczot, 2006). This allows for rapid degradation of H_2O_2 before the damaging ROS can diffuse to other parts of the cell. Its evolutionary conservation suggests that it is essential in systems that have evolved over the centuries, enabling the survival of organisms in aerobic environments. CAT is a tetrameric enzyme comprising four identical, tetrahedrally

arranged subunits, with a heme group and NADPH in the active centre of each subunit (Kirkman and Gaetani, 1984).

It is thought that CAT plays a critical role in maintaining the integrity of muscle (Stauber et al., 1977). Decreases in the activities of CAT occur in the skeletal muscles of starved rodents (Di Simplicio et al., 1997) and fasted penguins (Rey et al., 2008), and in hindlimb unloading models (Lawler et al., 2003). In contrast, an increase in the activity of Cat occurs in the foot muscle of aestivating land snails (Hermes-Lima and Storey, 1995). These results indicate that CAT could prevent muscle atrophy by protecting the skeletal muscle against oxidative damage.

1.5.3. Gpx

GPX are considered to be the frontline of defence against ROS. There are two types of GPX – the selenium-dependent GPX (SeGPX) and the selenium-independent GPX (non-SeGPX). SeGPX, which includes GPX1 to 4, is able to reduce both organic and inorganic peroxides such as H_2O_2, while non-SeGPX (GPX5 to 8) catalyses the reduction of organic peroxide only (Almar et al., 1998). The various isozymes are found in different cellular locations and vary in substrate specificity as well. The selenol in Se-GPX reacts with H_2O_2 to selenenic acid, which is then reduced by reduced glutathione (GSH) to form oxidized glutathione (GSSG) and water (Flohé, 1989; Toppo et al., 2009; Flohé et al., 2011). GPX1 is the most abundant isozyme, found in the cytosol of nearly all mammalian tissues, and has a preferred substrate of H_2O_2; GPX4 is expressed at lower levels in almost every mammalian cell, and prefers to reduce lipid hydroperoxides (Brigelius-Flohé, 1999). Among the SeGPX, GPX4 protects membranes from oxidative damage as it possesses the ability to reduce both

H_2O_2 and hydroperoxides in complex lipids including phospholipids, cholesterol and cholesterolester hydroperoxides, even when these lipids are found inserted into biomembranes or lipoproteins (Thomas et al., 1990). GPX4 can translate oxidative stress into cell death (Seiler et al., 2008).

Unlike CAT, there are no significant changes in GPX activity or protein expression in the skeletal muscle of starved mice (Di Simplicio et al., 1997) or fasted penguins (Rey et al., 2008). This suggests that CAT probably plays a more important role than GPX in antioxidant defense in cases of food deprivation. However, decreases in GPX levels take place in rat muscle upon hindlimb unloading (Lawler et al., 2003). In contrast, increases in the activities of SeGpx and total Gpx occur in the foot muscle of land snails (Ramos-Vasconcelos et al., 2003; Nowakowska et al., 2011, 2014) and in the muscle of spadefoot toads (Grundy and Storey, 1998) during aestivation. Therefore, Gpx is implicated in protecting the muscle against oxidative damage.

1.5.4. General changes in expression of *CuZnsod*/CuZnSod, *Mnsod*/MnSod, *cat*/Cat, *gpx1*/Gpx1 and *gpx4*/Gpx4, and levels of several oxidative stress markers during fasting or muscle disuse

SOD: SOD activity decreased in the skeletal muscle of fasted mice (Di Simplicio et al., 1997). An increase in CuZnSOD was reported in limb immobilization models (Kondo et al., 1991, 1993). This increase is also observed in the skeletal muscles of rats upon hindlimb unloading (Lawler et al., 2003). However, the same study (Lawler et al., 2003) reported a decrease in MnSOD activity. It was thought that there could be an upregulation of superoxide anions in the cytosol instead of the mitochondria in

skeletal muscles with unloading, and that the increased CuZnSOD activity could offer some protection against superoxide anions (Lawler et al., 2003).

CAT: CAT activity decreases in the skeletal muscles of starved rodents (Di Simplicio et al., 1997) and fasted penguins (Rey et al., 2008). CAT levels decreases in hindlimb unloading models and is associated with disuse muscle atrophy (Lawler et al., 2003). Overexpression of CAT attenuates disuse-induced atrophy significantly by abolishing immobilization-induced transactivation of nuclear factor κB and FOXO (Dodd et al., 2010).

GPX: No significant changes in GPX activity or protein expression has been reported in the skeletal muscle of starved mice (Di Simplicio et al., 1997) or fasted penguins (Rey et al., 2008). However, in disuse mammalian models, there were decreases in GPX levels in rat muscle upon hindlimb unloading (Lawler et al., 2003).

Oxidative stress biomarkers: Fasting can cause a depletion of extracellular glutathione concentrations (Vogt and Richie, 1993; Di Simplicio et al., 1997), which can result in fasting-induced muscle atrophy. Increases in xanthine oxidase activity, lipid peroxidation and [GSSG]/[GSH] ratio were observed in limb immobilization models (Kondo et al., 1991, 1993). Similar increases in lipid peroxidation and protein oxidation, together with muscle fibre atrophy, were reported in rodents following hindlimb unloading (Lawler et al., 2003; Brocca et al., 2010; Desaphy et al., 2010). Prolonged skeletal muscle inactivity due to immobilization leads to chronic increases in production of ROS and oxidative damage in quiescent muscle fibres (Kondo et al., 1991).

2. Introduction

2.1. African lungfishes and aestivation

Lungfishes are freshwater fishes belonging to the class Sarcoterygii that hold an important position in the evolution of vertebrates with regard to the water-land transition. This is because lungfishes possess lungs, and some of them can survive emersion for a long period. There are six extant lungfishes worldwide, of which four (*Protopterus annectens*, *P. aethiopicus*, *P. amphibicus*, and *P. dolloi*) are found in Africa. African lungfishes are obligate air-breathers and can undergo aestivation in subterranean mud cocoon for up to four years (Smith, 1931; see Ip and Chew, 2010; Ballantyne and Frick, 2010 and Chew et al., 2015 for reviews). Aestivation is a state of corporal torpor adopted by some animals to survive in arid conditions at high temperature without food and water intake for an extended period (Ip and Chew, 2010; Chew et al., 2015).

African lungfishes can be induced to aestivate in completely dried mucus cocoon in plastic boxes in the laboratory (Chew et al., 2004; Ip et al., 2005a; Loong et al., 2005, 2008a, b, 2012a). There are three phases of aestivation: induction, maintenance and arousal. During the induction phase, the aestivating lungfish detects environmental cues and turns them into internal signals that will instill the necessary behavioural, structural, physiological, and biochemical changes in preparation of aestivation. It hyperventilates and secretes mucus which turns into a dry mucus cocoon within 6–8 days. Aestivation begins when the lungfish is completely encased in a cocoon, and there is a complete cessation of feeding and locomotion. During the maintenance phase, the lungfish has to prevent cell death, preserve the biological

structures and sustain a slow rate of waste production to avoid polluting the internal environment. The lungfish can perpetuate to aestivate under such conditions for more than a year in the laboratory. The lungfish can be aroused from aestivation upon the addition of water. It struggles out of the cocoon and swims sluggishly to the water surface to gulp air. During the arousal phase, it has to excrete the accumulated waste products and feed for repair and growth. Feeding begins approximately 7–10 days after arousal, and the lungfish grows and develops normally thereafter. It is apparent that metabolic changes would vary between the three phases of aestivation, but majority of studies in the literature focused predominantly on the maintenance phase.

2.2. Aestivation and muscle atrophy

During periods of fasting, energy stores are mobilized from several tissues as a provision of nutrients for energy production. Unlike lipids and carbohydrates, however, there is no known protein store in animals, and proteins would have to be mobilized from biological structures of specific functions. Fasting-induced muscle atrophy occurs through enhanced protein degradation and reduced protein synthesis in the skeletal muscle (Tomas et al., 1979; Goldberg et al., 1980; Löfberg et al., 2002). Similar processes also occur during skeletal muscle disuse, leading to disuse-induced muscle atrophy in mammals (Childs, 2003). Various studies have reported an immediate decline in the rate of basal protein synthesis after unloading, and this rate stays suppressed throughout the period of disuse (Goldspink, 1977; Booth and Seider, 1979; Paddon-Jones et al., 2006; Glover et al., 2008; Lang et al., 2012; Kelleher et al., 2013). Decreased protein synthesis is thus a prominent attribute of muscle atrophy in mammalian disuse models (Rennie et al., 2010; Marimuthu et al., 2011). Other than

decreased protein synthesis, another prominent feature that contributes to disuse muscle atrophy in non-hibernating mammals is the induction of protein catabolism (Lecker and Goldberg, 2002; Jackman and Kandarian, 2004; Marimuthu et al., 2011). Studies have reported a coordinated increase in the expression of genes involved in the ubiquitin-proteasome pathway, proteolysis and lysosome proteolysis in skeletal muscles of various mammalian models of disuse muscle atrophy (Wittwer et al., 2002; Chopard et al., 2009; Bialek et al., 2011).

During aestivation, there is a complete cessation of feeding and locomotor activities in the African lungfish, which results in the possibility of muscle atrophy induced by fasting and disuse. However, aestivating *P. annectens* loses less than 10% of its skeletal mass after 6 months of aestivation without food supply (Y. K. Ip, unpublished results). It has to preserve its muscle structure and strength by suppressing proteolysis and amino acid catabolism during the maintenance phase of aestivation so that it can struggle out of the cocoon upon subsequent arousal (Chew et al., 2015). Hence, the aestivating African lungfish represents a rare case of a fish being able to suppress muscle atrophy despite long periods of fasting and inactivity. Without food supply, protein synthesis would either come to a halt or be reduced to an extremely low level through endogenous nitrogen recycling. This should theoretically exacerbate muscle atrophy resulting from the increased catabolism of muscle tissue for energy supply (Yacoe, 1983; Wickler et al., 1987, 1991; Steffen et al., 1991). As muscle mass preservation is dependent on the balance between the rate of protein synthesis (muscle formation) and the rate of protein degradation (muscle degradation), the author aimed to determine the changes in expression of various

genes/proteins, which are known to be involved in muscle formation or degradation, in the skeletal muscle of *P. annectens* during three phases of aestivation.

Prolonged skeletal muscle disuse results in a loss of muscle protein and atrophy of muscle fibre, which is associated with increased biomarkers of oxidative stress in in humans and many other mammals (Kondo et al., 1991; Arbogast et al., 2007; Falk et al., 2011; Hussain et al., 2010; Jaber et al., 2011; Levine et al., 2008; Min et al., 2011; Powers et al., 2011; Whidden et al., 2009, 2010). Reactive oxygen species (ROS) can act as signalling molecules in situations of muscle disuse such as immobilization (Kondo et al., 1991, 1993), limb suspension/unloading (Lawler et al., 2003) and denervation (Muller et al., 2007). Oxidative stress leads to the upregulation of several degradative pathways related to skeletal muscle atrophy (Hudson and Franklin, 2002; Powers et al., 2005). The role of ROS and oxidative stress in disuse atrophy is supported by the attenuation of immobilisation atrophy in mice administered with mitochondria-targeting antioxidants (Min et al., 2011). Furthermore, a suppression of mitochondrial ROS production in the disused skeletal muscle of striped burrowing frogs protects the muscle against potential oxidative injury and facilitates muscle mass preservation during aestivation in preparation for arousal (Reilly et al., 2014). Although many studies have investigated antioxidant levels in muscles of aestivators and hibernators during the maintenance and/or arousal phases of aestivation and hibernation, respectively (Ramos-Vasconcelos and Hermes-Lima, 2003; Hudson et al., 2006; Allan and Storey, 2012; James et al., 2013; Young et al., 2013a, b; Reilly et al., 2014), there is little information on the oxidative defense mechanisms or oxidative damages involved. The author decided to determine

the changes in expression of various genes/proteins involved in oxidative defense or acted as oxidative stress markers in the skeletal muscle of *P. annectens* during three phases of aestivation.

2.3. Fasting and muscle disuse generally lead to muscle atrophy

Skeletal muscle atrophy can occur as a result of immobilization and/or starvation in multiple animal models. Under these conditions, muscle wasting involves increased proteolysis and reduced protein synthesis (Sandri et al., 2004).

During long periods of food deprivation, there is a need to mobilize energy stores from various tissues for energy production. Under adverse conditions, skeletal muscle can act as a source of energy, as muscle protein can be broken down to amino acids (Daniel, 1977), which can be later converted to glucose. However, this can result in skeletal muscle atrophy as reported in several animal models (Wing and Goldberg, 1993; Medina et al., 1995; Jagoe et al., 2002; Ørngreen et al., 2003; Allen et al., 2010; Seiliez et al., 2011). Muscle atrophy can also occur due to disuse (Fitts et al., 1986; Taillandier et al., 1996; Morey-Holton and Globus, 2002; Marimuthu et al., 2011). In cases of food deprivation, levels of glucocorticoids (endocrine hormones) are increased (Lecker et al., 1999; Braun et al., 2011) leading to fasting-induced muscle atrophy through increased proteolysis and decreased protein synthesis in the muscle (Tomas et al., 1979; Goldberg et al., 1980; Löfberg et al., 2002). However, glucocorticoids do not seem to be necessary for muscle atrophy induced by disuse (Tischler, 1994) or denervation (Watson et al., 2012). In humans, disuse muscle atrophy is attributed to decreased protein synthesis and no significant change in protein breakdown in human disuse models (Ferrando et al., 1996; Biolo et al., 2004;

Paddon-Jones et al., 2006; Glover et al., 2008), although measuring protein degradation in humans is difficult (Bodine, 2013). Unlike human disuse models, various studies on hind limb unweighting in rodents have attributed disuse muscle atrophy to increased protein breakdown (Taillander et al., 1996; Tawa et al., 1997; Bodine et al., 2001; Gomes et al., 2001; Ikemoto et al., 2001).

Animals that undergo torpor are protected against muscle atrophy despite long periods of immobilization and food deprivation (Grundy and Storey, 1998; Hudson and Franklin, 2002; Lohuis et al., 2007; Mantle et al., 2009; Cotton and Harlow, 2010; Lee et al., 2010; Gao et al., 2012; Andres-Mateos et al., 2013). In the case of African lungfishes, they do not consume any food nor is there any locomotor activity during the maintenance phase of aestivation. As such, the skeletal muscles of African lungfish may undergo atrophy due to both fasting and disuse during aestivation. Although it was observed that fasting can initiate physiological and biochemical changes in a manner similar to aestivation (Fishman et al., 1986), a drastic increase in protein degradation, as in the case of fasting alone (Ip et al., 2005b), does not occur in aestivating African lungfishes. Hence, it is apparent that aestivating lungfishes can effectively preserve muscle structure and strength during the maintenance phase of aestivation (i.e. a period of 6 months in this study), in preparation for arousal, by suppressing proteolysis and amino acid catabolism (Chew et al., 2015). In order to differentiate the effects of fasting and muscle disuse, it was essential to analyze the effects of aestivation on the genes/proteins involved in muscle formation and those involved in muscle degradation.

2.4. Objectives and hypotheses

2.4.1. Molecular characterization of various genes/proteins involved in muscle formation or muscle degradation in *P. annectens*

The first objective of this study was to clone and sequence the cDNA coding region of genes known to be involved in muscle formation [*peroxisome proliferator-activated receptor-γ coactivator-1α* (*ppargc-1α*), *myogenic differentiation 1* (*myod1*), *myogenin* (*myog*), *mitogen-activated protein kinases 1* (*mapk1*) and *3* (*mapk3*)] and muscle degradation [*histone deacetylase 1* (*hdac1*), *forkhead box O1* (*foxO1*), *forkhead box O3* (*foxO3*), *myostatin* (*mstn*) and *F-box protein 32* (*fbxo32*)] from the muscle of *P. annectens*. Efforts were made to investigate the dendrogamic relationship of each gene/protein involved in muscle formation and muscle degradation. It was hoped that information obtained would shed light on the evolutionary relationship of lungfishes to tetrapods and teleosts.

2.4.2. Effects of aestivation on the expression of various genes/proteins involved in muscle formation or muscle degradation in the skeletal muscle of *P. annectens*

The second objective was to determine the mRNA expression levels and, where possible, the protein abundances of genes/proteins known to be involved in muscle formation (*ppargc-1α*/Ppargc-1α, *myod1*/Myod1, *myog*/Myog, *mapk1*/Mapk1 and *mapk3*/Mapk3) and muscle degradation (*hdac1*/Hdac1, *foxO1*/FoxO1, *foxO3*/FoxO3, *tp53*/Tp53, *mstn*/Mstn and *fbxo32*/Fbxo32) in the muscle of *P. annectens* during the three phases of aestivation. During the induction phase, fasting had just begun and the lungfish still exhibited some locomotor activity, especially for the first 1 to 3 days. Moreover, the aestivating lungfish performed tissue reconstruction (Chew et al.,

2015), which could naturally involve increased protein turnover in certain organs. There could be an increased supply or mobilization of protein/amino acids from the skeletal muscle as the fish was deprived of food. Hence, it was hypothesized that muscle formation might be reduced or remain unchanged, while muscle degradation may remain unchanged or enhanced, during the induction phase.

During the maintenance phase, the lack of food supply and locomotor activity subjected the skeletal muscle of the aestivating lungfish to possible atrophy induced by fasting and muscle disuse, respectively. However, there was a need to preserve muscle structure and strength in preparation for arousal (Chew et al., 2015). It was thus hypothesized that the expression of genes/proteins involved in muscle formation and particularly in muscle degradation could be down-regulated during the maintenance phase of aestivation.

During the arousal phase, fasting continued but the lungfish resumed locomotor activity. The aroused fish had to perform tissue reconstruction/regeneration which depicted increased protein turnover in certain organs, with possible increased protein/amino acid mobilization from the skeletal muscle. Hence, the hypothesis tested was that the expression of genes/proteins involved in muscle formation would decrease, while the expression of genes/proteins involved in muscle degradation might increase in the skeletal muscle of the aroused fish.

2.4.3. Effects of aestivation on the expression of genes/proteins, and their activities where applicable, involved in oxidative defense or acted as oxidative stress markers in the skeletal muscle of *P. annectens*

The third objective was to determine the mRNA and protein expression levels of copper-zinc superoxide dismutase (*CuZnsod*/CuZnSod), manganese superoxide dismutase (*Mnsod*/MnSod), catalase (*cat*/Cat), glutathione peroxidases 1 (*gpx1*/Gpx1) and 4 (*gpx4*/Gpx4) in the muscle of *P. annectens* during the three phases of aestivation. In order to assess whether the skeletal muscle of the aestivating fish suffered oxidative damages, efforts were also made to determine the specific activities of CuZnSod, MnSod, total Sod, Cat, selenium-dependent Gpx (SeGpx), total Gpx, glutathione reductase (Gr) and glutathione-S-transferase (Gst), the concentrations of total glutathione equivalent (total GSH-eq), reduced and oxidized glutathione (GSH and GSSG), and oxidative damage products [lipid hydroperoxides (LOOH), thiobarbituric acid reactive substances (TBARS) and carbonyl proteins] in the muscle of *P. annectens* during the three phases of aestivation.

During the induction phase, *P. annectens* could be confronted with oxidative stress due to hyperventilation and possibly an increased metabolic rate due to tissue reconstruction (Chew et al., 2015). It was thus predicted that the expression of certain genes/proteins involved in oxidative defense or acted as oxidative stress markers would be up-regulated in the skeletal muscle of the aestivating fish during this short period. During the maintenance phase, it was hypothesised that the expression of certain genes/proteins involved in oxidative defense would be enhanced in the muscle to protect it from oxidative damages and related atrophy. Since the skeletal muscle of

the aestivating fish had little muscle loss (as compared to human disuse models), the expression of oxidative stress markers were hypothesized to remain unchanged or decrease in the skeletal muscle during the maintenance phase of aestivation. During the arousal phase, there was an increase in oxygen consumption, which could result in increased oxidative stress. Up-regulation of various enzymes involved in oxidative defense have been reported in aestivators to protect against ischemia-reperfusion related oxidative stress associated with the transition from aestivation to arousal (Hermes-Lima and Storey, 1995; Hermes-Lima and Zenteno-Savín, 2002; Ramos-Vasconcelos and Hermes-Lima, 2003; Ramos-Vasconcelos et al., 2005; Nowakowska et al., 2009). It was thus hypothesised that the expression of genes/proteins involved in oxidative defense would be up-regulated in the skeletal muscle of *P. annectens* during the arousal phase of aestivation.

3. Materials and methods

3.1. Animals

Specimens of *P. annectens* (80–120 g body mass) were imported from Central Africa through a local fish farm in Singapore. Specimens were maintained in plastic aquaria filled with dechlorinated tap water at 25°C in the laboratory. Water was changed daily. No attempt was made to separate the sexes. Fish were acclimated to laboratory conditions for at least two weeks. During the acclimatization period, fish were fed with frozen fish meat. This study was performed in accordance with approved protocol IACUC 035/09 granted by the Institutional Animal Care and Use Committee of the National University of Singapore.

3.2. Experimental conditions and collection of samples

Lungfishes were induced to aestivate at 27–29°C and 85–90% humidity individually in plastic tanks (L29 cm x W19 cm x H17.5 cm) containing 15 ml dechlorinated tap water (made to Salinity 0.3 with seawater), following the procedure of Chew et al. (2004). It took approximately 6 days for the lungfish to be encased in a brown dried mucus cocoon. In this study, these 6 days were counted as part of the aestivation period. Hence, for a lungfish aestivated for 12 days, it would have spent approximately 6 days within the dried mucus cocoon. The lungfish were allowed to aestivate for 6 months. In order to maintain a high humidity (>90%) within the tank, 1–2 ml of water was sprayed onto the side of the tank daily. After 6 months of aestivation, some lungfish were aroused by adding 200 ml of water into the tank and breaking up the cocoon manually. After a few minutes, the lungfish would swim sluggishly in the water; another 800 ml of water was added to cover the fish. Some

lungfish were killed with an overdose of neutralized 0.05% MS222 for tissue sampling after 3 or 6 days (the induction phase), or after 12 days (the early maintenance phase) or 6 months (the prolonged maintenance phase) of aestivation (*N*=4 for each group). Some lungfish were killed after 1, 3 or 6 days of arousal from 6 months of aestivation (the arousal phase) without food (*N*=4 for each group). The eye, brain, gills, heart, liver, spleen, pancreas, gut, kidney, lung, muscle and skin were quickly excised and freeze-clamped with aluminum tongs pre-cooled in liquid nitrogen, and kept at -80°C until analysis. The lungfish kept in fresh water (*N*=4) served as controls and were killed after food was withheld for 96 h.

3.3. Cloning, sequencing, dendrogemic analysis and tissue expression

3.3.1. Total RNA extraction and cDNA synthesis

Total RNA was extracted from all the samples extracted from *P. annectens* using Tri Reagent™ (Sigma-Aldrich Co., St. Louis, MO, USA), and purified using the Qiagen RNeasy Mini Kit (Qiagen GmbH, Hilden, Germany). RNA was quantified spectrophotometrically using a BioSpec-nano (Shimadzu, Tokyo, Japan) and RNA integrity assessed electrophoretically before storing at -80°C. Assessment of RNA quality to verify RNA integrity prior to cDNA synthesis was performed electrophoretically. First strand cDNA was synthesized from 4 µg of total RNA using oligo$(dT)_{18}$ primer and the RevertAid™ first strand cDNA synthesis kit (Fermentas International Inc., Burlington, ON, Canada).

3.3.2. Polymerase Chain Reaction (PCR) and cloning

The full coding sequences of *tp53*, *CuZnsod*, *Mnsod*, *cat*, *gpx1* and *gpx4* have been obtained previously from the author's laboratory (Ong, 2010; 2011; Ching, 2012).

The partial coding sequence of *ppargc-1α* was obtained from Genbank with the accession number FJ710608.

Partial sequences of *myod1*, *myog*, *mapk1*, *mapk3*, *hdac1*, *foxO1*, *foxO3*, *mstn*, and *fbxo32* were obtained using gene-specific primers (Table 1) designed from the highly conserved regions based on multiple alignments of the respective sequences from various fish species available in Genbank (http://www.ncbi.nlm.nih.gov/Genbank/). PCR was performed using Dreamtaq polymerase (Fermentas International Inc.), according to the manufacturer's instructions. The thermal cycling conditions were 95°C for 3 min, followed by 40 cycles of 95°C for 30 s, 60°C for 30 s, 72°C for 2 min and a final extension of 72°C for 10 min. PCR products were separated by gel electrophoresis and bands of estimated molecular masses were excised and purified by FavorPrep™ Gel Purification Mini Kit (Favorgen Biotech Corp., Ping Tung, Taiwan) according to the manufacturer's instructions. PCR products were cloned into pGEM®-T Easy vector (Promega Corporation, Madison, WI, USA). The ligated vector was transformed into JM109 competent cells and plated onto Luria-Bertani agar with 100 μg ml^{-1} ampicillin, 50 μg ml^{-1} X-gal and 0.5 mmol l^{-1} IPTG. Selected white colonies were grown overnight in Luria-Bertani broth with ampicillin. The plasmids were extracted using the resin-based plasmid miniprep kit (Axygen Biosciences, Union city, CA, USA). Sequencing was performed using BigDye® Terminator v3.1 Cycle Sequencing Kit (Thermo Fisher Scientific, Waltham, MA, USA) and sequenced using the 3130XL Genetic Analyzer (Thermo Fisher Scientific). Sequence assembly and analysis were performed using Bioedit v7.1.3 (Hall, 1999).

Table 1. The primer sequences used for PCR.

Gene	Primer sequence (5'to 3')
myod1	Forward: CACATCTCTTTGCTCATTCC
	Reverse: CCCTCTGCTCCTGTTTCT
myog	Forward: GAGCACCCTGATGAACCC
	Reverse: ACTGTGATGCTGTCCACGAT
mapk1	Forward: GTGTGTTCTTCTAGTCATGG
	Reverse: TTCTGAAGTCCTAGCCCT
mapk3	Forward: CTCAAATCCCTCAGCAAC
	Reverse: ATCAGCTCTTTCAGTTTCTCC
hdac1	Forward: GCGGTTGTATAGATAGAGTGAGT
	Reverse: CAAGGAATGCCAATGCTA
foxO1	Forward: TCGCCATAACTTGTCACTTC
	Reverse: GCCCATTACTGTTGATACCA
foxO3	Forward: GAACTCAATCCGACACAATCT
	Reverse: CACTGCCCTCATCTTGCT
mstn	Forward: GACGTGCTGGGAGATGAC
	Reverse: CAATAATCCAGTCCCAGCC
fbxo32	Forward: TGTCTCAGCCAAGAAACGA
	Reverse: GGTTGATGAAGTCTTGTGGG

3.3.3. Rapid amplification of cDNA ends (RACE)

Total RNA (1 µg) isolated from the muscle of freshwater *P. annectens* was reverse transcribed into 5'-RACE-Ready cDNA and 3'-RACE-Ready cDNA using SMARTer™ RACE cDNA Amplification kit (Clontech Laboratories, Mountain View, CA, USA). RACE-PCR were performed using Advantage® 2 PCR kit (Clontech Laboratories), with gene-specific RACE primers (Table 2), designed based on partial cDNA sequences of *ppargc-1α*, *myod1*, *myog*, *mapk1*, *mapk3*, *hdac1*, *foxO1*, *foxO3*, *mstn*, and *fbxo32* to generate the 5' and 3' cDNA fragments respectively. The cycling conditions involved 30 cycles of 94°C for 30 s, 65°C for 30 s, and 72°C for 4 min. RACE-PCR products were separated using gel electrophoresis, purified and sequenced. Multiple sequencing was performed in both directions to obtain the full coding sequence.

3.3.4. Deduced amino acid sequences and dendrogramic analysis

The amino acid sequences of Ppargc-1α, Myod1, Myog, Mapk1, Mapk3, Hdac1, FoxO1, FoxO3, Mstn, and Fbxo32 were translated from their respective nucleotide sequences using ExPASy Proteomic server (http://web.expasy.org/translate/). The deduced amino acid sequences were aligned and compared with selected Ppargc-1α/PPARGC-1α, Myod1/MYOD1, Myog/MYOG, Mapk1/MAPK1, Mapk3/MAPK3, Hdac1/HDAC1, FoxO1/FOXO1, FoxO3/FOXO3, Mstn/MSTN, and Fbxo32/FBXO32 sequences from various animal species using BioEdit. Potential nuclear localization signals were identified using cNLS Mapper (Kosugi et al., 2009) and potential nuclear export signals were identified using LocNES (Xu et al., 2014).

Table 2. The primer sequences used for RACE PCR.

Gene	Primer type	Primer sequence (5'to 3')
ppargc-1α	5'-RACE	CAGCAAGTTGGCCTCATTCTCGT
	3'-RACE	TGCATTTGCTGCTCTTGAGAATGG
myod1	5'-RACE	GGGTCATCATAGAAGTCATCTGCTGG
	3'-RACE	TGTAAAGCCTGCAAGAGAAAGACCAC
myog	5'-RACE	CTGCACTGCTCCATTCTGGACTG
	3'-RACE	CAGTCCAGAATGGAGCAGTGCAG
mapk1	5'-RACE	GTGTGCCAACGCTTCTTCCACTT
	3'-RACE	CAGTGATGAGCCTACAGCAGAATCACCA
mapk3	5'-RACE	TCGCAGGATCTGGTAGAGGAAGTAG
	3'-RACE	ATGAGCCCGTGGCAGAGGAACCC
hdac1	5'-RACE	CCCTCCAGCCCAATTCACTGCAATATCA
	3'-RACE	CTTGCGAATGCTTCCTCATGCTCCT
foxO1	5'-RACE	GATTGAGCATCCACCAGGAACTCTTC
	3'-RACE	TAAACCCTGCAACCCACCCTCATCAAG
foxO3	5'-RACE	ACTGCTGCGTGAAGTAGGACTGCCA
	3'-RACE	CCCAATGCTGTACCCTAGTCCTACCCAT
mstn	5'-RACE	TCCACTTTCAGAGAACGAATGCCT
	3'-RACE	AAGAAGGGCTGCAACCATTTCTG
fbxo32	5'-RACE	GTGCAGCAGCTCTCTGGATTGTTGG
	3'-RACE	TCCAAAGGTGTTACTTGTCTCTTTCCAG

The sequences of the proteins listed above were aligned using ClustalX2, and the various dendrograms were constructed through maximum likelihood analyses. Using ModelGenerator v0.85 (Keane et al., 2006), the best-fitting evolutionary model under the Akaike Information Criterion for all the proteins listed above was Jones-Taylor-Thornton. The maximum likelihood analyses were run using RaxML v8.2.5 (Stamatakis, 2014) with the number of bootstraps listed in Table 3. Trees were determined to have converged after a certain number of replicates (Table 3) by the bootstrap convergence criterion. The selected animal species and their respective amino acid accession numbers used in the dendrogramic analyses are presented in Appendix 1.

3.3.5. Gene expression in various tissues/organs

PCR was performed on the cDNAs of muscle, heart, brain, eye, gills, kidney, lung, skin, liver, spleen, pancreas, and gut of freshwater *P. annectens* (*N*=1) using gene-specific qPCR primers (Table 4) to detect the mRNA expression levels of each gene in various tissues. Each PCR was carried out in 10 µl reaction vols. using Dreamtaq polymerase (Fermentas International Inc.) with thermal cycling conditions: 95°C for 3 min, followed by 28 cycles of 95°C for 30 s, 55°C for 30 s, 72°C for 30 s and a final extension of 72°C for 10 min. PCR products were then separated by electrophoresis in 2% agarose gel.

3.4. qPCR

Since it was essential to compare the mRNA expression levels of various genes involved in muscle formation, muscle degradation and oxidative defense in the same tissue, the method of absolute quantification with reference to a standard curve was

Table 3. Best-fitting evolutionary models, number of bootstraps and number of replicates required for convergence for dendrogramic analyses.

Protein	Number of bootstraps ran	Number of replicates required for convergence
Ppargc-1α	1000	800
Myod1 and Myog	1000	450
Mapk1 and Mapk3	1000	950
Hdac1	1000	400
FoxO1 and FoxO3	1000	400
Mstn	8000	7750
Fbxo32	1000	400

Table 4. Primer sequences used for qPCR.

Gene	Primer sequence (5' to 3')	Primer concentration (μmol l^{-1})	Efficiency (%)
ppargc-1α	Forward: GATGAAAGTGAGGATGATGG Reverse: AAGATTTGGGTGGTGAGAC	0.4	86.1
myod1	Forward: CATCTACAAACCCAAACCAAAG Reverse: CCTGTGTAATCCATCATGCC	0.2	87.1
myog	Forward: GTGAGAATTACTTCCCAACCAG Reverse: TCCTCAACTCCCAAACCA	0.2	91.5
mapk1	Forward: GTGCCTTGGAATAGACTGTT Reverse: AATGGTGATTCTGCTGTAGG	0.2	92.7
mapk3	Forward: GGTGTGGAATCGGTGAAG Reverse: AGTATGTCTGGTGTTCAAAGGG	0.4	89.7
hdac1	Forward: ATGTTGGGAGGAGGTGGT Reverse: TCGTTGGTGTTCTGATTTGTC	0.2	85.9

Table 4. (continued)

Gene	Primer sequence (5’ to 3’)	Primer concentration (μmol l^{-1})	Efficiency (%)
foxO1	Forward: GCACCATGTTACACAGTTCAC Reverse: TGTTGATACCAGGGAAAGGA	0.2	86.0
foxO3	Forward: CAAATAGCATGAGCCTTCC Reverse: CCACCCATATTCTGAGATGA	0.2	93.6
tp53	Forward: AATTATACGTGCCACTGCTG Reverse: GACCATCTTTATGTTCTGTGCT	0.3	97.9
mstn	Forward: CCACTACAGCAACTTCTTGACC Reverse: ACATTTAGGCTTTCCCTCCA	0.2	92.0
fbxo32	Forward: TCGGAAGGAGCAGTATGG Reverse: GGTTGATGAAGTCTTGTGGG	0.2	85.9
CuZn-sod	Forward: ATGTAGGTGATCTTGGAAATGTG Reverse: TGCCCAAGTCATCTTCTTTCTC	0.25	99.6

Table 4. (continued)

Gene	Primer sequence (5’ to 3’)	Primer concentration ($\mu mol\ l^{-1}$)	Efficiency (%)
Mnsod	Forward: ACTCTTCCAGACCTCCCA Reverse: CTCCATTGAATTTCAGAGCAG	0.2	98.2
cat	Forward: CCAGAAAGAGTTGTACATGCC Reverse: CAGCAACAGTGGAGAAACGA	0.25	100.1
gpx1	Forward: AATTCGTTGAAATATGTCCGTCC Reverse: CGCATCATCACTGGGATAAGG	0.15	94.6
gpx4	Forward: GAAGGGCAGGTGGTAAAGAG Reverse: ATGGAATGCTACAGGTAATTTGG	0.2	95.5

adopted in this study. While relative quantitation methods produce only fold-change data, they do not allow the interpretation of which gene being the predominant one being expressed in a certain condition. Although absolute quantification provides more information, it is not commonly adopted because of the lack of internal standard to avoid technical errors, and the necessity to create reliable standards for quantification and include these standards in every qPCR.

RNA (4 μg) from the muscle of *P. annectens* were extracted using the Qiagen RNeasy Plus Mini Kit (Qiagen GmbH), and reverse-transcribed using random hexamer primers with RevertAid^{TM} first strand cDNA synthesis kit (Thermo Fisher Scientific). To determine the absolute quantity of transcripts of the genes involved in muscle formation, muscle degradation and oxidative defense in a qPCR reaction, efforts were made to produce a pure amplicon (standard) of a defined region of the cDNA, as defined by the gene-specific set of qPCR primers (Table 4), from the muscle of *P. annectens* following the method of Gerwick et al. (2007). PCR was performed with a specific set of qPCR primers and cDNA as a template in a final volume of 25 μl with the following cycling conditions: initial denaturation 95°C for 3 min, followed by 40 cycles of 95°C for 30 s, 60°C for 30 s and 72°C for 30 s and 1 cycle of final extension of 72°C for 10 min. The PCR product was separated in a 2% agarose gel then excised and purified. The nucleotide fragments in the purified product was cloned using pGEM®-T Easy vector (Promega Corporation). The presence of the insert in the recombinant clones was confirmed by sequencing. The cloned circular plasmid was quantified using a BioSpec-nano (Shimadzu).

qPCR was performed in triplicates using a StepOnePlus™ Real-Time PCR System (Thermo Fisher Scientific). The mRNA expression levels of the genes involved in muscle formation, muscle degradation and oxidative defense were determined using gene-specific qPCR primers (Table 4). The standard cDNA (template) was serially diluted (from 10^6 to 10^2 specific copies per 2 µl). The qPCR reactions contained 5 µl of KAPA SYBR® FAST Master Mix (2X) ABI Prism™ (Kapa Biosystems, Woburn, MA, USA), forward and reverse qPCR primers each and 1 ng of sample cDNA or various quantities of standard in a total volume of 10 µl. Cycling conditions were 95°C for 20 s (1 cycle), followed by 40 cycles of 95°C for 3 s and 62°C for 30 s. Data (C_t values) were collected at each elongation step. A melt curve analysis was performed after each run by increasing the temperature from 60°C to 95°C in 0.3°C increments to confirm the presence of a single product only. The PCR products obtained were also separated in a 2% agarose gel to verify the presence of a single band. A standard curve was obtained from plotting threshold cycle (C_t) on the Y-axis and the natural log of concentration (copies μl^{-1}) on the X-axis. The C_t slope, PCR efficiency, Y-intercept and correlation coefficient (r^2) were calculated using the default setting of StepOne™ Software v2.1 (Thermo Fisher Scientific). Diluted standards were stored at -20°C. The concentrations used and the PCR efficiencies of each qPCR primer pair are indicated in Table 4. The quantity of transcript in an unknown sample was determined from the linear regression line derived from the standard curve and expressed as copies of transcript per ng total RNA.

3.5. SDS-PAGE and Western blotting

A commercial firm (GenScript, Piscataway, NJ, USA) was engaged to raise a rabbit polyclonal antibody against the epitope sequence of the translated amino acid sequences of Ppargc-1α, Myod1, Myog, Mapk, Hdac1, FoxO1, FoxO3, Mstn, Fbxo32, Cat, Gpx1 and Gpx4 of *P. annectens*. Commercial antibodies for CuZnSod (FL-154: sc-11407, Santa Cruz Biotechnology Inc., Texas, USA) and MnSod (DD-17, Sigma-Aldrich Co.) were purchased. The epitope sequences for each primary antibody are indicated in Table 5.

Western blotting was performed on the muscle samples obtained from the control fish and fish that had undergone 6 days, or 6 months of aestivation, or 1 or 3 days of arousal from 6 months of aestivation. Individual samples were homogenized thrice at 24,000 r.p.m. for 20 s each with 10 s intervals in five volumes (w/v) of ice cold buffer containing 50 mmol l^{-1} Tris HCl, (pH 7.4), 1 mmol l^{-1} EDTA, 150 mmol l^{-1} NaCl, 1 mmol l^{-1} NaF, 1 mmol l^{-1} Na_3VO_4, 1% NP-40, 1% sodium deoxycholate, 1 mmol l^{-1} phenylmethylsulfonyl fluoride, and 1× HALT protease inhibitor cocktail (Thermo Fisher Scientific) using LabGEN homogenizer 125 (Cole-Parmer Instrument Company, Chicago, IL, USA). The homogenate was centrifuged at 10,000 × g for 20 min at 4°C. The protein concentration in the supernatant obtained was determined according to the method of Bradford (1976) and adjusted to 10 µg $µl^{-1}$ with Laemmli buffer (Laemmli, 1970). Samples were heated at 95°C for 5 min, and then kept at -80°C until analysis.

Table 5. Epitope sequences of translated amino acids based on which antibodies were designed against, the amount of protein loaded from the muscle of *P. annectens* and the dilution used for each primary antibody for Western blotting.

Antibody	Epitope sequence	Protein load (µg)	Dilution
Anti-Ppargc-1α	CSRSRSPYRHRTRYD	100	1:300
Anti-Myod1	CETGAEGSPSSPHGG	200	1:300
Anti-Myog	GVEEKLSPVSGISPC	20	1:300
Anti-Mapk	DNVNKIRVAIKKISC	100	1:300
Anti-Hdac1	CDKTEAKGVKEETKP	100	1:300
Anti-FoxO1	CSKMTSLPSLSEMSS	20	1:500
Anti-FoxO3	CRQTPMQTIQENKQT	200	1:500
Anti-Mstn	TEPDFAIPMEGKPKC	200	1:500
Anti-Fbxo32	VKTGDGWKRYKNDVC	100	1:500
Anti-CuZnSod	Amino acids 1–154 of human CuZnSOD (FL-154: sc-11407; Santa Cruz Biotechnology Inc.)	100	1:800
Anti-MnSod	CDVWEHAYYLQYKNVRPD (DD-17; Sigma-Aldrich Co.)	100	1:1000
Anti-Cat	TQKRNPQTNLKDPDC	100	1:500
Anti-Gpx1	CPDGVPYKRYSRKFL	200	1:500
Anti-Gpx4	CGPMDDPVVIEKDLP	200	1:500

The amount of protein load and the dilution used for each primary antibody are indicated in Table 5. Proteins were separated by SDS-PAGE according to the method of Laemmli (1970) using a vertical mini-slab apparatus (Bio-Rad Laboratories, Hercules, CA, USA). Proteins were then electrophoretically transferred onto PVDF membranes using a transfer apparatus (Bio-Rad Laboratories).

For Ppargc-1α, Mapk, Hdac1, FoxO1, FoxO3, Mstn, Fbxo32, MnSod, Gpx1 and Gpx4, detection was performed using Pierce™ SuperSignal™ West Pico Rabbit Fast Western Kit (Thermo Fisher Scientific), as per manufacturer's instructions. Bands were visualized by chemiluminescence (Western Lightning™, PerkinElmer Life Sciences, Boston, MA, USA) using X-ray film (Thermo Fisher Scientific) and were processed by a Kodak X-Omat 3000 RA processor (Kodak, Rochester, NY, USA).

For Myod1, Myog, CuZnSod and Cat, after transfer, each membrane was blocked with 10% skim milk in TTBS (0.05% Tween 20 in Tris-buffered saline: 20 mmol l^{-1} Tris-HCl; 500 mmol l^{-1} NaCl, pH 7.6) for 1 h before being incubated overnight at 4°C with the respective primary antibodies diluted in 1% bovine serum albumin in TTBS. For Myod1, Myog and Cat, the membranes were incubated in goat anti-rabbit horseradish peroxidase secondary antibody (1:5,000 dilution for Myod1 and Myog; 1:8,000 dilution for Cat; Santa Cruz Biotechnology Inc.) for 1 h and rinsed. Bands were visualized by chemiluminescence (Western Lightning™) using X-ray film (Thermo Fisher Scientific) and were processed by a Kodak X-Omat 3000 RA processor (Kodak). For CuZnSod, the membranes were incubated in goat anti-rabbit alkaline phosphatase-conjugated secondary antibody (1:8,000 dilution; Santa

Cruz Biotechnology Inc.) for 1 h, rinsed and then incubated for 30 min in a solution of 5-bromo-4-chloro-3-indolyl phosphate *p*-toluidine salt and nitro-blue tetrazolium chloride (Invitrogen, Carlsbad, CA, USA) for color development.

The blots were scanned using CanonScan 4400F flatbed scanner in TIFF format at 300 dpi resolution. Densitometric quantification of the band intensities was performed using ImageJ (version 1.40, NIH), calibrated with a calibrated 37 step reflection scanner scale (1″× 8″; Stouffer #R3705-1C). It would be very difficult to find a reference protein, the expression of which would be unaffected throughout the three phases of aestivation. Hence, results were expressed as arbitrary densitometric unit per μg protein, i.e. with reference to the protein abundance, as reported elsewhere for L-Gulono-γ-lactone oxidase (Ching et al., 2014), Na^+/K^+-ATPase (Hiong et al., 2014), Betaine-homocysteine methyltransferase 1 (Ong et al., 2015) and Coagulation factor II/Fibrinogen gamma chain (Hiong et al., 2015a) expression in *P. annectens* during aestivation.

3.6. Enzyme assays

The frozen muscle samples were homogenized three times at 24,000 r.p.m. for 20 s each with 10 s intervals in 5 volumes (w/v) of ice-cold 50 mmol l^{-1} potassium phosphate buffer containing 0.5 mmol l^{-1} EDTA at pH 7.2, and 10 μmol l^{-1} phenylmethylsulfonyl fluoride (added just before homogenization) using LabGEN homogenizer 125 (Cole-Parmer Instrument Company). The homogenates were centrifuged at 15,000 × *g* for 15 min at 5°C to obtain the supernatants, which were used directly for various enzyme assays. Protein amounts were determined by the

Bradford method (Bradford, 1976) with bovine gamma globulin as the standard for comparison.

3.6.1. Determination of CuZnSod, MnSod and total Sod activities

Total Sod activities were determined using SOD Assay Kit-WST (19160, Sigma-Aldrich Co.) according to the manufacturer's protocol. Bovine SOD (S7571, Sigma-Aldrich Co.) was diluted according to the kit's recommendation as the standard for comparison. To measure MnSod activity, 0.042 mmol l^{-1} potassium cyanide was added to each sample. CuZnSod is specifically inhibited by potassium cyanide (Kasemset and Oberley, 1984). CuZnSod activity for each sample was calculated as the difference between total Sod and MnSod activities. Results were expressed in mU per mg protein.

3.6.2. Determination of Cat activity

The Cat assay mixture contained 50 mmol l^{-1} potassium phosphate buffer, pH 7.0 and 10 mmol l^{-1} H_2O_2. Sample extracts were added to start the reaction, where the decay of H_2O_2 was followed at 240 nm in a quartz cuvette (ε = 0.0394 L $mmol^{-1}$ cm^{-1}), as described by Aebi (1974). The specific activity of Cat was expressed as nmol of H_2O_2 decomposed per min per mg protein.

3.6.3. Determination of SeGpx and total Gpx activities

Two separate assays were conducted for determining the activities of SeGpx and total Gpx. For SeGpx, the reaction was initiated by adding 0.5 mmol l^{-1} hydrogen peroxide (H_2O_2) to the standard assay mixture of 50 mmol l^{-1} potassium phosphate buffer, pH 7.0, 1 mmol l^{-1} EDTA, 2 mmol l^{-1} NaN_3, 0.2 mmol l^{-1} NADPH, 1 i.u. Gr (Sigma-Aldrich Co.) and 5 mmol l^{-1} GSH (Ahmad and Pardini, 1988). The same assay was

used to quantify total Gpx, except that H_2O_2 was replaced with 1.2 mmol l^{-1} cumene hydroperoxide. The specific activities of SeGpx and total Gpx were expressed in nmol NADPH oxidized per min per mg protein.

3.6.4. Determination of Gr activity

The assay medium for Gr consisted of 50 mmol l^{-1} potassium phosphate buffer, pH 7.4, 1 mmol l^{-1} EDTA, 0.2 mmol l^{-1} NADPH and 5 mmol l^{-1} GSSG, and the rate of NADPH oxidation was followed at 340 nm. The specific activity of Gr was expressed in nmol of NADPH oxidized per min per mg protein.

3.6.5. Determination of Gst activity

Gst was assayed according to Grundy and Storey (1998). The enzyme activity was measured by monitoring the rate of formation of S-2,4-dinitrophenylglutathione (a conjugate of GSH and 1-chloro-2,4-dinitrobenzene) at 340 nm (ε = 9.6 L $mmol^{-1}$ cm^{-1}). The reaction was started by adding the supernatant to an assay containing 50 mmol l^{-1} potassium phosphate buffer, pH 6.5, 1 mmol l^{-1} EDTA, 5 mmol l^{-1} GSH and 2 mmol l^{-1} 1-chloro-2,4-dinitrobenzene. The specific activity of Gst was expressed in nmol of conjugate generated per min per mg protein.

3.7. Determination of total and oxidized glutathione

The frozen tissue sample was homogenized three times at 24,000 r.p.m. using LabGEN homogenizer 125 (Cole-Parmer Instrument Company) for 20 s each with 10 s intervals in 5 volumes (w/v) of ice-cold 5% sulfosalicylic acid which had been bubbled in nitrogen gas for 10 min. After bubbling for another 10 s, the homogenate was centrifuged at 15,000 × *g* for 5 min at 4°C. The supernatant was removed, neutralized (pH 6.5–7) with 3 mol l^{-1} Trizma base and separated into two portions for

the measurement of total GSHeq and GSSG according to the method of Griffith (1980). For total GSHeq, an aliquot of the supernatant was introduced to a reaction mixture containing 100 mmol l^{-1} potassium phosphate buffer, pH 7.5, 0.25 mmol l^{-1} NADPH, 4 mmol l^{-1} EDTA and 0.6 mmol l^{-1} 5,5-dithiobis-2-nitrobenzoic acid (DTNB) in a final volume of 1.2 ml. The reaction was initiated by the addition of 0.9 i.u. Gr (Sigma-Aldrich Co.) and the absorbance monitored at 412 nm. The second portion of the supernatant was incubated with 170 mmol l^{-1} 2-vinylpyridine for 1 h at 30°C to derivatize any GSH present in the sample. GSSG in this portion was quantified using the same method. GSH content was calculated as the difference between the contents of total GSHeq and GSSG. Results were expressed in nmol per g wet mass.

3.8. Determination of levels of oxidative damage products

3.8.1. Determination of products of lipid peroxidation

Two methods were adopted to determine lipid peroxidation in this study. The first method used xylenol orange to quantify LOOH (Hermes-Lima et al., 1995). The samples were homogenized three times for 20 s each with 10 s intervals, in 20 volumes (w/v) of HPLC grade methanol using LabGEN homogenizer 125 (Cole-Parmer Instrument Company) at 24,000 r.p.m. Following that, centrifugation was carried out for 5 min at 15,000 × *g* at 4°C to obtain the supernatant. An assay mixture consisting of 0.25 mmol l^{-1} ferrous sulfate, 25 mmol l^{-1} sulfuric acid, 0.1 mmol l^{-1} xylenol orange (added in the stated order) was incubated for 30 min at 25°C. Following incubation, 1 ml of the assay mixture was added to 15 µl of supernatant and the reaction was allowed to occur at 25°C for 12 h before the absorbance was

determined at 580 nm. Next, 5 µl of 1 mmol l^{-1} cumene hydroperoxide was added as an internal standard and further incubated for 30 min at 25°C before determining the absorbance again at 580 nm. The results were calculated according to the equation of Hermes-Lima et al. (1995) and the LOOH content expressed as cumene hydroperoxide equivalents per g wet mass.

The second method quantified TBARS as an index of lipid peroxidation (Hermes-Lima and Storey, 1995). The frozen sample was homogenized as stated above, in 20 volumes (w/v) of ice-cold 1.1% phosphoric acid. Then, 0.4 ml of the homogenate was added to an equal volume of a mixture of 1% thiobarbituric acid, 0.1 mmol l^{-1} butylated hydroxytoluene solution, 50 mmol l^{-1} sodium hydroxide, and 0.2 ml of 7% phosphoric acid. After heating for 15 min at 98°C, the sample was vigorously mixed with 1.5 ml of butanol, and centrifuged at 2,000 × *g* for 5 min using a Beckman J2-21/E centrifuge (Beckman Coulter Inc., Fullerton, CA, USA). The organic layer was transferred to glass cuvettes, and the optical densities at 532 nm and 600 nm were determined using a Shimadzu UV-160A spectrophotometer (Shimadzu). Blanks were prepared by replacing the thiobarbituric acid with 3 mmol l^{-1} hydrochloric acid. The results were calculated as Sample (A_{532} - A_{600}) - Blank (A_{532} - A_{600}) as recommended by Ramos-Vasconcelos and Hermes-Lima (2003). TBARS was quantified based on the extinction coefficient of 156 L $mmol^{-1}$ cm^{-1}, and expressed in nmol per g wet mass.

3.8.2. Determination of carbonyl proteins

The assay for carbonyl protein quantifies the oxidative damage to proteins (Stadtman and Levine, 2000). Ice-cold 5% sulfosalicylic acid was used as the homogenization

medium for the tissues (1:20, w/v). The homogenized sample was centrifuged at 15,000 × *g* for 5 min to obtain the pellet, which was mixed with 10 mmol l^{-1} 2,4-dinitrophenyl-hydrazine in 2 mmol l^{-1} hydrochloric acid, vortexed every 15 min and kept for 1 h at room temperature. The sample was then centrifuged at 15,000 × *g* for 3 min after the addition of 20% trichloroacetic acid. Excess 2,4-dinitrophenyl-hydrazine was removed by washing the pellet three times using 1 ml of ethanol:ethyl acetate (1:1, v/v), followed with the addition of 6 mmol l^{-1} guanidine chloride. An incubation period of 15 min at 37°C was allowed before recording the absorbance at 360 nm. Sample blanks were prepared using 2 mmol l^{-1} hydrochloric acid instead of 2,4-dinitrophenyl-hydrazine. The carbonyl protein content was calculated using the extinction coefficient of 22 L $mmol^{-1}$ cm^{-1}, and expressed in µmol per g wet mass.

3.9. Statistical analyses

Results were presented as means ± standard errors of the mean (S.E.M.). Statistical analyses were performed using SPSS version 18 (SPSS Inc, Chicago, USA). Homogeneity of variance was checked using Levene's Test. Differences between means were tested using one-way analysis of variance followed by multiple comparisons of means by either the Tukey or Dunnett T3 post-hoc test, depending on the homogeneity of variance of the data set. Differences with $P<0.05$ were reported as statistically significant.

4. Results

4.1. Genes/proteins involved in muscle formation

4.1.1. *ppargc-1α*/ Ppargc-1α

4.1.1.1. Nucleotide sequence, translated amino acid sequence and dendrogramic analysis

The complete coding sequence of *ppargc-1α* from *P. annectens* comprised 2394 bp. The deduced Ppargc-1α sequence consisted of 798 amino acids with an estimated molecular mass of 90.8 kDa (Appendix 2a), and shared the highest amino acid sequence identity with reptilian PPARGC-1α (65.5–67.2%), followed by mammalian PPARGC-1α (65.2–66.3%), coelacanth Ppargc-1α (66.2–66.3%), amphibian Ppargc-1α (50.3–63.3%), elasmobranch Ppargc-1α (63.1%), and teleost Ppargc-1α (32.8–48.1%; Table 6).

An alignment of Ppargc-1α from *P. annectens* with those of human, rat, frog, coelacanth, zebrafish and shark revealed high conservation in most of the important domains (Fig. 1). Amino acid positions reported henceforth will be in relation to the ruler represented in the figure. The two activation domains (AD), AD1 (position 32–42) and AD2 (position 85–98) are highly conserved in all species compared. The LXXLL motif, essential in mediating nuclear receptor-coactivator interactions, was also highly conserved in all species compared. The PPAR-γ binding domain showed the least conservation among other domains, with fish and elasmobranch Ppargc-1α being the most dissimilar to those of other organisms. While all three p38-MAPK phosphorylation sites (T309, S312, T349) were conserved in all species compared, only one of the two AMPK phosphorylation sites (T179, S621) was conserved among

them. S621 was well conserved, while T179 was conserved only in tetrapods (Fig. 1). The Ppargc-1α of *P. annectens* also contained a conserved RNA-binding domain and two domains rich in serine and arginine residues, also known as SR-rich domains.

The Ppargc-1α of *P. annectens* was grouped in a clade together with PPARGC-1α of tetrapods, Ppargc-1α of *L. chalumnae* and Ppargc-1α of elasmobranches, separated from Ppargc-1α of teleosts (Fig. 2).

4.1.1.2. Gene expression of *ppargc-1α* in various tissues/organs

The expression of *ppargc-1α* was the highest in the kidney, heart and gills of *P. annectens* kept in fresh water (Fig. 3). The expression of *ppargc-1α* was also detected in the muscle, brain, eye, skin, liver, pancreas and gut, but was undetectable in the lung and spleen.

4.1.1.3. mRNA expression of *ppargc-1α*

There were significant decreases in the mRNA expression level of *ppargc-1α* in the muscle of *P. annectens* after 3 days (by 45.7%; $P<0.05$) or after 6 months of aestivation (by 36.4%; $P<0.05$), as compared to the freshwater control (Fig. 4a). By contrast, there was a significant increase in the mRNA expression of *ppargc-1α* after 6 days of arousal from 6 months of aestivation (2.59-fold; $P<0.05$; Fig. 4b).

4.1.1.4. Protein abundance of Ppargc-1α

There were no significant changes in the protein abundance of Ppargc-1α in the muscle of *P. annectens* after 6 days or 6 months of aestivation, or after 1 day or 3 days of arousal from 6 months of aestivation (Fig. 5).

Table 6. The percentage similarity between the deduced amino acid sequence of peroxisome proliferator-activated receptor gamma, coactivator 1 alpha (Ppargc-1α) from the muscle of *Protopterus annectens* and PPARGC-1α/Ppargc-1α sequences from other animal species obtained from GenBank (accession numbers in brackets). Sequences are arranged in a descending order of similarity.

Classification	Species	Similarity
Reptiles	*Pelodiscus sinensis* PPARGC-1α isoform 2 (XP_006138222.1)	67.2%
	Chelonia mydas PPARGC-1α (XP_007058167.1)	66.5%
	Pelodiscus sinensis PPARGC-1α isoform 1 (XP_006138221.1)	65.5%
Mammals	*Homo sapiens* PPARGC-1α (NP_037393.1)	66.3%
	Rattus norvegicus PPARGC-1α (NP_112637.1)	65.6%
	Mus musculus PPARGC-1α (NP_032930.1)	65.2%
Coelacanth	*Latimeria chalumnae* Ppargc-1α (XP_005997925.1)	66.3%
Amphibian	*Xenopus (Silurana) tropicalis* Ppargc-1α isoform 1 (XP_002936759.2)	63.3%
	Xenopus (Silurana) tropicalis Ppargc-1α isoform 2 (XP_004911281.1)	63.2%
Elasmobranch	*Callorhinchus milii* Ppargc-1α (XP_007887233.1)	63.1%
Teleosts	*Ictalurus punctatus* Ppargc-1α (AHH38878.1)	48.1%
	Esox lucius Ppargc-1α (XP_012995921.1)	47.8%
	Cynoglossus semilaevis Ppargc-1α (XP_008324663.1)	47.5%
	Fundulus heteroclitus Ppargc-1α isoform 3 (XP_012720393.1)	47.1%
	Esox lucius Ppargc-1α isoform 1 (XP_012995919.1)	46.4%
	Larimichthys crocea Ppargc-1α (XP_010732114.1)	46.3%
	Esox lucius Ppargc-1α isoform 2 (XP_012995920.1)	46.3%
	Oryzias latipes Ppargc-1α isoform 3 (XP_011485675.1)	44.9%
	Danio rerio Ppargc-1α (XP_002667577.3)	44.0%
	Takifugu rubripes Ppargc-1α (XP_011605089.1)	42.1%
	Oryzias latipes Ppargc-1α isoform 1 (XP_011485673.1)	33.5%
	Oryzias latipes Ppargc-1α isoform 2 (XP_011485674.1)	33.5%

Fig. 1. Molecular characterization of peroxisome proliferator-activated receptor gamma, coactivator 1 alpha (Ppargc-1α) from the muscle of *Protopterus annectens*. Multiple amino acid alignment of Ppargc-1α from the muscle of *P. annectens* with six other known PPARGC-1α/Ppargc-1α from *Homo sapiens* (NP_037393.1), *Rattus norvegicus* (NP_112637.1), *Xenopus* (*Silurana*) *tropicalis* (XP_002936759.2), *Latimeria chalumnae* (XP_005997925.1), *Danio rerio* (XP_002667577.3) and *Callorhinchus milii* (XP_007887233.1). Identical amino acids are indicated by shaded residues. The yellow boxes represent the activation domains (AD) 1 and 2. An LXXLL motif is underlined. The open box indicates the PPARγ-binding domain. The open triangles indicate the three p38 mitogen-activated protein kinase phosphorylation sites (T309, S312, T349), while the closed triangles indicate the two AMP kinase phosphorylation sites (T179, S621). Two serine-arginine-rich (SR-rich) domains are indicated by dotted lines. The RNA-binding domain is double-underlined.

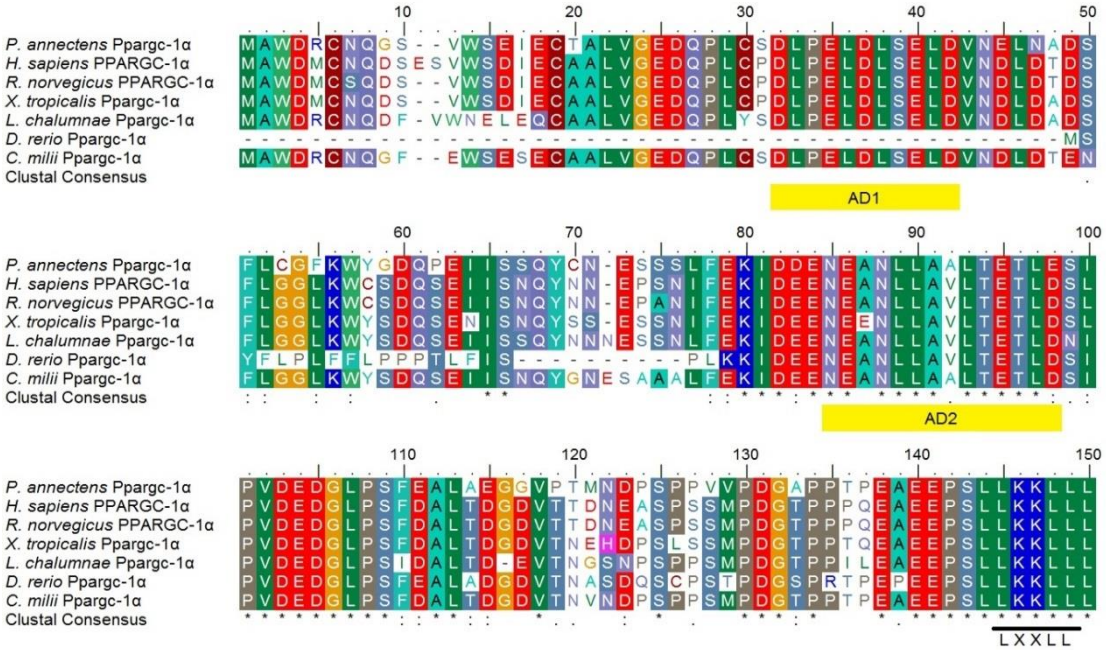

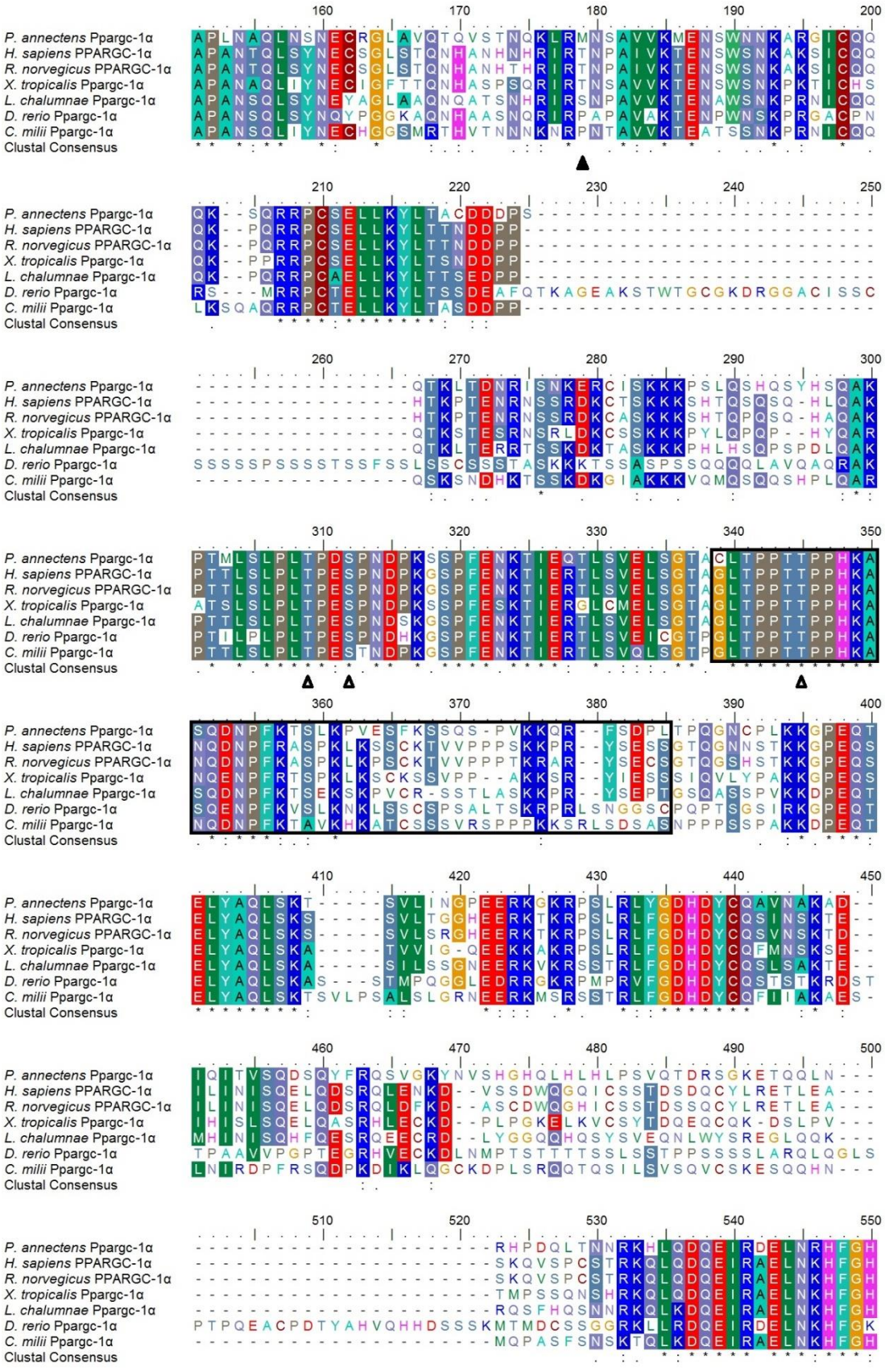
160 170 180 190 200
P. annectens Ppargc-1α
H. sapiens PPARGC-1α
R. norvegicus PPARGC-1α
X. tropicalis Ppargc-1α
L. chalumnae Ppargc-1α
D. rerio Ppargc-1α
C. milii Ppargc-1α
Clustal Consensus
210 220 230 240 250
260 270 280 290 300
310 320 330 340 350
360 370 380 390 400
410 420 430 440 450
460 470 480 490 500
510 520 530 540 550

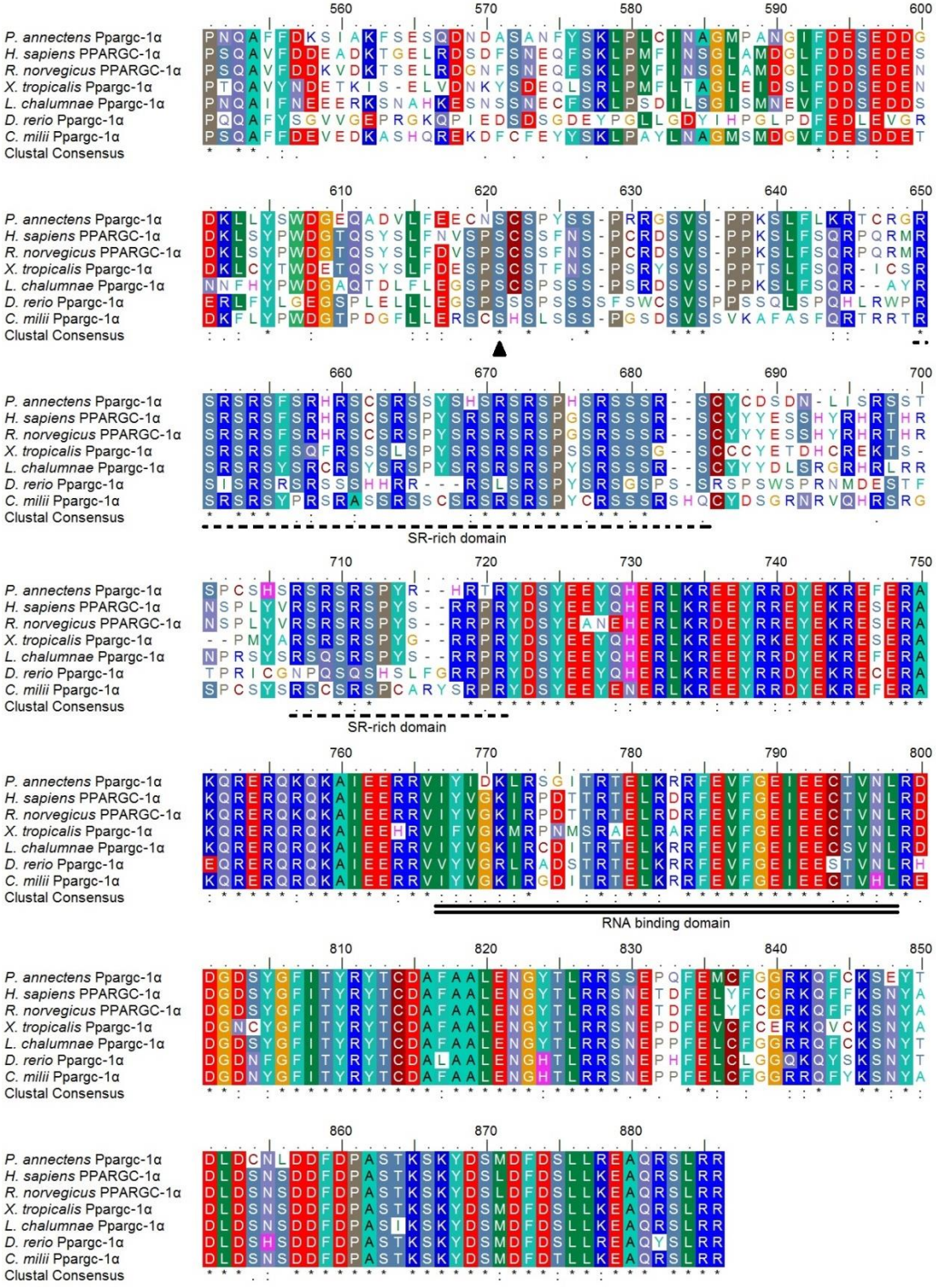
P. annectens Ppargc-1α
H. sapiens PPARGC-1α
R. norvegicus PPARGC-1α
X. tropicalis Ppargc-1α
L. chalumnae Ppargc-1α
D. rerio Ppargc-1α
C. milii Ppargc-1α
Clustal Consensus
SR-rich domain
SR-rich domain
RNA binding domain

Fig. 2. A dendrogram of peroxisome proliferator-activated receptor gamma, coactivator 1 alpha (PPARGC-1α/Ppargc-1α) including that of *Protopterus annectens*. Numbers presented at each branch point represent bootstrap percentages from 1000 replicates. Ppargc-1α from *Hydra vulgaris* is used as the outgroup for the dendrogram.

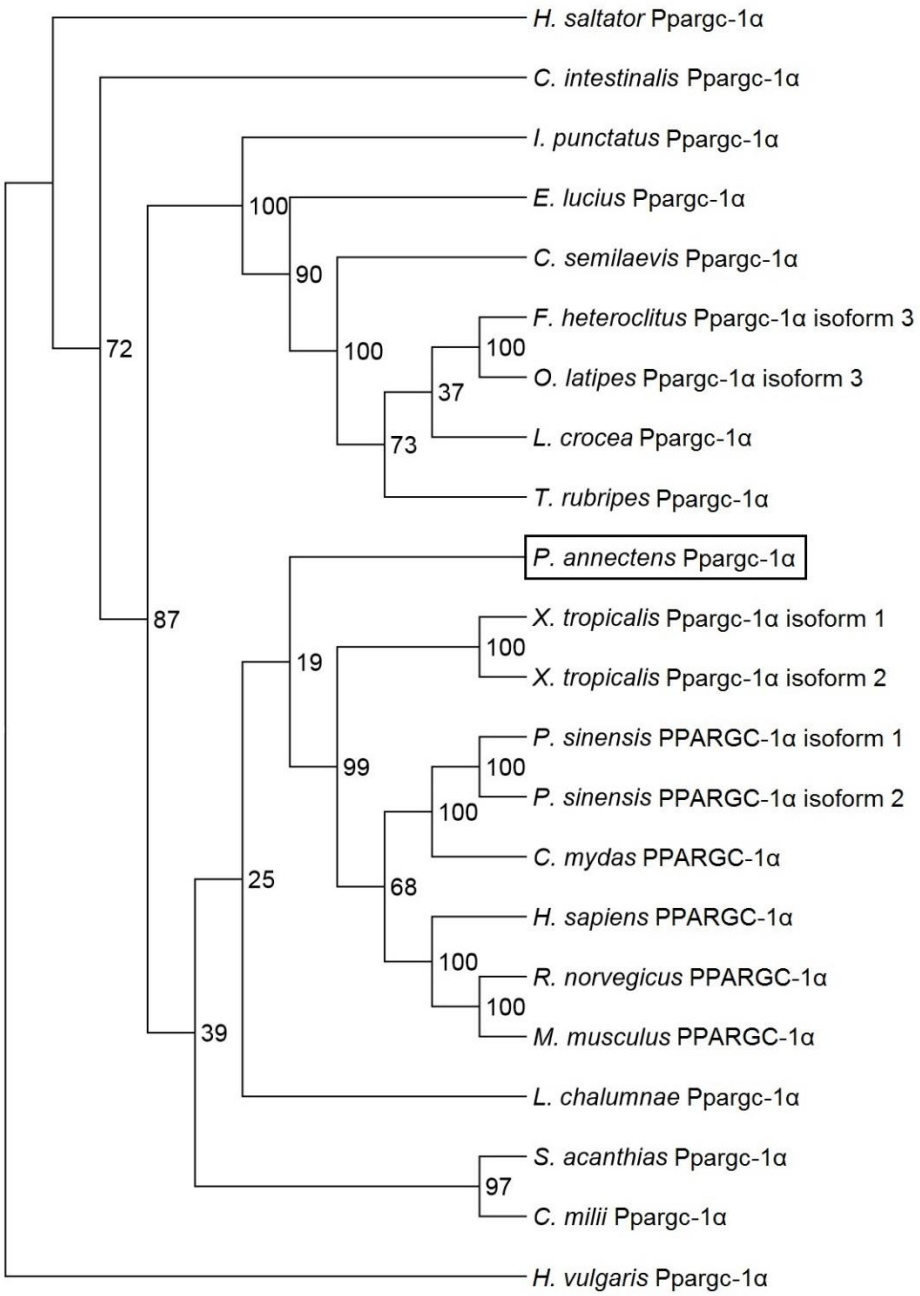

Fig. 3. The gene expression of *peroxisome proliferator-activated receptor gamma, coactivator 1 alpha* (*ppargc-1α*) in various tissues/organs of *Protopterus annectens*. Expression of *ppargc-1α* were examined in the muscle (M), heart (H), brain (B), eye (E), gills (Gi), kidney (K), Lung (Lu), skin (Sk), liver (Li), spleen (Sp), pancreas (P), and gut (Gu) of *Protopterus annectens* (*N*=1) kept in fresh water.

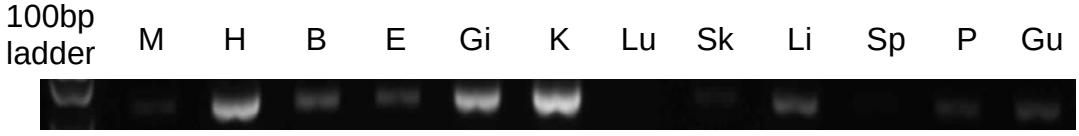

Fig. 4. mRNA expression levels of *peroxisome proliferator-activated receptor-γ coactivator-1α* (*ppargc-1α*) in the muscle of *Protopterus annectens*. Absolute quantification (×10^2 copies of transcript per ng total RNA) of *ppargc-1α* transcripts in the muscle of *P. annectens* kept in (a) fresh water on day 0 (FW; control), after 3 or 6 days (d; the induction phase), or 12 d or 6 months (mon; the maintenance phase) of aestivation; (b) fresh water on day 0 (FW; control), after 6 mon (the maintenance phase) of aestivation, or after 1 d, 3 d or 6 d of arousal (Ar; the arousal phase) from 6 mon of aestivation. Results represent means ± S. E. M (*N*=4). Means not sharing the same letter are significantly different (*P*<0.05).

(a)

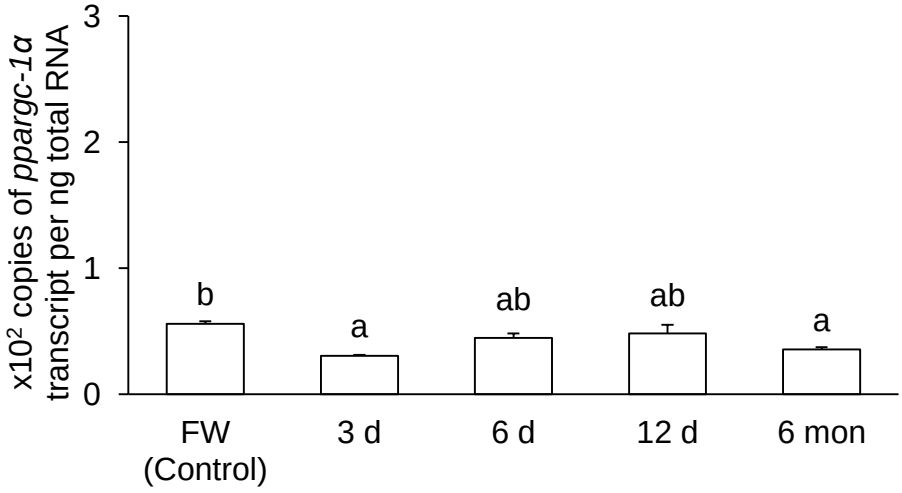

(b)

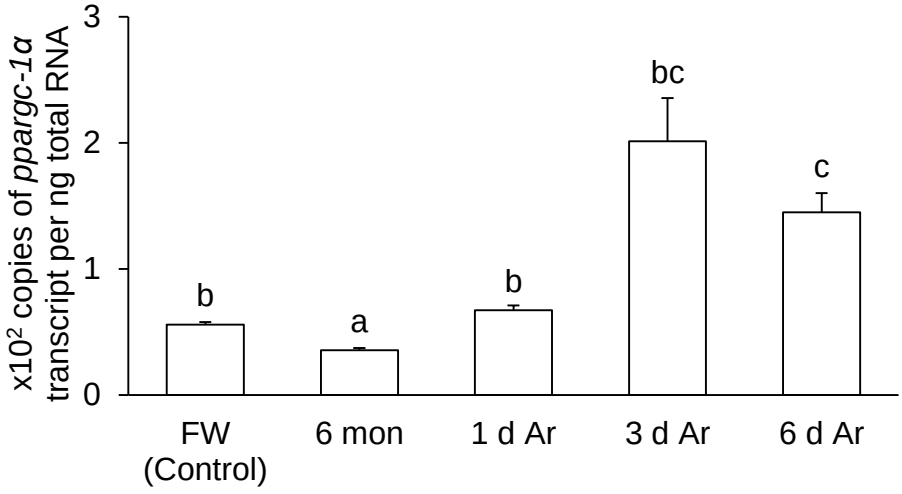

Fig. 5. Protein abundance of Peroxisome proliferator-activated receptor gamma, coactivator 1 alpha (Ppargc-1α) in the muscle of *Protopterus annectens*. Protein abundance of Ppargc-1α in the muscle of *P. annectens* kept in fresh water on day 0 (FW; control), after 6 days (d; induction phase) or 6 months (mon; maintenance phase) of aestivation in air, or after 1 d or 3 d of arousal (Ar; arousal phase) from 6 mon of aestivation in air. (a) An example of immunoblot of Ppargc-1α. (b) The protein abundance of Ppargc-1α expressed as arbitrary densitometric units per 100 μg protein. Results represent mean ± S.E.M. (*N*=3). Means not sharing the same letter are significantly different (*P*<0.05).

(a)

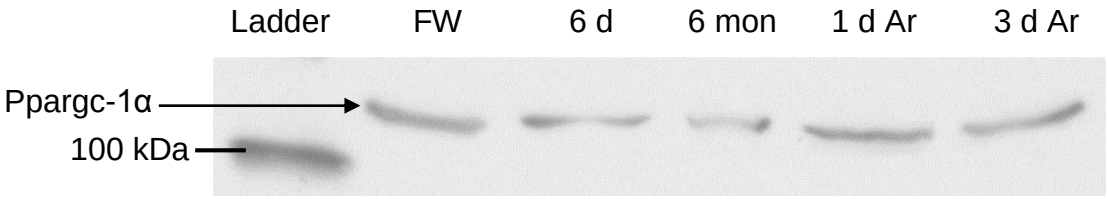

(b)

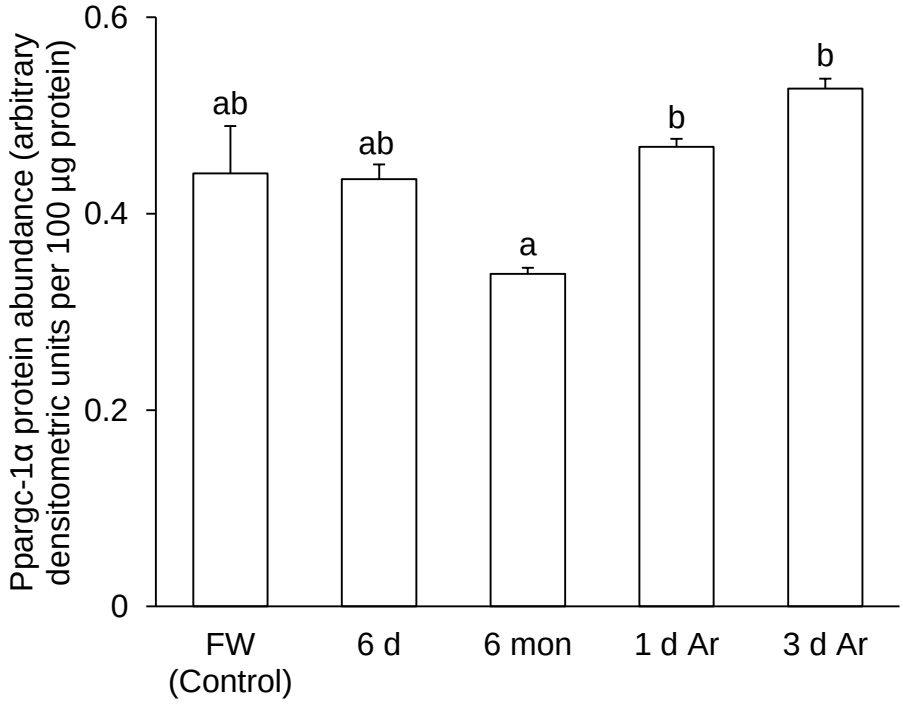

4.1.2. *myod1* and *myog*/Myod1 and Myog

4.1.2.1. Nucleotide sequence, translated amino acid sequence and dendrogramic analysis

The complete coding sequence of *myod1* from *P. annectens* consisted of 831 bp. The putative Myog sequence comprised 277 amino acids with an estimated molecular mass of 31.1 kDa (Appendix 2b), and shared the highest amino acid sequence identity with Myod1 of *L. chalumnae* (84.8%), followed by amphibian Myod1 (67.6–75.7%), teleost Myod1 (44.0–75.3%), Myod1 of *C. milii* (74.1%) and mammalian MYOD1 (59.6–61.3%; Table 7). An alignment of Myod1 from *P. annectens* with MYOD1/Myod1 of human, mouse, frog, zebrafish and shark revealed a high conservation of the bHLH domain (Fig. 6). The basic region of the bHLH domain was conserved in all 6 species. The LXXLL motif was found to be conserved in the Myod1 of *P. annectens*. The myogenic recognition motif (MRM), which contains two adjacent amino acids, alanine and threonine, was highly conserved in all species compared.

The complete coding sequence of *myog* from *P. annectens* consisted of 711 bp. The deduced Myog sequence comprised 237 amino acids with an estimated molecular mass of 26.8 kDa (Appendix 2c), and shared the highest amino acid sequence identity with Myog of *L. chalumnae* (67.9%), followed by MYOG of *P. sinensis* (67%), amphibian Myog (65.8–66.2%), mammalian MYOG (59.9–60.3%), teleost Myog (51.9–58.6%) and Myog of *H. signifer* (46.6%; Table 8). An alignment of *P. annectens* Myog with those of human, frog, coelacanth, zebrafish and stingray showed high conservation in the basic helix-loop-helix (bHLH), alanine-threonine

dipeptide, histidine/cysteine-rich and C-terminal helix III domains (Fig. 7). This suggested that Myog of *P. annectens* possessed similar myogenic regulatory functions as human MYOG.

The Myod1 of *P. annectens* was grouped in a clade together with MYOD1 of tetrapods, Myod1 of *L. chalumnae* and the cartilaginous fish *C. milii*, separated from Myod1 of teleosts (Fig. 8). The Myog of *P. annectens* was grouped in a clade together with MYOG of amphibians and Myog of *L. chalumnae*, separated from MYOG of mammals and *P. sinensis*, and Myog of teleosts and *H. signifer* (Fig. 8).

4.1.2.2. Gene expression of *myod1* in various tissues/organs

The expression of *myod1* was the highest in the skeletal muscle of *P. annectens* kept in fresh water; it was weakly detected in the eye and skin, but undetectable in the gills, heart, brain, kidney, lung, liver, spleen, pancreas and gut (Fig. 9a). Similarly, the skeletal muscle of *P. annectens* kept in fresh water had the highest *myog* expression level, and *myog* expression was weak in the eye but undetectable in other organs (Fig. 9b).

4.1.2.3. mRNA expression of *myod1* and *myog*

There was a significant increase in the mRNA expression level of *myod1* in the muscle of *P. annectens* after 3 days of aestivation (2.02-fold; $P<0.05$), as compared to the control (Fig. 10a). However, there was a significant decrease in the mRNA expression level of *myod1* in the muscle of *P. annectens* after 12 days of aestivation (by 59%; $P<0.05$). The mRNA expression of *myod1* remained unchanged in the muscle of *P. annectens* during the arousal phase (Fig. 10b).

There were significant increases in the mRNA expression level of *myog* in the muscle of *P. annectens* after 3 days (1.55-fold; $P<0.05$) or 6 days (1.45-fold; $P<0.05$) or after 6 months of aestivation (1.61-fold; $P<0.05$), as compared to the control (Fig. 11a). Likewise, there was a significant increase in the mRNA expression level of *myog* in the muscle of *P. annectens* after 6 days of arousal from 6 months of aestivation (2.51-fold; $P<0.05$), as compared to the freshwater control (Fig. 11b).

4.1.2.4. Protein abundance of Myod1 and Myog

A significant increase in the protein abundance of Myod1 in the muscle of *P. annectens* occurred after 6 months of aestivation (1.58-fold; $P<0.05$), as compared to the control (Fig. 12). In contrast, there were no significant changes in the protein abundance of Myog in the muscle of *P. annectens* after 6 days or 6 months of aestivation, or after 1 day or 3 days of arousal from 6 months of aestivation (Fig. 13).

Table 7. The percentage similarity between the deduced amino acid sequence of myogenic differentiation 1 (Myod1) from the muscle of *Protopterus annectens* and MYOD1/Myod1 sequences from other animal species obtained from GenBank (accession numbers in brackets). Sequences are arranged in a descending order of similarity.

Classification	Species	Similarity
Coelacanth	*Latimeria chalumnae* Myod1 (XP_005990556.1)	84.8%
Amphibians	*Xenopus laevis* Myod1A (NP_001079366.1)	75.7%
	Xenopus (Silurana) tropicalis Myod1 (NP_988972.1)	75.7%
	Xenopus laevis Myod1B (NP_001081292.1)	67.6%
Teleosts	*Danio rerio* Myod1 (AAI14262.1)	75.3%
	Cyprinus carpio Myod1 (BAA33565.1)	75.3%
	Megalobrama amblycephala Myod1 (AHW49178.1)	74.6%
	Salmo salar Myod1 (CAD89607.1)	70.1%
	Oncorhynchus mykiss Myod1 (Q91205.1)	70.1%
	Salmo salar Myod2 (NP_001117026.1)	69.1%
	Takifugu rubripes Myod1 (BAE79389.1)	57.3%
	Hippoglossus hippoglossus Myod1 (CAF34063.1)	44.0%
Elasmobranch	*Callorhinchus milii* Myod1 (XP_007885677.1)	74.1%
Mammals	*Mus musculus* MYOD1 (AAI03620.1)	61.3%
	Rattus norvegicus MYOD1 (AAI27481.1)	61.3%
	Homo sapiens MYOD1 (AAH64493.1)	59.6%

Fig. 6. Molecular characterization of myogenic differentiation 1 (Myod1) from the muscle of *Protopterus annectens*. Multiple amino acid alignment of Myod1 from the muscle of *P. annectens* with five other known MYOD1/Myod1 from *Homo sapiens* (AAH64493.1), *Mus musculus* (AAI03620.1), *Xenopus* (*Silurana*) *tropicalis* (NP_988972.1), *Danio rerio* (AAI14262.1) and *Callorhinchus milii* (XP_007885677.1). Identical amino acids are indicated by shaded residues. The open box indicates the basic helix-loop-helix domain, and the basic region (DRRKAATMRERRR) is underlined. The LXXLL motif is denoted with a dash line. The arrows indicate the myogenic recognition motif.

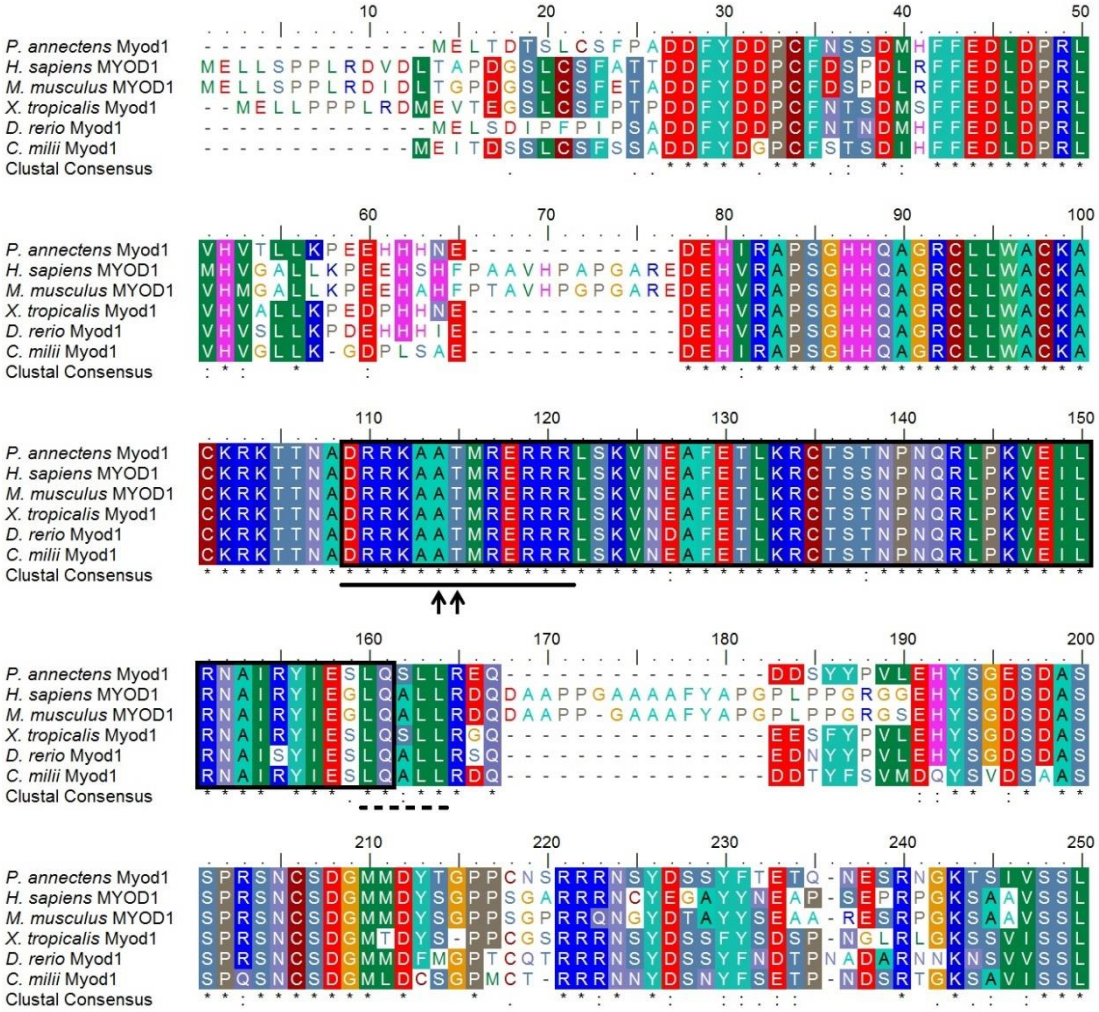

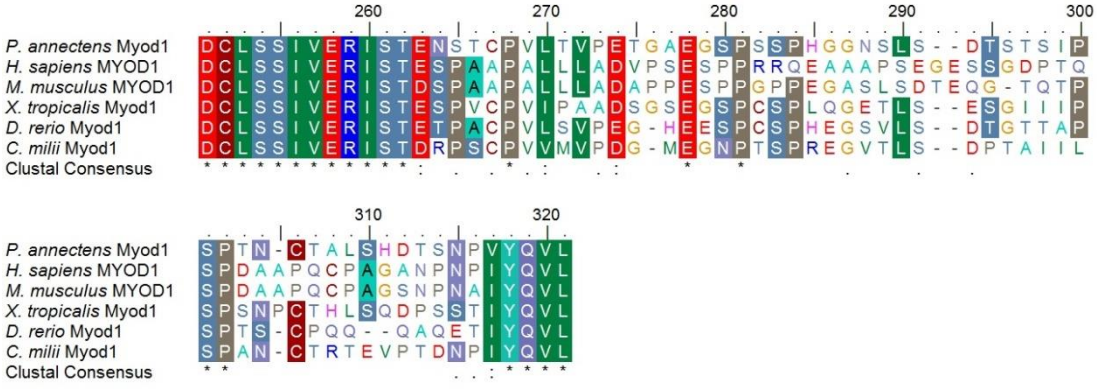
260
270
280
290
300
P. annectens Myod1
H. sapiens MYOD1
M. musculus MYOD1
X. tropicalis Myod1
D. rerio Myod1
C. milii Myod1
Clustal Consensus
310
320
P. annectens Myod1
H. sapiens MYOD1
M. musculus MYOD1
X. tropicalis Myod1
D. rerio Myod1
C. milii Myod1
Clustal Consensus

Table 8. The percentage similarity between the deduced amino acid sequence of myogenin (Myog) from the muscle of *Protopterus annectens* and MYOG/Myog sequences from other animal species obtained from GenBank (accession numbers in brackets). Sequences are arranged in a descending order of similarity.

Classification	Species	Similarity
Coelacanth	*Latimeria chalumnae* Myog (XP_005987662.1)	67.9%
Reptile	*Pelodiscus sinensis* MYOG (BAJ53267.1)	67.0%
Amphibians	*Xenopus laevis* Myog (NP_001079326.1)	66.2%
	Xenopus (Silurana) tropicalis Myog (NP_001016725.1)	65.8%
Mammals	*Homo sapiens* MYOG (NP_002470.2)	60.3%
	Mus musculus MYOG (AAB59676.1)	59.9%
	Rattus norvegicus MYOG (NP_058811.2)	59.9%
Teleosts	*Ictalurus furcatus* Myog (AAS48404.1)	58.6%
	Ictalurus punctatus Myog (AAS48084.1)	58.6%
	Ameiurus catus Myog (AAS67040.1)	58.3%
	Sternopygus macrurus Myog (AAQ97203.1)	58.3%
	Cyprinus carpio Myog (BAA33564.1)	57.6%
	Tachysurus fulvidraco Myog (ADP24122.1)	57.5%
	Devario aequipinnatus Myog (ABB00908.1)	57.3%
	Danio rerio Myog (NP_571081.1)	56.9%
	Epinephelus coioides Myog (ADJ95349.1)	53.5%
	Oreochromis niloticus Myog (NP_001266455.1)	53.5%
	Sparus aurata Myog (ABR22022.1)	53.5%
	Oreochromis aureus Myog (ADA84044.1)	53.1%
	Hippoglossus hippoglossus Myog (CAD32316.1)	52.7%
	Paralichthys olivaceus Myog (ABO43958.1)	52.7%
	Sander lucioperca Myog (AEN02543.1)	52.7%
	Siniperca chuatsi Myog (ADX41684.1)	52.3%
	Morone saxatilis Myog (AAL66388.1)	52.2%
	Salmo salar Myog (NP_001117072.1)	52.1%
	Trachidermus fasciatus Myog (AFP28936.1)	51.9%
Elasmobranch	*Himantura signifer* Myog	46.6%

Fig. 7. Molecular characterization of myogenin (Myog) from the muscle of *Protopterus annectens*. Multiple amino acid alignment of Myog from the muscle of *P. annectens* with five other known MYOG/Myog from *Homo sapiens* (NP_002470.2), *Xenopus laevis* (NP_001079326.1), *Latimeria chalumnae* (XP_005987662.1), *Danio rerio* (NP_571081.1) and *Himantura signifer* (KX494984). Identical amino acids are indicated by shaded residues. The basic helix-loop-helix domain is indicated by an open box and the basic region is indicated by a dotted line (positions 85–100). The His/Cys-rich domain (positions 81–97) is underlined and the Helix III domain (positions 230–243) is indicated by a yellow box. The alanine-threonine dipeptide is indicated by arrows.

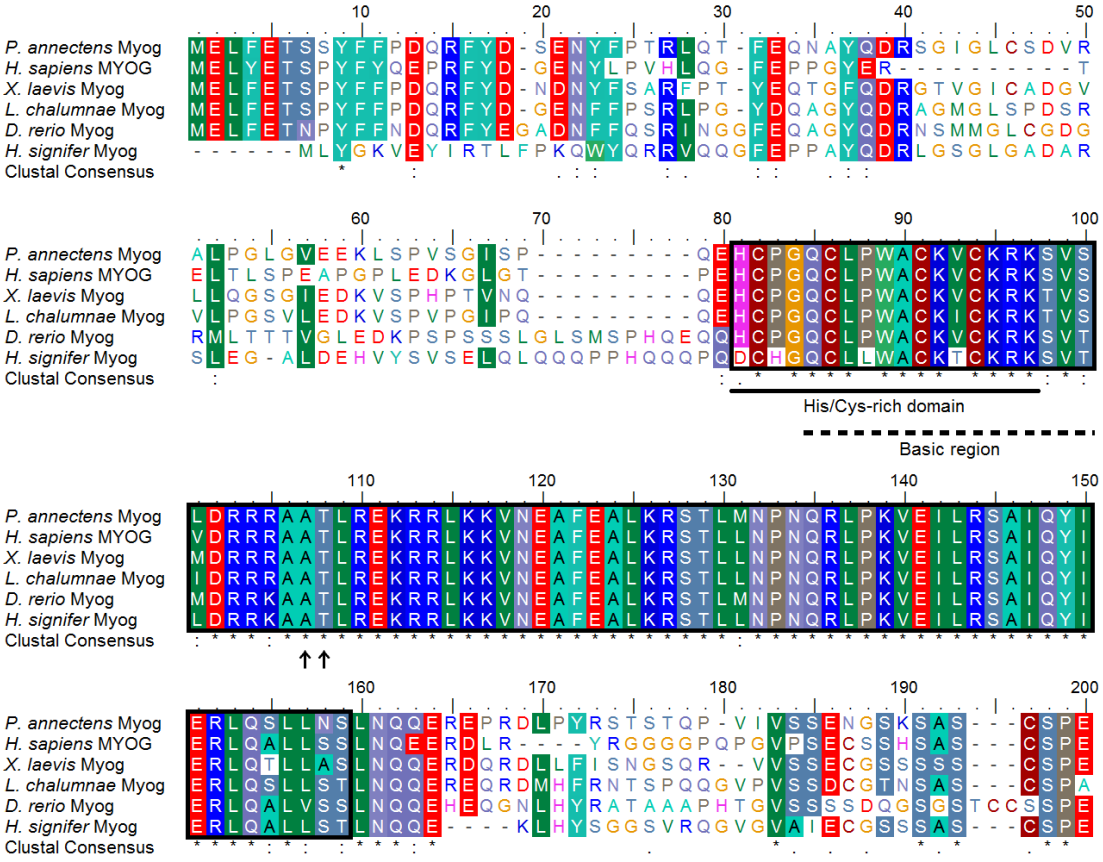

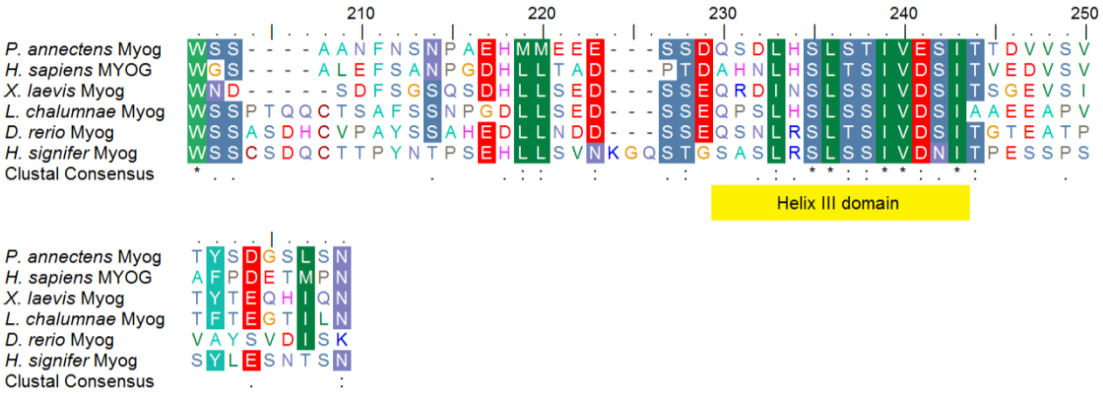
210
220
230
240
250
P. annectens Myog
H. sapiens MYOG
X. laevis Myog
L. chalumnae Myog
D. rerio Myog
H. signifer Myog
Clustal Consensus
Helix III domain

Fig. 8. A dendrogram of myogenic differentiation 1 (MYOD1/Myod1) and myogenin (MYOG/Myog) including those of *Protopterus annectens*. Numbers presented at each branch point represent bootstrap percentages from 1000 replicates. Myogenic regulatory factor (MRF) from *Phallusia mammillata* is used as the outgroup for the dendrogram. MDF: Myogenic determination factor.

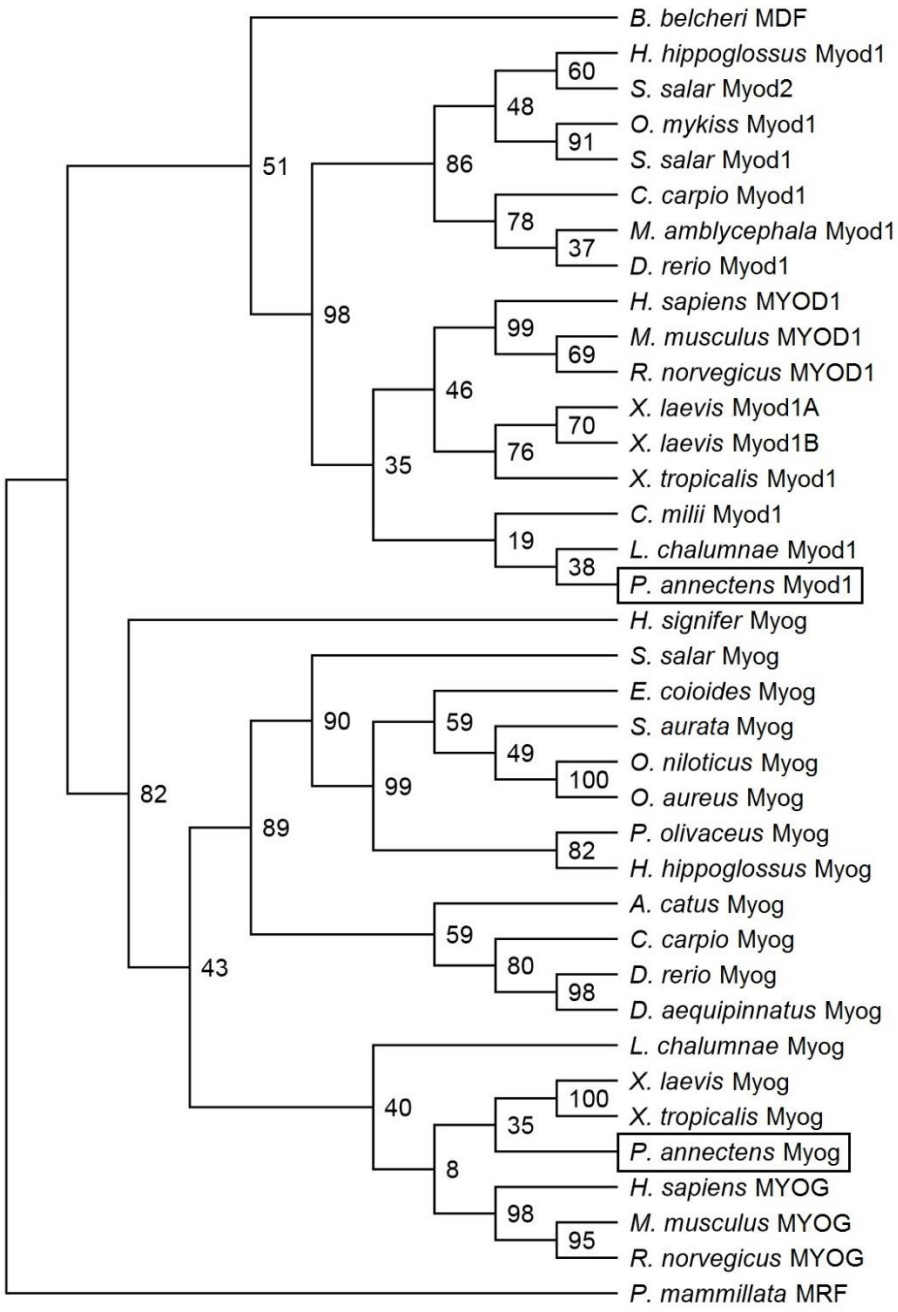

Fig. 9. The gene expression of *myogenic differentiation 1* (*myod1*) and *myogenin* (*myog*) in various tissues/organs of *Protopterus annectens*. Expression of (a) *myod1* and (b) *myog* were examined in the muscle (M), heart (H), brain (B), eye (E), gills (Gi), kidney (K), Lung (Lu), skin (Sk), liver (Li), spleen (Sp), pancreas (P), and gut (Gu) of *Protopterus annectens* (*N*=1) kept in fresh water.

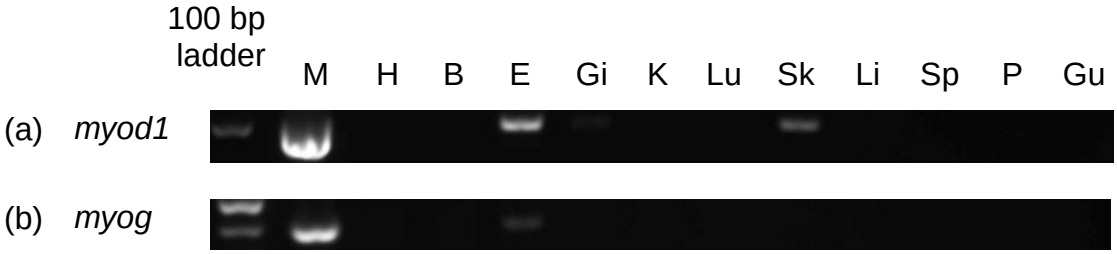

Fig. 10. mRNA expression levels of *myogenic differentiaton 1* (*myod1*) in the muscle of *Protopterus annectens*. Absolute quantification ($\times 10^3$ copies of transcript per ng total RNA) of *myod1* transcripts in the muscle of *P. annectens* kept in (a) fresh water on day 0 (FW; control), after 3 or 6 days (d; the induction phase), or 12 d or 6 months (mon; the maintenance phase) of aestivation; (b) fresh water on day 0 (FW; control), after 6 mon (the maintenance phase) of aestivation, or after 1 d, 3 d or 6 d of arousal (Ar; the arousal phase) from 6 mon of aestivation. Results represent means ± S. E. M (N=4). Means not sharing the same letter are significantly different (P<0.05).

(a)

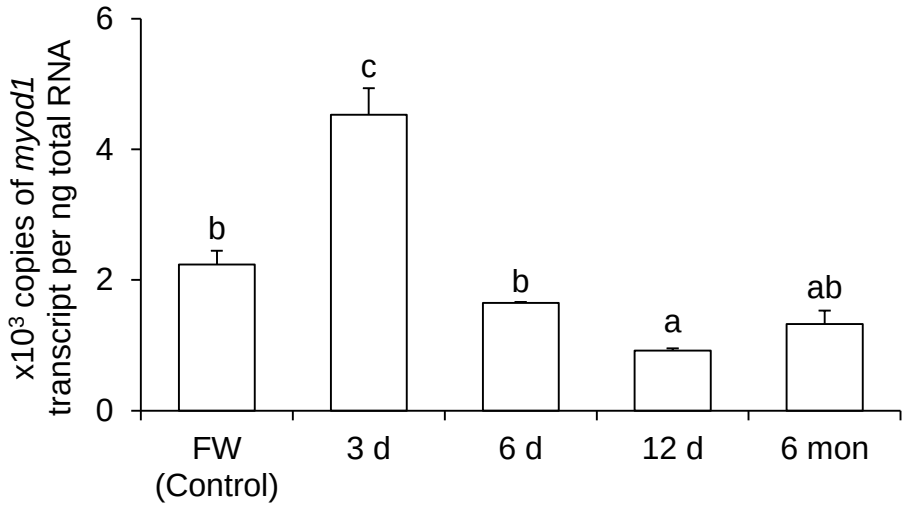

(b)

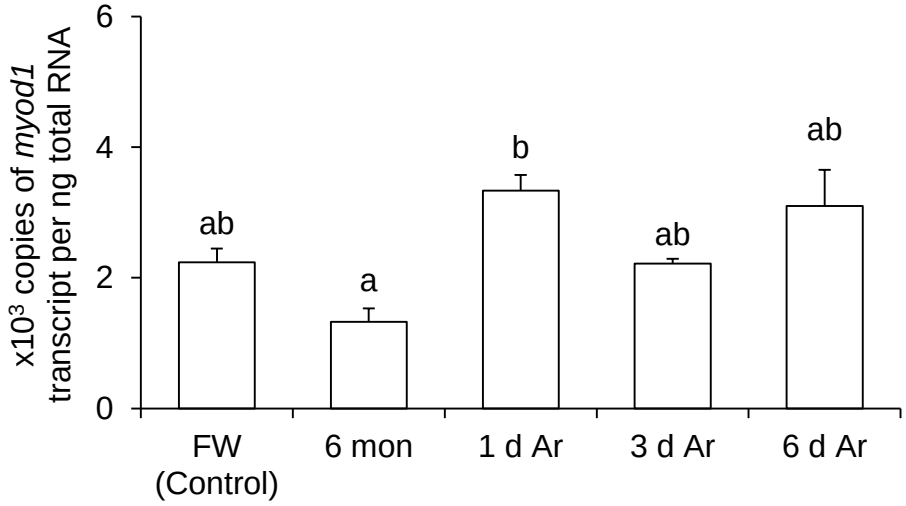

Fig. 11. mRNA expression levels of *myogenin* (*myog*) in the muscle of *Protopterus annectens*. Absolute quantification (×10^2 copies of transcript per ng total RNA) of *myog* transcripts in the muscle of *P. annectens* kept in (a) fresh water on day 0 (FW; control), after 3 or 6 days (d; the induction phase), or 12 d or 6 months (mon; the maintenance phase) of aestivation; (b) fresh water on day 0 (FW; control), after 6 mon (the maintenance phase) of aestivation, or after 1 d, 3 d or 6 d of arousal (Ar; the arousal phase) from 6 mon of aestivation. Results represent means ± S. E. M (*N*=4). Means not sharing the same letter are significantly different (*P*<0.05).

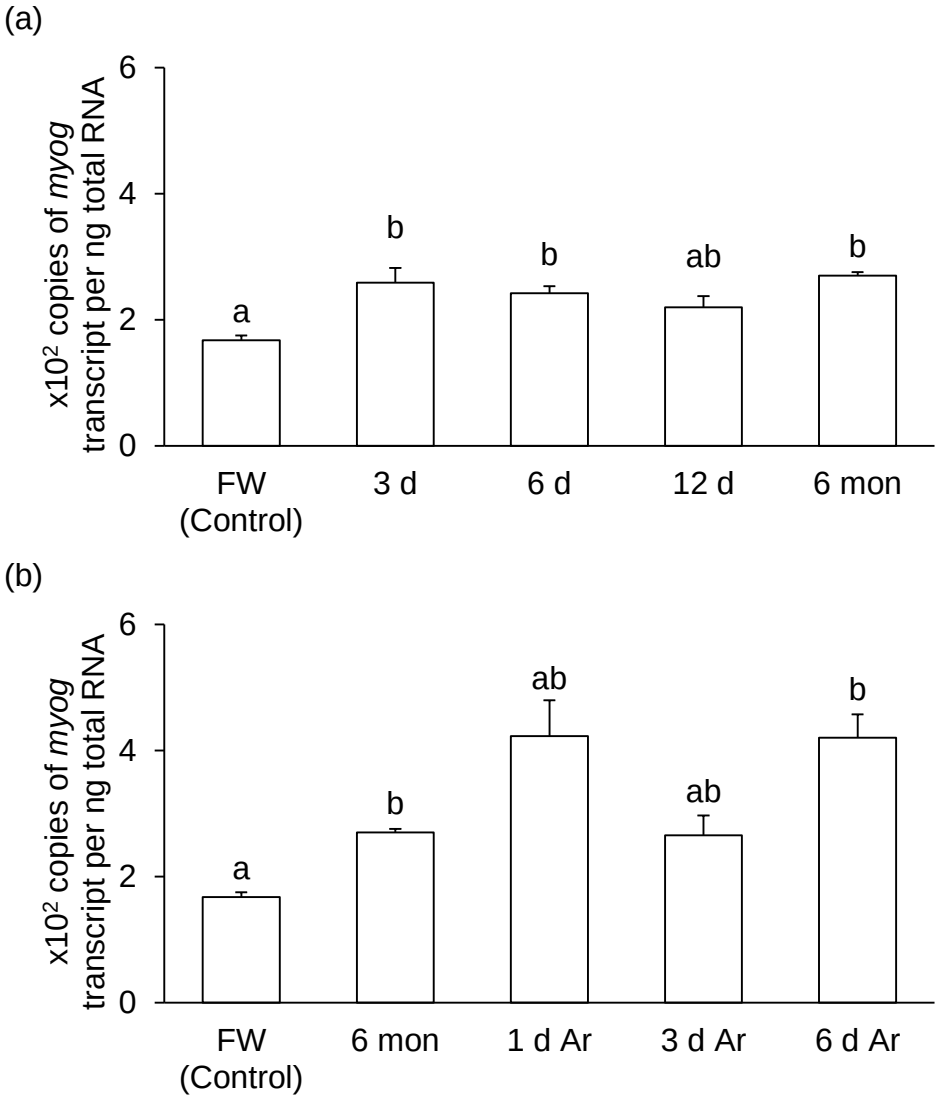

Fig. 12. Protein abundance of myogenic differentiation 1 (Myod1) in the muscle of *Protopterus annectens*. Protein abundance of Myod1 in the muscle of *P. annectens* kept in fresh water on day 0 (FW; control), after 6 days (d; induction phase) or 6 months (mon; maintenance phase) of aestivation in air, or after 1 d or 3 d of arousal (Ar; arousal phase) from 6 mon of aestivation in air. (a) An example of immunoblot of Myod1. (b) The protein abundance of Myod1 expressed as arbitrary densitometric units per 200 μg protein. Results represent mean ± S.E.M. (*N*=3). Means not sharing the same letter are significantly different ($P<0.05$).

(a)

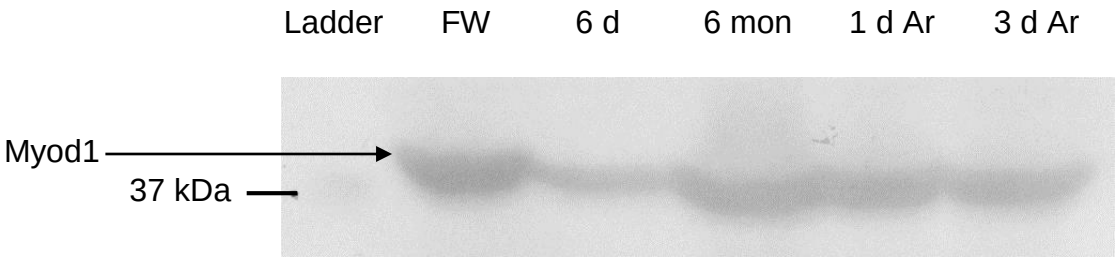

(b)

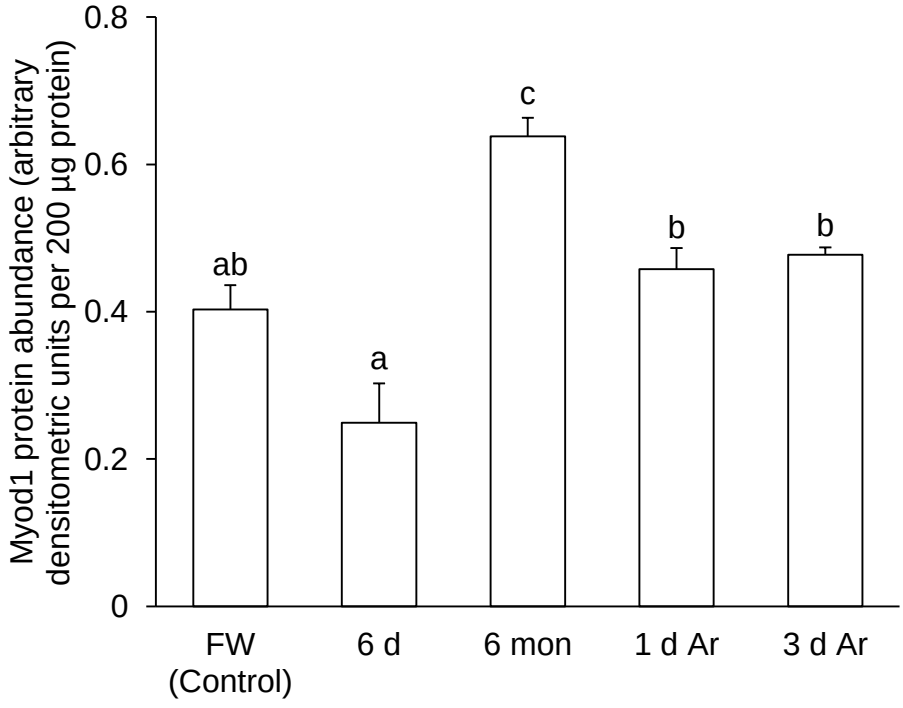

Fig. 13. Protein abundance of myogenin (Myog) in the muscle of *Protopterus annectens*. Protein abundance of Myog in the muscle of *P. annectens* kept in fresh water on day 0 (FW; control), after 6 days (d; induction phase) or 6 months (mon; maintenance phase) of aestivation in air, or after 1 d or 3 d of arousal (Ar; arousal phase) from 6 mon of aestivation in air. (a) An example of immunoblot of Myog. (b) The protein abundance of Myog expressed as arbitrary densitometric units per 20 µg protein. Results represent mean ± S.E.M. (N=3). Means not sharing the same letter are significantly different (P<0.05).

(a)

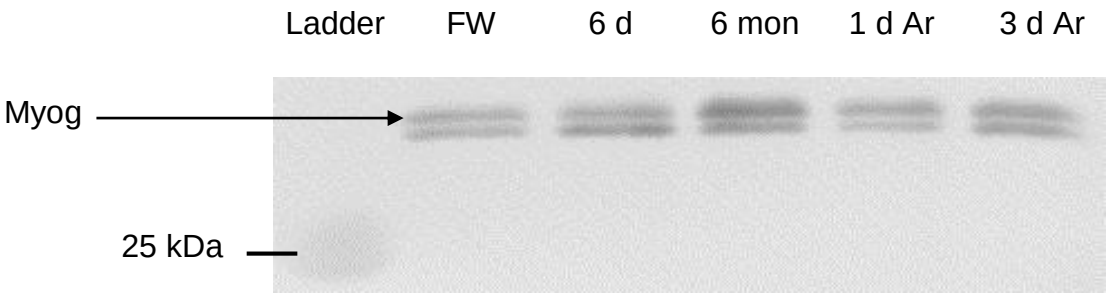

(b)

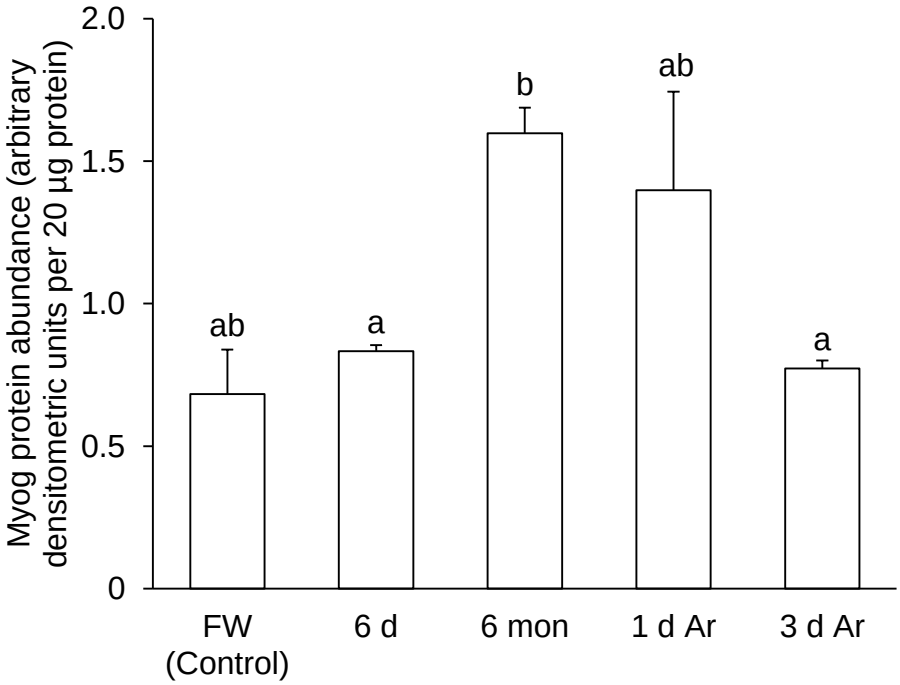

4.1.3. *mapk1* and *mapk3*/Mapk1 and Mapk3

4.1.3.1. Nucleotide sequences, translated amino acid sequences and dendrogramic analyses

The complete coding sequence of *mapk1* and *mapk3* from *P. annectens* consisted of 1092 bp and 1140 bp respectively. The deduced Mapk1 sequence comprised 364 amino acids with an estimated molecular mass of 41.9 kDa (Appendix 2d), and shared the highest amino acid sequence identity with amphibian Mapk1 (92.8–93.4%), followed by mammalian MAPK1 (92.3–92.5%), Mapk1 of *L. chalumnae* (91.5%), MAPK1 of *C. p. bellii* (91.3%), teleost Mapk1 (80.6–90.5%) and Mapk1 of *C. milii* (88.6%; Table 9). The putative Mapk3 sequence consisted of 380 amino acids and had an estimated molecular mass of 43.2 kDa (Appendix 2e). The Mapk3 of *P. annectens* shared the highest amino acid sequence identity with MAPK3 of *C. p. bellii* (91.5%), followed by mammalian MAPK3 (78.9–86.6%) and teleost Mapk3 (80.6–86.3%; Table 10).

Both Mapk1 and Mapk3 of *P. annectens* were analyzed together as they possessed similar domains. A comparison of *P. annectens* Mapk1 and Mapk3 with MAPK1/Mapk1 and MAPK3/Mapk3 from various organisms revealed a highly conserved kinase domain (Fig. 14), which consist of the signature TXY motif. This motif comprises the regulatory residues T221 and Y223 (reference in accordance to the ruler in Fig. 14). A conserved nuclear translocation signal (NTS) was found in all MAPK/Mapk compared, indicating that Mapk1 and Mapk3 of *P. annectens* could be translocated to the nucleus. In addition, the cytoplasmic retention sequence (CRS)/common docking (CD) motif reported in human MAPK1 (Rubinfeld et al.,

1999; Tanoue et al., 2000) was found to be highly conserved for all MAPK/Mapk compared.

The Mapk1 of *P. annectens* was grouped in a clade together with MAPK1 of tetrapods and Mapk1 of *L. chalumnae*, separated from Mapk1 of teleosts (Fig. 15). Likewise, the Mapk3 of *P. annectens* was grouped in a clade together with MAPK3 of tetrapods, separated from Mapk3 of teleosts (Fig. 15).

4.1.3.2. Gene expression of *mapk1* and *mapk3* in various tissues/organs

The brain of *P. annectens* kept in fresh water had the highest expression level of *mapk1* (Fig. 16a). The expression of *mapk1* was detected in the heart, eye, gills, kidney, lung, skin, liver, spleen, pancreas and gut, and barely detectable in the muscle. The brain and gills of freshwater *P. annectens* had the highest expression level of *mapk3* (Fig. 16b). The expression of *mapk3* was detected in the muscle, heart, eye, kidney, lung, skin, liver, spleen, pancreas and gut.

4.1.3.3. mRNA expression of *mapk1* and *mapk3*

There was a significant decrease in the mRNA expression level of *mapk1* in the muscle of *P. annectens* after 6 months of aestivation (by 48.8%; $P<0.05$), as compared to the freshwater control (Fig. 17a). By contrast, there was a significant increase in the mRNA expression of *mapk1* after 3 days of arousal from 6 months of aestivation (3.25-fold; $P<0.05$), as compared to the control (Fig. 17b).

There were significant decreases in the mRNA expression levels of *mapk3* in the muscle of *P. annectens* after 3 days (by 51.3%; $P<0.05$) or 6 days (by 61.6%; $P<0.05$) or 12 days (by 69.1%; $P<0.05$) or after 6 months of aestivation (by 62.7%; $P<0.05$), as compared to the control (Fig. 18a). Similarly, there were significant

decreases in the mRNA expression of *mapk3* after 1 day (by 74.1% $P<0.05$) or 3 days (by 53.7%; $P<0.05$) or 6 days of arousal from 6 months of aestivation (by 55.2%; $P<0.05$) as compared to the freshwater control (Fig. 18b).

4.1.3.4. Protein abundance of Mapk

There were no significant changes in the protein abundance of Mapk in the muscle of *P. annectens* after 6 days or 6 months of aestivation, or after 1 day or 3 days of arousal from 6 months of aestivation, as compared to the control (Fig. 19).

Table 9. The percentage similarity between the deduced amino acid sequence of mitogen-activated protein kinase 1 (Mapk1) from the muscle of *Protopterus annectens* and MAPK1/Mapk1 sequences from other animal species obtained from GenBank (accession numbers in brackets). Sequences are arranged in a descending order of similarity.

Classification	Species	Similarity
Amphibians	*Xenopus (Silurana) tropicalis* Mapk1 (NP_001017127.1)	93.4%
	Xenopus laevis Mapk1 (NP_001083548.1)	92.8%
Mammals	*Homo sapiens* MAPK1 (NP_620407.1)	92.5%
	Bos taurus MAPK1 (NP_786987.1)	92.5%
	Mus musculus MAPK1 (NP_036079.1)	92.3%
	Rattus norvegicus MAPK1 (NP_446294.1)	92.3%
Coelacanth	*Latimeria chalumnae* Mapk1 (XP_005990239.1)	91.5%
Teleosts	*Danio rerio* Mapk1 (NP_878308.2)	90.5%
	Oreochromis niloticus Mapk1 (XP_003444522.1)	90.2%
	Maylandia zebra Mapk1 (XP_004555701.1)	90.2%
	Fundulus heteroclitus Mapk1 (XP_012720765.1)	89.9%
	Poecilia formosa Mapk1 (XP_007547416.1)	89.4%
	Clupea harengus Mapk1 (XP_012671405.1)	89.4%
	Poecilia reticulata Mapk1 (XP_008417574.1)	89.4%
	Notothenia coriiceps Mapk1 (XP_010778600.1)	81.4%
	Astyanax mexicanus Mapk1 (XP_007229493.1)	80.6%
Elasmobranch	*Callorhinchus milii* Mapk1 (AFP02819.1)	88.6%
Lungfish	*P. annectens* Mapk3	83.9%

Table 10. The percentage similarity between the deduced amino acid sequence of mitogen-activated protein kinase 3 (Mapk3) from the muscle of *Protopterus annectens* and MAPK3/Mapk3 sequences from other animal species obtained from GenBank (accession numbers in brackets). Sequences are arranged in a descending order of similarity.

Classification	Species	Similarity
Reptile	*Chrysemys picta bellii* MAPK3 (XP_005290239.1)	91.5%
Mammals	*Mus musculus* MAPK3 (NP_036082.1)	86.6%
	Rattus norvegicus MAPK3 (NP_059043.1)	86.3%
	Homo sapiens MAPK3 isoform 1 (NP_002737.2)	86.0%
	Bos taurus MAPK3 (NP_001103488.1)	85.0%
	Homo sapiens MAPK3 isoform 2 (NP_001035145.1)	78.9%
Teleosts	*Scleropages formosus* Mapk3 (KKX11163.1)	86.3%
	Astyanax mexicanus Mapk3 (XP_007234538.1)	86.2%
	Danio rerio Mapk3 (NP_958915.1)	85.7%
	Clarias batrachus Mapk3 (AKC01948.1)	84.4%
	Stegastes partitus Mapk3 (XP_008303580.1)	80.8%
	Larimichthys crocea Mapk3 (KKF25582.1)	80.6%
Lungfish	*P. annectens* Mapk1	83.9%

Fig. 14. Molecular characterization of mitogen-activated protein kinase 1 (Mapk1) and Mapk3 from the muscle of *Protopterus annectens*. Multiple amino acid alignment of Mapk1 and Mapk3 from the muscle of *P. annectens* with *Homo sapiens* MAPK1 (NP_620407.1), *H. sapiens* MAPK3 isoform 1 (NP_002737.2), *Mus musculus* MAPK1 (NP_036079.1), *M. musculus* MAPK3 (NP_036082.1), *Xenopus laevis* Mapk1 (NP_001083548.1), *Latimeria chalumnae* Mapk1 (XP_005990239.1), *Danio rerio* Mapk1 (NP_878308.2), *D. rerio* Mapk3 (NP_958915.1) and *Callorhinchus milii* Mapk1 (AFP02819.1). Identical amino acids are indicated by shaded residues. The open box indicates the kinase domain. The dotted line indicates the activation loop. The conserved TXY motif is underlined, and the regulatory residues that undergo phosphorylation are denoted by open triangles. The nuclear translocation signal (NTS) is indicated by the yellow box. The cytoplasmic retention sequence/common docking motif is double-underlined.

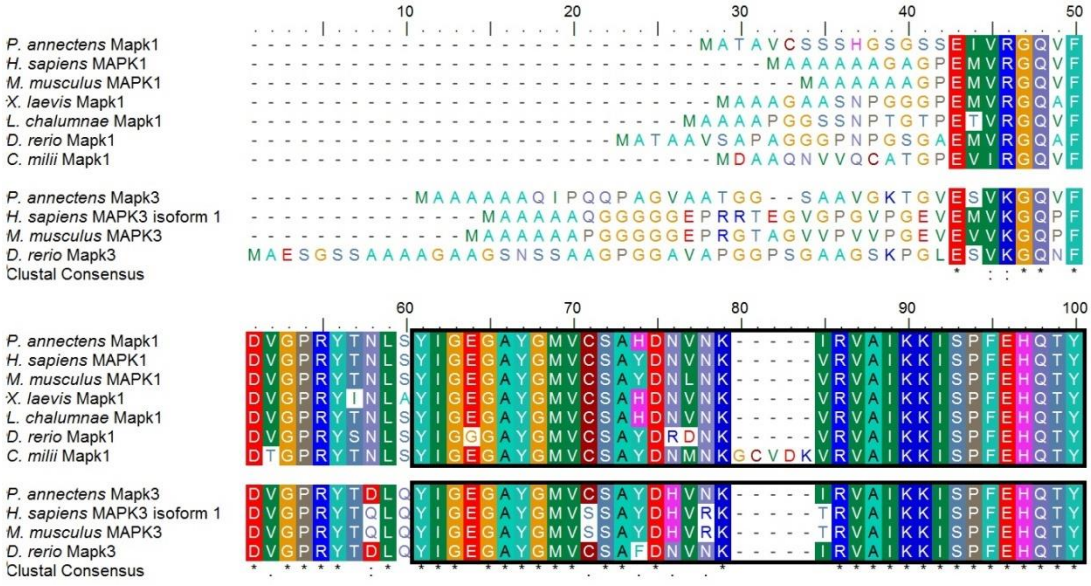

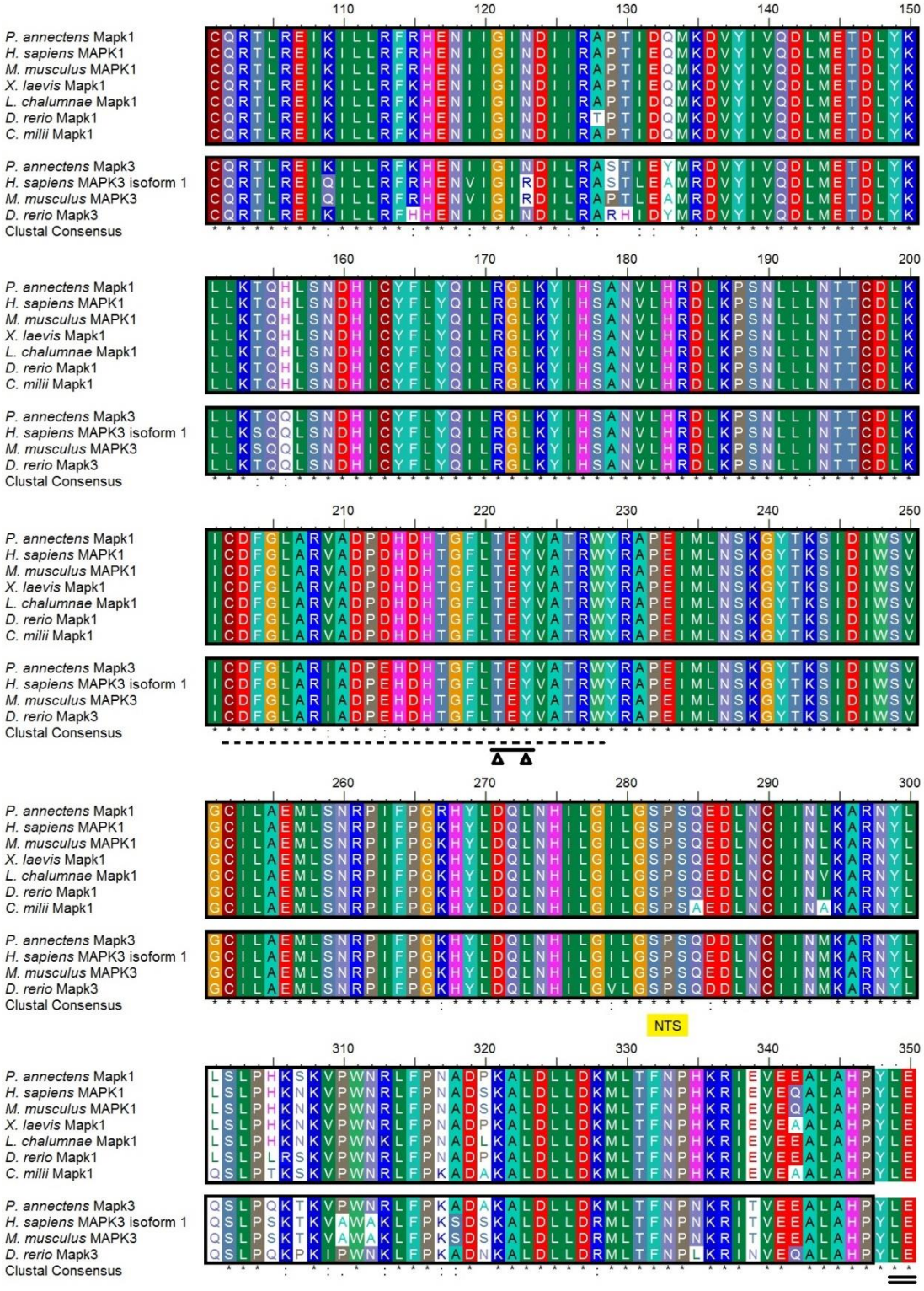
110
120
130
140
150
P. annectens Mapk1
H. sapiens MAPK1
M. musculus MAPK1
X. laevis Mapk1
L. chalumnae Mapk1
D. rerio Mapk1
C. milii Mapk1
P. annectens Mapk3
H. sapiens MAPK3 isoform 1
M. musculus MAPK3
D. rerio Mapk3
Clustal Consensus
160
170
180
190
200
P. annectens Mapk1
H. sapiens MAPK1
M. musculus MAPK1
X. laevis Mapk1
L. chalumnae Mapk1
D. rerio Mapk1
C. milii Mapk1
P. annectens Mapk3
H. sapiens MAPK3 isoform 1
M. musculus MAPK3
D. rerio Mapk3
Clustal Consensus
210
220
230
240
250
P. annectens Mapk1
H. sapiens MAPK1
M. musculus MAPK1
X. laevis Mapk1
L. chalumnae Mapk1
D. rerio Mapk1
C. milii Mapk1
P. annectens Mapk3
H. sapiens MAPK3 isoform 1
M. musculus MAPK3
D. rerio Mapk3
Clustal Consensus
260
270
280
290
300
P. annectens Mapk1
H. sapiens MAPK1
M. musculus MAPK1
X. laevis Mapk1
L. chalumnae Mapk1
D. rerio Mapk1
C. milii Mapk1
P. annectens Mapk3
H. sapiens MAPK3 isoform 1
M. musculus MAPK3
D. rerio Mapk3
Clustal Consensus
NTS
310
320
330
340
350
P. annectens Mapk1
H. sapiens MAPK1
M. musculus MAPK1
X. laevis Mapk1
L. chalumnae Mapk1
D. rerio Mapk1
C. milii Mapk1
P. annectens Mapk3
H. sapiens MAPK3 isoform 1
M. musculus MAPK3
D. rerio Mapk3
Clustal Consensus

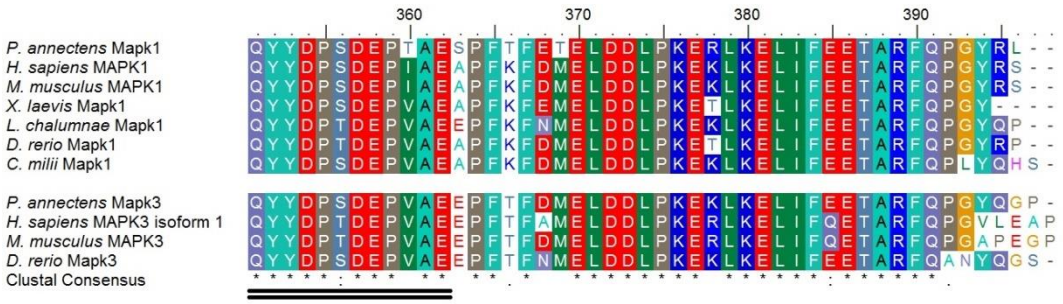
360
370
380
390
P. annectens Mapk1
H. sapiens MAPK1
M. musculus MAPK1
X. laevis Mapk1
L. chalumnae Mapk1
D. rerio Mapk1
C. milii Mapk1
P. annectens Mapk3
H. sapiens MAPK3 isoform 1
M. musculus MAPK3
D. rerio Mapk3
Clustal Consensus

Fig. 15. A dendrogram of mitogen-activated protein kinase 1 (MAPK1/Mapk1) and 3 (MAPK3/Mapk3) including those of *Protopterus annectens*. Numbers presented at each branch point represent bootstrap percentages from 1000 replicates. Mapk from *Hydra vulgaris* is used as the outgroup for the dendrogram.

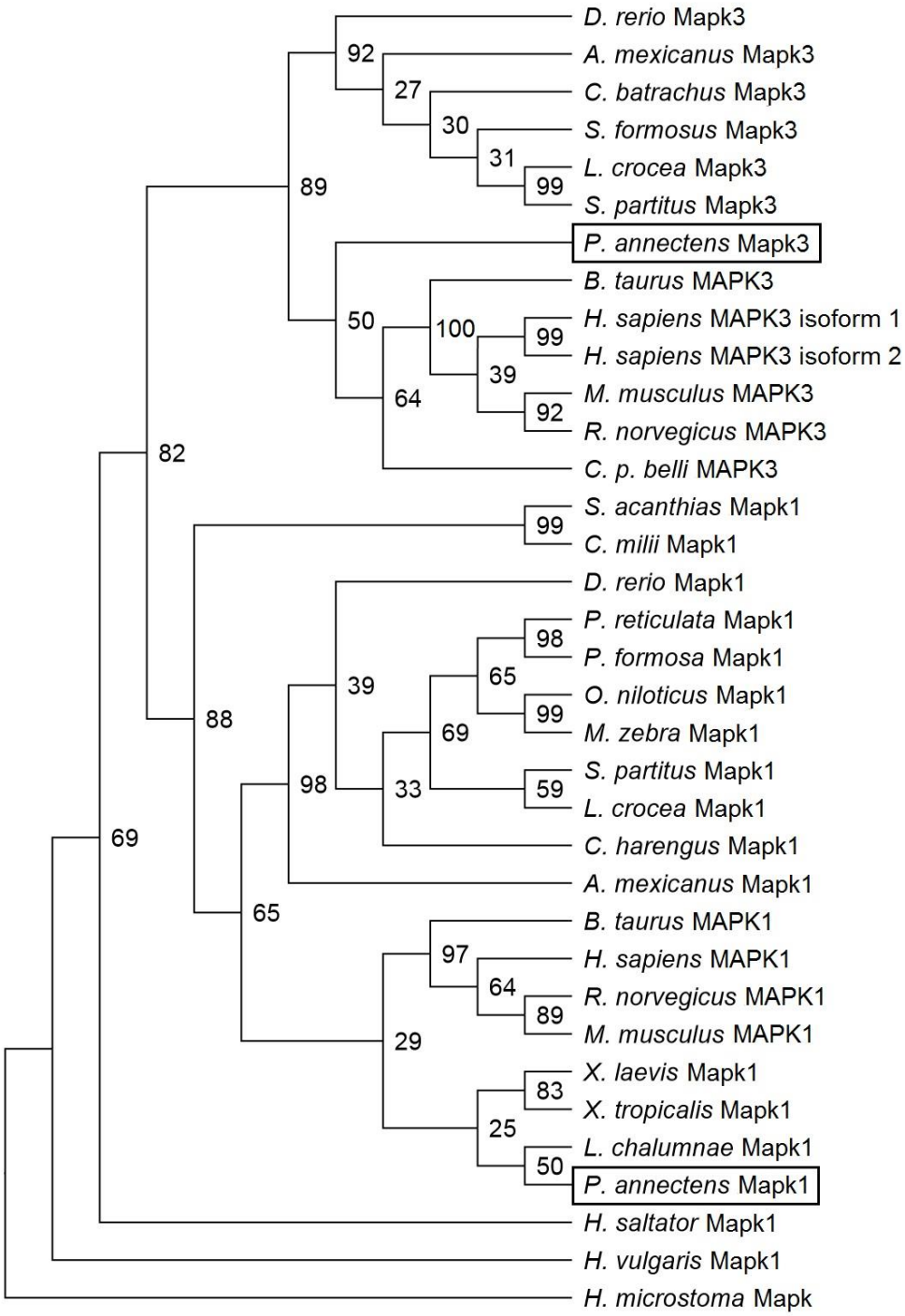

Fig. 16. The gene expression of *mitogen-activated protein kinase 1* (*mapk1*) and *mapk3* in various tissues/organs of *Protopterus annectens*. Expression of (a) *mapk1* and (b) *mapk3* were examined in the muscle (M), heart (H), brain (B), eye (E), gills (Gi), kidney (K), Lung (Lu), skin (Sk), liver (Li), spleen (Sp), pancreas (P), and gut (Gu) of *Protopterus annectens* (*N*=1) kept in fresh water.

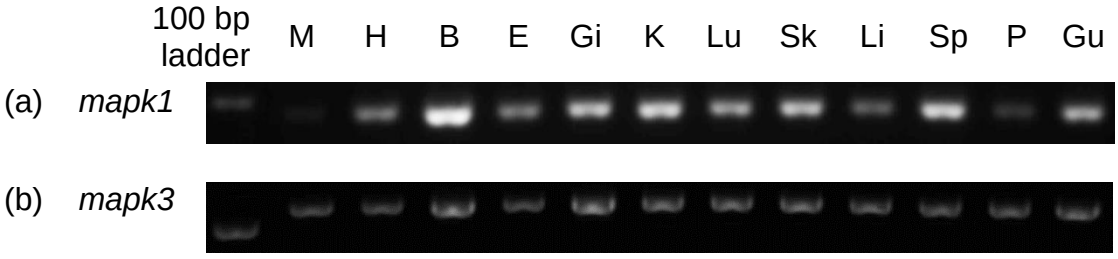

Fig. 17. mRNA expression levels of *mitogen-activated protein kinase 1* (*mapk1*) in the muscle of *Protopterus annectens*. Absolute quantification (copies of transcript per ng total RNA) of *mapk1* transcripts in the muscle of *P. annectens* kept in (a) fresh water on day 0 (FW; control), after 3 or 6 days (d; the induction phase), or 12 d or 6 months (mon; the maintenance phase) of aestivation; (b) fresh water on day 0 (FW; control), after 6 mon (the maintenance phase) of aestivation, or after 1 d, 3 d or 6 d of arousal (Ar; the arousal phase) from 6 mon of aestivation. Results represent means ± S. E. M (N=4). Means not sharing the same letter are significantly different (P<0.05).

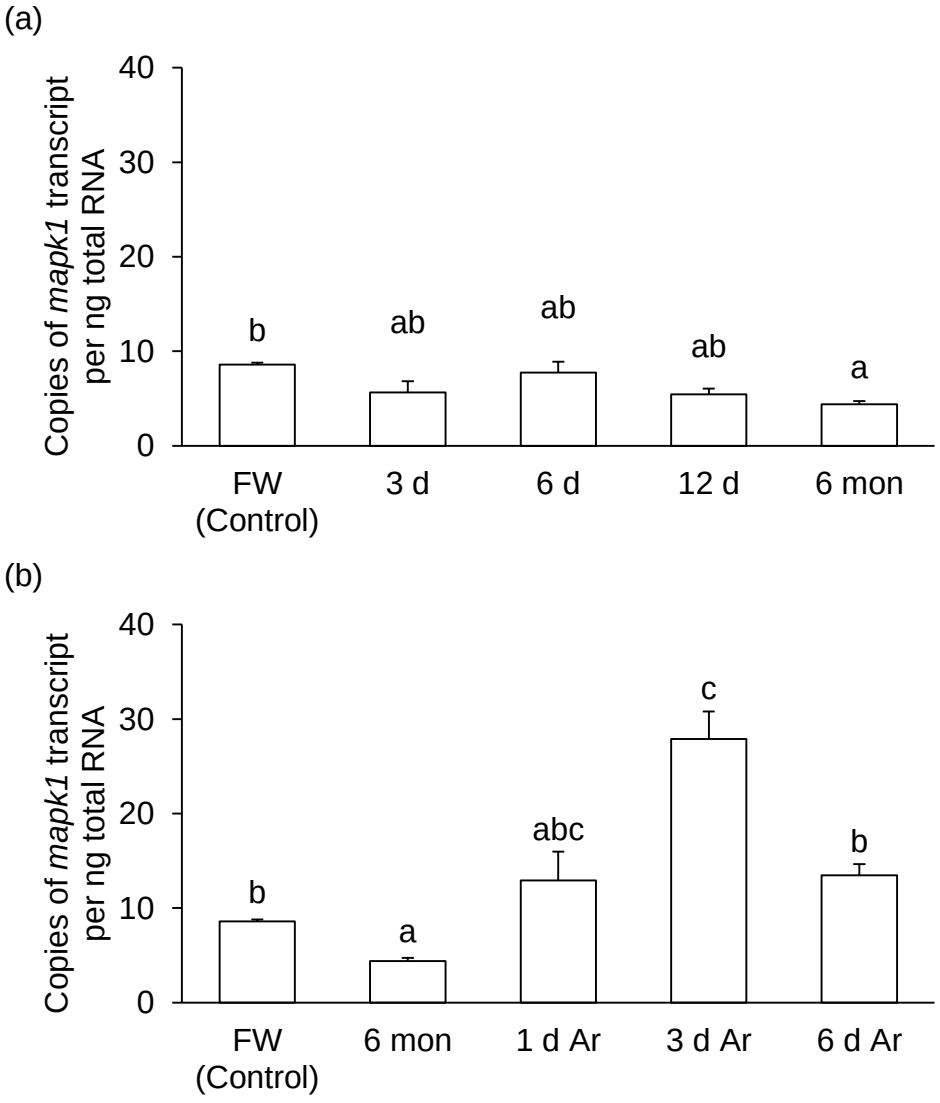

Fig. 18. mRNA expression levels of *mitogen-activated protein kinase 3* (*mapk3*) in the muscle of *Protopterus annectens*. Absolute quantification (×10^2 copies of transcript per ng total RNA) of *mapk3* transcripts in the muscle of *P. annectens* kept in (a) fresh water on day 0 (FW; control), after 3 or 6 days (d; the induction phase), or 12 d or 6 months (mon; the maintenance phase) of aestivation; (b) fresh water on day 0 (FW; control), after 6 mon (the maintenance phase) of aestivation, or after 1 d, 3 d or 6 d of arousal (Ar; the arousal phase) from 6 mon of aestivation. Results represent means ± S. E. M (*N*=4). Means not sharing the same letter are significantly different (*P*<0.05).

(a)

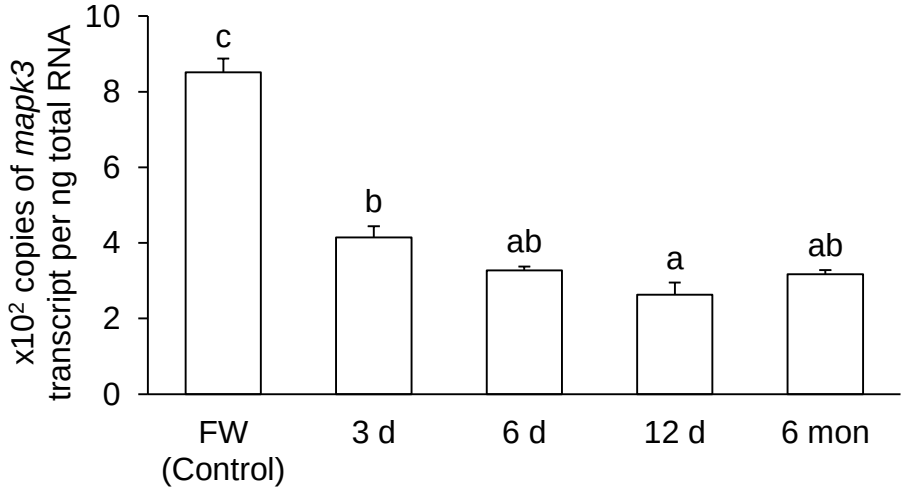

(b)

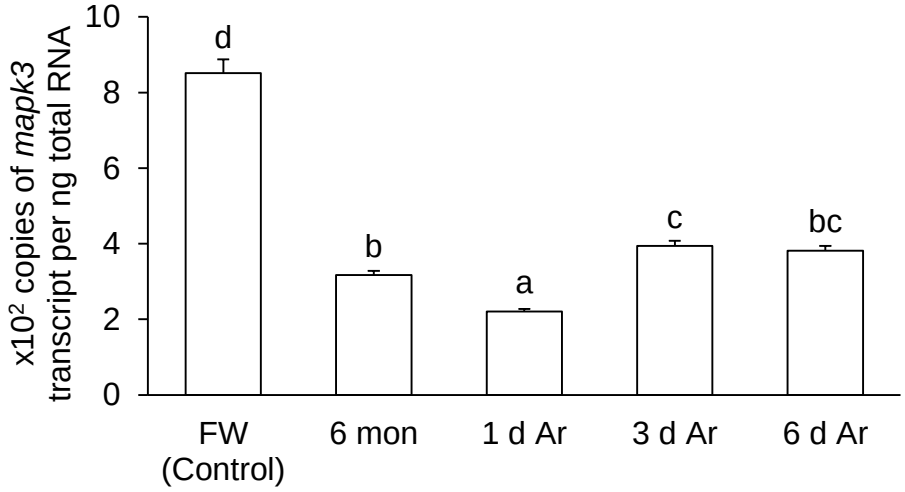

Fig. 19. Protein abundance of mitogen-activated protein kinase (Mapk) in the muscle of *Protopterus annectens*. Protein abundance of Mapk in the muscle of *P. annectens* kept in fresh water on day 0 (FW; control), after 6 days (d; induction phase) or 6 months (mon; maintenance phase) of aestivation in air, or after 1 d or 3 d of arousal (Ar; arousal phase) from 6 mon of aestivation in air. (a) An example of immunoblot of Mapk. (b) The protein abundance of Mapk is expressed as arbitrary densitometric units per 100 μg protein. Results represent mean ± S.E.M. (N=3). Means not sharing the same letter are significantly different (P<0.05).

(a)

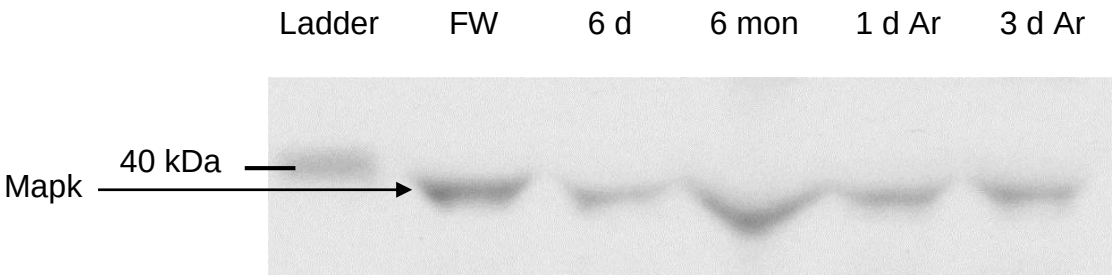

(b)

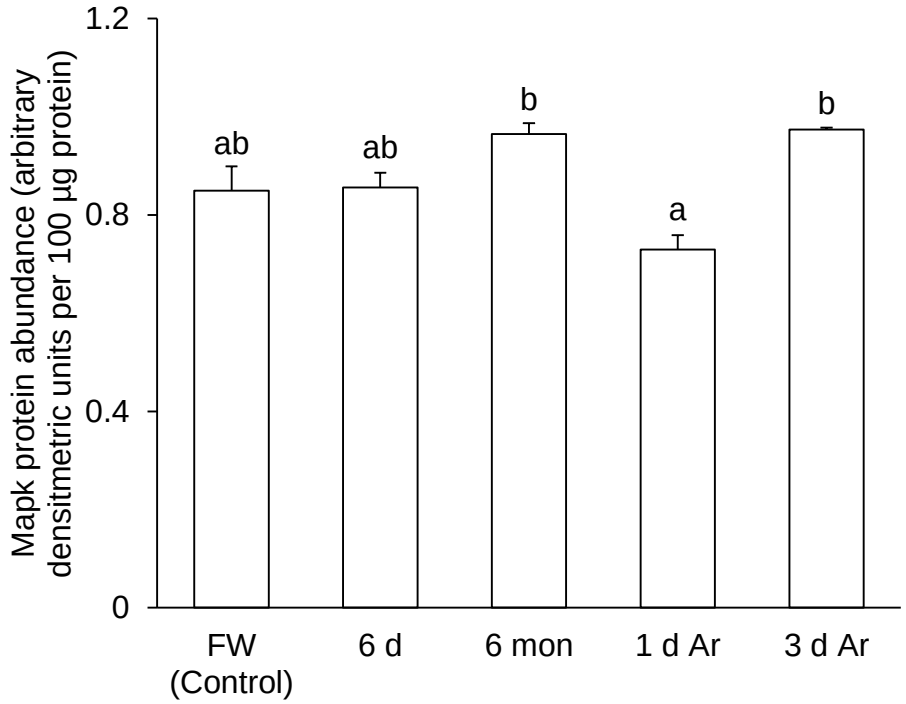

4.2. Genes/proteins involved in muscle degradation

4.2.1. *hdac1*/Hdac1

4.2.1.1. Nucleotide sequence, translated amino acid sequence and dendrogramic analysis

The complete coding sequence of *hdac1* from *P. annectens* consisted of 1488 bp. The putative Hdac1 protein sequence consisted of 496 amino acids and had an estimated molecular mass of 56.5 kDa (Appendix 2f). The Hdac1 of *P. annectens* shared the highest amino acid sequence identity with amphibian Hdac1 (88.3–89.3%), followed by teleosts Hdac1 (81.2–89.1%), mammalian HDAC1 (87.9–88.1%), and elasmobranch Hdac1 (86.8%; Table 11).

Amino acid positions reported here are in reference to the ruler as presented in Fig. 20. A comparison of *P. annectens* Hdac1 with HDAC1/Hdac1 of human, mouse, frog, zebrafish and shark demonstrated a high conservation in the HDAC association domain (HAD; position 1–52) and the active site at the N terminus (position 54–326), especially for the zinc binding sites (D177, H179, D265) and the residues that form the active site pocket (H141, H142, G150, F151, D175, D177, H179, D182, F206, D265, L272; Fig. 20). The two serine residues, S422 and S424, which were well conserved for all species compared, are phosphorylated by casein kinase 2 (CSNK2). Out of the six lysine residues (K219, K221, K433, K439, K440 and K442) which undergo acetylation in human HDAC1, all but K433 were conserved in *P. annectens*. This particular site had been substituted by arginine in *P. annectens*. A predicted nuclear localization sequence (NLS) was found in the Hdac1 of *P. annectens* and was in the same region as the known NLS for human HDAC1. Three potential NES were

also found in the Hdac1 of *P. annectens*, bearing the signature conserved leucine-rich motifs (LXXLXL and/or LXXXLXXL; Fig. 20).

The Hdac1 of *P. annectens* was grouped in a clade together with HDAC1 of tetrapods, separated from Hdac1 of teleosts (Fig. 21).

4.2.1.2. Gene expression of *hdac1* in various tissues/organs

The highest expression of *hdac1* was observed in the gills of *P. annectens* kept in fresh water (Fig. 22). Besides the gills, the expression of *hdac1* was detected in the muscle, heart, brain, eye, kidney, lung, skin, liver, spleen, pancreas and gut.

4.2.1.3. mRNA expression of *hdac1*

There were no significant changes in the mRNA expression of *hdac1* in the muscle of *P. annectens* during the induction, maintenance or arousal phases when compared to the freshwater control (Fig. 23).

4.2.1.4. Protein abundance of Hdac1

There was a significant increase in the protein abundance of Hdac1 in the muscle of *P. annectens* after 3 days of arousal from 6 months of aestivation (4.13-fold; $P<0.05$), as compared to the control (Fig. 24).

Table 11. The percentage similarity between the deduced amino acid sequence of histone deacetylase 1 (Hdac1) from the muscle of *Protopterus annectens* and HDAC1/Hdac1 sequences from other animal species obtained from GenBank (accession numbers in brackets). Sequences are arranged in a descending order of similarity.

Classification	Species	Similarity
Amphibians	*Xenopus (Silurana) tropicalis* Hdac1 (AAH90604.1)	89.3%
	Xenopus laevis Hdac1 (NP_001079396.1)	88.3%
Teleosts	*Danio rerio* Hdac1 (NP_775343.1)	89.1%
	Notothenia coriiceps Hdac1 (XP_010770908.1)	87.5%
	Cynoglossus semilaevis Hdac1 (XP_008314048.1)	87.5%
	Stegastes partitus Hdac1 (XP_008282430.1)	87.3%
	Takifugu rubripes Hdac1 (AAL89665.1)	86.7%
	Esox lucius Hdac1 isoform X1 (XP_010877522.1)	86.6%
Mammals	*Mus musculus* HDAC1 (NP_032254.1)	88.1%
	Rattus norvegicus HDAC1 (NP_001020580.1)	88.1%
	Homo sapiens HDAC1 (NP_004955.2)	87.9%
Elasmobranch	*Callorhinchus milii* Hdac1 (AFO97213.1)	86.8%

Fig. 20. Molecular characterization of histone deacetylase 1 (Hdac1) from the muscle of *Protopterus annectens*. Multiple amino acid alignment of Hdac1 from the muscle of *P. annectens* with five other known HDAC1/Hdac1 from *Homo sapiens* (NP_004955.2), *Mus musculus* (NP_032254.1), *Xenopus* (*Silurana*) *tropicalis* (AAH90604.1), *Danio rerio* (NP_775343.1) and *Callorhinchus milii* (AFO97213.1). Identical amino acids are indicated by shaded residues. The HDAC association domain is denoted with dotted lines. The open box indicates the catalytic domain. Open triangles denote the residues that form the active site pocket. Zinc binding sites are indicated by open circles. The known nuclear localization sequence (NLS) for *H. sapiens* and *M. musculus* and the predicted NLS for *P. annectens* are underlined. The yellow boxes indicate the potential nuclear export signal (NES) domains. The arrows denote the serine residues that are phosphorylated by casein kinase 2, while the lysine residues that undergo acetylation are indicated by open squares.

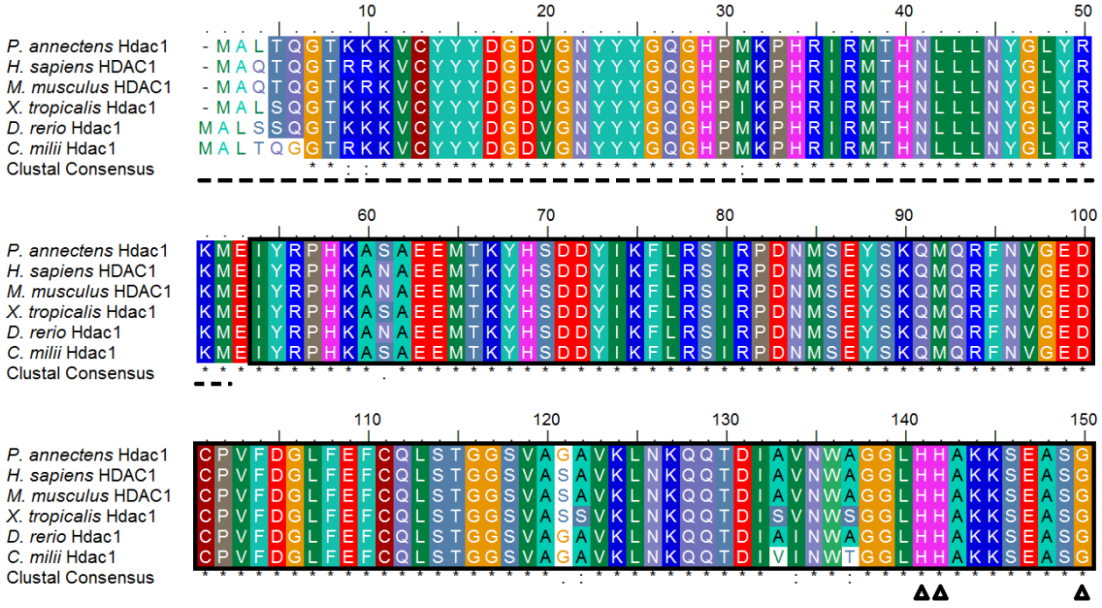

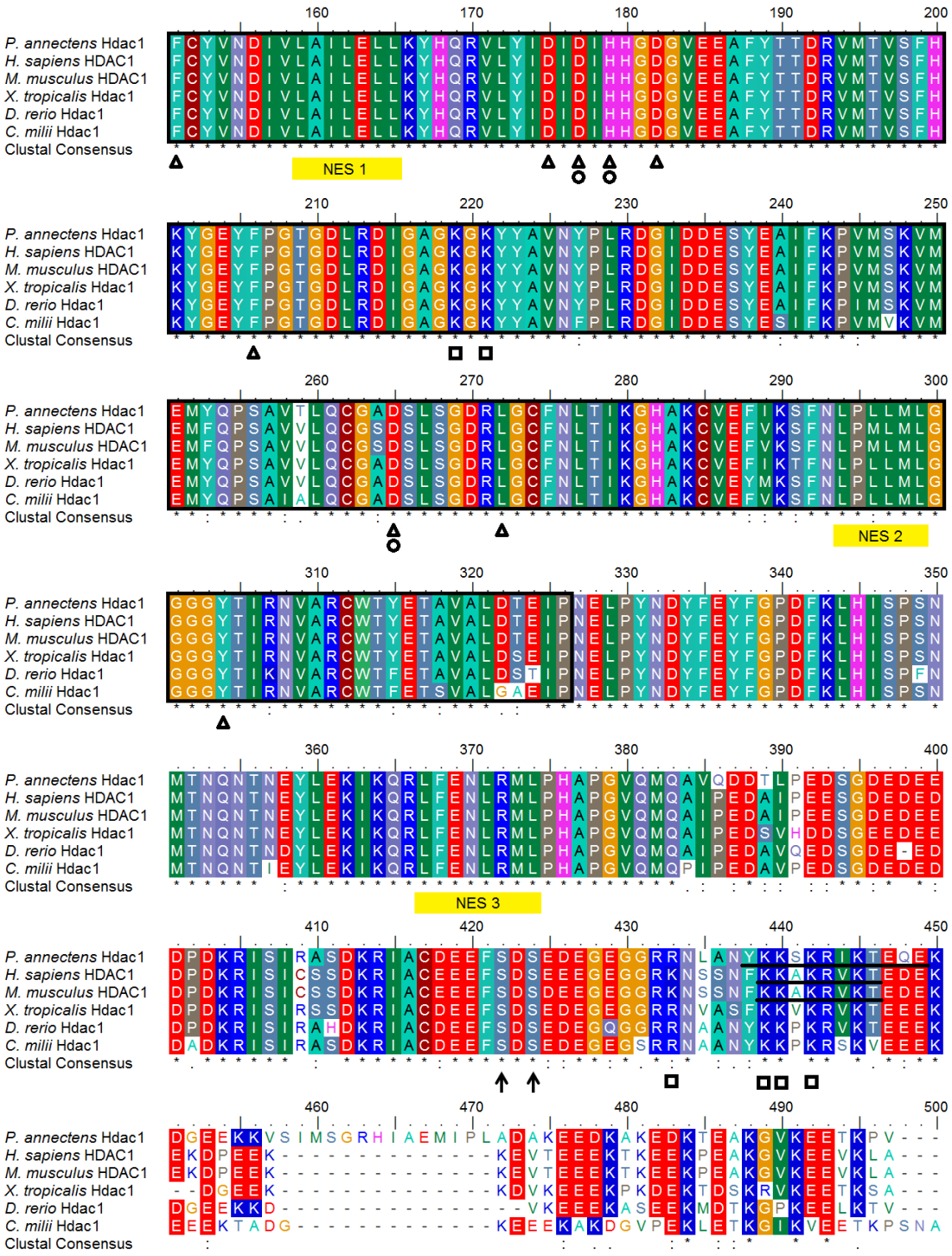
160
170
180
190
200
P. annectens Hdac1
H. sapiens HDAC1
M. musculus HDAC1
X. tropicalis Hdac1
D. rerio Hdac1
C. milii Hdac1
Clustal Consensus
NES 1
210
220
230
240
250
260
270
280
290
300
NES 2
310
320
330
340
350
360
370
380
390
400
NES 3
410
420
430
440
450
460
470
480
490
500

Fig. 21. A dendrogram of histone deacetylase 1 (HDAC1/Hdac1) including that of *Protopterus annectens*. Numbers presented at each branch point represent bootstrap percentages from 1000 replicates. Hdac1 from *Strongylocentrotus purpuratus* is used as the outgroup for the dendrogram.

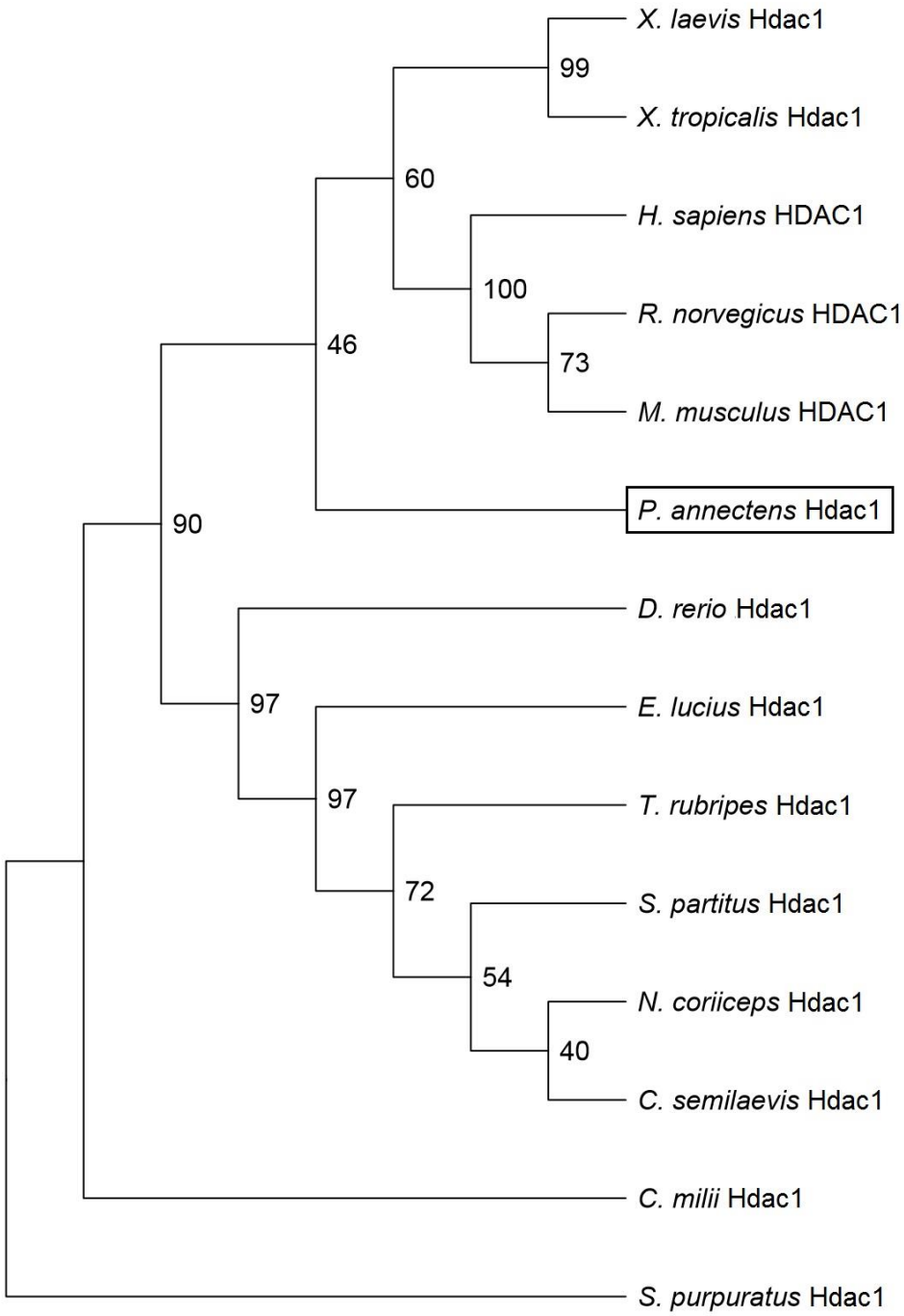

Fig. 22. The gene expression of *histone deacetylase 1* (*hdac1*) in various tissues/organs of *Protopterus annectens*. Expression of *hdac1* were examined in the muscle (M), heart (H), brain (B), eye (E), gills (Gi), kidney (K), Lung (Lu), skin (Sk), liver (Li), spleen (Sp), pancreas (P), and gut (Gu) of *Protopterus annectens* (*N*=1) kept in fresh water.

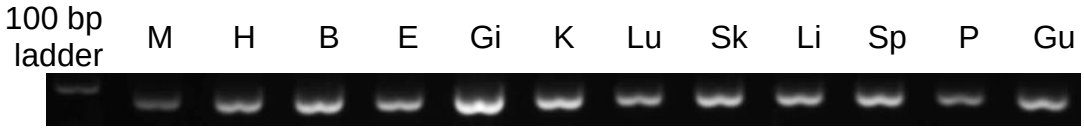

Fig. 23. mRNA expression levels of *histone deacetylase 1* (*hdac1*) in the muscle of *Protopterus annectens*. Absolute quantification (x10^2 copies of transcript per ng total RNA) of *hdac1* transcripts in the muscle of *P. annectens* kept in (a) fresh water on day 0 (FW; control), after 3 or 6 days (d; the induction phase), or 12 d or 6 months (mon; the maintenance phase) of aestivation; (b) fresh water on day 0 (FW; control), after 6 mon (the maintenance phase) of aestivation, or after 1 d, 3 d or 6 d of arousal (Ar; the arousal phase) from 6 mon of aestivation. Results represent means ± S. E. M (*N*=4).

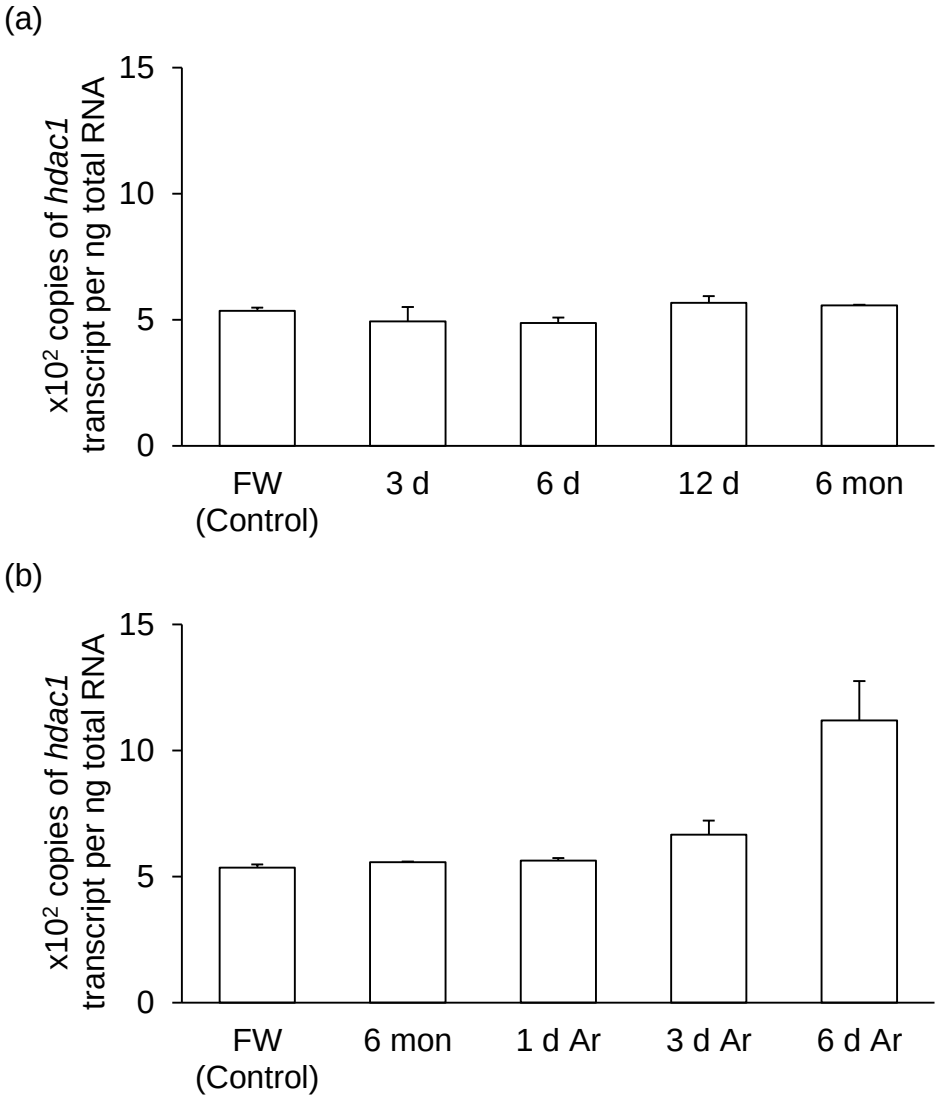

Fig. 24. Protein abundance of histone deacetylase 1 (Hdac1) in the muscle of *Protopterus annectens*. Protein abundance of Hdac1 in the muscle of *P. annectens* kept in fresh water on day 0 (FW; control), after 6 days (d; induction phase) or 6 months (mon; maintenance phase) of aestivation in air, or after 1 d or 3 d of arousal (Ar; arousal phase) from 6 mon of aestivation in air. (a) An example of immunoblot of Hdac1. (b) The protein abundance of Hdac1 is expressed as arbitrary densitometric units per 100 µg protein. Results represent mean ± S.E.M. (N=3). Means not sharing the same letter are significantly different (P<0.05).

(a)

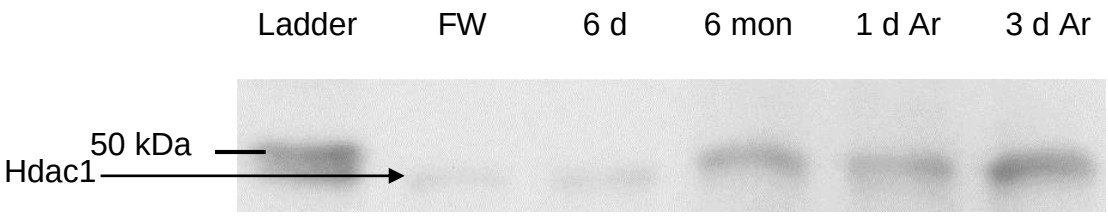

(b)

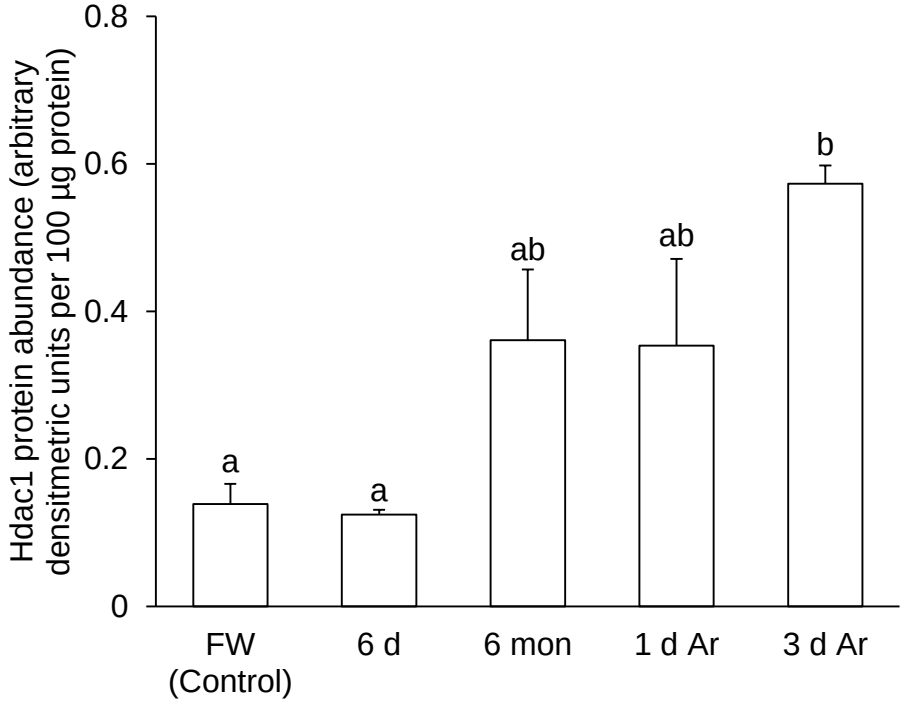

4.2.2. *foxO1* and *foxO3*/FoxO1 and FoxO3

4.2.2.1. Nucleotide sequences, translated amino acid sequences and dendrogramic analyses

The complete coding sequences of *foxO1* and *foxO3* from *P. annectens* consisted of 1932 bp and 2001 bp respectively. The deduced FoxO1 sequence comprised 644 amino acids with an estimated molecular mass of 70.1 kDa (Appendix 2g), while the putative FoxO3 sequence consisted of 667 amino acids and had an estimated molecular mass of 71.9 kDa (Appendix 2h). The FoxO1 of *P. annectens* shared the highest amino acid sequence identity with mammalian FOXO1 (62.0–63.7%), followed by amphibian FoxO1 (61.2%) and zebrafish FoxO1b (51.2%; Table 12). Likewise, the FoxO3 of *P. annectens* shared the highest amino acid sequence identity with mammalian FOXO3 (64.0–64.1%), followed by amphibian FoxO3 (62.9%) and zebrafish FoxO3 (52.2%; Table 12). It was observed that both FoxO1 and FoxO3 of *P. annectens* shared less than 38% sequence identity to other members of the FOXO/FoxO family (Table 12).

Analysis of multiple amino acid alignment of FOXO1/FoxO1 and FOXO3/FoxO3 revealed four main domains in FOXO proteins: (1) a forkhead DNA binding domain (DBD); (2) a NLS located downstream of the forkhead DNA binding domain; (3) a NES and (4) a C terminus transactivation domain (Fig. 25). The forkhead DBD and the transactivation domains showed high conservation in all sequences compared. The FoxO1 and FoxO3 of *P. annectens* contained a NLS and a NES each, which were in similar regions as the known NLS and NES in human

FOXO1 and FOXO3. This indicated that the FoxO1 and FoxO3 of *P. annectens* could be localized to both the nucleus and cytoplasm.

FOXO proteins are regulated by several post-translational modifications, including phosphorylation and acetylation. There were three AKT kinase and serum and glucocorticoid-inducible kinase (SGK) consensus phosphorylation sites in *P. annectens* FoxO1 and FoxO3 (T32, S266, S333; Fig. 25). All three AKT sites contained the AKT consensus phosphorylation motif, RXRXXS/T, which was highly conserved for all FOXO/FoxO compared. Phosphorylation of FOXO1 by AKT at S333 allows for the binding of CSNK1, which then sequentially phosphorylates FOXO1 at S336 and S339 (Rena et al., 2002, 2004). While S336 is conserved for all sequences compared, S339 was substituted by glycine in *P. annectens* FoxO1 but remained conserved in *P. annectens* FoxO3. S343, which was highly conserved in all FOXO/FoxO sequences compared, can be phosphorylated by dual tyrosine phosphorylated regulated kinase-1A (DYRK1A). Acetylation of FOXO at sites K256, K259, K273, K276, K307 and K611 are mediated by p300 or cyclic-AMP responsive element binding (CREB)-binding protein (CBP), all of which were conserved in *P. annectens* FoxO1 and FoxO3.

MAPK1 and MAPK3 target S311, S364 and S455 in FOXO3 (Yang et al., 2008a, b), where all but S455 were conserved in *P. annectens* FoxO3 (Fig. 25). S455 was substituted by proline in the FoxO3 of *P. annectens*. FOXO3 is also targeted by AMPK at T193, S427, S443, S596, S631 and S673. In *P. annectens* FoxO3, T193, S427, S631 and S673 were conserved while S443 and S596 were substituted by asparagine.

A dendrogram for both FoxO1 and FoxO3 including those of *P. annectens* was generated despite a lack of available FOXO/FoxO sequences in GenBank. The dendrogram agrees with the sequence identity, grouping the different members of the FOXO/FoxO family together; the FoxO1 of *P. annectens* was grouped together with other known FOXO1/FoxO1, separated from FOXO3/FoxO3 and FOXO4/FoxO4, while the FoxO3 of *P. annectens* was grouped together with other known FOXO3/FoxO3, separated from FOXO1/FoxO1 and FOXO4/FoxO4 (Fig. 26).

4.2.2.2. Gene expression of *foxO1* and *foxO3* in various tissues/organs

The highest expression of *foxO1* was observed in the gills and liver of *P. annectens* kept in fresh water (Fig. 27a). The expression of *foxO1* was detected in the muscle, heart, brain, eye, kidney, skin, spleen, pancreas and gut, but undetected in the lung. The expression of *foxO3* was the highest in the heart, brain, eye and gills of *P. annectens* kept in fresh water (Fig. 27b). The expression of *foxO3* was detected in the muscle, kidney, lung, skin, liver, spleen, pancreas and gut.

4.2.2.3. mRNA expression of *foxO1* and *foxO3*

There were significant decreases in the mRNA expression levels of *foxO1* in the muscle of *P. annectens* after 6 days (by 44.2%; $P<0.05$) or 12 days (by 36.4%; $P<0.05$) or after 6 months of aestivation (by 60.6%; $P<0.05$), as compared to the freshwater control (Fig. 28a). By contrast, there was a significant increase in the mRNA expression of *foxO1* after 6 days of arousal from 6 months of aestivation (4.23-fold; $P<0.05$; Fig. 28b).

There were significant increases in the mRNA expression levels of *foxO3* in the muscle of *P. annectens* after 3 days (2.08-fold; $P<0.05$) or 6 days of aestivation

(1.64-fold; $P<0.05$), as compared to the control (Fig. 29a). There was a significant increase in the mRNA expression of *foxO3* after 6 days of arousal from 6 months of aestivation (2.28-fold; $P<0.05$; Fig. 29b).

4.2.2.4. Protein abundance of FoxO1 and FoxO3

There was a significant decrease in the protein abundance of FoxO1 in the muscle of *P. annectens* after 1 day of arousal from 6 months of aestivation (by 79.5%; $P<0.05$), as compared to the freshwater control (Fig. 30). In contrast, there were no significant changes in the protein abundance of FoxO3 in the muscle of *P. annectens* after 6 days or 6 months of aestivation, or after 1 day or 3 days of arousal from 6 months of aestivation as compared to the control (Fig. 31).

Table 12. The percentage similarity between the deduced amino acid sequence of forkhead box O1 (FoxO1) and FoxO3 from the muscle of *Protopterus annectens* and FOXO/FoxO sequences from other animal species obtained from GenBank (accession numbers in brackets). Sequences are arranged in a descending order of similarity to *P. annectens* FoxO1.

Classification	Species	Similarity to *P. annectens* FoxO1	Similarity to *P. annectens* FoxO3
Lungfish	*P. annectens* FoxO1	100%	35.1%
	P. annectens FoxO3	35.1%	100%
Mammals	*Mus musculus* FOXO1 (NP_062713.2)	63.7%	37.4%
	Homo sapiens FOXO1 (AAH21981.1)	62.0%	36.8%
	Homo sapiens FOXO3 (AAH68552.1)	36.1%	64.1%
	Mus musculus FOXO3 (NP_062714.1)	35.7%	64.0%
	Homo sapiens FOXO4 isoform 1 (NP_005929.2)	31.8%	30.6%
	Rattus norvegicus FOXO4 (NP_001100413.1)	31.0%	30.3%
	Mus musculus FOXO4 (NP_061259.1)	30.7%	30.3%
	Homo sapiens FOXO4 isoform 2 (NP_001164402.1)	29.3%	28.0%
Amphibians	*Xenopus laevis* FoxO1 (NP_001086417.1)	61.2%	37.4%
	Xenopus laevis FoxO3 (NP_001086418.1)	36.1%	62.9%
	Xenopus laevis FoxO4 (ACO24746.1)	34.0%	33.0%
Teleosts	*Danio rerio* FoxO1b (AAI63020.1)	51.2%	30.8%
	Danio rerio FoxO3 (NP_571160.1)	34.3%	52.2%

Fig. 25. Molecular characterization of forkhead box O1 and O3 (FoxO1 and FoxO3) from the muscle of *Protopterus annectens*. Multiple amino acid alignment of FoxO1 and FoxO3 from the muscle of *P. annectens* with *Homo sapiens* FOXO1 (AAH21981.1), *H. sapiens* FOXO3 (AAH68552.1), *Mus musculus* FOXO1 (NP_062713.2), *M. musculus* FOXO3 (NP_062714.1), *Xenopus laevis* FoxO1 (NP_001086417.1), *X. laevis* FoxO3 (NP_001086418.1), *Danio rerio* FoxO1b (AAI63020.1) and *D. rerio* FoxO3 (NP_571160.1). Identical amino acids are indicated by shaded residues. The forkhead DNA-binding domain is indicated with an open box. Regions of nuclear localization sequence (NLS) and nuclear export sequence (NES) are indicated by yellow boxes, with the sequences (known for human and predicted for *P. annectens*) underlined. The open triangles indicate the residues in both FOXO1 and FOXO3 that are phosphorylated by protein kinase AKT/serum-and glucocorticoid-inducible kinase, while the dotted lines indicate the AKT consensus phosphorylation motif (RXRXXS/T). In both FOXO1 and FOXO3, the open circles denote the residues that are phosphorylated by casein kinase 1, while the open square indicates the serine residue that is phosphorylated by dual tyrosine phosphorylated regulated kinase-1A. Lysine residues which undergo acetylation by p300/cyclic-AMP responsive element binding (CREB)-binding protein in both FOXO1 and FOXO3 are denoted by the symbol #. The symbol ‡ indicates the serine residues in FOXO3 that undergo phosphorylation by mitogen-activated protein kinases 1 and 3. The residues that undergo AMP-activated protein kinase phosphorylation in FOXO3 are indicated by arrows. The transactivation domain for both FOXO1 and FOXO3 is double-underlined.

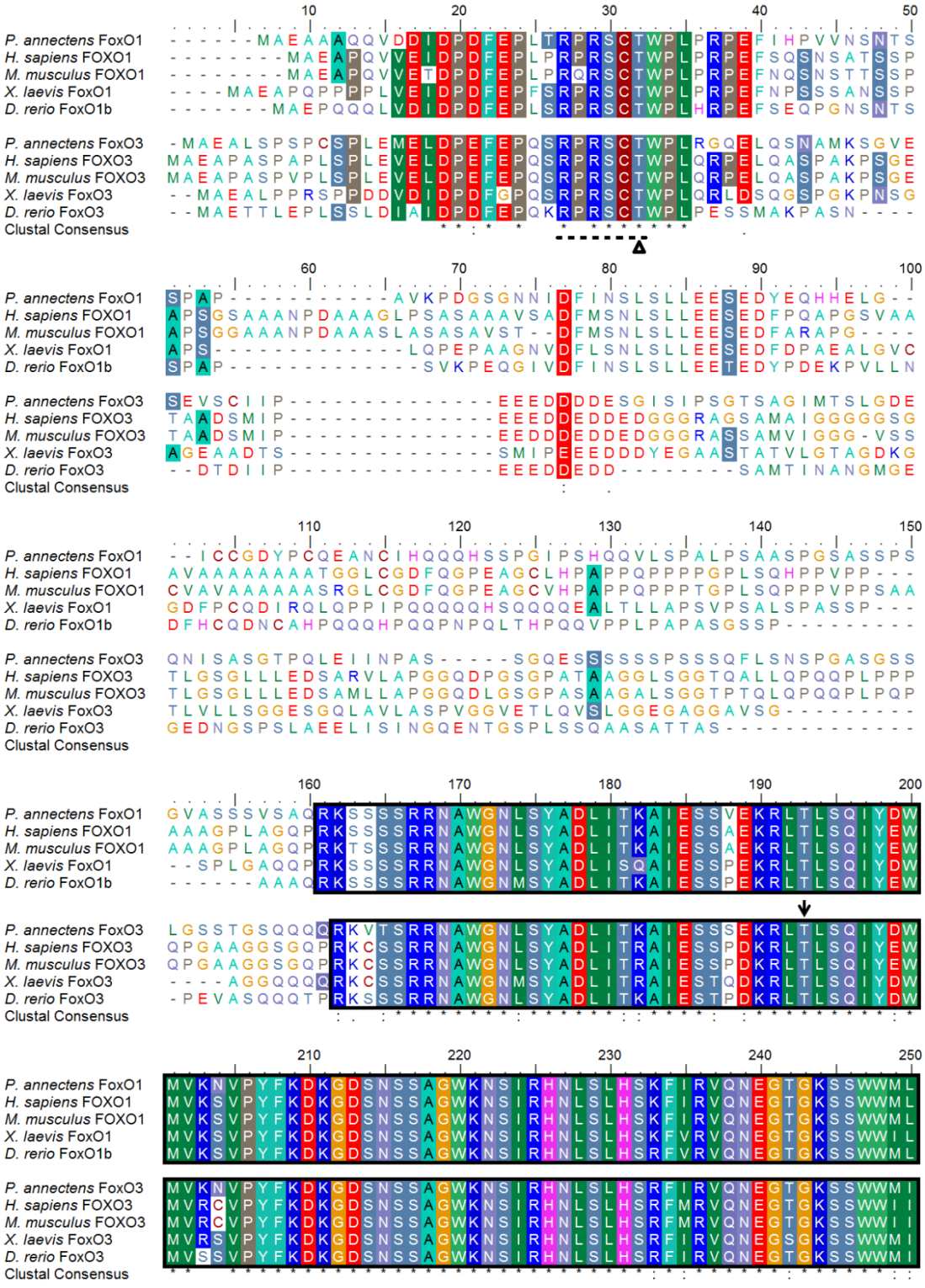
P. annectens FoxO1
H. sapiens FOXO1
M. musculus FOXO1
X. laevis FoxO1
D. rerio FoxO1b
P. annectens FoxO3
H. sapiens FOXO3
M. musculus FOXO3
X. laevis FoxO3
D. rerio FoxO3
Clustal Consensus

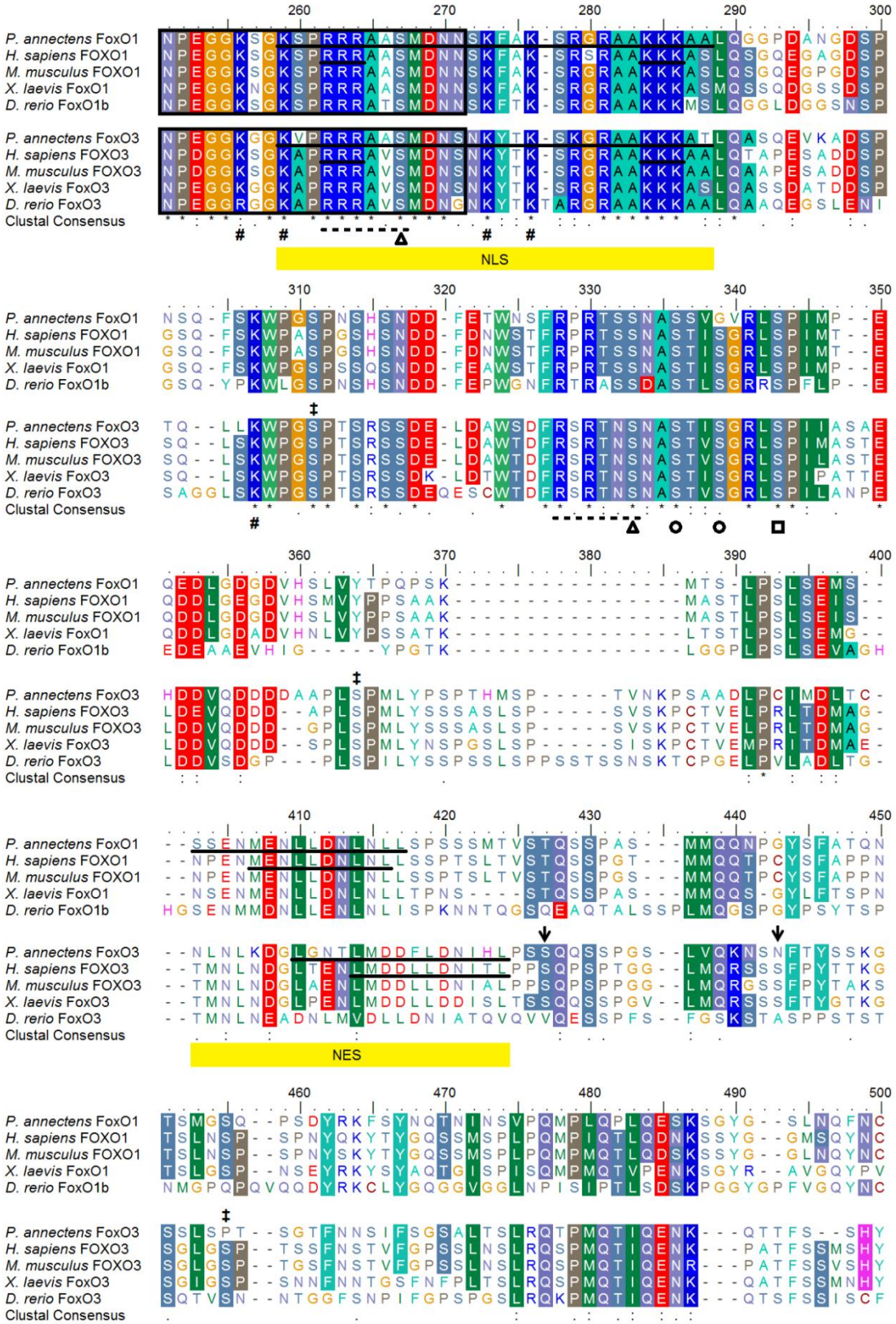
260
270
280
290
300
P. annectens FoxO1
H. sapiens FOXO1
M. musculus FOXO1
X. laevis FoxO1
D. rerio FoxO1b
P. annectens FoxO3
H. sapiens FOXO3
M. musculus FOXO3
X. laevis FoxO3
D. rerio FoxO3
Clustal Consensus
NLS
310
320
330
340
350
P. annectens FoxO1
H. sapiens FOXO1
M. musculus FOXO1
X. laevis FoxO1
D. rerio FoxO1b
P. annectens FoxO3
H. sapiens FOXO3
M. musculus FOXO3
X. laevis FoxO3
D. rerio FoxO3
Clustal Consensus
360
370
380
390
400
P. annectens FoxO1
H. sapiens FOXO1
M. musculus FOXO1
X. laevis FoxO1
D. rerio FoxO1b
P. annectens FoxO3
H. sapiens FOXO3
M. musculus FOXO3
X. laevis FoxO3
D. rerio FoxO3
Clustal Consensus
410
420
430
440
450
P. annectens FoxO1
H. sapiens FOXO1
M. musculus FOXO1
X. laevis FoxO1
D. rerio FoxO1b
P. annectens FoxO3
H. sapiens FOXO3
M. musculus FOXO3
X. laevis FoxO3
D. rerio FoxO3
Clustal Consensus
NES
460
470
480
490
500
P. annectens FoxO1
H. sapiens FOXO1
M. musculus FOXO1
X. laevis FoxO1
D. rerio FoxO1b
P. annectens FoxO3
H. sapiens FOXO3
M. musculus FOXO3
X. laevis FoxO3
D. rerio FoxO3
Clustal Consensus

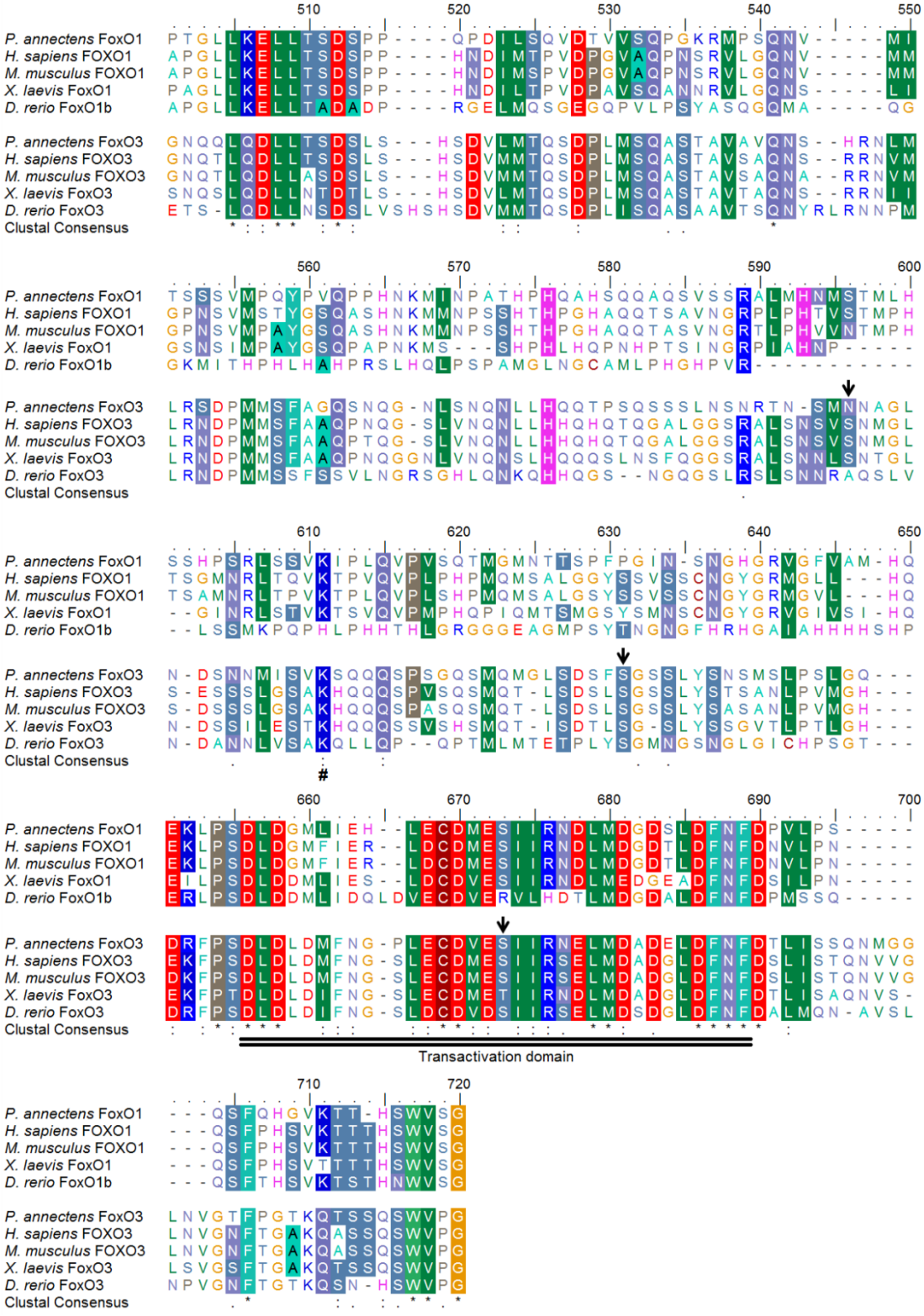
510
520
530
540
550
P. annectens FoxO1
H. sapiens FOXO1
M. musculus FOXO1
X. laevis FoxO1
D. rerio FoxO1b
P. annectens FoxO3
H. sapiens FOXO3
M. musculus FOXO3
X. laevis FoxO3
D. rerio FoxO3
Clustal Consensus
560
570
580
590
600
610
620
630
640
650
660
670
680
690
700
710
720
Transactivation domain

Fig. 26. A dendrogram of forkhead box O (FOXO/FoxO) including those of *Protopterus annectens*. Numbers presented at each branch point represent bootstrap percentages from 1000 replicates. FoxO from *Cerapachys biroi* is used as the outgroup for the dendrogram.

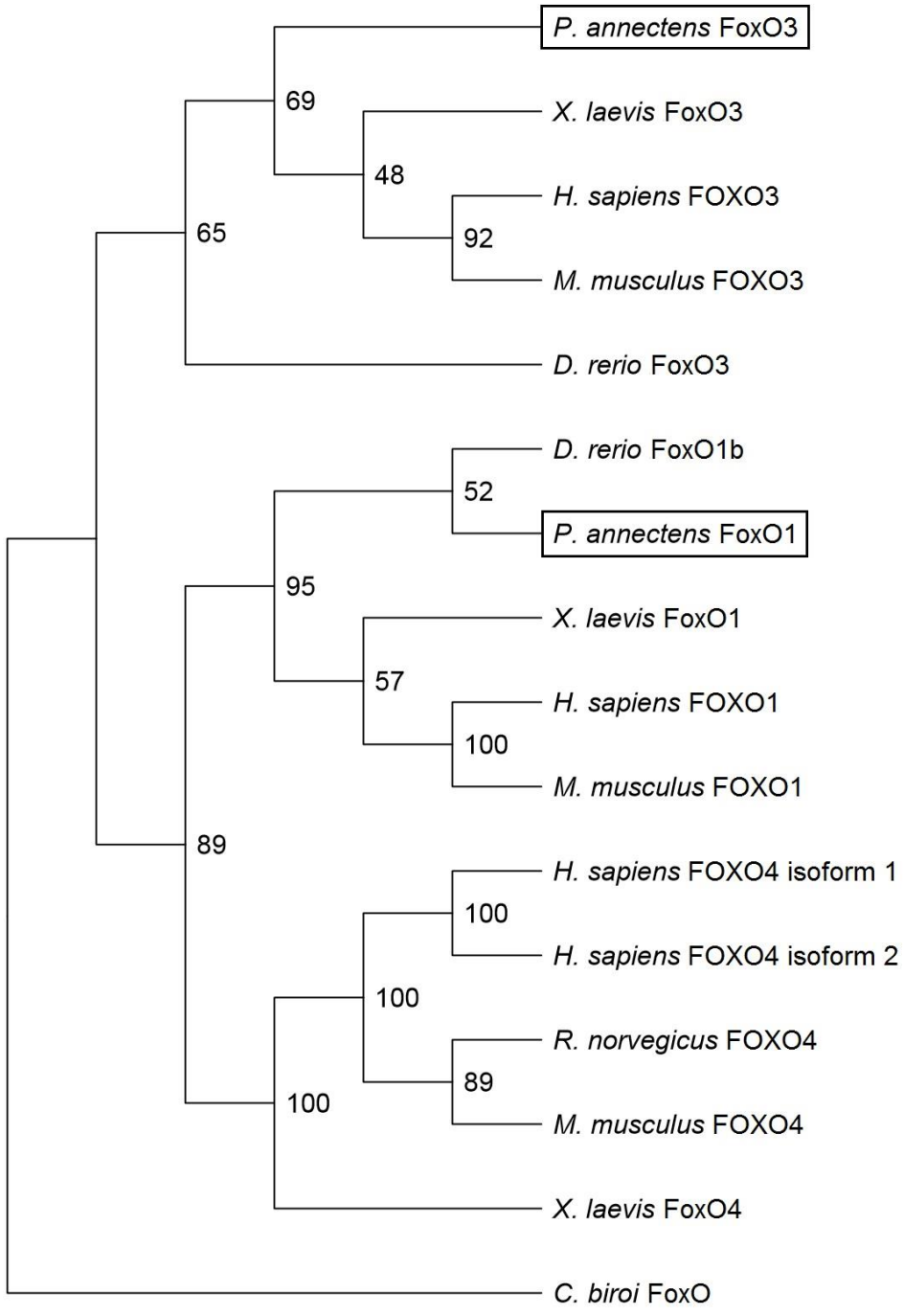

Fig. 27. The gene expression of *forkhead box O1* (*foxO1*) and *O3* (*foxO3*) in various tissues/organs of *Protopterus annectens*. Expression of (a) *foxO1* and (b) *foxO3* were examined in the muscle (M), heart (H), brain (B), eye (E), gills (Gi), kidney (K), Lung (Lu), skin (Sk), liver (Li), spleen (Sp), pancreas (P), and gut (Gu) of *Protopterus annectens* (*N*=1) kept in fresh water.

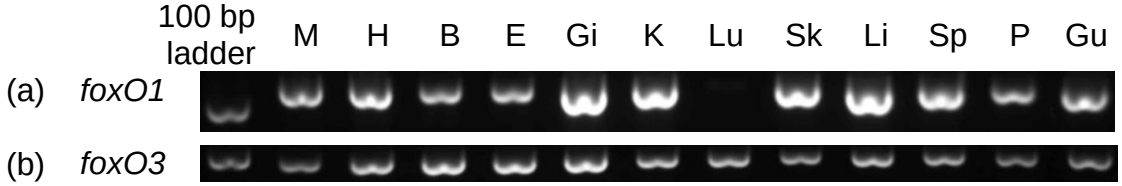

Fig. 28. mRNA expression levels of *forkhead box O1* (*foxO1*) in the muscle of *Protopterus annectens*. Absolute quantification (×10^2 copies of transcript per ng total RNA) of *foxO1* transcripts in the muscle of *P. annectens* kept in (a) fresh water on day 0 (FW; control), after 3 or 6 days (d; the induction phase), or 12 d or 6 months (mon; the maintenance phase) of aestivation; (b) fresh water on day 0 (FW; control), after 6 mon (the maintenance phase) of aestivation, or after 1 d, 3 d or 6 d of arousal (Ar; the arousal phase) from 6 mon of aestivation. Results represent means ± S. E. M (*N*=4). Means not sharing the same letter are significantly different (*P*<0.05).

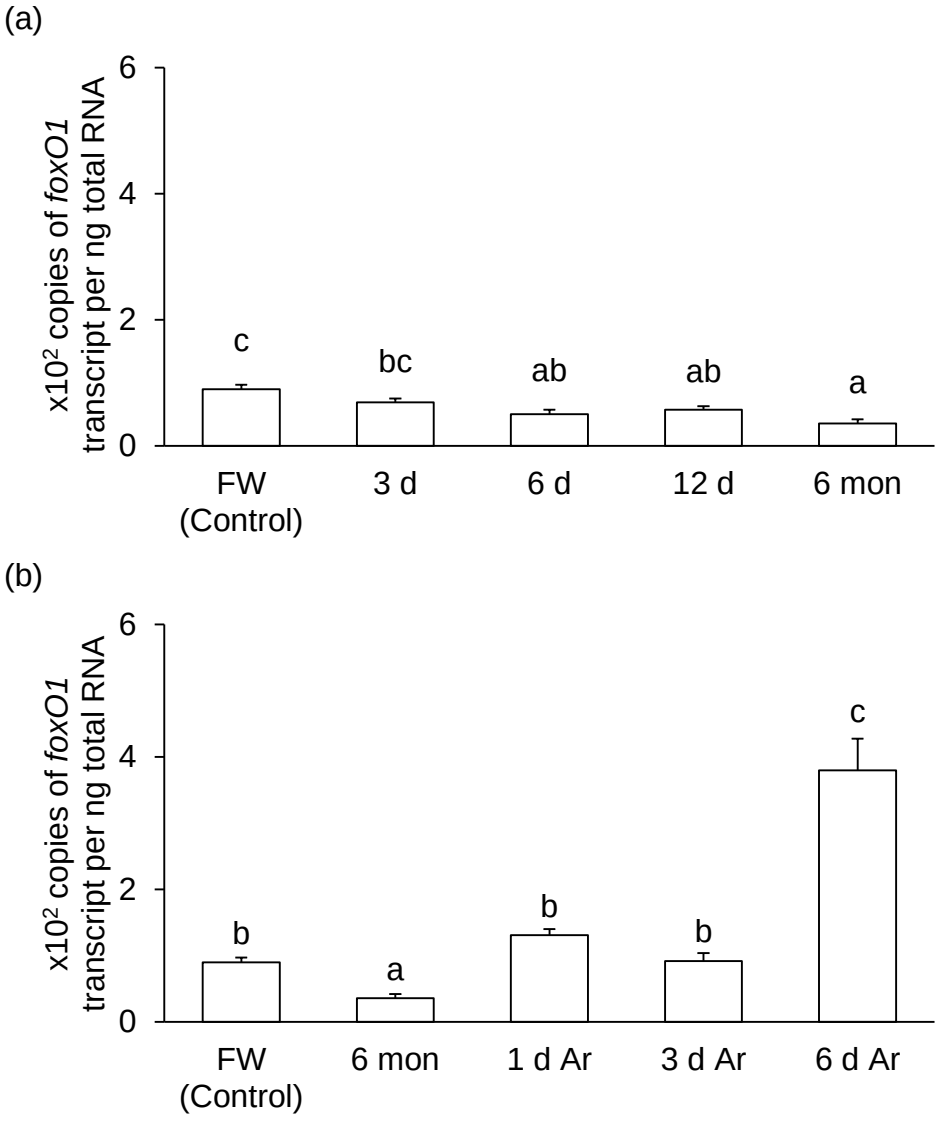

Fig. 29. mRNA expression levels of *forkhead box O3* (*foxO3*) in the muscle of *Protopterus annectens*. Absolute quantification (×10^2 copies of transcript per ng total RNA) of *foxO3* transcripts in the muscle of *P. annectens* kept in (a) fresh water on day 0 (FW; control), after 3 or 6 days (d; the induction phase), or 12 d or 6 months (mon; the maintenance phase) of aestivation; (b) fresh water on day 0 (FW; control), after 6 mon (the maintenance phase) of aestivation, or after 1 d, 3 d or 6 d of arousal (Ar; the arousal phase) from 6 mon of aestivation. Results represent means ± S. E. M (*N*=4). Means not sharing the same letter are significantly different (*P*<0.05).

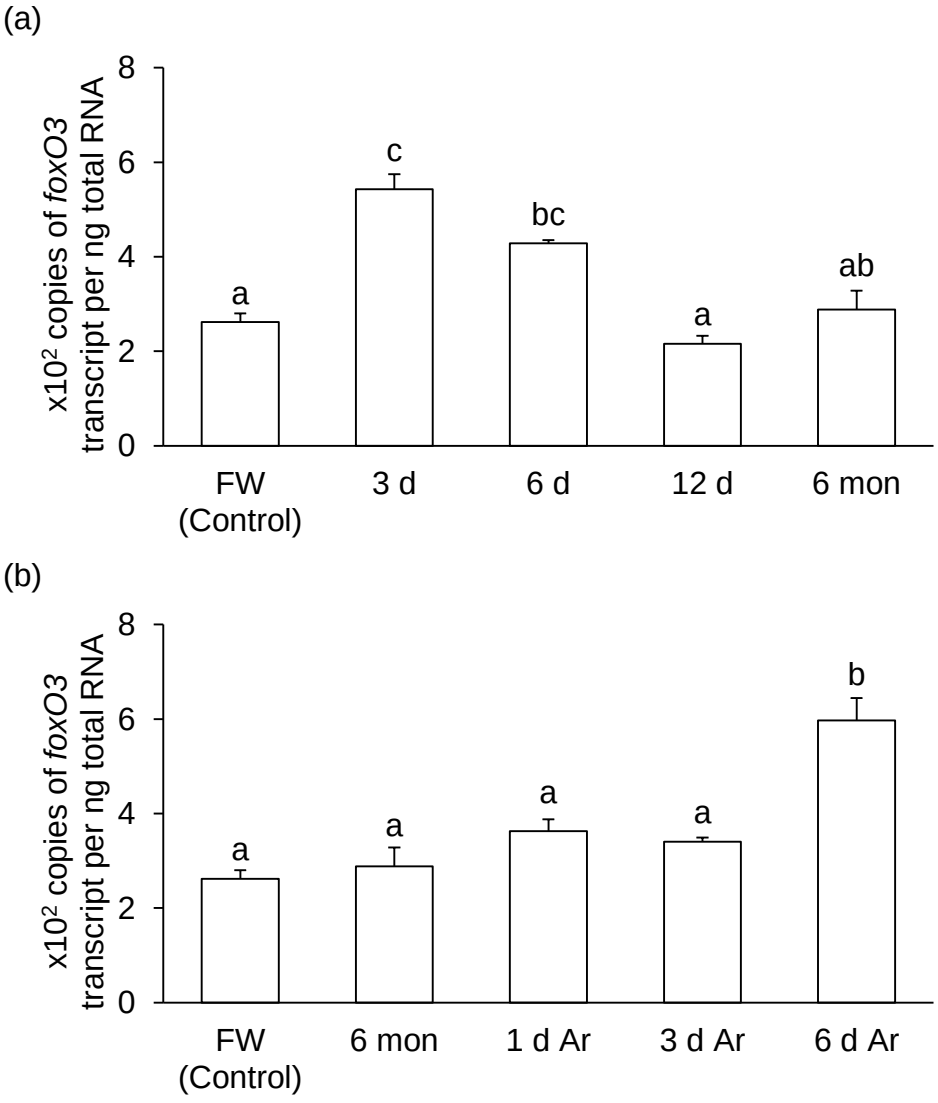

Fig. 30. Protein abundance of forkhead box O1 (FoxO1) in the muscle of *Protopterus annectens*. Protein abundance of FoxO1 in the muscle of *P. annectens* kept in fresh water on day 0 (FW; control), after 6 days (d; induction phase) or 6 months (mon; maintenance phase) of aestivation in air, or after 1 d or 3 d of arousal (Ar; arousal phase) from 6 mon of aestivation in air. (a) An example of immunoblot of FoxO1. (b) The protein abundance of FoxO1 is expressed as arbitrary densitometric units per 20 μg protein. Results represent mean ± S.E.M. (N=3). Means not sharing the same letter are significantly different (P<0.05).

(a)

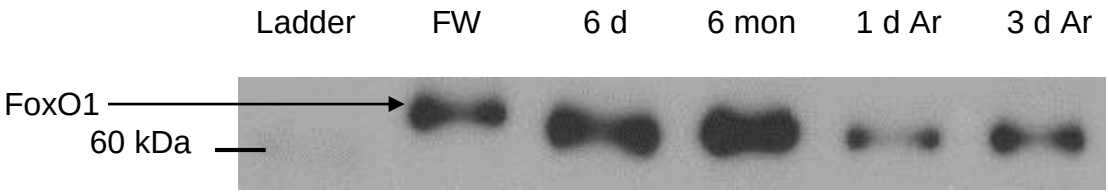

(b)

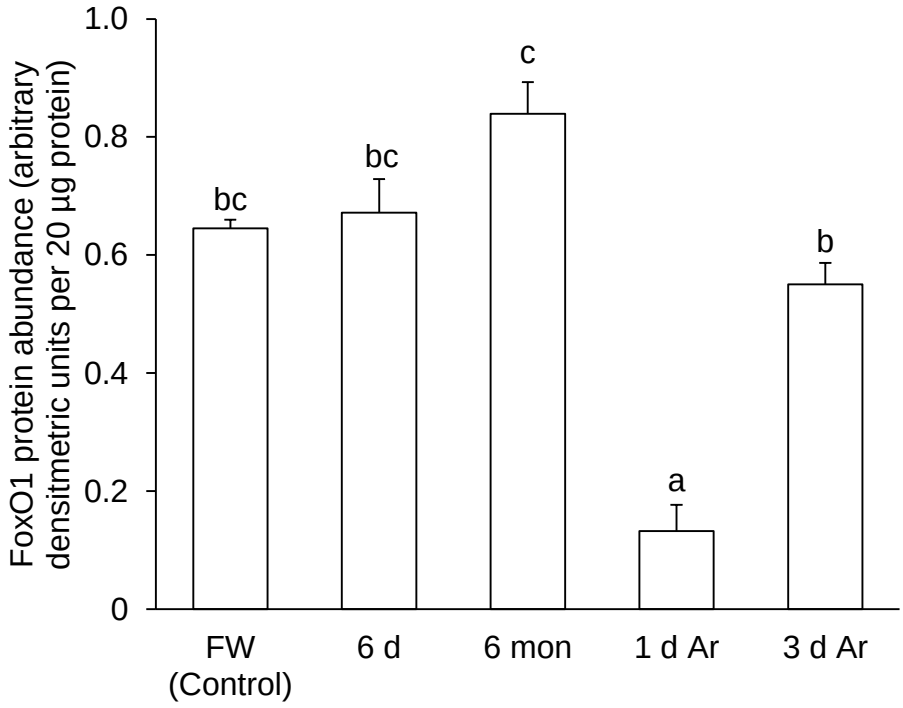

Fig. 31. Protein abundance of forkhead box O3 (FoxO3) in the muscle of *Protopterus annectens*. Protein abundance of FoxO3 in the muscle of *P. annectens* kept in fresh water on day 0 (FW; control), after 6 days (d; induction phase) or 6 months (mon; maintenance phase) of aestivation in air, or after 1 d or 3 d of arousal (Ar; arousal phase) from 6 mon of aestivation in air. (a) An example of immunoblot of FoxO3. (b) The protein abundance of FoxO3 is expressed as arbitrary densitometric units per 200 μg protein. Results represent mean ± S.E.M. (*N*=3).

(a)

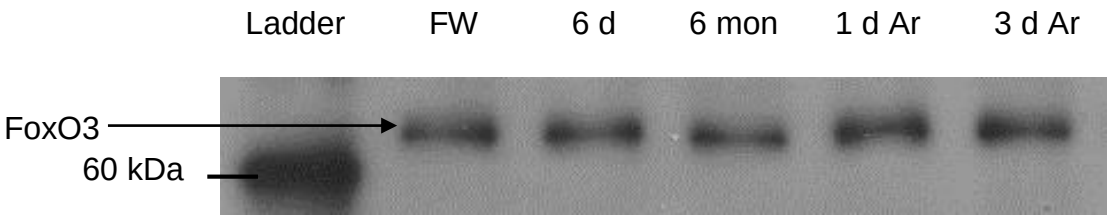

(b)

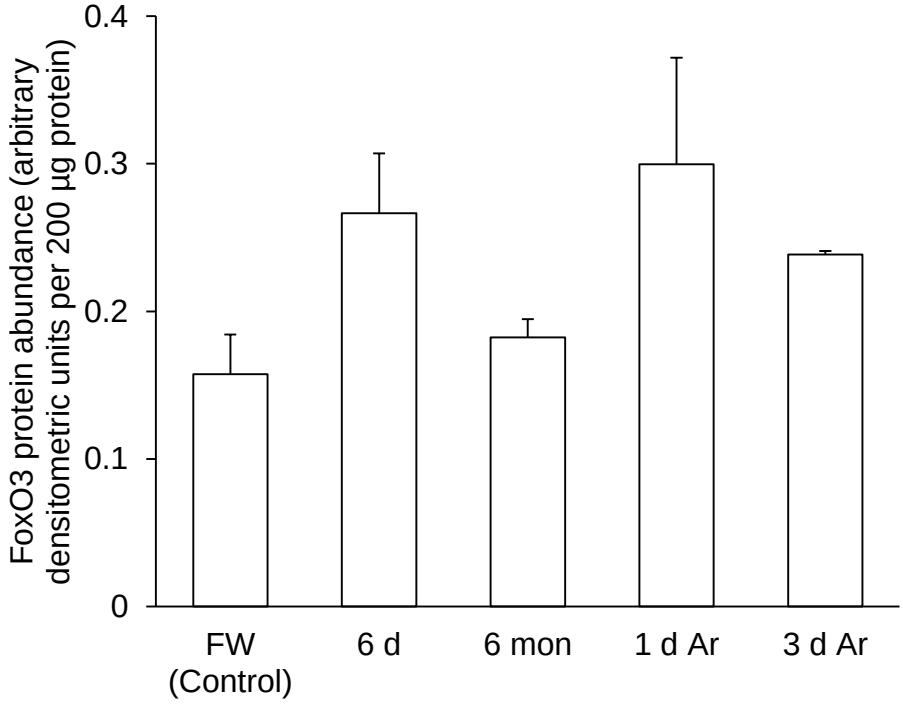

4.2.3. *tp53*

4.2.3.1. Gene expression of *tp53* in various tissues/organs

The gills, kidney, skin, liver and spleen of *P. annectens* kept in fresh water had the highest expression levels of *tp53* (Fig. 32). The expression of *tp53* was detected in the brain, eye, pancreas and gut, weakly detectable in the muscle and lung but undetectable in the heart.

4.2.3.2. mRNA expression of *tp53*

There was a significant increase in the mRNA expression of *tp53* in the muscle of *P. annectens* after 6 days of aestivation (2.29-fold; $P<0.05$), as compared to the control (Fig. 33a). There were significant increases in the mRNA expression levels of *tp53* in the muscle of *P. annectens* after 1 day (1.75-fold; $P<0.05$) or 3 days (3.36-fold; $P<0.05$) or 6 days of arousal from 6 months of aestivation (4.37-fold; $P<0.05$), as compared with the freshwater control (Fig. 33b).

Fig. 32. The gene expression of *tumour protein 53* (*tp53*) in various tissues/organs of *Protopterus annectens*. Expression of *tp53* were examined in the muscle (M), heart (H), brain (B), eye (E), gills (Gi), kidney (K), Lung (Lu), skin (Sk), liver (Li), spleen (Sp), pancreas (P), and gut (Gu) of *Protopterus annectens* (*N*=1) kept in fresh water.

Fig. 33. mRNA expression levels of *tumour protein 53* (*tp53*) in the muscle of *Protopterus annectens*. Absolute quantification ($\times 10^2$ copies of transcript per ng total RNA) of *tp53* transcripts in the muscle of *P. annectens* kept in (a) fresh water on day 0 (FW; control), after 3 or 6 days (d; the induction phase), or 12 d or 6 months (mon; the maintenance phase) of aestivation; (b) fresh water on day 0 (FW; control), after 6 mon (the maintenance phase) of aestivation, or after 1 d, 3 d or 6 d of arousal (Ar; the arousal phase) from 6 mon of aestivation. Results represent means ± S. E. M (N=4). Means not sharing the same letter are significantly different (P<0.05).

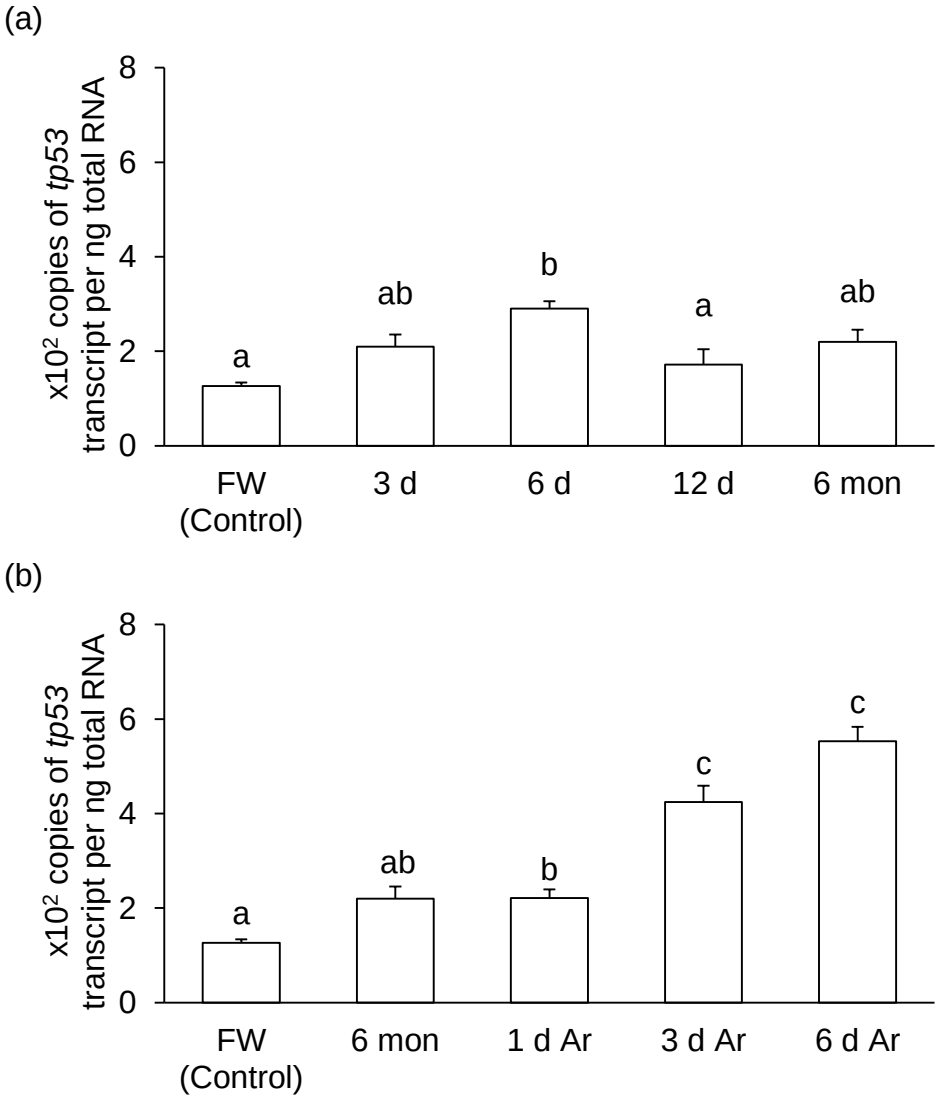

4.2.4. *mstn*/Mstn

4.2.4.1. Nucleotide sequence, translated amino acid sequence and dendrogramic analysis

The complete coding sequence of *mstn* from *P. annectens* comprised 1128 bp. The deduced Mstn sequence consisted of 376 amino acids with an estimated molecular mass of 42.9 kDa (Appendix 2i), and shared the highest amino acid sequence identity with mammalian MSTN (69.1–70.8%), followed by coelacanth Mstn (66.5%), teleost Mstn (31.1–62.5%) and amphibian Mstn (61.6%; Table 13).

A comparison of the Mstn from *P. annectens* with MSTN/Mstn of human, mouse, frog, coelacanth and zebrafish showed that *P. annectens* Mstn consisted of a conserved TGF-β propeptide domain, a RXXR proteolytic cleavage site (RSRR) and a bioactive TGF-β domain (Fig. 34). The proteolytic site allows the mature peptide to be released. The Mstn of *P. annectens* also contained nine cysteine residues after the proteolytic site that were conserved in all Mstn and inhibin/activin-like members of the TGF-β family. A putative signal peptide was predicted in the NH_2-terminus, and cleavage was predicted to occur between amino acid positions 21 and 22 of *P. annectens* Mstn.

The Mstn of *P. annectens* was grouped in a clade together with Mstn of *L. chalumnae* and MSTN of tetrapods, separated from Mstn of teleosts (Fig. 35).

4.2.4.2. Gene expression of *mstn* in various tissues/organs

The muscle and eye of *P. annectens* kept in fresh water had the highest expression levels of *mstn* (Fig. 36). The expression of *mstn* was not detected in the heart, brain, gills, kidney, lung, skin, liver, spleen, pancreas and gut.

4.2.4.3. mRNA expression of *mstn*

There were significant increases in the mRNA expression levels of *mstn* in the muscle of *P. annectens* after 6 days (3.23-fold; $P<0.05$) or 12 days of aestivation (4.06-fold; $P<0.05$), as compared to the control (Fig. 37a). By contrast, the mRNA expression of *mstn* remained unchanged in the muscle of *P. annectens* during the arousal phase (Fig. 37b).

4.2.4.4. Protein abundance of Mstn

There was a significant decrease in the protein abundance of Mstn in the muscle of *P. annectens* after 1 day of arousal from 6 months of aestivation (by 41.4%; $P<0.05$) when compared to the control (Fig. 38).

Table 13. The percentage similarity between the deduced amino acid sequence of myostatin (Mstn) from the muscle of *Protopterus annectens* and MSTN/Mstn sequences from other animal species obtained from GenBank (accession numbers in brackets). Sequences are arranged in a descending order of similarity.

Classification	Species	Similarity
Mammals	*Homo sapiens* MSTN (ABI48513.1)	70.8%
	Mus musculus MSTN (AAI05675.1)	69.6%
	Rattus norvegicus MSTN (AAB86691.1)	69.1%
Coelacanth	*Latimeria chalumnae* Mstn (XM_005996542.1)	66.5%
Teleosts	*Labeo fimbriatus* Mstn (AEN75197.1)	62.5%
	Cyprinus carpio Mstn 1a (ACY01745.1)	62.3%
	Danio rerio Mstn (AAB86693.1)	62.3%
	Oncorhynchus mykiss Mstn 1a (AAZ85121.1)	62.0%
	Salmo salar Mstn 1b (CAC59700.1)	61.7%
	Salmo salar Mstn 1a (ABN72586.1)	61.7%
	Catla catla Mstn (AEN75196.1)	61.5%
	Oncorhynchus mykiss Mstn 1b (ABA42586.1)	61.5%
	Cyprinus carpio Mstn 1b (ACY01746.1)	61.2%
	Takifugu rubripes Mstn 1 (AAR88255.1)	59.4%
	Cynoglossus semilaevis Mstn (ABU25352.1)	58.1%
	Ameiurus catus Mstn (AAS48405.1)	57.3%
	Clarias macrocephalus Mstn (AFS49710.1)	56.7%
Amphibian	*Xenopus (Silurana) tropicalis* Mstn (XP_002931542.1)	61.6%

Fig. 34. Molecular characterization of myostatin (Mstn) from the muscle of *Protopterus annectens*. Multiple amino acid alignment of Mstn from the muscle of *P. annectens* with five other known MSTN/Mstn from *Homo sapiens* (ABI48513.1), *Mus musculus* (AAI05675.1), *Xenopus* (*Silurana*) *tropicalis* (XP_002931542.1), *Latimeria chalumnae* (XM_005996542.1) and *Danio rerio* (AAB86693.1). Identical amino acids are indicated by shaded residues. The signal peptide (21 amino acids long) is underlined. The open box indicates the proteolytic cleavage site (RXXR), which separates the TGF-β propeptide domain (position 39–260) from the TGF-β domain (position 284–379). The arrows indicate the conserved cysteine residues present in all TGF-β family members.

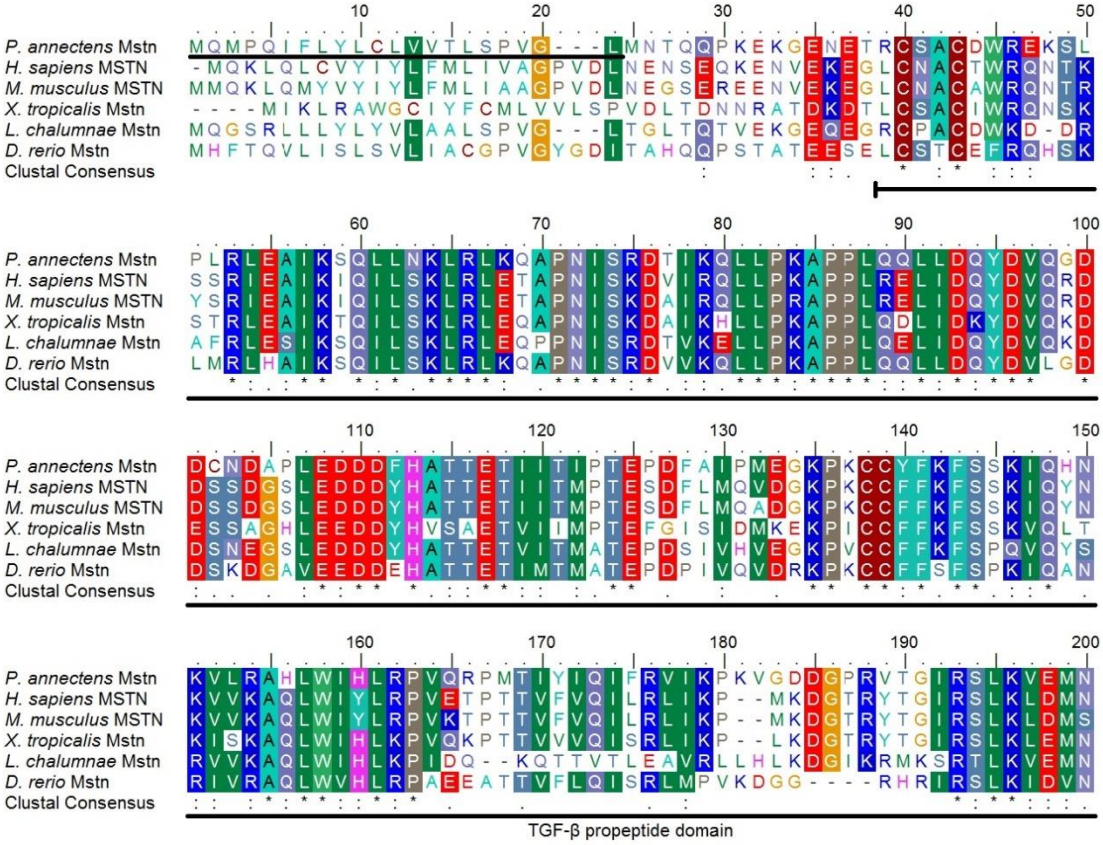

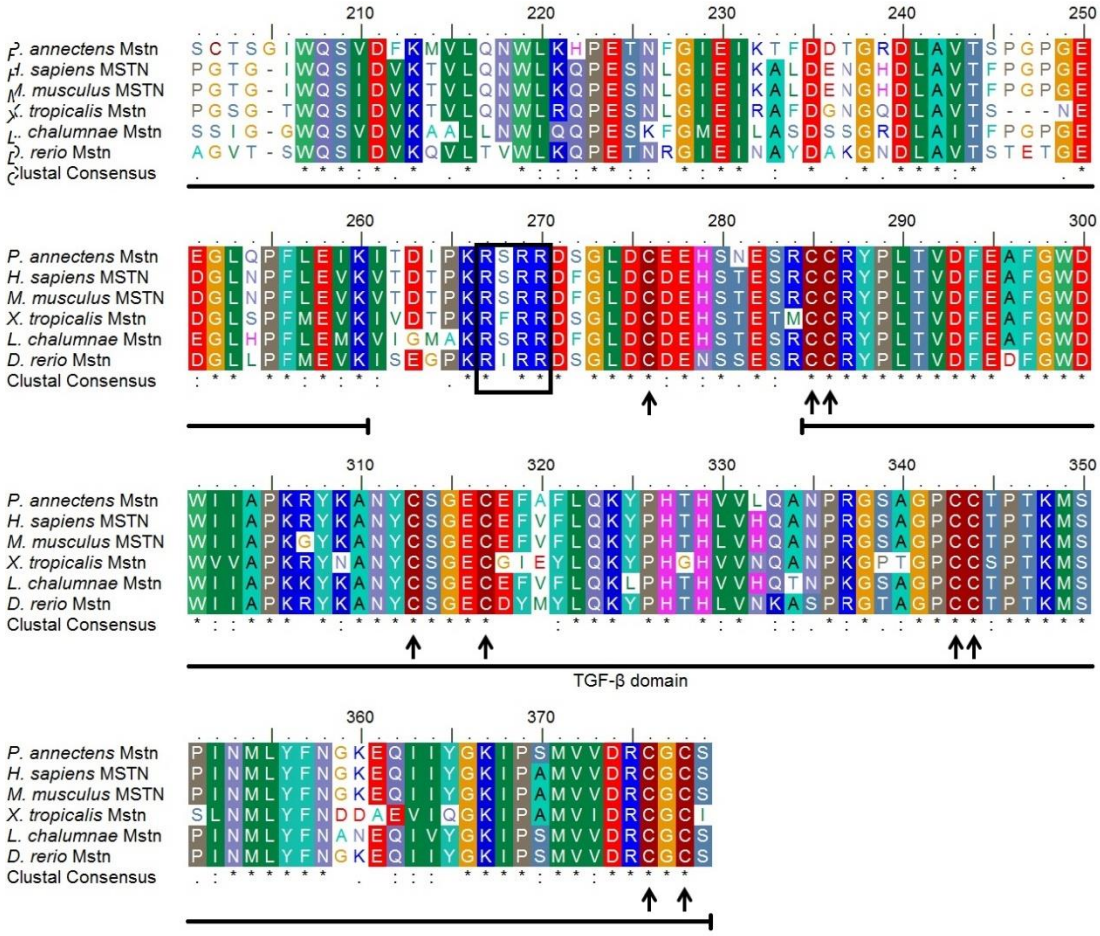
P. annectens Mstn
H. sapiens MSTN
M. musculus MSTN
X. tropicalis Mstn
L. chalumnae Mstn
D. rerio Mstn
Clustal Consensus
TGF-β domain

Fig. 35. A dendrogram of myostatin (MSTN/Mstn) including that of *Protopterus annectens*. Numbers presented at each branch point represent bootstrap percentages from 8000 replicates. Mstn from *Nematostella vectensis* is used as the outgroup for the phylogenetic analysis.

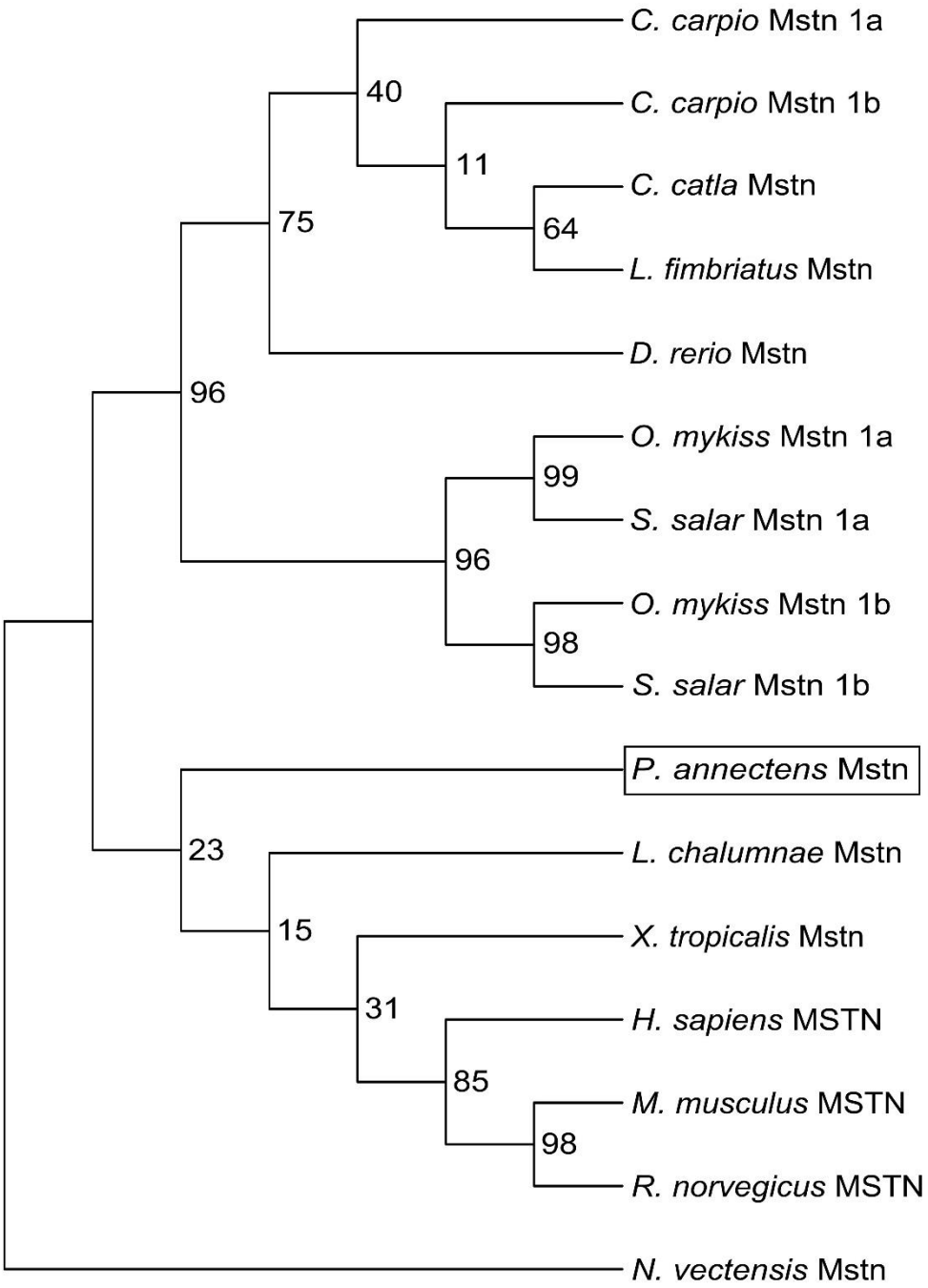

Fig. 6. The gene expression of *myostatin* (*mstn*) in various tissues/organs of *Protopterus annectens*. Expression of *mstn* were examined in the muscle (M), heart (H), brain (B), eye (E), gills (Gi), kidney (K), Lung (Lu), skin (Sk), liver (Li), spleen (Sp), pancreas (P), and gut (Gu) of *Protopterus annectens* (*N*=1) kept in fresh water.

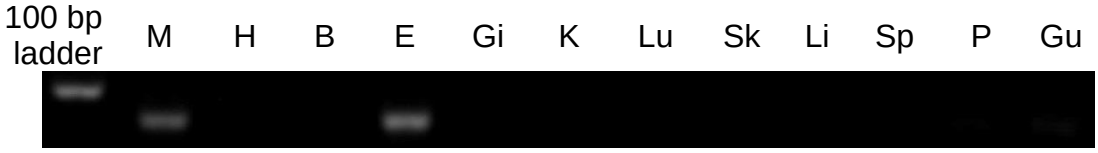

Fig. 37. mRNA expression levels of *myostatin* (*mstn*) in the muscle of *Protopterus annectens*. Absolute quantification (copies of transcript per ng total RNA) of *mstn* transcripts in the muscle of *P. annectens* kept in (a) fresh water on day 0 (FW; control), after 3 or 6 days (d; the induction phase), or 12 d or 6 months (mon; the maintenance phase) of aestivation; (b) fresh water on day 0 (FW; control), after 6 mon (the maintenance phase) of aestivation, or after 1 d, 3 d or 6 d of arousal (Ar; the arousal phase) from 6 mon of aestivation. Results represent means ± S. E. M (N=4). Means not sharing the same letter are significantly different (P<0.05).

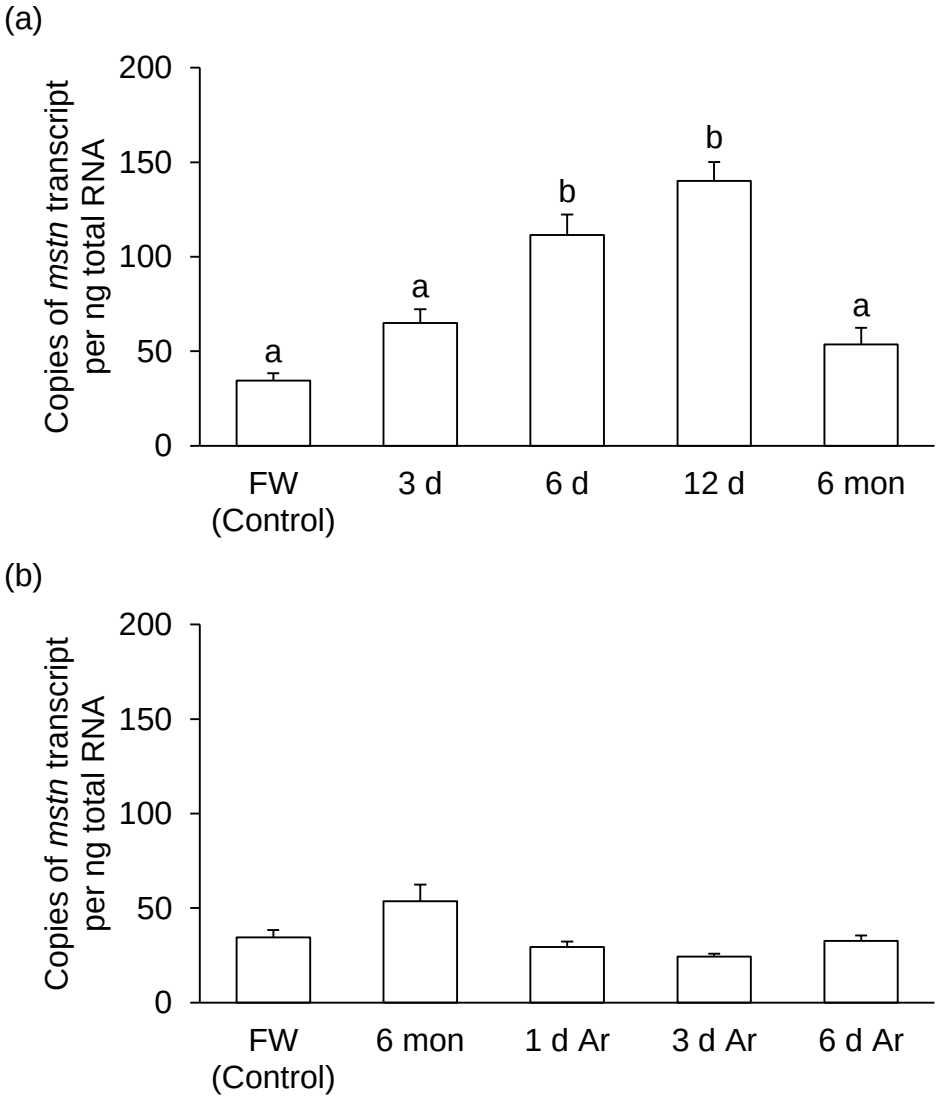

Fig. 38. Protein abundance of myostatin (Mstn) in the muscle of *Protopterus annectens*. Protein abundance of Mstn in the muscle of *P. annectens* kept in fresh water on day 0 (FW; control), after 6 days (d; induction phase) or 6 months (mon; maintenance phase) of aestivation in air, or after 1 d or 3 d of arousal (Ar; arousal phase) from 6 mon of aestivation in air. (a) An example of immunoblot of Mstn. (b) The protein abundance of Mstn is expressed as arbitrary densitometric units per 200 µg protein. Results represent mean ± S.E.M. (N=3). Means not sharing the same letter are significantly different (P<0.05).

(a)

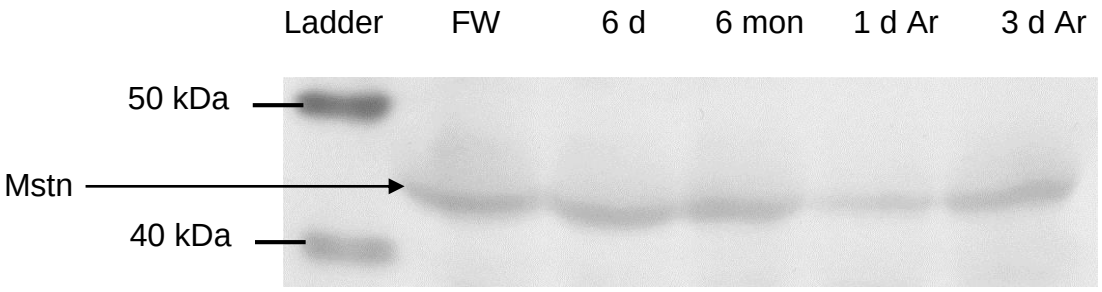

(b)

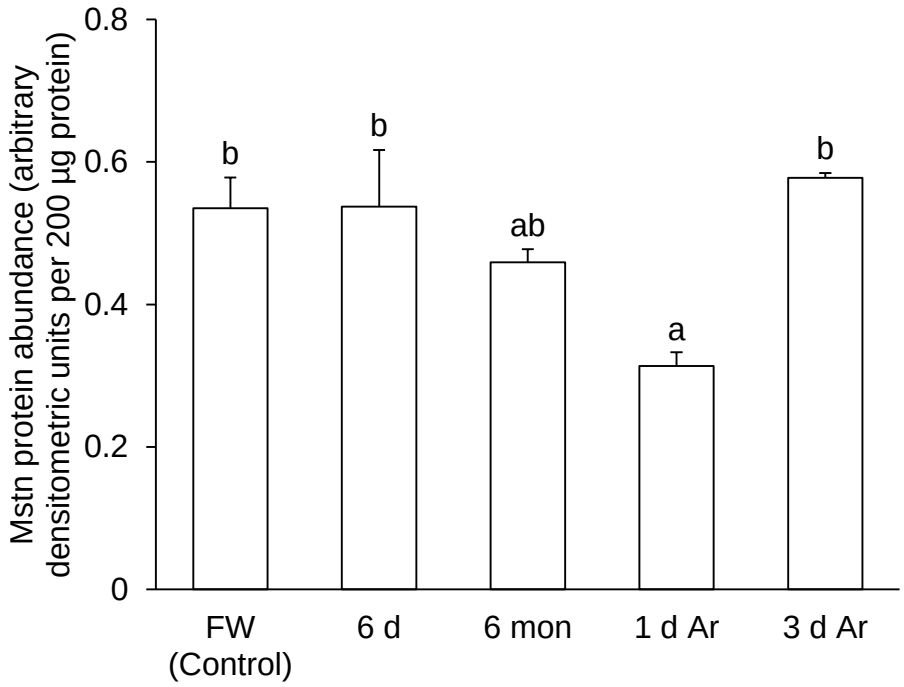

4.2.5. *fbxo32*/Fbxo32

4.2.5.1. Nucleotide sequence, translated amino acid sequence and dendrogramic analysis

The complete coding sequence of *fbxo32* from *P. annectens* consisted of 1062 bp. The deduced Fbxo32 sequence comprised 354 amino acids with an estimated molecular mass of 41.8 kDa (Appendix 2j), and shared the highest amino acid sequence identity with reptilian FBXO32 (58.2–80.3%) and coelacanth Fbxo32 (80.3%), followed by mammalian FBXO32 (77.8–79.2%), elasmobranch Fbxo32 (77%), teleost Fbxo32 (69.4–72.8%) and amphibian Fbxo32 (62.1%; Table 14).

An alignment of Fbxo32 from *P. annectens* with those from human, mouse, frog, rainbow trout and shark revealed that it contained a SV40-type monopartite NLS containing the basic amino acids KKRRK, which was highly conserved for all protein sequences compared (Fig. 39). The Fbxo32 from *P. annectens* was also found to contain a putative bipartite NLS located between position 276–304 (with reference to the ruler in Fig. 39), suggesting that *P. annectens* Fbxo32 could be localized to the nucleus. A conserved F-box domain was also found in *P. annectens* Fbxo32. A leucine-charged domain (LCD) containing an inverted LXXLL motif was found to be conserved in the Fbxo32 of *P. annectens*.

The Fbxo32 of *P. annectens* was grouped in a clade together with FBXO32 of tetrapods, Fbxo32 of *L. chalumnae* and Fbxo32 of the cartilaginous fish, *C. milii*, separated from Fbxo32 of teleosts (Fig. 40).

4.2.5.2. Gene expression of *fbxo32* in various tissues/organs

The muscle of *P. annectens* kept in fresh water had the highest expression level of *fbxo32* (Fig. 41). Apart from the muscle, *fbxo32* expression was detected in the heart, brain, eye, gills, kidney, lung, skin, liver, spleen, pancreas and gut.

4.2.5.3. mRNA expression of *fbxo32*

Significant increases in the mRNA expression levels of *fbxo32* were observed in the muscle of *P. annectens* after 3 days (4.81-fold; $P<0.05$) or 6 days (2.5-fold; $P<0.05$), or 12 days of aestivation (1.82-fold; $P<0.05$), as compared to the control (Fig. 42a). There were significant increases in the mRNA expression levels of *fbxo32* after 1 day (2.29-fold; $P<0.05$) or 6 days of arousal from 6 months of aestivation (4.34-fold; $P<0.05$; Fig. 42b).

4.2.5.4. Protein abundance of Fbxo32

There were significant decreases in the protein abundance of Fbxo32 in the muscle of *P. annectens* after 6 days (by 64.6%; $P<0.05$), or after 1 day of arousal from 6 months of aestivation (by 69.7%; $P<0.05$), as compared to the freshwater control (Fig. 43).

Table 14. The percentage similarity between the deduced amino acid sequence of F-box protein 32 (Fbxo32) from the muscle of *Protopterus annectens* and FBXO32/Fbxo32 sequences from other animal species obtained from GenBank (accession numbers in brackets). Sequences are arranged in a descending order of similarity.

Classification	Species	Similarity
Reptiles	*Chrysemys picta bellii* FBXO32 (XP_005288831.1)	80.3%
	Pelodiscus sinensis FBXO32 isoform X1 (XP_006137545.1)	80.1%
	Chelonia mydas FBXO32 (XP_007070931.1)	72.3%
	Pelodiscus sinensis FBXO32 isoform X2 (XP_006137546.1)	58.2%
Coelacanth	*Latimeria chalumnae* Fbxo32 isoform X1 (XP_006000858.1)	80.3%
Mammals	*Homo sapiens* FBXO32 isoform 1 (NP_478136.1)	79.2%
	Rattus norvegicus FBXO32 (NP_598205.1)	78.2%
	Mus musculus FBXO32 (NP_080622.1)	77.8%
Elasmobranch	*Callorhinchus milii* Fbxo32 (XP_007898752.1)	77.0%
Teleosts	*Poecilia reticulata* Fbxo32 (XP_008430324.1)	72.8%
	Astyanax mexicanus Fbxo32 (XP_007250892.1)	72.2%
	Danio rerio Fbxo32 (NP_957211.1)	71.9%
	Larimichthys crocea Fbxo32 (XP_010738325.1)	71.7%
	Oncorhynchus mykiss Fbxo32 (NP_001180255.1)	71.3%
	Stegastes partitus Fbxo32 (XP_008275201.1)	70.8%
	Salmo salar Fbxo32 (NP_001171956.1)	70.5%
	Esox lucius Fbxo32 (XP_010891067.1)	70.2%
	Notothenia coriiceps Fbxo32 (XP_010780879.1)	69.4%
Amphibian	*Xenopus (Silurana) tropicalis* Fbxo32 (AAH92557.1)	62.1%

Fig. 39. Molecular characterization of F-box protein 32 (Fbxo32) from the muscle of *Protopterus annectens*. Multiple amino acid alignment of Fbxo32 from the muscle of *P. annectens* with five other known FBXO32/Fbxo32 from *Homo sapiens* (NP_478136.1), *Mus musculus* (NP_080622.1), *Xenopus* (*Silurana*) *tropicalis* (AAH92557.1), *Oncorhynchus mykiss* (NP_001180255.1) and *Callorhinchus milii* (XP_007898752.1). Identical amino acids are indicated by shaded residues. The open box indicates the F-box domain. The putative nuclear localization sequences are underlined. The leucine-charged domain is denoted by a yellow box, with the inverted LXXLL motif indicated.

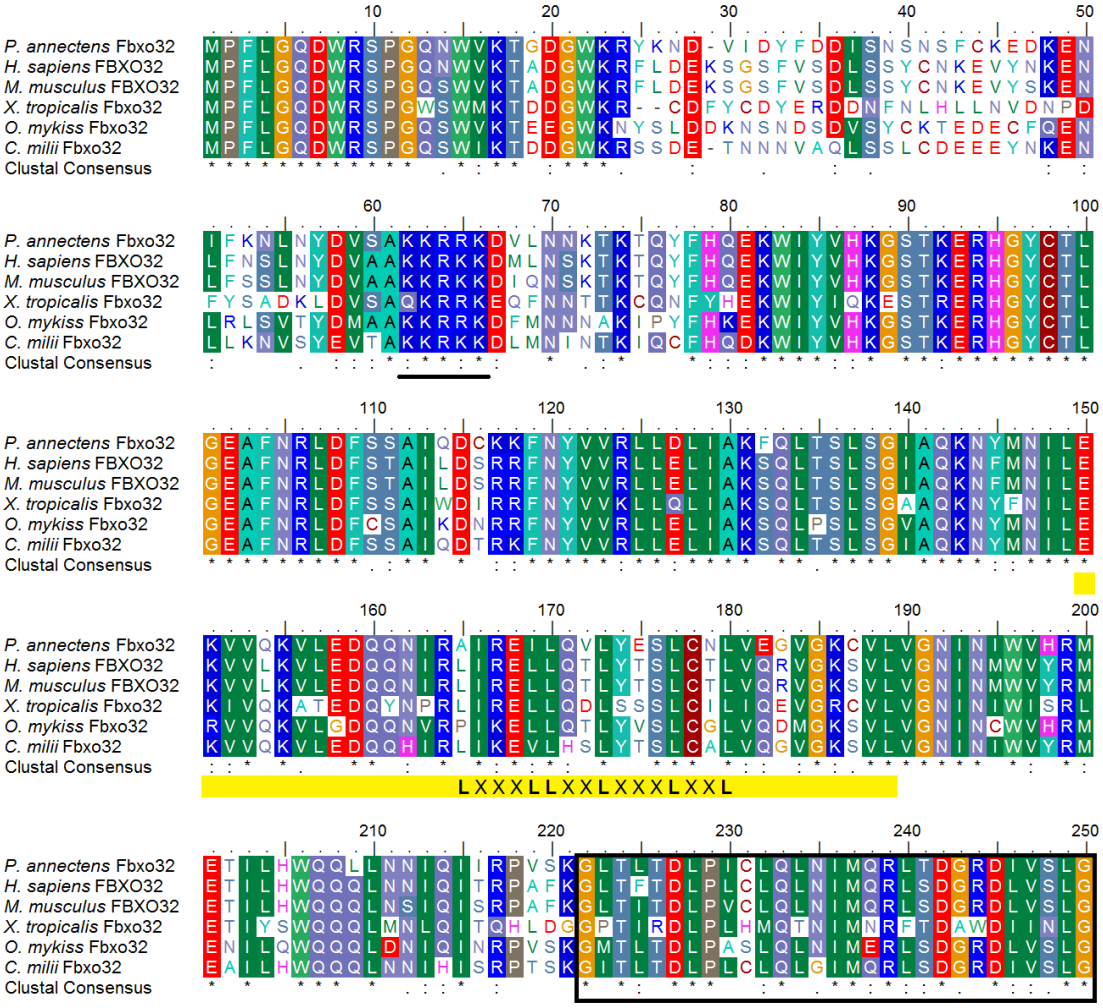

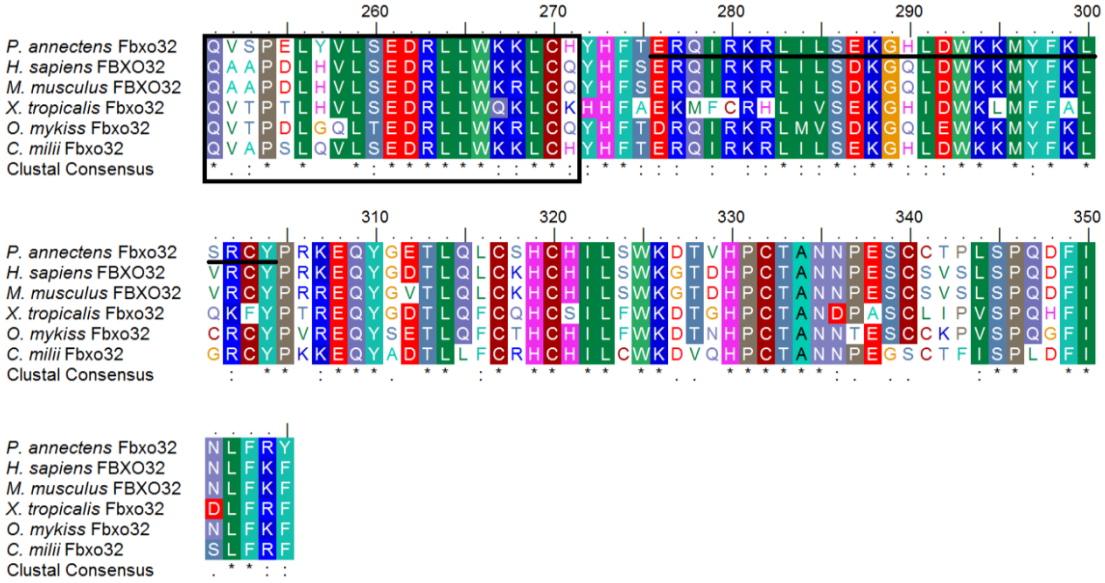
260
270
280
290
300
P. annectens Fbxo32
H. sapiens FBXO32
M. musculus FBXO32
X. tropicalis Fbxo32
O. mykiss Fbxo32
C. milii Fbxo32
Clustal Consensus
310
320
330
340
350
P. annectens Fbxo32
H. sapiens FBXO32
M. musculus FBXO32
X. tropicalis Fbxo32
O. mykiss Fbxo32
C. milii Fbxo32
Clustal Consensus

P. annectens Fbxo32
H. sapiens FBXO32
M. musculus FBXO32
X. tropicalis Fbxo32
O. mykiss Fbxo32
C. milii Fbxo32
Clustal Consensus

Fig. 40. A dendrogram of F-box protein 32 (FBXO32/Fbxo32) including that of *Protopterus annectens*. Numbers presented at each branch point represent bootstrap percentages from 1000 replicates. Fbxo32 from *Strongylocentrotus purpuratus* is used as the outgroup for the dendrogram.

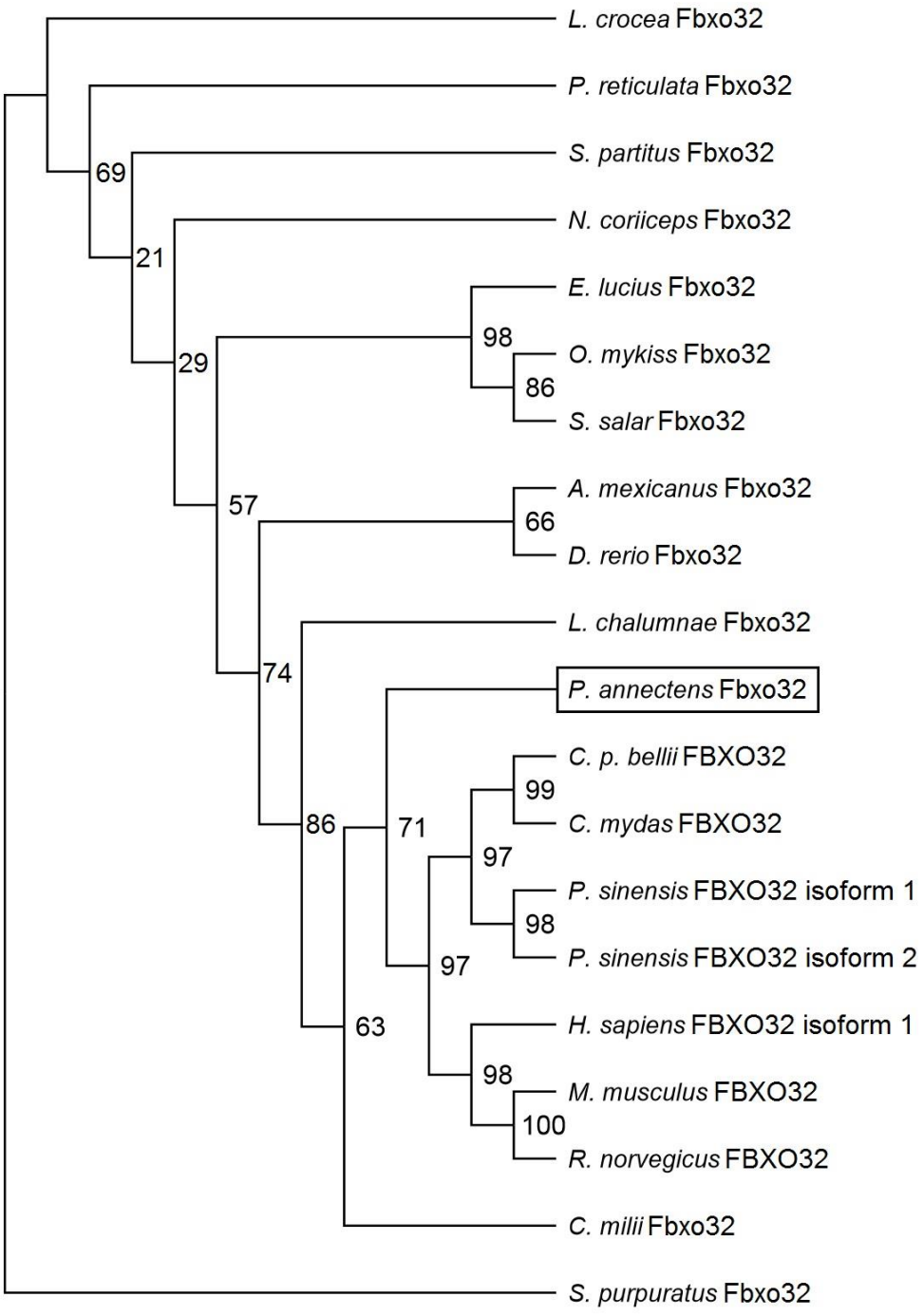

Fig. 41. The gene expression of *F-box protein 32* (*fbxo32*) in various tissues/organs of *Protopterus annectens*. Expression of *fbxo32* were examined in the muscle (M), heart (H), brain (B), eye (E), gills (Gi), kidney (K), Lung (Lu), skin (Sk), liver (Li), spleen (Sp), pancreas (P), and gut (Gu) of *Protopterus annectens* (*N*=1) kept in fresh water.

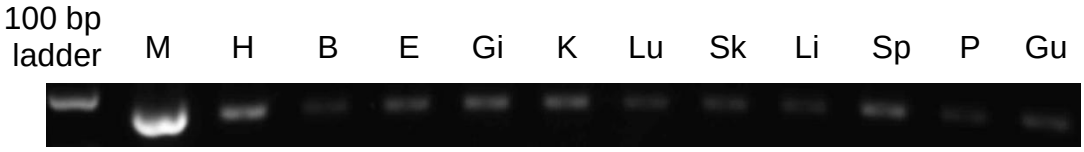

Fig. 42. mRNA expression levels of *F-box protein 32* (*fbxo32*) in the muscle of *Protopterus annectens*. Absolute quantification (x 10^4 copies of transcript per ng total RNA) of *fbxo32* transcripts in the muscle of *P. annectens* kept in (a) fresh water on day 0 (FW; control), after 3 or 6 days (d; the induction phase), or 12 d or 6 months (mon; the maintenance phase) of aestivation; (b) fresh water on day 0 (FW; control), after 6 mon (the maintenance phase) of aestivation, or after 1 d, 3 d or 6 d of arousal (Ar; the arousal phase) from 6 mon of aestivation. Results represent means ± S. E. M (*N*=4). Means not sharing the same letter are significantly different (*P*<0.05).

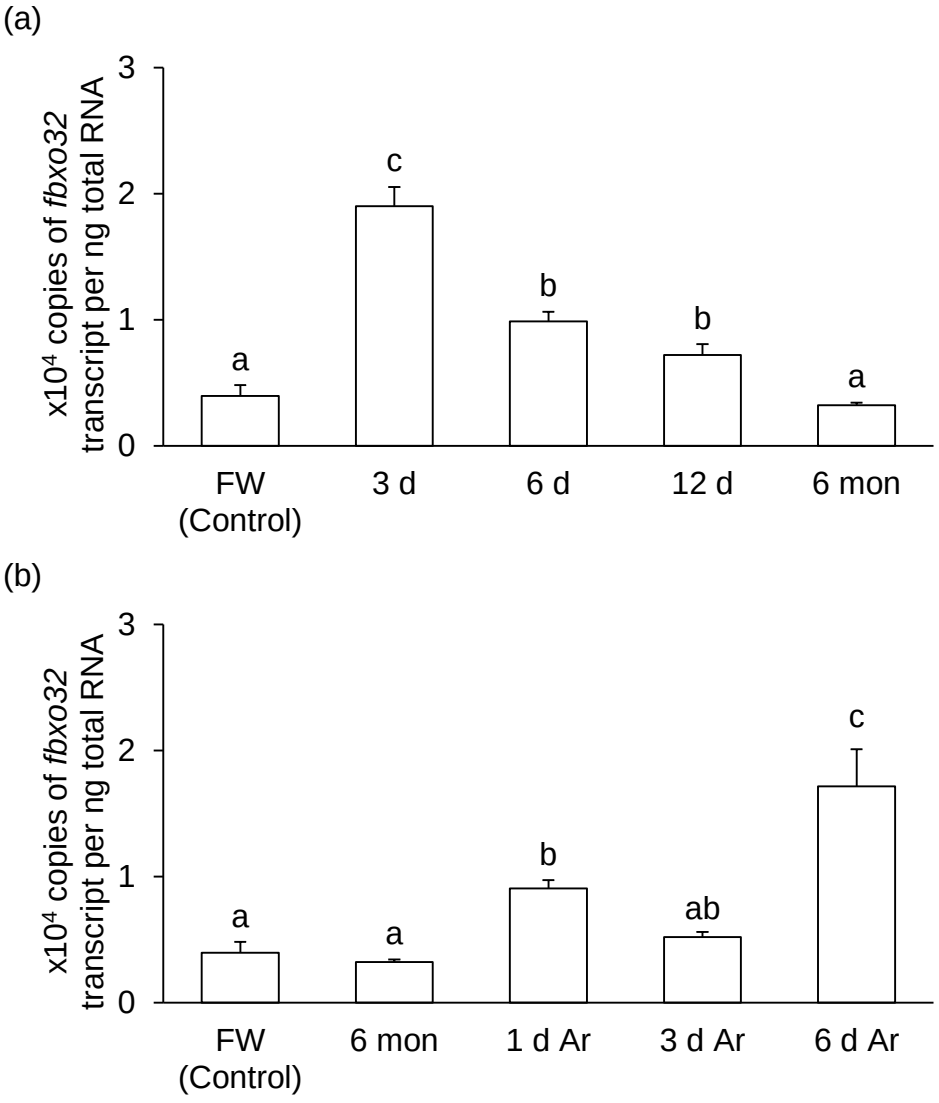

Fig. 43. Protein abundance of F-box protein 32 (Fbxo32) in the muscle of *Protopterus annectens*. Protein abundance of Fbxo32 in the muscle of *P. annectens* kept in fresh water on day 0 (FW; control), after 6 days (d; induction phase) or 6 months (mon; maintenance phase) of aestivation in air, or after 1 d or 3 d of arousal (Ar; arousal phase) from 6 mon of aestivation in air. (a) An example of immunoblot of Fbxo32. (b) The protein abundance of Fbxo32 expressed as arbitrary densitometric units per 100 µg protein. Results represent mean ± S.E.M. (N=3). Means not sharing the same letter are significantly different (P<0.05).

(a)

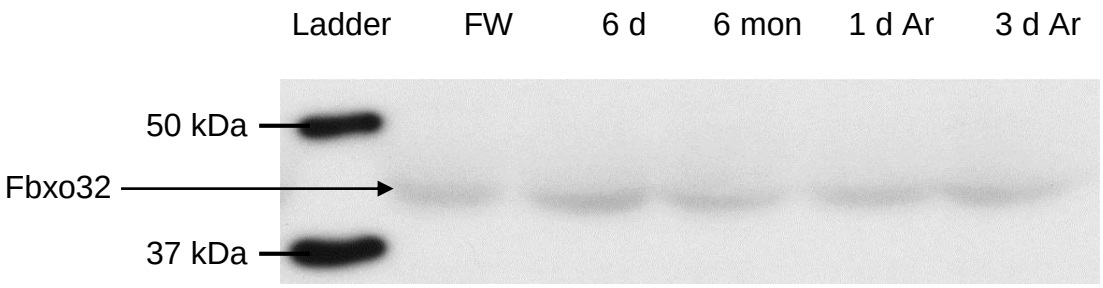

(b)

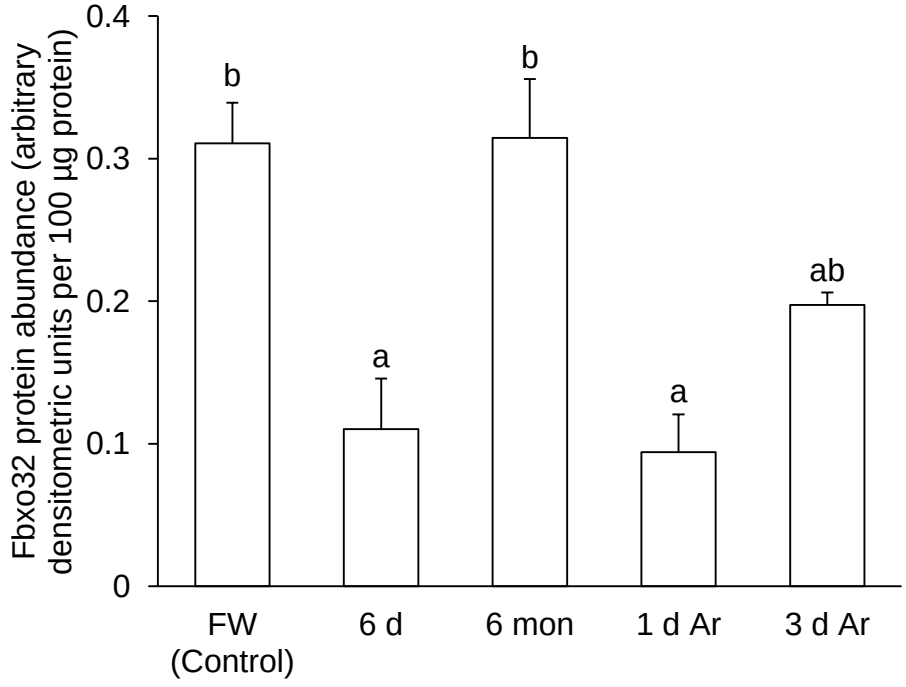

4.3. Genes/proteins involved in oxidative defense

4.3.1. *CuZnsod* and *Mnsod*/CuZnSod and MnSod

4.3.1.1. Gene expression of *CuZnsod* and *Mnsod* in various tissues/organs

The expression of *CuZnsod* was detected in the muscle, heart, brain, eye, gills, kidney, lung, skin, liver, spleen, pancreas and gut of *P. annectens* kept in fresh water (Fig. 44a). The gills of freshwater *P. annectens* had the highest expression level of *Mnsod* (Fig. 44b). Besides the gills, *Mnsod* expression was detected in the muscle, heart, brain, eye, kidney, lung, skin, liver, spleen, pancreas and gut.

4.3.1.2. mRNA expression of *CuZnsod* and *Mnsod*

There were significant decreases in the mRNA expression levels of *CuZnsod* in the muscle of *P. annectens* after 3 days (by 27.9%; $P<0.05$) or 6 days (by 29.2%; $P<0.05$) or 12 days (by 48%; $P<0.05$) or after 6 months of aestivation (by 38.8%; $P<0.05$), as compared to the control (Fig. 45a). The mRNA expression of *CuZnsod* after 1 day of arousal from 6 months of aestivation was not significantly different from that of the control, but decreased significantly (by 36.1%; $P<0.05$) after 3 days of arousal from 6 months of aestivation, before returning to the control level after 6 days of arousal from 6 months of aestivation (Fig. 45b).

There were significant decreases in the mRNA expression levels of *Mnsod* in the muscle of *P. annectens* after 3 days (by 35.6%; $P<0.05$) or 6 days (by 34.3%; $P<0.05$) or 12 days (by 38.4%; $P<0.05$) or after 6 months of aestivation (by 64.2%; $P<0.05$), as compared to the control (Fig. 46a). The mRNA expression of *Mnsod* decreased significantly after 1 day (by 54.8%; $P<0.05$) or 6 days of arousal from 6

months of aestivation (by 38.2%; $P<0.05$), as compared to the freshwater control (Fig. 46b).

4.3.1.3. Protein abundance of CuZnSod and MnSod

There were significant increases in the protein abundance of CuZnSod in the muscle of *P. annectens* after 6 months of aestivation (2.7-fold; $P<0.05$), or after 1 day (2.76-fold; $P<0.05$) or 3 days of arousal from 6 months of aestivation (2.03-fold; $P<0.05$), as compared to the freshwater control (Fig. 47).

There were no significant changes in the protein abundance of MnSod in the muscle of *P. annectens* after 6 days or 6 months of aestivation, or after 1 day or 3 days of arousal from 6 months of aestivation as compared to the control (Fig. 48).

Fig. 44. The gene expression of *copper-zinc superoxide dismutase* (*CuZnsod*) and *manganese sod* (*Mnsod*) in various tissues/organs of *Protopterus annectens*. Expression of (a) *CuZnsod* and (b) *Mnsod* were examined in the muscle (M), heart (H), brain (B), eye (E), gills (Gi), kidney (K), Lung (Lu), skin (Sk), liver (Li), spleen (Sp), pancreas (P), and gut (Gu) of *Protopterus annectens* (*N*=1) kept in fresh water.

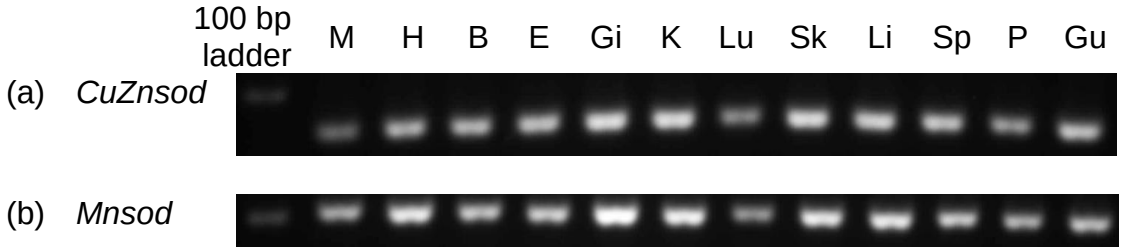

Fig. 45. mRNA expression levels of *copper-zinc superoxide dismutase* (*CuZnsod*) in the muscle of *Protopterus annectens*. Absolute quantification (×10^2 copies of transcript per ng total RNA) of *CuZnsod* transcripts in the muscle of *P. annectens* kept in (a) fresh water on day 0 (FW; control), after 3 or 6 days (d; the induction phase), or 12 d or 6 months (mon; the maintenance phase) of aestivation; (b) fresh water on day 0 (FW; control), after 6 mon (the maintenance phase) of aestivation, or after 1 d, 3 d or 6 d of arousal (Ar; the arousal phase) from 6 mon of aestivation. Results represent means ± S. E. M (N=4). Means not sharing the same letter are significantly different (P<0.05).

(a)

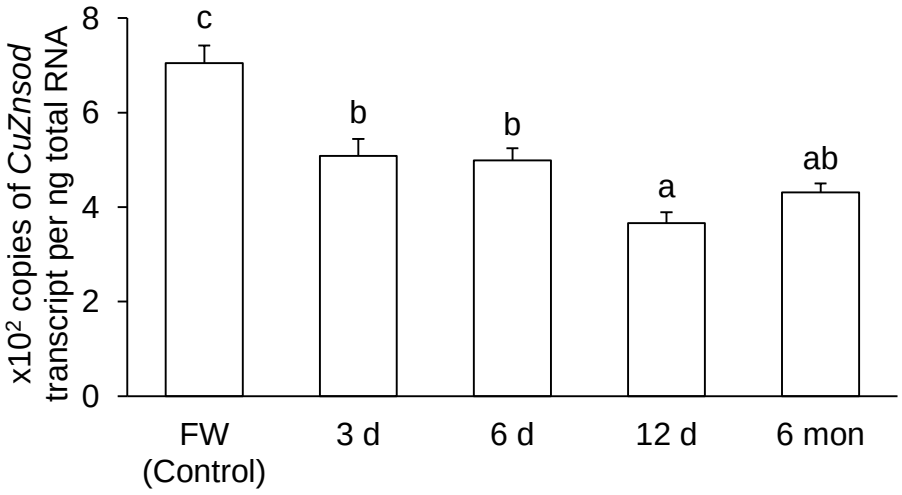

(b)

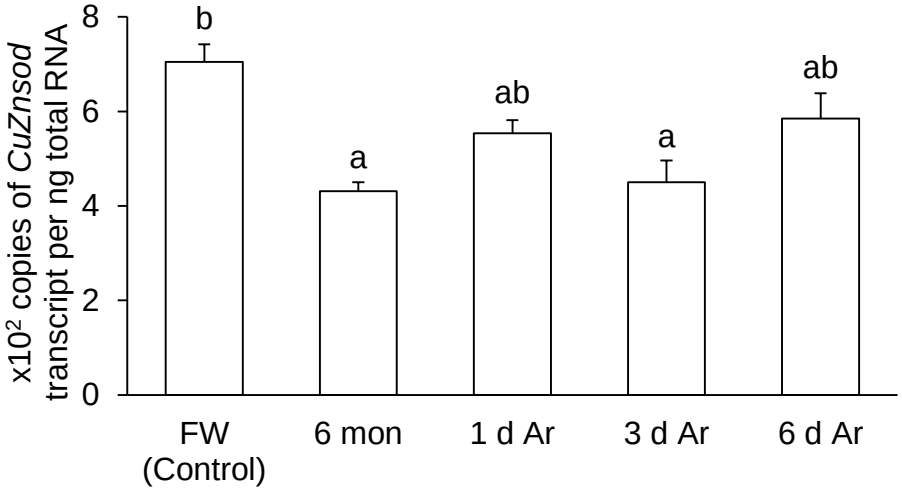

Fig. 46. mRNA expression levels of *manganese superoxide dismutase* (*Mnsod*) in the muscle of *Protopterus annectens*. Absolute quantification (×10^2 copies of transcript per ng total RNA) of *Mnsod* transcripts in the muscle of *P. annectens* kept in (a) fresh water on day 0 (FW; control), after 3 or 6 days (d; the induction phase), or 12 d or 6 months (mon; the maintenance phase) of aestivation; (b) fresh water on day 0 (FW; control), after 6 mon (the maintenance phase) of aestivation, or after 1 d, 3 d or 6 d of arousal (Ar; the arousal phase) from 6 mon of aestivation. Results represent means ± S. E. M (N=4). Means not sharing the same letter are significantly different (P<0.05).

(a)

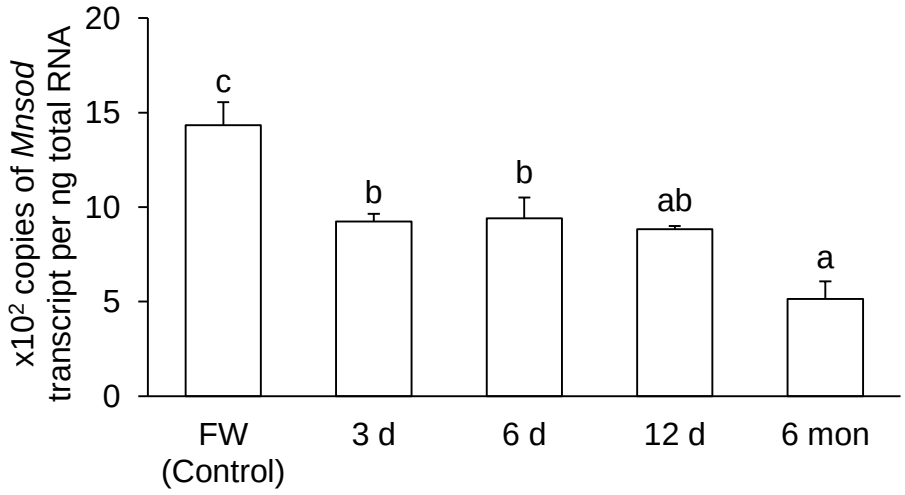

(b)

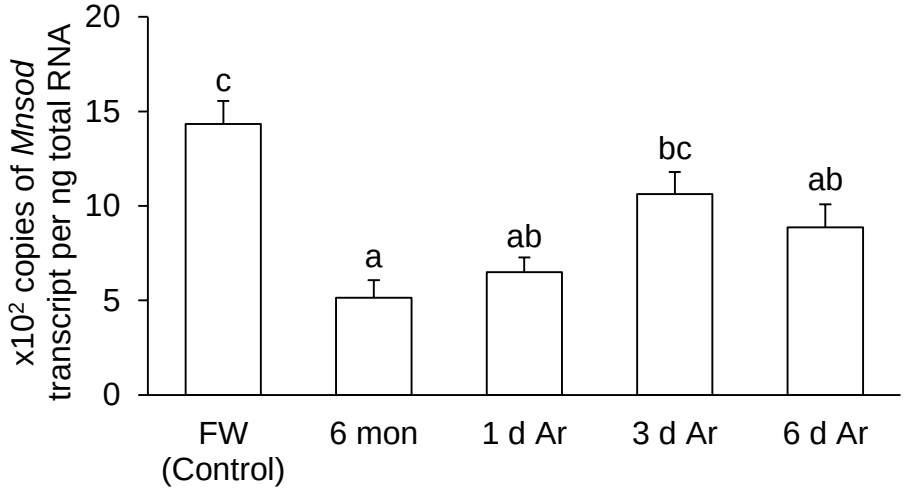

Fig. 47. Protein abundance of copper-zinc superoxide dismutase (CuZnSod) in the muscle of *Protopterus annectens*. Protein abundance of CuZnSod in the muscle of *P. annectens* kept in fresh water on day 0 (FW; control), after 6 days (d; induction phase) or 6 months (mon; maintenance phase) of aestivation in air, or after 1 d or 3 d of arousal (Ar; arousal phase) from 6 mon of aestivation in air. (a) An example of immunoblot of CuZnSod. (b) The protein abundance of CuZnSod expressed as arbitrary densitometric units per 100 μg protein. Results represent mean ± S.E.M. (N=3). Means not sharing the same letter are significantly different (P<0.05).

(a)

(b)

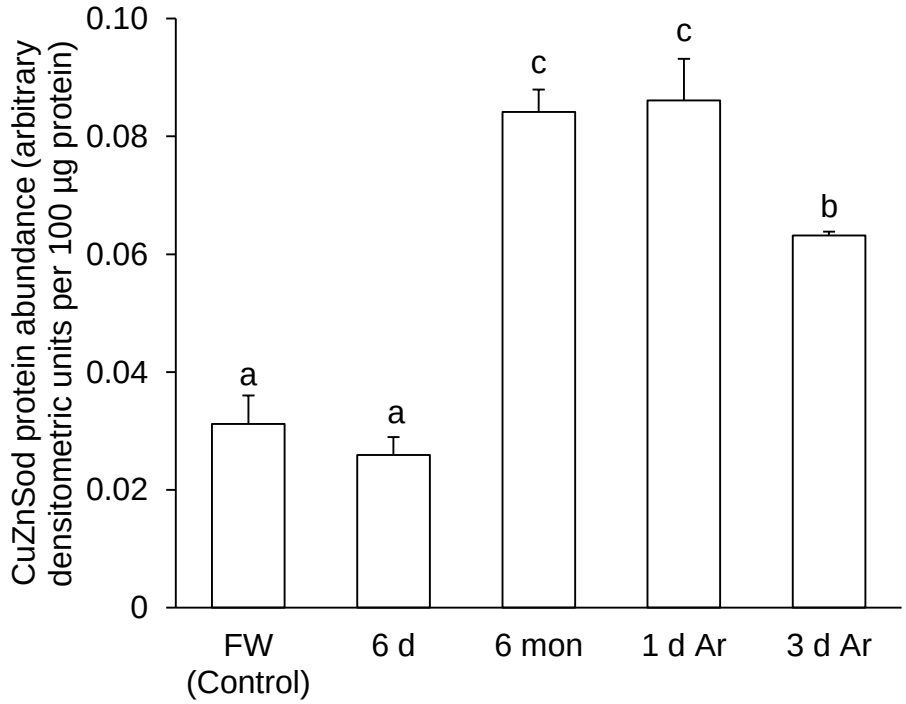

Fig. 48. Protein abundance of manganese superoxide dismutase (MnSod) in the muscle of *Protopterus annectens*. Protein abundance of MnSod in the muscle of *P. annectens* kept in fresh water on day 0 (FW; control), after 6 days (d; induction phase) or 6 months (mon; maintenance phase) of aestivation in air, or after 1 d or 3 d of arousal (Ar; arousal phase) from 6 mon of aestivation in air. (a) An example of immunoblot of MnSod. (b) The protein abundance of MnSod expressed as arbitrary densitometric units per 100 μg protein. Results represent mean ± S.E.M. (*N*=3).

(a)

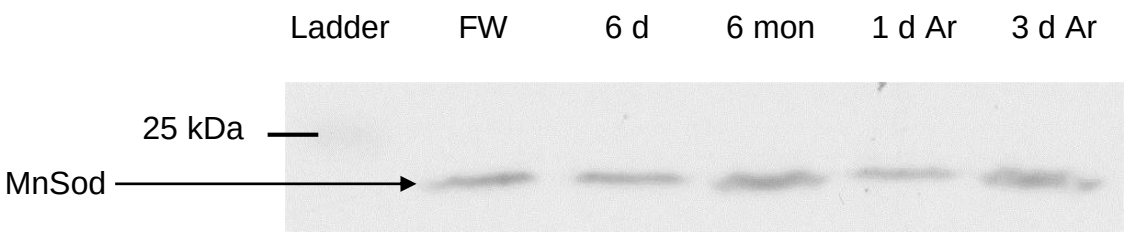

(b)

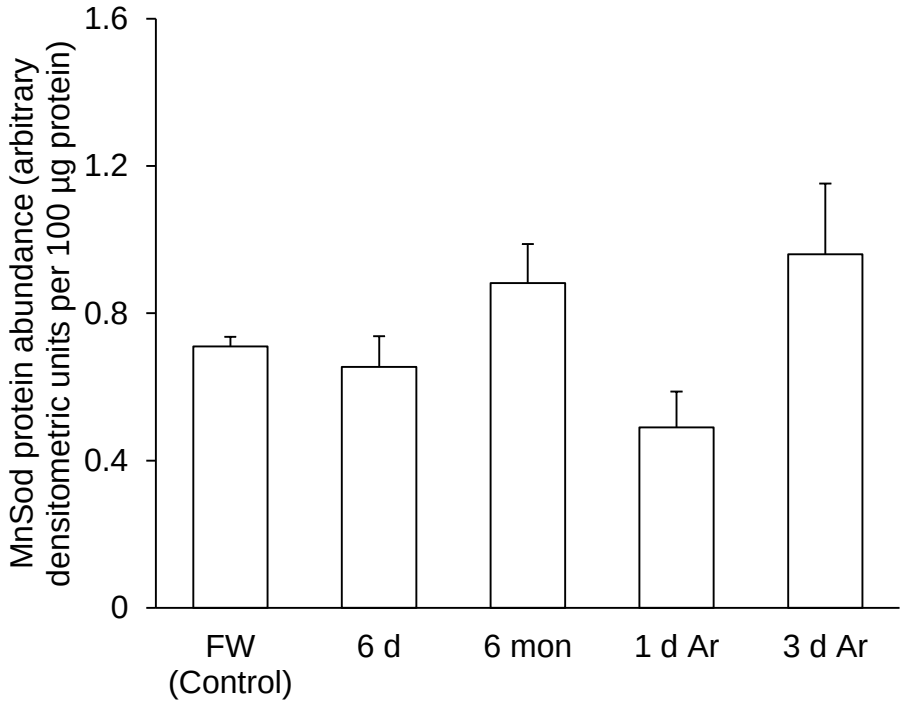

4.3.2. *cat*/Cat

4.3.2.1. Gene expression of *cat* in various tissues/organs

The highest expression level of *cat* was observed in the liver of *P. annectens* kept in fresh water (Fig. 49). Besides the liver, *cat* expression was detected in the muscle, heart, brain, eye, gill, kidney, lung, skin, spleen, pancreas and gut.

4.3.2.2. mRNA expression of *cat*

There were no significant changes in the mRNA expression levels of *cat* in the muscle of *P. annectens* during the induction, maintenance and arousal phases when compared to the freshwater control (Fig. 50).

4.3.2.3. Protein abundance of Cat

There were significant increases in the protein abundance of Cat in the muscle of *P. annectens* after 6 days of aestivation (4.11-fold; $P<0.05$) or after 1 day of arousal from 6 months of aestivation (4.97-fold; $P<0.05$), as compared to the freshwater control (Fig. 51).

Fig. 49. The gene expression of *catalase* (*cat*) in various tissues/organs of *Protopterus annectens*. Expression of *cat* were examined in the muscle (M), heart (H), brain (B), eye (E), gills (Gi), kidney (K), Lung (Lu), skin (Sk), liver (Li), spleen (Sp), pancreas (P), and gut (Gu) of *Protopterus annectens* (*N*=1) kept in fresh water.

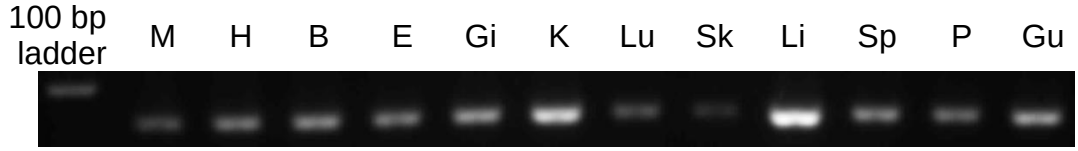

Fig. 50. mRNA expression levels of *catalase* (*cat*) in the muscle of *Protopterus annectens*. Absolute quantification (×10^2 copies of transcript per ng total RNA) of *cat* transcripts in the muscle of *P. annectens* kept in (a) fresh water on day 0 (FW; control), after 3 or 6 days (d; the induction phase), or 12 d or 6 months (mon; the maintenance phase) of aestivation; (b) fresh water on day 0 (FW; control), after 6 mon (the maintenance phase) of aestivation, or after 1 d, 3 d or 6 d of arousal (Ar; the arousal phase) from 6 mon of aestivation. Results represent means ± S. E. M (*N*=4). Means not sharing the same letter are significantly different (*P*<0.05).

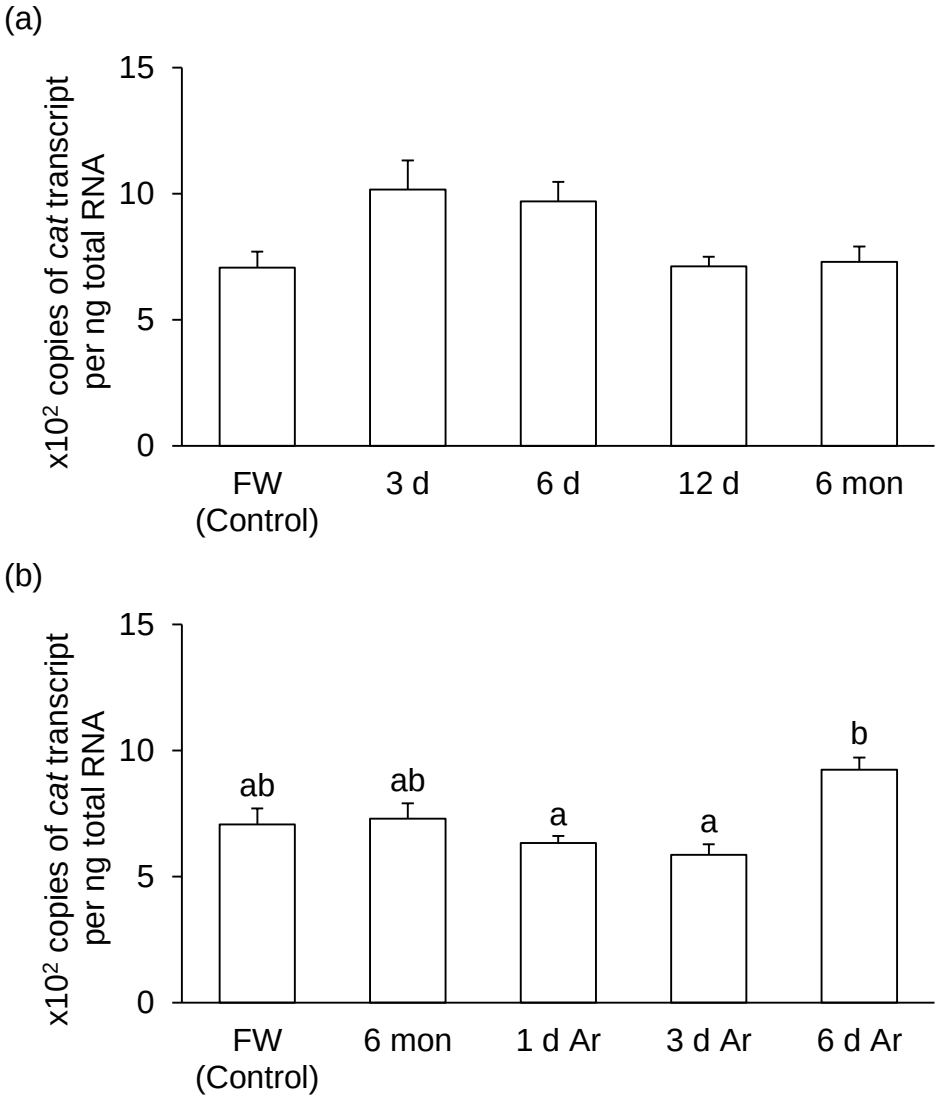

Fig. 51. Protein abundance of catalase (Cat) in the muscle of *Protopterus annectens*. Protein abundance of Cat in the muscle of *P. annectens* kept in fresh water on day 0 (FW; control), after 6 days (d; induction phase) or 6 months (mon; maintenance phase) of aestivation in air, or after 1 d or 3 d of arousal (Ar; arousal phase) from 6 mon of aestivation in air. (a) An example of immunoblot of Cat. (b) The protein abundance of Cat expressed as arbitrary densitometric units per 100 μg protein. Results represent mean ± S.E.M. (*N*=3). Means not sharing the same letter are significantly different ($P<0.05$).

(a)

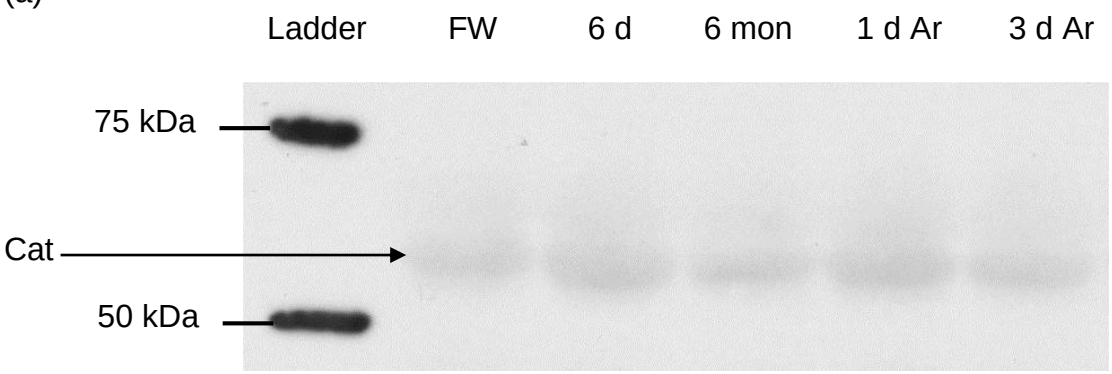

(b)

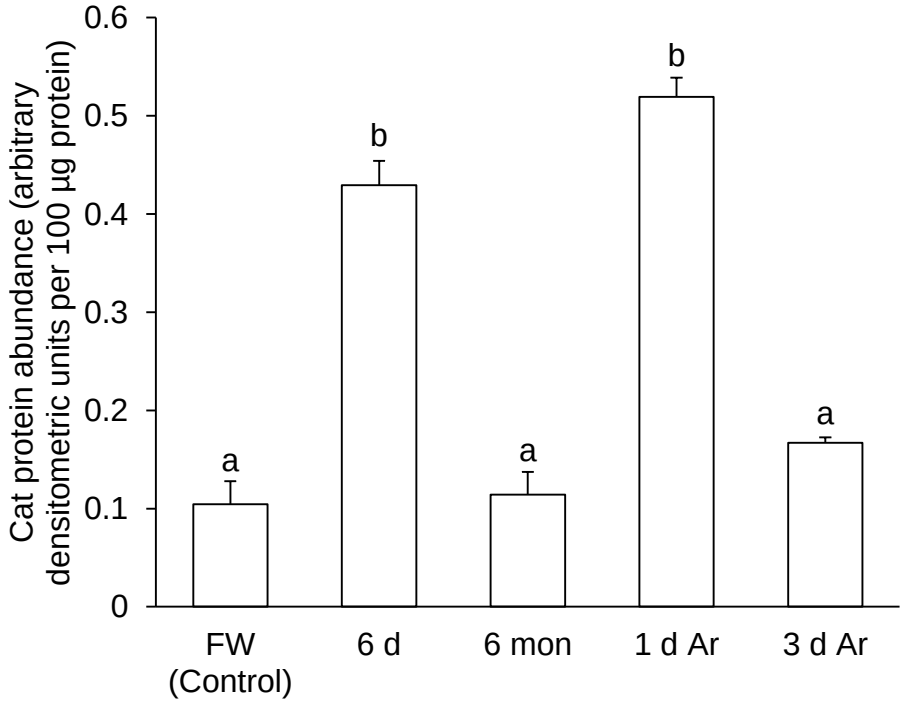

4.3.3. *gpx1* and *gpx4*/Gpx1 and Gpx4

4.3.3.1. Gene expression of *gpx1* and *gpx4* in various tissues/organs

The highest expression levels of *gpx1* were detected in the gills, kidney and skin of freshwater *P. annectens* (Fig. 52a). The expression of *gpx1* was detected in the muscle, heart, brain, eye, lung, liver, spleen, pancreas and gut. The expression of *gpx4* was detected in the muscle, heart, brain, eye, gills, kidney, lung, skin, liver, spleen, pancreas and gut of *P. annectens* kept in fresh water (Fig. 52b).

4.3.3.2. mRNA expression of *gpx1* and *gpx4*

There were significant decreases in the mRNA expression levels of *gpx1* in the muscle of *P. annectens* after 3 days (by 73.1%; $P<0.05$) or 6 days (by 57.6%; $P<0.05$) or 12 days (by 69.2%; $P<0.05$) or after 6 months of aestivation (by 66.2%; $P<0.05$), as compared to the freshwater control (Fig. 53a). The mRNA expression of *gpx1* decreased significantly after 1 day (by 67.9%; $P<0.05$) or 3 days of arousal from 6 months of aestivation (by 70.2%; $P<0.05$), and returned to the control level after 6 days of arousal from 6 months of aestivation (Fig. 53b).

There was a significant increase in the mRNA expression level of *gpx4* in the muscle of *P. annectens* after 6 months of aestivation (2.46-fold; $P<0.05$), as compared to the freshwater control (Fig. 54a). A significant increase in the mRNA expression level of *gpx4* occurred after 3 days of arousal from 6 months of aestivation (2.21-fold; $P<0.05$; Fig. 54b).

4.3.3.3. Protein abundance of Gpx1 and Gpx4

The protein abundance of Gpx1 in the muscle of *P. annectens* increased significantly after 3 days of arousal from 6 months of aestivation (3.04-fold; $P<0.05$), as compared

to the freshwater control (Fig. 55). The protein abundance of Gpx4 in the muscle of *P. annectens* increased significantly after 6 months of aestivation (6-fold; $P<0.05$), as compared to the control (Fig. 56).

Fig. 52. The gene expression of *glutathione peroxidase 1* (*gpx1*) and *4* (*gpx4*) in various tissues/organs of *Protopterus annectens*. Expression of (a) *gpx1* and (b) *gpx4* were examined in the muscle (M), heart (H), brain (B), eye (E), gills (Gi), kidney (K), Lung (Lu), skin (Sk), liver (Li), spleen (Sp), pancreas (P), and gut (Gu) of *Protopterus annectens* (*N*=1) kept in fresh water.

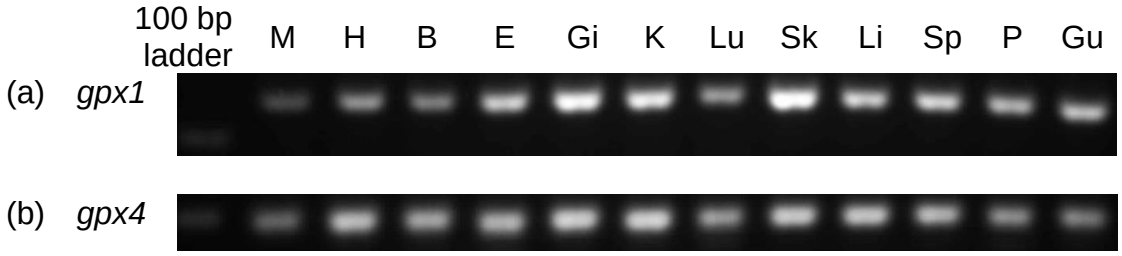

Fig. 53. mRNA expression levels of *glutathione peroxidase 1* (*gpx1*) in the muscle of *Protopterus annectens*. Absolute quantification (copies of transcript per ng total RNA) of *gpx1* transcripts in the muscle of *P. annectens* kept in (a) fresh water on day 0 (FW; control), after 3 or 6 days (d; the induction phase), or 12 d or 6 months (mon; the maintenance phase) of aestivation; (b) fresh water on day 0 (FW; control), after 6 mon (the maintenance phase) of aestivation, or after 1 d, 3 d or 6 d of arousal (Ar; the arousal phase) from 6 mon of aestivation. Results represent means ± S. E. M (N=4). Means not sharing the same letter are significantly different (P<0.05).

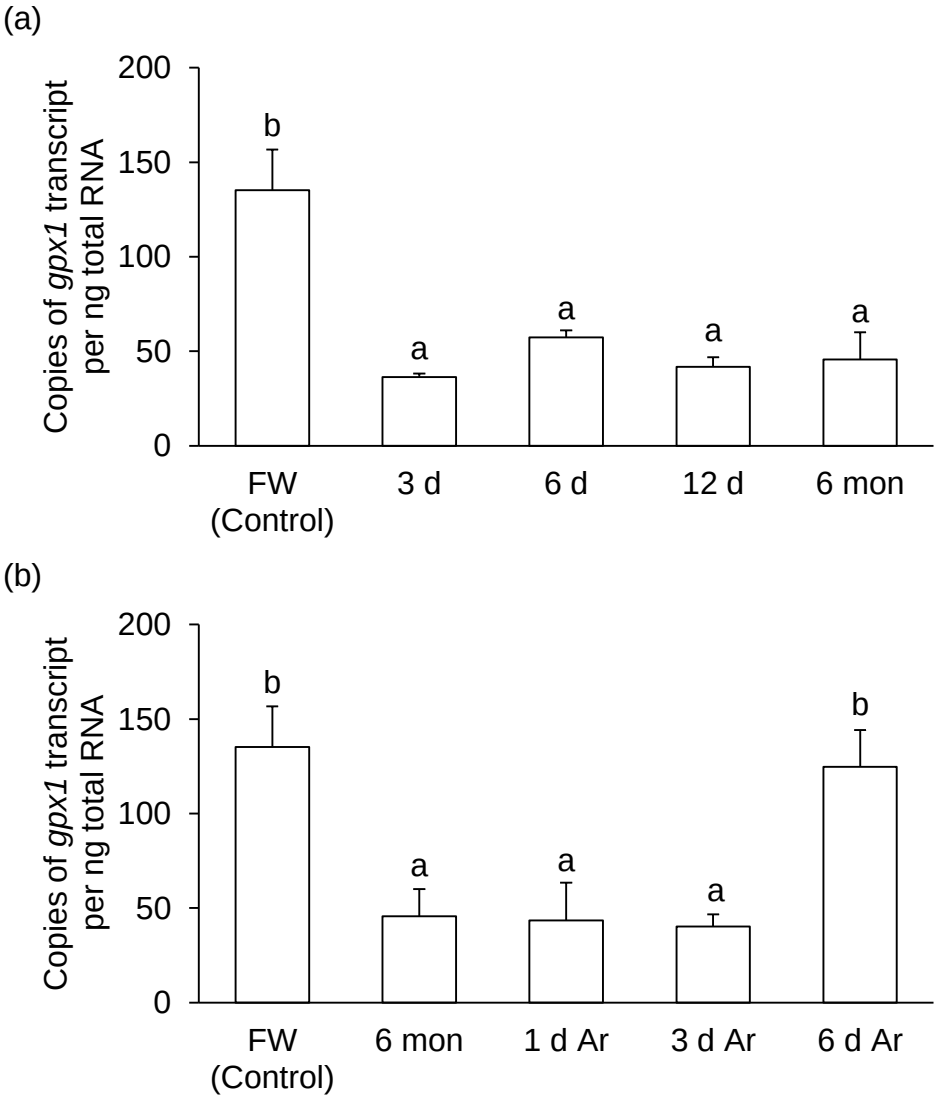

Fig. 54. mRNA expression levels of *glutathione peroxidase 4* (*gpx4*) in the muscle of *Protopterus annectens*. Absolute quantification ($\times 10^2$ copies of transcript per ng total RNA) of *gpx4* transcripts in the muscle of *P. annectens* kept in (a) fresh water on day 0 (FW; control), after 3 or 6 days (d; the induction phase), or 12 d or 6 months (mon; the maintenance phase) of aestivation; (b) fresh water on day 0 (FW; control), after 6 mon (the maintenance phase) of aestivation, or after 1 d, 3 d or 6 d of arousal (Ar; the arousal phase) from 6 mon of aestivation. Results represent means ± S. E. M (N=4). Means not sharing the same letter are significantly different (P<0.05).

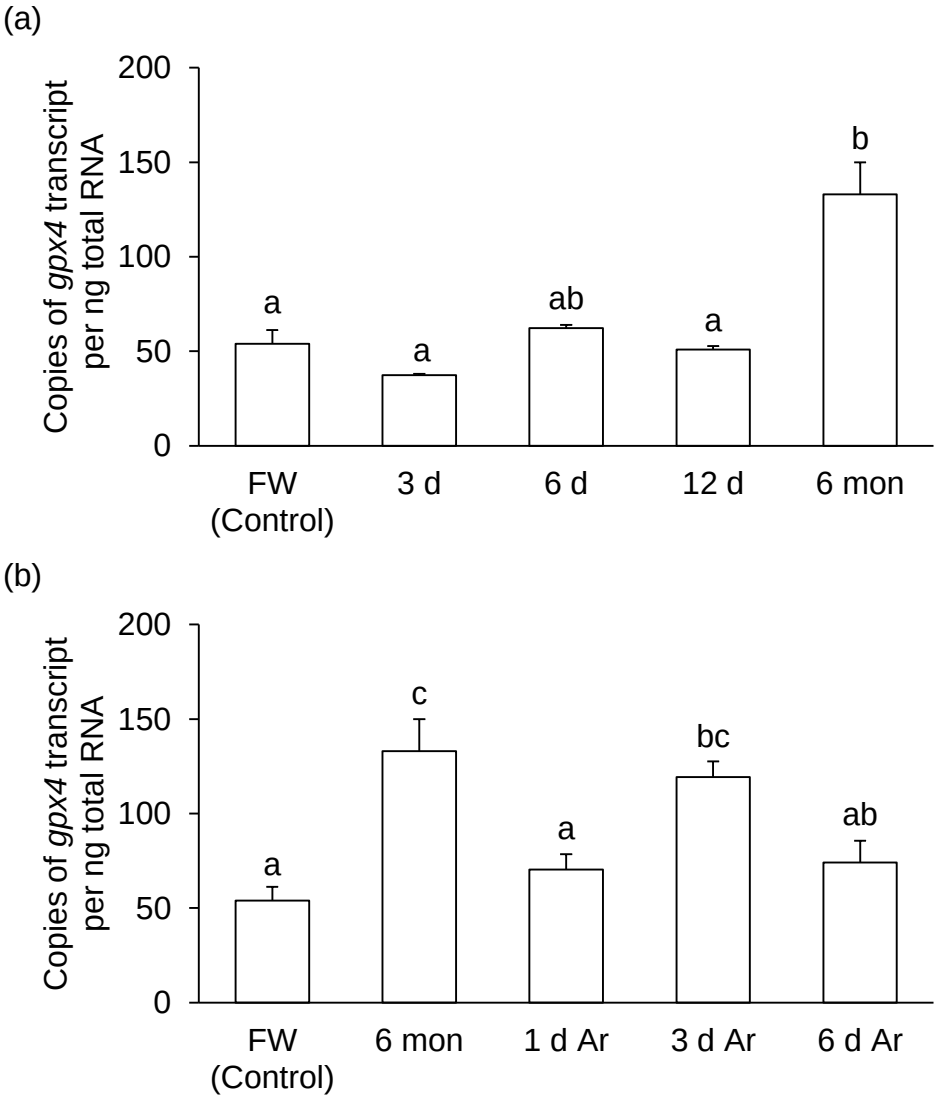

Fig. 55. Protein abundance of glutathione peroxidase 1 (Gpx1) in the muscle of *Protopterus annectens*. Protein abundance of Gpx1 in the muscle of *P. annectens* kept in fresh water on day 0 (FW; control), after 6 days (d; induction phase) or 6 months (mon; maintenance phase) of aestivation in air, or after 1 d or 3 d of arousal (Ar; arousal phase) from 6 mon of aestivation in air. (a) An example of immunoblot of Gpx1. (b) The protein abundance of Gpx1 expressed as arbitrary densitometric units per 200 µg protein. Results represent mean ± S.E.M. (N=3). Means not sharing the same letter are significantly different (P<0.05).

(a)

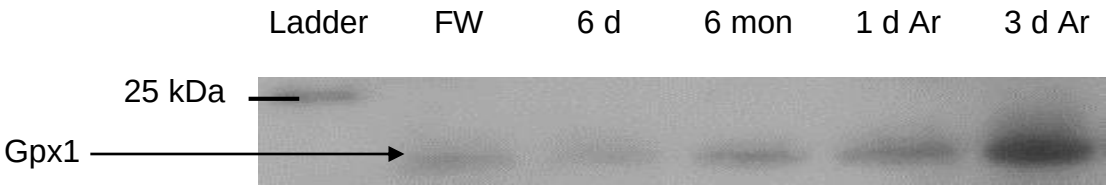

(b)

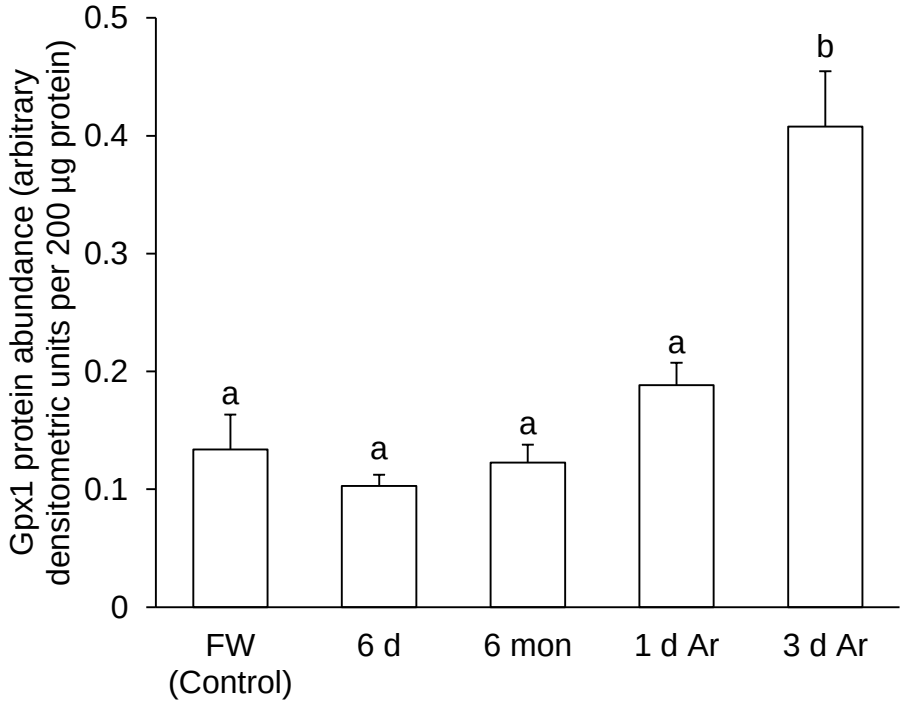

Fig. 56. Protein abundance of glutathione peroxidase 4 (Gpx4) in the muscle of *Protopterus annectens*. Protein abundance of Gpx4 in the muscle of *P. annectens* kept in fresh water on day 0 (FW; control), after 6 days (d; induction phase) or 6 months (mon; maintenance phase) of aestivation in air, or after 1 d or 3 d of arousal (Ar; arousal phase) from 6 mon of aestivation in air. (a) An example of immunoblot of Gpx4. (b) The protein abundance of Gpx4 expressed as arbitrary densitometric units per 200 µg protein. Results represent mean ± S.E.M. (N=3). Means not sharing the same letter are significantly different (P<0.05).

(a)

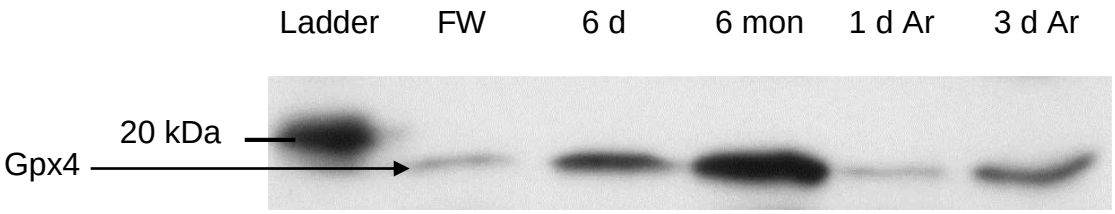

(b)

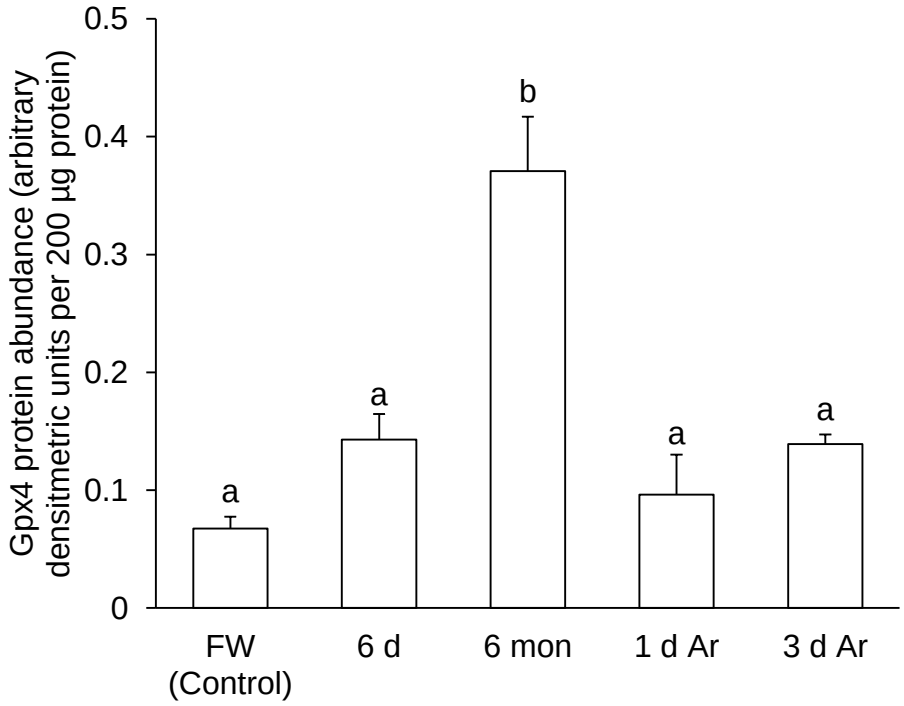

4.3.4. Activities of various enzymes involved in oxidative defense in the muscle of *P. annectens* during three phases of aestivation

4.3.4.1. Sod

There were no significant changes in the activities of CuZnSod and total Sod after 6 days or 6 months of aestivation, or after 3 days of arousal from 6 months of aestivation as compared to the control (Table 15). There was a significant increase in the activity of MnSod (12.2-fold; $P<005$) after 3 days of arousal from 6 months of aestivation (Table 15).

4.3.4.2. Cat

There were no significant changes in Cat activity after 6 days or 6 months of aestivation, or after 3 days of arousal from 6 months of aestivation when compared to the freshwater control (Table 15).

4.3.4.3. Gpx

There were significant increases in the activities of SeGpx (4.08-fold; $P<005$) and total Gpx (8.20-fold; $P<0.05$) after 6 months of aestivation when compared to the control (Table 15). The activities of SeGpx and total Gpx returned to the control levels after 3 days of arousal from 6 months of aestivation.

4.3.4.4. Gr

There was a significant increase in the activity of Gr after 6 days of aestivation (2.36-fold; $P<0.05$), as compared to the control, after which it returned to the control level after 6 months of aestivation or after 3 days of arousal from 6 months of aestivation (Table 15).

Table 15. Specific activities [nmol min^{-1} mg^{-1} protein except superoxide dismutase (Sod)] of copper-zinc Sod (CuZnSod; mU mg^{-1} protein), manganese Sod (MnSod), total Sod, catalase (Cat), selenium-dependent glutathione peroxidase (SeGpx), total Gpx, glutathione reductase (Gr), and glutathione-S-transferase (Gst) from the muscle of *Protopterus annectens* kept in fresh water on day 0 (FW; control), after 6 days (d; induction phase) or 6 months (mon; maintenance phase) of aestivation in air, or after 3 d of arousal (Ar; arousal phase) from 6 mon of aestivation in air. Results represent mean ± S.E.M. (N=4). Means not sharing the same letter are significantly different (P<0.05).

Antioxidant enzymes	FW (Control)	6 d (Induction phase)	6 mon (Maintenance phase)	3 d Ar (Arousal phase)
CuZnSod	24.28 ± 3.58	27.63 ± 4.92	45.85 ± 10.70	27.63 ± 6.66
MnSod	0.78 ± 0.28[a]	0.86 ± 0.31[a]	1.15 ± 0.32[a]	9.51 ± 1.78[b]
Total Sod	25.08 ± 3.40	28.45 ± 4.99	47.00 ± 10.52	37.15 ± 5.85
Cat	480 ± 69[ab]	754 ± 122[b]	268 ± 81[a]	394 ± 101[ab]
SeGpx	2.80 ± 0.53[a]	6.39 ± 0.36[ab]	11.4 ± 3.3[b]	4.00 ± 0.35[a]
Total Gpx	1.39 ± 0.30[a]	0.93 ± 0.43[a]	11.4 ± 3.8[b]	1.72 ± 0.59[a]
Gr	0.275 ± 0.018[a]	0.650 ± 0.048[b]	0.303 ± 0.034[a]	0.383 ± 0.079[a]
Gst	3.95 ± 0.70[ab]	3.10 ± 0.35[a]	5.82 ± 1.69[ab]	6.23 ± 0.54[b]

4.3.4.5. Gst

There were no significant changes in Gst activity after 6 days or 6 months of aestivation, or after 3 days of arousal from 6 months of aestivation when compared to the freshwater control (Table 15).

4.3.5. Total GSHeq, GSH, GSSG and GSSG/GSH in the muscle of *P. annectens* during three phases of aestivation

The content of total GSHeq in the muscle of *P. annectens* increased significantly after 6 months of aestivation (3.86–fold; $P<0.05$), or after 3 days of arousal from 6 months of aestivation (3.11–fold; $P<0.05$), as compared to the control (Table 16). Likewise, there were significant increases in the content of GSH in the muscle of *P. annectens* after 6 months of aestivation (3.71–fold; $P<0.05$), or after 3 days of arousal from 6 months of aestivation (3.08–fold; $P<0.05$), as compared to the freshwater control. There were significant increases in the GSSG content in the muscle of *P. annectens* after 6 days (20.0–fold; $P<0.05$), or 6 months of aestivation (89.0–fold; $P<0.05$), as compared to the freshwater control. The GSSG/GSH ratio increased significantly after 6 days (44.0–fold; $P<0.05$), or 6 months of aestivation (28.6–fold; $P<0.05$), as compared to the control.

Table 16. Contents (nmol g^{-1} wet mass) of total glutathione equivalents (total GSHeq), reduced glutathione (GSH), oxidized glutathione (GSSG) and the GSSG/GSH ratio in the muscle of *Protopterus annectens* kept in fresh water on day 0 (FW; control), after 6 days (d; induction phase) or 6 months (mon; maintenance phase) of aestivation in air, or after 3 d of arousal (Ar; arousal phase) from 6 mon of aestivation in air. Results represent mean ± S.E.M. (*N*=4). Means not sharing the same letter are significantly different (*P*<0.05).

	FW (Control)	6 d (Induction phase)	6 mon (Maintenance phase)	3 d Ar (Arousal phase)
Total GSHeq	8.41 ± 1.90[a]	5.43 ± 0.25[a]	32.5 ± 5.1[b]	26.2 ± 0.4[b]
GSH	8.40 ± 1.90[a]	5.12 ± 0.24[a]	31.2 ± 4.5[b]	25.8 ± 0.4[b]
GSSG	0.00750 ± 0.00750[a]	0.150 ± 0.021[b]	0.668 ± 0.329[c]	0.155 ± 0.118[abc]
GSSG/GSH	0.000674 ± 0.000674[a]	0.0296 ± 0.0039[b]	0.0193 ± 0.0069[b]	0.00611 ± 0.00469[ab]

4.3.6. Oxidative damage products in the muscle of *P. annectens* during three phases of aestivation

There were no significant changes in the contents of LOOH and TBARS in the muscle of *P. annectens* during the three phases of aestivation, as compared to the freshwater control (Fig. 57). However, there were significant decreases in the content of carbonyl proteins in the muscle of *P. annectens* after 6 months of aestivation (by 45.1%; $P<0.05$), or after 3 days of arousal from 6 months of aestivation (by 26.4%; $P<0.05$; Fig. 57).

Fig. 57. Oxidative damage products in the muscle of *Protopterus annectens*. Contents of lipid hydroperoxides (µmol cumene hydroperoxide equivalents (CHE) g-1 wet mass; □), thiobarbituric acid reactive substances (TBARS; nmol g-1 wet mass; ▩) and carbonyl proteins (µmol g-1 wet mass; ▨) in the muscle of P. annectens kept in fresh water on day 0 (FW; control), after 6 days (d; induction phase) or 6 months (mon; maintenance phase) of aestivation in air, or after 3 d of arousal (Ar; arousal phase) from 6 mon of aestivation in air. Results represent mean ± S.E.M. (N=4). Means not sharing the same letter (a, b, c for TBARS and x, y, z for carbonyl proteins) are significantly different (P<0.05).

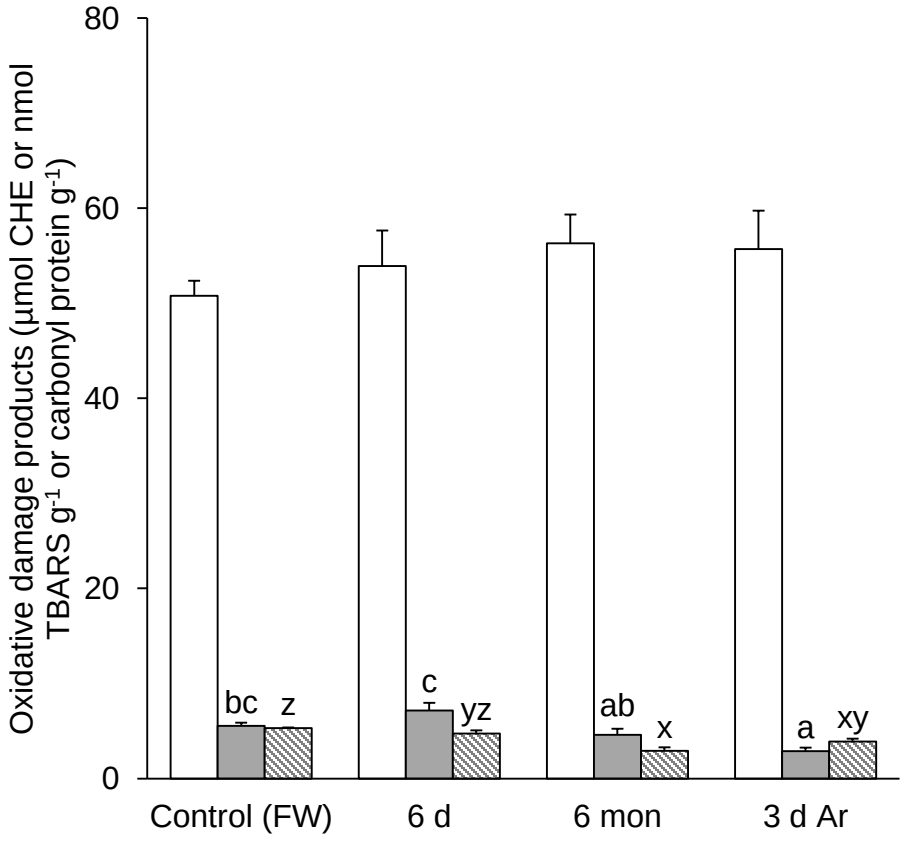

5. Discussion

5.1. Molecular characterization of various genes/proteins involved in muscle formation and degradation from *P. annectens*

5.1.1. Molecular characterization of proteins involved in muscle formation

5.1.1.1. Ppargc-1α

The N terminus of Ppargc-1α containing the ADs and the LXXLL motif is well conserved in the Ppargc-1α of *P. annectens.* The ADs are crucial to to PPARGC-1α transcriptional activity (Sadana and Park, 2007), and facilitate the transcriptional activation of target genes by recruiting histone remodeling proteins upon interaction with DNA-bound proteins (Puigserver et al., 1999, 2003). The deletion of AD1 and AD2 results in a decrease in the induction of various PPARGC-1α-regulated genes such as *phosphoenolpyruvate carboxykinase* and *carnitine palmitoyltransferase-I*, but does not affect the recruitment of PPARGC-1α to its target genes (Sadana and Park, 2007). The negatively-charged amino acids and leucine residues are important for the transcriptional induction of the target genes of PPARGC-1α (Sadana and Park, 2007). The LXXLL motif, essential for the interactions with members of the nuclear hormone receptor superfamily (Vega et al., 2000; Wu et al., 2002a; Oberkofler et al., 2003), mediates essential interactions of PPARGC-1α with nuclear receptors (Heery et al., 1997; Puigserver et al., 1998). Although this motif is found in the N terminus, it does not play a role in the transcriptional activation function of PPARGC-1α (Puigserver et al., 1999; Zhang et al., 2004), which has been attributed to the N terminus (Huss et al., 2002).

The PPAR-γ binding domain is relatively well-conserved in the Ppargc-1α of *P. annectens* and across species (LeMoine et al., 2010), indicating similar binding capacities. The PPAR-γ binding domain mediates ligand-independent interactions with nuclear receptors during brown fat differentiation (Puigserver et al., 1998).

p38-MAPK and AMPK phosphorylation regulates PPARGC-1α activity. p38 stress-activated MAPK phosphorylation of PPARGC-1α not only results in increased stability and half-life (Puigserver et al., 2001), but also enhances the transcription of PPARGC-1α (Knutti et al., 2001). The three p38-MAPK phosphorylation sites are in a region previously demonstrated to play a key regulatory role in PPARGC-1α binding to transcription factors (Puigserver et al., 1999). As these sites are conserved in the Ppargc-1α of *P. annectens*, it can be deduced that p38-Mapk regulates Ppargc-1α via phosphorylation at these sites. In murine muscle cells, AMPK phosphorylation of PPARGC-1α promotes mitochondrial biogenesis (Jäger et al., 2007). Mutations of both regulatory sites abolish PPARGC-1α coactivating activity on its own promoter (Jäger et al., 2007). The presence of two conserved sites in the PPARGC-1α/ Ppargc-1α of tetrapods but only one conserved site (T179) in the Ppargc-1α of other species, including that of *P. annectens*, suggests that there may be potential differences in the responsiveness of PPARGC-1α to AMPK in these species (LeMoine et al., 2010). This might have critical consequences on the role of PPARGC-1α/Ppargc-1α in metabolic pathways mediated by AMPK, as observed in the absence of Ppargc-1α induction in zebrafish subjected to endurance training (McClelland et al., 2006).

The C terminus of PPARGC-1α contains RNA-binding domains which are actively involved in mRNA processing and elongation (Puigserver et al., 1998, 2003;

Rodgers et al., 2005). Proteins containing paired RNA-binding domains and SR-rich domains can interact with the C-terminal domain of RNA polymerase II, and this indicates a putative link between transcription and RNA processing (Yuryev et al., 1996). It has been shown that PPARGC-1α forms a complex with the phosphorylated form of RNA polymerase II and other factors involved in elongation which includes cyclin-dependent kinase 9 and cyclin T, indicating that the RNA-binding domain and SR-rich domain in the C terminus of PPARGC-1α are responsible for maintaining these interactions (Monsalve et al., 2000). As the Ppargc-1α of *P. annectens* comprises conserved RNA-binding domain and SR-rich domains, it is likely to interact with RNA polymerase II in a similar manner.

5.1.1.2. Myod1

The Myod1 of *P. annectens* consists of three conserved motifs – bHLH, MRM and LXXLL. The bHLH motif serves as an interface for dimerization of Myod1, which brings the basic regions of Myod1 together, forming a bipartite DNA-binding domain that recognizes the E-box sequence CANNTG, which activates muscle transcription (Davis et al., 1990; Brennan et al., 1991; Edmondson et al., 1992). The MRM within the bHLH region confers both myogenic potential and susceptibility to inhibition induced by TGF-β (Martin et al., 1992). Although the MRM is crucial for the activation of muscle-specific transcription, it is not necessary for DNA binding (Davis et al., 1990; Brennan et al., 1991; Weintraub et al., 1991). The core LXXLL motif sequence in the Myod1 of *P. annectens* allows it to bind to Fbxo32. Fbxo32 associates with Myod1 via an inverted LXXLL motif located in a series of helical leucine-charged residue-rich domains (Tintignac et al., 2005). A mutation (L164Q) in

the LXXLL motif can repress Myod1 ubiquitination and degradation induced by Fbxo32 (Tintignac et al, 2005).

5.1.1.3. Myog

The conserved bHLH domain in the Myog of *P. annectens* allows for ubiquitous bHLH protein binding, which forms complexes that bind to the DNA sequence E-box and activate muscle-specific transcription (Davis et al., 1990; Brennan et al., 1991; Edmondson et al., 1992). The Myog of *P. annectens* consists of a sub-domain of 12 amino acids (positions 103–114 in reference to Fig. 11) of the basic region (RRRAATLREKRR) necessary for DNA binding and heterodimerization with the bHLH protein E12 (Codina et al., 2008). The alanine-threonine dipeptide containing A107 and T108 is necessary in conferring muscle specificity to the basic domain (Brennan et al., 1991; Davis and Weintraub, 1992; Heidt et al., 2007). The alanine-threonine dipeptide, histidine/cysteine rich domain and helix III domain are the functional domains responsible for transcriptional activation, chromatin remodeling, nuclear localization and heterodimerization in myogenic regulatory factors, which includes MYOG (Vandromme et al., 1995; Gerber et al., 1997; Delgado-Olguín et al., 2011; Izzi et al. 2013). The conservation of the bHLH, alanine-threonine dipeptide, histidine/cysteine-rich and helix III domains indicates a high evolutionary constraint and the importance of the function of MYOG/Myog in vertebrates (Rescan, 2001; Berghella et al., 2008).

5.1.1.4. Mapk

The Mapk1 and Mapk3 of *P. annectens* consist of the signature TXY motif in the activation loop which comprises the regulatory residues T221 and Y223 (reference in

accordance to the ruler in Fig. 16). Human MAPK activity is tightly controlled by the dual phosphorylation of T183 and Y185 (corresponding to T221 and Y223 according to the ruler in Fig. 16), which leads to over 1000-fold activation of MAPK1 and MAPK3 (Ahn et al., 1991; Payne et al., 1991; Robbins and Cobb, 1992; Robbins et al., 1993). Both covalently bound phosphates are essential in maintaining high activity (Seger et al., 1992; Robbins et al., 1993). It has been reported that the replacement of T183 with alanine or Y185 with phenylalanine abolishes MAPK activity (Robbins et al., 1993). Mutating the phosphorylated residues to glutamate, however, does not yield a constitutively active MAPK, which is the case for some protein kinases (Mansour et al., 1994). Robbins et al. (1993) and Zhang et al. (1994) demonstrated that once tyrosine was phosphorylated in the mutant MAPK1/T183E, the mutated enzyme had 10% of the activity of the wild type MAPK, indicating that glutamate could mimic phosphothreonine but not phosphotyrosine (Canagarajah et al., 1997).

Nuclear localization of proteins is primarily mediated by a NLS present within the sequence of these nuclear proteins (Schlenstedt, 1996). Importins, which are special carrier proteins, facilitate protein transport across the nuclear pore complexes (NPC; Tran and Wente, 2006). However, not all cytonuclear shuttling proteins contain the NLS; some nuclear proteins use NLS-independent mechanisms for their passage through the NPC. One such mechanism is the presence of a NTS in the sequence of cytonuclear shuttling proteins, which have been identified in human MAPK1 (Chuderland et al., 2008), which lacks a canonical NLS. A mutation or deletion of three residues (SPS) in the NTS results in cytoplasmic retention of the

mutants (Chuderland et al., 2008). The NTS is phosphorylated upon stimulation and induces nuclear translocation of MAPK1 (Chuderland et al., 2008). The phosphorylated SPS domain acts by binding to importin7 and MAPK1 is released from nuclear pore proteins, consequently facilitating the nuclear translocation of MAPKs (Chuderland et al., 2008). Since the SPS domain is present in both Mapk1 and Mapk3 of *P. annectens*, it can be deduced that both Mapks of *P. annectens* are localized to the nucleus via the SPS domain.

The Mapk1 and Mapk3 of *P. annectens* consist of the CRS/CD motif outside the catalytic region, which comprises hydrophobic and negatively-charged residues essential in establishing hydrophobic and electrostatic interactions with the hydrophobic and positively charged residues of D domains, respectively (Tanoue et al., 2000; Enslen and Davis, 2001). D domains are one of the two docking motifs involved in MAPK interactions with their substrates, activators and inactivating phosphatases (see Tanoue and Nishida, 2003 for review). A replacement of the negatively charged amino acids with neutral ones disrupts the docking interactions (Tanuoe et al., 2000). As the docking interactions of MAPKs with their substrates, activators and phosphatases are mutually exclusive, the docking interactions through the CRS/CD domain can regulate the signal transduction of the MAPK cascade (Tanoue and Nishida, 2003).

5.1.2. Molecular characterization of proteins involved in muscle degradation

5.1.2.1. Hdac1

The Hdac1 of *P. annectens* has highly conserved domains–(1) the HAD necessary for HDAC1 homodimerisation, enzymatic activity and association with HDAC2 and

other proteins (Taplick et al., 2001; Luo et al., 2009); (2) the zinc-binding catalytic domain which contains several conserved histidine and aspartate residues and forms the active site pocket of HDAC1 (Finnin et al., 1999; Taplick et al., 2001; Marmorstein, 2001); (3) a lysine-rich C terminus containing the NLS (Taplick et al., 2001); and (4) three leucine-rich NES motifs (Kim et al., 2010). Deletion/mutation experiments have demonstrated that the N terminus HAD is essential for HDAC1 homodimerisation and enzyme activity (Taplick et al., 2001). A mutant HDAC1 without the NLS motif can be translocated to the nucleus by associating with an intact HDAC1 protein (Taplick et al., 2001). A structural study by Finnin et al. (1999) has revealed the conserved residues which make up the active site, and these residues are also conserved in the Hdac1 of *P. annectens*. The active site consists of a tubular pocket, a zinc-binding site and two aspartate-histidine charge-relay systems (Finnin et al., 1999). A site-directed mutagenesis of the histidine and aspartate residues in the charge-relay system abolishes the deacetylase activity (Hassig et al., 1998; Kadosh and Struhl, 1998). The deacetylase activity is manifested only after incubation with zinc chloride *in vitro* (Finnin et al., 1999), which is consistent with the proposition that HDAC1 activity required a metal cofactor (Hassig et al., 1998). The conservation of the core residues in the HAD and the active site pocket in the Hdac1 of *P. annectens* indicates it possesses deacetylase activity.

It has been established that the C terminus of *Xenopus* Hdac1 is essential for the nuclear location of HDAC1 (Ryan et al., 1999; Vermaak et al., 1999). Indeed, the deletion of the C terminus of mouse HDAC1 results in the cytoplasmic retention of the mutant (Taplick et al., 2001). The C terminus, which is rich in charged amino

acids, is essential for the nuclear localization of HDAC1 in the absence of the HAD (Taplick et al., 2001). The NLS of mouse HDAC1 shares high similarity with the *c-myc* NLS (Dang and Lee, 1988) and is responsible for the transporting of GFP into the nucleus (Taplick et al., 2001). HDAC1 can also be exported out of the nucleus (Kim et al., 2010). A mutation of the NES in HDAC1 interferes with the formation of a complex with chromosome region maintenance 1 (CRM1), and prevents the nuclear export of the mutant HDAC1 (Kim et al., 2010). As the mouse HDAC1 NLS motif is identical to the NLS of human HDAC1 and similar to the predicted NLS in *P. annectens* Hdac1, it can be deduced that the Hdac1 of *P. annectens* is localized to the nucleus. Furthermore, the presence of conserved NES motifs in the Hdac1 of *P. annectens*, which is similar to the NES originally described in viral proteins (Wen et al., 1995), indicates that it can be exported out of the nucleus by forming a complex with CRM1.

The HDAC1 protein is a target for a number of post-translational modifications such as phosphorylation and acetylation (Pflum et al., 2001; Qiu et al., 2006). CSNK2, the main kinase responsible for HDAC1 phosphorylation (Cai et al., 2001; Sun et al., 2007), phosphorylates S421 and S423 of HDAC1 (corresponding to S422 and S424 according to the ruler in Fig. 23), which are conserved in the Hdac1 of *P. annectens*. This indicated that the Hdac1 of *P. annectens* can be phosphorylated through these two serine residues by CSNK2. Mutations in these two serine residues lead to reduced deacetylase and transcriptional repression activities, as well as weakened interaction with RbAP48, Sin3a, CoREST and MTA-2 (Pflum et al., 2001). CSNK2-dependent phosphorylation of HDAC1 is constitutive throughout the cell

cycle, althought it is dispensable for the intrinsic HDAC1 activity *in vitro* (Cai et al., 2001; Karwowska-Desaulniers et al., 2007). An increase in CSNK2-dependent phosphorylation of HDAC1 in response to hypoxic conditions is correlated with increased HDAC enzymatic activity (Pluemsampant et al., 2008), suggesting that phosphorylation is an essential signaling factor of various pathways which converge on HDAC1 to deliver the appropriate biological responses.

An acetylation of HDAC1 leads to a dramatic reduction in its enzymatic and repression activities both *in vivo* and *in vitro* (Qiu et al., 2006). Six lysine residues can undergo acetylation in HDAC1 (Qiu et al., 2006). All these lysine residues, except K433 which is replaced with arginine, are conserved in the Hdac1 of *P. annectens*. It has been established that K433 is the key residue for HDAC1 acetylation (Qiu et al., 2006; Luo et al., 2009). A similar phenomenon can be observed in HDAC2, but HDAC2 is not acetylated *in vitro* by p300 although all other lysine residues were conserved in HDAC2 (Luo et al., 2009). A mutation of R433 to lysine leads to the acetylation of HDAC2 by p300 *in vitro*, though to a lesser extent compared to HDAC1 (Luo et al., 2009). This suggests that the Hdac1 of *P. annectens* could be refractory to acetylation by p300, and might undergo acetylation by other acetyltransferases such as CBP and histone acetyltransferases instead.

5.1.2.2. FoxO

The nuclear-cytoplasmic shuttling of FOXO proteins is regulated by phosphorylation, which disrupts FOXO transcriptional activities and promotes FOXO protein degradation. FOXO proteins undergo phosphorylation by several kinases–AKT (also referred to as protein kinase B), SGK, CSNK1 and DYRK1A. Both AKT and SGK

are known to target the same substrate motifs (Brunet et al., 1999, 2001), but it is unclear if one can substitute for the other in FOXO regulation. Although both AKT and SGK phosphorylation of FOXO lead to the cytoplasmic localization and inhibition, AKT preferentially phosphorylates S256 (corresponding to S266 in Fig. 28) while SGK prefers S319 (corresponding to S333 in Fig. 28) (Brunet et al., 2001). Upon phosphorylation by AKT or SGK, FOXO3 binds to 14-3-3 proteins and remains in the cytoplasm, thus abolishing its function as a transcription factor (Brunet et al., 1999, 2001). The majority of the 14-3-3 proteins are localized to the cytoplasm, but they bind to FOXO proteins in the nucleus (Brunet et al., 2002) before being exported into the cytoplasm. 14-3-3 mediates the masking of the NLS in FOXO proteins, preventing the re-entry of FOXO into the nucleus (Brunet et al., 2002; Zhao et al., 2004). Moreover, the phosphorylation of FOXO at S256 introduces a negative charge in the basic NLS, contributing to the cytoplasmic retention of FOXO (Rena et al., 2001). As all three phosphorylation sites are conserved in both FoxO proteins of *P. annectens*, it is probable that *P. annectens* FoxO1 and FoxO3 can be phosphorylated by Akt and Sgk, and similarly exported to the cytoplasm by binding to 14-3-3 proteins.

The phosphorylation of FOXO1 by AKT at site 319 (corresponding to S333 in Fig. 28) creates a consensus sequence for the binding with CSNK1, which subsequently leads to the phosphorylation of S322 and S325 (corresponding to S336 and S339 in Fig. 28) and potentiates the export of FOXO1 to the cytoplasm (Rena et al., 2002, 2004). Phosphorylation of sites S322 and S325 would enhance the formation of FOXO1 with the export machinery (Ran and Exportin/Crm1) to promote

nuclear export (Rena et al., 2002; Zhao et al., 2004). Since both S336 and S339 are conserved in the FoxO3 of *P. annectens*, it is highly likely that FoxO3 of *P. annectens* can be phosphorylated by CSNK1. By contrast, only S336 is conserved in the FoxO1 of *P. annectens*. Hence either the FoxO1 of *P. annectens* is phosphorylated by CSNK1 at only one site, or there is another phosphorylation site targeted by CSNK1 yet to be identified.

FOXO consists of a site (S329) which can be phosphorylated by DYRK1A; this is independent of AKT or CSNK1 activity and is unaffected by growth signals (Woods et al., 2001). This site is conserved in both FoxO proteins of *P. annectens*. A mutation of this serine residue (S329, corresponding to S343 in Fig. 28) to alanine results in the retention of FoxO1 in the nucleus (Woods et al., 2001). The phosphorylation of several serine residues near S329, together with S329, stabilizes the interaction with the nuclear export protein Ran, thereby promoting nuclear export of FoxO1 (Rena et al., 2002).

FOXO activity is also modulated by acetylation, and all known acetylation sites are conserved in both FoxO1 and FoxO3 of *P. annectens*. However, the effect of acetylation on FOXO activity is still unclear. Acetylation was reported to enhance FOXO activity (Brunet et al., 2004; Motta et al., 2004), while other studies demonstrated impaired FOXO activity upon acetylation (Brunet et al., 2004; Motta et al., 2004; Daitoku et al., 2004; van der Horst et al., 2004). Although acetylation of FOXO is generally thought to be inhibitory, the recruitment of CBP/p300 to promoter regions by FOXO proteins induces histone acetylation, acting as a positive signal for transcription initiation (Daitoku et al., 2004). Transient transfection experiments

reveal that p300 potently stimulates FOXO1-induced transcription of IGF-binding protein-1 (Perrot and Rechler, 2005). Yet, an acetylation of FOXO, mediated by CBP/p300 (Brunet et al., 2004; Daitoku et al., 2004; van der Heide and Smidt, 2005; Wang et al., 2012), was demonstrated to reduce DNA binding and to increase its sensitivity to phosphorylation by AKT which provides negative regulation (Matsuzaki et al., 2005). CBP/p300 does not only serves as an essential cofactor (Nasrin et al., 2000; Kwon et al., 2004) in FOXO-mediated transcriptional activity, but also inhibits FOXO activity by acetylation (van der Heide and Smidt, 2005; Wang et al., 2012). FOXO acetylation also inhibits ubiquitination, and as both ubiquitination and acetylation occur on lysine residues, these two post-translational modifications can be inversely correlated as they compete for the same lysine residues (Daitoku et al., 2011).

One of the growth factor-controlled inhibitory pathways involves the phosphorylation of FOXO3 by MAPK1/3, which results in MDM2-mediated ubiquitination and FOXO3 protein degradation (Yang et al., 2008a, b). The mutation of the three serine residues to alanine leads to decreased phosphorylation by MAPK and increased resistance to degradation by MDM2 (Yang et al., 2008a, b). For the FoxO3 of *P. annectens*, one of the serine residues in the phosphorylation cluster S295/345/426 (corresponding to S311/364/455 in Fig. 28) is replaced with proline. However, a serine residue is present next to this particular proline residue, which corresponded to the MAPK phosphorylation consensus motif of serine/threonine-proline (Davis, 1993; Songyang et al., 1996), in the FoxO3 of *P. annectens*. This motif is present in all three phosphorylation sites. Hence, it is probable that S454

(according to the ruler in Fig. 28) is one of the three targets of MAPK1/3 (together with the other two serine residues) in the FoxO3 of *P. annectens*.

AMPK phosphorylates nuclear FOXO3 in response to nutrient deprivation, increasing the transcriptional activity of FOXO3 and possibly modulating differential promoter recognition without affecting localization (Greer et al., 2007). Greer et al. (2007) has identified at least six regulatory phosphorylation sites that are targeted by AMPK, where four of these are conserved in the FoxO3 of *P. annectens*. The other two sites are substituted with asparagine, which is not a known target for phosphorylation. Mutation of these six sites to alanine leads to an 84% reduction in phosphorylation in the mutant as compared with the wildtype FOXO3 (Greer et al., 2007). S413 (corresponding to S443 in Fig. 28) is a key residue in activating the transcriptional activity of FOXO3 upon phosphorylation by AMPK (Greer et al., 2007). The replacement of this key residue and another serine residue by asparagine in the FoxO3 of *P. annectens* indicates that AMPK phosphorylation may occur at some other serine/threonine residues. Indeed, it has been reported that there are other phosphorylation sites, especially at the C terminus, in FOXO3, as the 6A mutant can still be phosphorylated to some extent by AMPK (Greer et al., 2007). Although the exact mechanism of FOXO3 transcriptional activation by AMPK remains uncertain, AMPK phosphorylation of FOXO3 can increase the interaction with CBP/p300, which affects FOXO3 activity and promoter recognition through acetylation (Wang et al., 2012). AMPK phosphorylation of FOXO has been associated with neuronal cell death (Davila et al., 2012), FOXO-induced autophagy (Chiacchiera and Simone, 2009) and muscle atrophy (Sanchez et al., 2012).

5.1.2.3. Mstn

The Mstn of *P. annectens* consists of a signal peptide for secretion, a propeptide domain, a furin cleavage site (RSRR) and a bioactive domain consisting of nine cysteine residues which are characteristic of vertebrate MSTN/Mstn and inhibins (McPherron et al., 1997; see review by Lee, 2004 and Joulia-Ekaza and Cabello 2006). The proteolytic furin cleavage site serves to release the processed mature peptide. The cysteine residues in the bioactive domain are essential for the dimerization of the two MSTN subunits (Hu et al., 1998; Daopin et al., 1992). The conservation of the above mentioned sites across various animal species including *P. annectens* indicated a conservation of function in the Mstn of *P. annectens*.

5.1.2.4. Fbxo32

Fbxo32 from *P. annectens* has a F-box functional domain. F-box proteins usually contain a carboxy-terminal substrate-recognition domain, which allows F-box proteins to be further classified into one of three families (Jin et al., 2004). F-box proteins that contain Trp-Asp repeats belong to the FBW family, while F-box proteins containing leucine-rich repeats belong to the FBL family. Both families recognize phosphorylated protein substrates (Smith et al., 1999; Kobe and Kajava, 2001; Enkhbayar et al., 2004). F-box proteins in the FBX family lack specific binding domains and contain various other protein-protein interaction domains at the carboxyl-terminus, like zinc-finger, carbohydrate interacting (CASH) or proline-rich domains (Kipreos and Pagano, 2000; Cardozo and Pagano, 2004; Jin et al., 2004). Since the Fbxo32 of *P. annectens* lacks specific protein recognition domains, it belongs to the FBX family of F-box proteins (Jin et al., 2004). Although there are no

specific protein recognition domains, several protein substrates which undergo ubiquitination by FBXO32 have been identified, such as MyoD (Tintignac et al., 2005) and the subunit eIF3-f of the eukaryotic initiation factor eIF3 complex (Lagirand-Cantaloube et al., 2008; Csibi et al., 2009) in the skeletal muscle.

The Fbxo32 of *P. annectens* also consists of a putative bipartite NLS and a SV40-type monopartite NLS which are well conserved, and is a strong indication that the Fbxo32 of *P. annectens* is localized to the nucleus. Other mammalian (Gomes et al., 2001) FBXO32 and fish (Bower et al., 2010) Fbxo32 also contain NLS.

The Fbxo32 of *P. annectens* has a conserved LCD with an inverted LXXLL motif. The inverted LXXLL motif mediates direct binding to a LXXLL motif found in Myod family members (Tintignac et al., 2005), which results in the FBXO32-induced ubiquitination and degradation of Myod1.

5.2. Dendrogramic analyses of various proteins involved in muscle formation and degradation from *P. annectens*

Lungfishes share similarities with both amphibians and fishes, and are important animals for studies on the transition between fishes and tetrapods. Lungfishes are considered by many evolutionists as a sister group of amphibians (Forey, 1986), and many molecular phylogenetic studies support this view, favouring lungfishes as the closest living relatives of tetrapods (Zardoya et al., 1998; Tohyama et al., 2000; Takezaki et al., 2004; Hallstrom and Janke, 2009; Amemiya et al., 2013). Indeed, the various putative proteins involved in muscle formation and degradation in *P. annectens* were phylogenetically closer to tetrapods than to fishes. This supports the notion that lungfish is the intermediary form between fishes and tetrapods. As the

closest living sister group of land vertebrates, lungfishes would logically have some genes/proteins which are closer to those of other fishes such as carbamoyl phosphate synthetase III (Loong et al., 2012a) and argininosuccinate synthase (Chng et al., 2014), and other genes/proteins which share greater similarity with those of tetrapods, like argininosuccinate lyase (Chng et al., 2014), Na^+/K^+-ATPase α-subunit isoforms (Hiong et al., 2013), L-gulono-γ-lactone oxidase (Ching et al., 2014), betaine-homocysteine *S*-methyltransferase 1 (Ong et al., 2015) and coagulation factor 2 and fibrinogen gamma chain (Hiong et al., 2015a).

In this study, proteins involved in muscle formation in *P. annectens* were phylogenetically closer to tetrapods than to teleosts. Various domains of Ppargc-1α exhibited asymmetric evolutionary dynamics (LeMoine et al., 2010). Evolution of the middle domains was significantly faster in teleosts than in tetrapods as compared to the domains at each end, and was suggested to be due to divergent evolutionary pressures over these domains (LeMoine et al., 2010). Most fish Ppargc-1α have serine-rich insertions and a glutamine-rich insertion of variable length in the middle region (LeMoine et al., 2010), which are absent in lungfish and tetrapods. This supports the notion that the Ppargc-1α of *P. annectens* is phylogenetically closer to those of tetrapods than to those of fish. This holds true for both muscle regulatory factors, Myod1 and Myog, of *P. annectens*. Results from this study corroborate previous phylogenetic analyses (Macqueen and Johnston, 2006, 2008; Zhu et al., 2014), where fish Myod1 and Myog is separated from tetrapod MYOD1/Myod1 and MYOG/Myog respectively. Besides, no other isoforms of Myod1 or Myog were found in the muscle of *P. annectens*, which is similar to mammals but not fishes.

Multiple paralogs of Myod1 were reported in *Oncorhynchus mykiss* (Delalande and Rescan, 1999) and *Salmo salar* (Bower and Johnston, 2010). The same phenomenon was also observed for *P. annectens* Mapk1 and Mapk3, and corroborates previous phylogenetic analyses, where the teleost subgroups are isolated from tetrapods for each MAPK isoform (Krens et al., 2006; Li et al., 2011).

Similarly, proteins involved in muscle degradation in *P. annectens* were also phylogenetically closer to tetrapods than to teleosts. Phylogenetic analysis demonstrates that the evolution of HDACs preceded the evolution of histones, suggesting that the primary targets of HDACs may not be histones (Gregoretti et al., 2004). Currently, more than 50 non-histone proteins have been identified as targets of HDACs (Dokmanovic and Marks, 2005; Rosato and Grant, 2005; Minucci and Pelicci, 2006; Marks and Breslow, 2007; Xu et al., 2007), and they encompass proteins which play regulatory roles in cell proliferation, cell migration and cell death. The various classes of HDACs are conserved across divergent organisms, and are more closely related to their own class than to any other class of HDACs (Gregoretti et al., 2004). Previous phylogenetic studies of HDACs have focused on the classification and function instead of the evolution of individual HDACs (Gregoretti et al., 2004; Bradner et al., 2010). This is the first study that gives an indication of the evolution of HDAC1 across vertebrates, and demonstrates that *P. annectens* Hdac1 is phylogenetically closer to tetrapods than to teleosts. This also holds true for Mstn and Fbxo32 of *P. annectens*. There is evidence demonstrating that the evolution of fish *mstn* has been subjected to different duplication events (Kerr et al., 2005). Results from this study on *P. annectens* corroborate previous reports where tetrapod

MSTN/*Mstn* is separated from fish *mstn* (Kerr et al., 2005; Rodgers and Garikipati, 2008). Unlike mammalian *MSTN*, there are two copies of fish *mstn* (*mstn1* and *mstn2*). This is due to an early genome duplication event before the teleost radiation but after the divergence of ray- and lobe-finned fishes (Amores et al., 1998; Postlethwait et al., 1998). Although efforts were made to find *mstn* isoforms in the muscle of *P. annectens*, only 1 isoform was found, indicating that *P. annectens mstn* may not have undergone duplication, as in the case of tetrapods *MSTN*. Previous studies demonstrate that teleost Fbxo32 is separated from tetrapod FBXO32 (Cleveland and Evenhuis, 2010; Tacchi et al., 2010), and this is consistent with results from this study, further supporting the notion that the lungfish is the intermediary form between teleosts and tetrapods.

5.3. Ongoing transcription and translation of certain genes and proteins in *P. annectens* during aestivation

From the physiological point of view, aestivation is usually associated with metabolic depression, as metabolic fuel conservation is essential during long periods of torpor without food intake (Storey, 2002). Strong global suppression of gene expression and protein synthesis are integral parts of hypometabolism because transcription and translation are energy-intensive processes (Storey and Storey, 2010). However, it cannot be assumed that all protein syntheses are suppressed in every organ during the prolonged maintenance phase of aestivation. Certain genes or proteins are expected to be upregulated to overcome the various challenges associated with aestivation. Indeed, many more genes were upregulated than down-regulated in the brain of *P. annectens* during the induction and maintenance phases of aestivation, although one

would expect exactly the opposite during metabolic depression (Hiong et al., 2013). Although more genes related to protein synthesis were down-regulated than up-regulated in the liver of *P. annectens* during the maintenance phase of aestivation, this indicates that there is no complete suppression of the capacity of protein synthesis (Hiong et al., 2015b). Likewise, the mRNA expression levels of *carbamoyl phosphate synthase III* (Loong et al., 2012b), *argininosuccinate synthetase* and *argininosuccinate lyase* (Chng et al., 2014) increase in the liver of *P. annectens* during aestivation. Similarly, up- and down-regulation of the mRNA expression levels and/or protein abundance of Na^+/K^+-ATPase alpha-subunit isoforms (Hiong et al., 2013), L-gulono-γ-lactone oxidase (Ching et al., 2014), betaine-homocysteine methyltransferase 1 (Ong et al., 2015), coagulation factor II, fibrinogen gamma chain (Hiong et al., 2015a), heat shock protein 90, phospho-Akt, protein kinase B, nitric oxide synthase and hypoxia inducible factor 1α (Garofalo et al., 2015) have been observed in various organs/tissues of *P. annectens* during the three phases of aestivation. Results from this study demonstrated up- and down-regulation in the mRNA expression levels and/or protein abundance of various genes/proteins involved in muscle formation, muscle degradation and oxidative defense in the muscle of *P. annectens* during the three phases of aestivation. Thus, despite a general decrease in protein synthesis, there could be increases in syntheses of certain proteins in specific organs of *P. annectens* during aestivation as mentioned by Ip and Chew (2010).

The cellular machinery is responsible for directing gene and protein expression programs, and encompasses a diverse array of noncoding RNAs and

proteins whose complex interplay drives gene expression, handling of mRNA transcripts, protein synthesis, and post-translational processing to produce the final functional protein and deposit it in the correct subcellular destination (Tessier and Storey, 2014). Specifically, gene expression is regulated by epigenetic factors, signal transduction pathways, transcription factors and other components of the transcriptional apparatus, mRNA processing factors, components of the translational machinery, and the subcellular distribution of each of these factors (Tessier and Storey, 2014). The production and maintenance of protein are established by a dynamic balance of regulation of linked processes, which range from mRNA transcription, processing and degradation to protein translation, localization, modification and programmed destruction (Vogel and Marcotte, 2012). mRNA expression levels have been commonly used as proxies for the abundances and activities of the corresponding proteins, with the assumption that transcript abundances are the main determinant of protein abundances (Vogel and Marcotte, 2012). Although cellular protein concentrations correlate with the abundance of their corresponding mRNAs in both bacteria and eukaryotes, the correlation is not strong; they usually show a squared Pearson correlation coefficient of ~0.40, indicating that ~40% of the variation in protein abundance can be explained by knowing mRNA expression levels (de Sousa Abreu et al., 2009; Maier et al., 2009). The remaining ~60% of the variation can be accounted for by a combination of post-transcriptional regulation and measurement noise (de Sousa Abreu et al., 2009; Maier et al., 2009; Csárdi et al., 2015). It is therefore unsurprising that the changes in the mRNA

expression levels may not correlate with the changes in the corresponding protein abundances in the muscle of *P. annectens* during the three phases of aestivation.

Compared to aestivation, hibernation is described as a reversible state of suspended animation utilized as a survival strategy to survive long periods of winter with limited food (Wang and Lee, 1996). Hibernators display regulatory mechanisms which allow for a global reduction of transcription (Morin and Storey, 2006) and translation (Frerichs et al., 1998) during hibernation, but a small subset of stress-responsive pathways are activated to overcome the stresses associated with hibernation (Hittel and Storey, 2001; Eddy et al., 2005b, Yan et al., 2008). Moreover, it has been demonstrated that the total pool of mRNA remains stable (Frerichs et al., 1998), and that there are discrepancies between mRNA and protein expression profiles (Shao et al., 2010). These studies indicate that mRNA substrate availability alone neither provides a full understanding of the differential regulation of the hibernator proteome nor explains the inhibition of protein synthesis (Tessier and Storey, 2014). There are three regulatory mechanisms proposed, which are involved in the control of gene/protein expression and allow the hibernating cell to survive the stresses associated with cycles of torpor-arousal such as hypothermia and ischemia-reperfusion (Tessier and Storey, 2014). The first regulatory mechanism involves mRNA processing factors and other interacting proteins, which could protect and stabilize mRNA pools, and control the translation rate during torpor and arousal of hibernation (Tessier and Storey, 2014). Next, as a complementary mechanism to attain global reductions in translation, the regulation of initiation and elongation translation factors could be utilized to promote the preferential synthesis of essential

proteins and facilitate the evasion of cap-dependent inhibition (Tessier and Storey, 2014). Lastly, there could be a strict regulation of the subcellular organization and distribution of mRNA factors in intracellular compartments such as the nucleus and cytoplasm, allowing various components to differentially associate with cellular structures in aspects which regulate their activity, availability and net cellular response during hibernation (Tessier and Storey, 2014). It is interesting to note that the myocytes in the trabeculae associated with the free ventricular wall of *P. dolloi* demonstrated structural signs of low transcriptional and metabolic activity (heterochromatin, mitochondria of the dense type) in freshwater fish (Icardo et al., 2008). However, there was a partial reversal of these signs in aestivating lungfish (euchromatin, mitochondria with a light matrix), suggesting that aestivation triggered an increase in transcriptional and synthetic myocardial activities, particularly at the level of the ventricular septum (Icardo et al., 2008). Moreover, there were signs of hemodynamic remodeling in the heart of *P. annectens* during aestivation, as observed from the increases in endothelial-like nitric oxide synthase and heat-shock protein 90 (Amelio et al., 2013). It would seem that, similar to hibernation, during aestivation, the mRNA factors are compartmentalized in the nucleus and the subcellular organization and distribution of the transcriptional and/or translational machineries are strictly regulated, hence controlling gene and protein expression. Hence, aestivation cannot be considered as the result of a general metabolic depression; instead, aestivation encompasses the complex interplay between up-regulation and down-regulation of various cellular activities. Aestivation would logically entail variations in rates of protein degradation and protein synthesis, reconstructing cells

and tissues via a rapid protein turnover. As protein abundances are more direct determinants of cellular functions compared to mRNA expression levels (Vogel and Marcotte, 2012), the subsequent discussion will focus mainly on protein abundances. Any discussion on mRNA expression levels will only be done when necessary.

5.4. Molecular changes in expression of *ppargc-1α*/Ppargc-1α, *myod1*/Myod1, *myog*/Myog and *mapk*/Mapk, which are involved in muscle formation, occurring in the muscle of *P. annectens* during the three phases of aestivation

In general, genes/proteins involved in muscle formation are expected to be down-regulated in the skeletal muscle during periods of fasting or disuse. Indeed, there were decreases in the expression of *PPARGC-1α*/PPARGC-1α (Sandri et al., 2006; Sacheck et al., 2007). Furthermore, MAPK1/3 inhibition in both slow and fast muscles induces profound atrophy (Shi et al., 2009). However, there was an up-regulation in the expression of *MYOD1*/MYOD1 and *MYOG*/MYOG (Mozdziak et al., 1999; Alway et al., 2001; Moresi et al., 2010) in the skeletal muscle of rodents experiencing starvation or muscle disuse. It was thought that these changes help to protect skeletal muscle from atrophy induced by disuse or fasting (refer to section 1.3.5). Yet, previous studies have reported an up-regulation in the expression of *PPARGC-1α*/PPARGC-1α and *MAPK*/MAPK in the skeletal muscles of hibernating bats and squirrels (Eddy and Storey, 2003; Eddy et al., 2005a; MacDonald and Storey, 2005; Xu et al., 2013), demonstrating the protective effect of these genes/proteins in the skeletal muscle. These observations, together with results from this study, have been summarized in Table 17.

Table 17. Comparison of changes in expression of various genes/proteins involved in muscle formation in response to fasting-induced muscle atrophy, disuse-induced muscle atrophy (includes denervation, hindlimb suspension and unloading), hibernation and the three phases of aestivation. Decreases in expression are denoted with '-', while increases in expression are denoted with '+'. No significant changes in expression are denoted with '0'. 'N.A.' denotes no information is available.

Genes/Proteins	Fasting	Disuse	Hibernation	Aestivation		
				Induction	Maintenance	Arousal
ppargc-1α/ Ppargc-1α	-	-	+	0	0	0
myod1/Myod1	N.A.	+	N.A.	0	+	0
myog/Myog	N.A.	+	N.A.	0	0	0
mapk/Mapk	N.A.	N.A.	+	0	0	0

5.4.1. Induction phase

The induction phase lasted 6 to 9 days before the formation of a completely dried mucus cocoon, implying that the fasting is not severe. During this period, the skeletal muscles are still in use as there would still be occasional body movement, especially on the first 1 to 3 days. Furthermore, the aestivating fish has to undergo tissue reconstruction (Chew et al., 2015), which depicts an increase in protein turnover in certain organs, with perhaps an increased supply or mobilization of protein/amino acids from the skeletal muscle due to a lack of food supply. Hence, it is logical to predict that muscle formation may be reduced or remain unchanged. Indeed, results from this study demonstrated that there was a stable expression of Ppargc-1α, Myod1, Myog and Mapk1/3 in the muscle of *P. annectens* during the induction phase, which differs from the response to disuse or fasting in human or animal models (Table 17). This could be due to the short period of fasting and the incompleteness of muscle disuse, and consequently protein synthesis remained unchanged in the skeletal muscle of *P. annectens* during this period.

5.4.2. Maintenance phase

The maintenance phase of aestivation lasted for 6 months for the experimental fish in this study. During this period, fasting was severe and there was absolutely no locomotor activity, subjecting the skeletal muscles to possible atrophy induced by disuse and/or fasting. However, aestivating fish would have to preserve muscle structure and strength throughout the maintenance phase in preparation for arousal (Chew et al., 2015), suggesting that protein degradation is likely suppressed together with stable or reduced protein synthesis due to food deprivation. It is thus logical to

predict that muscle formation may remain unchanged or reduced. Indeed, in this study, the expression of Ppargc-1α, Myog and Mapk1/3 remained stable in the muscle of *P. annectens* during the maintenance phase, which differs from the response to disuse or fasting in human or animal models (Table 17). Interestingly, these results also differ from those reported in hibernators. In hibernators, various studies reported increases in the expression of *Ppargc-1α*/PPARGC-1α during hibernation, where there is little muscle atrophy (Eddy and Storey, 2003; Eddy et al., 2005a; Xu et al., 2013). An increase in MAPK1 expression also occurs in the skeletal muscles of Richardson's ground squirrels during hibernation (MacDonald and Storey, 2005). Since maintaining protein synthesis is involved in muscle mass preservation during hibernation inactivity (Fedorov et al., 2014; Hindle et al., 2015), the stable expression of Ppargc-1α, Myog and Mapk1/3 is likely to contribute to muscle mass preservation through maintaining protein synthesis.

The increase in Myod1 expression in the muscle of *P. annectens* during the maintenance phase was similar to results reported in mammalian disuse models (Table 17). However, a recent study demonstrated that increased MYOD1 expression might protect myofibres from atrophy induced by hindlimb suspension instead (Smith et al., 2014). MYOD1 is a master regulatory gene of muscle differentiation, and can convert non-muscle cells to muscle cells (Weintraub et al., 1989). Since it is necessary for *P. annectens* to preserve muscle structure and strength in preparation for arousal, it is logical to deduce that Myod1 contributes to muscle mass preservation by converting non-muscle cells to muscle cells during the maintenance phase of aestivation.

5.4.3. Arousal phase

During the early arousal phase of aestivation, *P. annectens* resumes some locomotor activity. As *P. annectens* would only start feeding after 7–10 days upon arousal, it would require fuel for ATP production, not only for locomotor activity but also for tissue reconstruction/regeneration. Hence, during the first 3 days of arousal, the fuel is likely to be of endogenous origins as feeding has yet to occur (Chew et al., 2015). There might be an increase in the mobilization of proteins/amino acids from the skeletal muscle, which could lead to a high protein turnover and an increase in nitrogenous waste production. A significant increase in urea-N excretion in *P. annectens* upon arousal from aestivation is attributed mainly to the urea accumulated in *P. annectens* during the maintenance phase (Hung et al., 2009). However, the excretion of accumulated urea in *P. dolloi* is known to be regulated by the level of internal ammonia (Ip et al., 2005c). Therefore, as proposed by Chew et al. (2015), it is probable that an increase in amino acid catabolism leads to an increase in ammonia production, thereby acting as a signal to enhance urea excretion in *P. annectens* upon arousal. It is thus logical to predict that muscle formation may be reduced or remain unchanged. Indeed, results from this study revealed that the stable expression of *ppargc-1α*/Ppargc-1α, *myod1*/Myod1, *myog*/Myog and Mapk1/3 in the muscle of *P. annectens* during the arousal phase is different from the response to fasting in mammalian models (Table 17). They suggest that protein synthesis remained unchanged in the skeletal muscle of *P. annectens* during this period.

5.5. Molecular changes in expression of *hdac1*/Hdac1, *foxo*/FoxO, *tp53*/TP53, *mstn*/Mstn and *fbxo32*/Fbxo32, which are involved in muscle degradation, occurring in the muscle of *P. annectens* during the three phases of aestivation

Atrophy in the skeletal muscles of rodents is induced by fasting or disuse, and this is generally accompanied by increases in the expression of *Hdac1*/HDAC1 (Beharry et al., 2014), *FoxO*/FOXO (Calnan and Brunet, 2008; Senf et al., 2010), *tp53*/TP53 (Fox et al., 2014), *Mstn*/MSTN (Carlson et al., 1999; Shao et al., 2007; Allen et al., 2009, 2010) and *Fbxo32*/FBXO32 (Bodine et al., 2001; Gomes et al., 2001; Jones et al., 2004; Sandri et al., 2004; Abadi et al., 2009; Allen et al., 2009; Gustafsson et al., 2010) (refer to section 1.4.6.). It is not clear if TP53 contributes to muscle atrophy induced by fasting, despite previous reports of increased TP53 activity in correlation with skeletal muscle atrophy *in vivo* under conditions of stress (Schwarzkopf et al., 2006, 2008; Edwards et al., 2007; Rodier et al., 2007; Didier et al., 2012), though TP53 may contribute to apoptosis-mediated muscle wasting since its expression in the muscle is increased after 14 days of space-flight (Ohnishi et al., 1999), and after 7 or 14 days of unloading (Siu and Alway, 2005a). It is apparent that these genes/proteins partake in muscle degradation, leading to muscle atrophy induced by fasting or disuse. However, in hibernators, it was reported that the protein expression of MSTN (Brooks et al., 2011) and the mRNA expression of *Fbxo32* remained stable (Velickovska et al., 2005; Velickovska and van Breukelen, 2007; Lee et al., 2010; Andres-Mateos et al., 2013; Dang et al., 2016), implying that there was a protective effect conferred on the skeletal muscles during hibernation. Observations from these studies, together with results from this study, have been summarized in Table 18.

Table 18. Comparison of changes in expression of various genes/proteins involved in muscle degradation in response to fasting-induced muscle atrophy, disuse-induced muscle atrophy (includes denervation, hindlimb suspension and unloading), hibernation and the three phases of aestivation. Decreases in expression are denoted with '-', while increases in expression are denoted with '+'. No significant changes in expression are denoted with '0'. Unavailable information is indicated 'N.A.'.

Genes/Proteins	Fasting	Disuse	Hibernation	Aestivation		
				Induction	Maintenance	Arousal
hdac1/Hdac1	+	+	N.A.	0	0	+
foxO1/FoxO1	+	+	N.A.	0	0	-
foxO3/FoxO3	+	+	N.A.	0	0	0
tp53/Tp53	N.A.	+	N.A.	+	0	+
mstn/Mstn	+	+	0	0	0	-
fbxo32/Fbxo32	+	+	0	-	0	-

5.5.1. Induction phase

As mentioned in section 5.4.1., fasting is not severe and muscle disuse is incomplete. Moreover, the aestivating lungfish has to undergo tissue reconstruction (Chew et al., 2015), leading to increased protein turnover in certain organs. Due to a lack of food supply, there could be an increased supply or mobilization of protein/amino acids from the skeletal muscle. Hence, it is logical to predict that muscle degradation may remain unchanged or enhanced, during the induction phase. Indeed, the expression of *hdac1*/Hdac1, FoxO, and Mstn in the skeletal muscle of *P. annectens* remained unchanged, and this could be explained by the short period of fasting and the incompleteness of muscle disuse. These results differed from those reported in mammals, where fasting and muscle disuse lead to increases in expression of almost all the genes/proteins of interest involved in muscle degradation (Table 18). These results also indicate that 6 days of fasting did not induce an increase in muscle degradation in *P. annectens*. However, unlike mammals, there was an increase and decrease in the expression of *tp53* and Fbxo32, respectively, in the skeletal muscle of *P. annectens* during the induction phase of aestivation.

A significant increase in the mRNA expression of *tp53* in the muscle of *P. annectens* during the induction phase indicates that (1) there might be some form of muscle wasting, or (2) there could be cellular stress caused by aestivation. A recent study showed that *TP53* directly represses *MYOG*/MYOG by binding to the *MYOG* promoter and suppresses muscle differentiation (Yang et al., 2015). It was thought that the repression of *MYOG* by *TP53* allows for DNA damage repair and proper chromosome segregation when there is intersection of the muscle differentiation

program with the cell cycle checkpoint control (Yang et al., 2015). However, this was not the case in the muscle of *P. annectens* during the induction phase as the Myog protein abundance remained unchanged despite an increase in the mRNA expression of *tp53*. It is thus likely that the increase in *tp53* expression could be purely due to cellular stress caused by aestivation. On the other hand, the decrease in the protein abundance of Fbxo32 in the muscle of *P. annectens* during the induction phase, indicates a decrease in the ubiquitination and proteolysis of muscle proteins and hence a suppression of muscle degradation.

5.5.2. Maintenance phase

During the maintenance phase, the aestivating lungfish must preserve muscle structure and strength to prepare for arousal (Chew et al., 2015) despite the extended period of severe fasting and muscle disuse (refer to section 5.4.2.). It is thus very likely that muscle degradation may be reduced or remain unchanged, during the maintenance phase to preserve muscle structure and strength.

In mammalian disuse or fasting models, the expression of almost all the genes/proteins involved in muscle degradation increased (Table 18), but this was not observed in the skeletal muscle of *P. annectens* during the maintenance phase of aestivation. The lack of changes in the expression of these genes/proteins of interest in the skeletal muscle of *P. annectens* indicates that 6 months of fasting and lack of locomotor activity did not induce an increase in muscle degradation. These results corroborate previous studies in hibernators. It has been demonstrated that the protein expression of MSTN remains unchanged in the skeletal muscle of thirteen-lined ground squirrels during hibernation (Brooks et al., 2011). Furthermore, the stable

Fbxo32 mRNA expression and the suppression of proteolytic degradation by proteasome in the skeletal muscles are apparently associated with the protection of hibernators from disuse muscle atrophy (Velickovska et al., 2005; Velickovska and van Breukelen, 2007; Lee et al., 2010; Andres-Mateos et al., 2013; Dang et al., 2016).

5.5.3. Arousal phase

The lungfish resumes some locomotor activity during the early arousal phase of aestivation, and requires endogenous fuel for ATP production due to a lack of food supply (Chew et al., 2015) (refer to section 5.4.3.). This might result in increased mobilization of proteins/amino acids from the skeletal muscle, subsequently leading to increased protein turnover and nitrogenous waste production. It is thus logical to predict that muscle degradation may be enhanced during the arousal phase.

However, contrary to our prediction, decreases in the expression of FoxO1, Mstn and Fbxo32 in the skeletal muscle of *P. annectens* occurred after 1 day of arousal from aestivation, suggesting that muscle degradation was still suppressed during the very early phase of arousal (Table 18). Although there was an increase in Hdac1 protein abundance in the skeletal muscle of *P. annectens* after 3 days of arousal, it was not accompanied by increases in the expression of other genes/proteins involved in muscle degradation or decrease in *myod1*/Myod1 expression. Class I HDACs are key regulators of FOXO and the muscle-atrophy program during both fasting and skeletal muscle disuse (Beharry et al., 2014). HDAC1 alone is adequate and required to activate FOXO and induce muscle fibre atrophy/degradation *in vivo*, and is pivotal to contractile dysfunction and muscle atrophy associated with muscle disuse (Beharry et al., 2014). The deacetylase activity of HDAC1 is necessary for

muscle atrophy to occur, and has been linked to the HDAC1-induction of several atrophy genes, including FBXO32, which requires the deacetylation of FOXO3a (Beharry et al., 2014). Since HDAC1 is also essential for the increased gene expression of other FOXO target genes involved in the inhibition of protein synthesis (*Eif4ebp1*) and in the ubiquitin proteasome pathway (*FBXO32* and *MuRF1*), HDAC1 could contribute to muscle atrophy/degradation by increasing FOXO-dependent transcription of target genes involved in various pathways which lead to increased protein turnover (Beharry et al., 2014), and repressing MYOD1 activity (Mal et al., 2001). In the case of arousing *P. annectens*, it is likely that the increase in Hdac1 could be for cell cycle progression and developmental events which might be crucial for the rebuild of muscle mass and strength upon subsequent feeding. Moreover, HDAC1 can deacetylate TP53, inhibiting TP53-dependent transcriptional activation, apoptosis and cell growth arrest (Luo et al., 2000). The increase in Hdac1 protein abundance could be a response to the increased mRNA expression of *tp53* in the muscle of *P. annectens* during the arousal phase, to reduce or arrest cell death. However, this proposition can only be confirmed by further studies to investigate the protein abundance of Tp53 in the muscle of *P. annectens* during aestivation.

5.6. Regulating muscle formation versus regulating muscle degradation

Taken together, these results suggest that, contrary to the author's prediction, muscle degradation was likely suppressed in the muscle of *P. annectens* during the induction phase (Table 18). Hence, it is unlikely that tissue reconstruction of certain organs involved the mobilization of amino acids from the skeletal muscle. Also, these results denote the importance of regulating muscle degradation over muscle formation

during the induction phase in the preservation of skeletal muscle structure in *P. annectens*.

During the maintenance phase, these results suggest that, contrary to the author's prediction, skeletal muscle formation was not suppressed in *P. annectens* during the maintenance phase (Table 17). Furthermore, FBXO32 promotes degradation of MYOD1 (Tintignac et al., 2005), and the rapid suppression of MYOD1 by FBXO32 leads to skeletal muscle wasting (Lagirand-Cantaloube et al., 2009). It has been reported that inhibiting MYOD1 proteolysis by FBXO32 prevents skeletal muscle atrophy *in vivo* (Lagirand-Cantaloube et al., 2009). Since there was no corresponding increase in the protein abundance of Fbxo32 in the muscle of *P. annectens* during the maintenance phase, this supports the notion that decreased myogenesis did not occur in the muscle of aestivating *P. annectens*. On the other hand, the absence of increased expressions of genes/proteins involved in muscle degradation in *P. annectens* during the maintenance phase of aestivation is unique and different from the mammalian fasting and disuse models, and suggested that preservation of skeletal muscle structure involves a suppression of fasting- or disuse-induced increase in muscle degradation. Overall, these results indicate that the regulation of both muscle formation and degradation is important in the preservation of skeletal muscle of *P. annectens* during the maintenance phase of aestivation.

During the early arousal phase of aestivation, our results denote unchanged protein synthesis and suppressed protein degradation in the muscle of *P. annectens* during the first 3 days of arousal from aestivation. Hence, it is unlikely that tissue reconstruction/regeneration of certain organs involved the mobilization of amino

acids from the skeletal muscle during this initial arousal period. However, the possibility of skeletal muscles being mobilized for tissue reconstruction during the subsequent period of arousal before feeding cannot be eliminated.

5.7. Molecular changes in expression of *CuZnsod*/CuZnSod, *Mnsod*/MnSod, *cat*/Cat, *gpx1*/Gpx1 and *gpx4*/Gpx4, and levels of several oxidative stress markers occurring in the muscle of *P. annectens* during the three phases of aestivation

In general, there is a down-regulation in the expression of genes/proteins involved in oxidative defence in the skeletal muscle of animals experiencing fasting or disuse (Di Simplicio et al., 1997; Lawler et al., 2003; Rey et al., 2008) (refer to section 1.5.4.). This phenomenon could explain the increases in the levels of several oxidative stress markers in the skeletal muscle of animals experiencing fasting or disuse (Kondo et al., 1991, 1993; Vogt and Richie, 1993; Di Simplicio et al., 1997; Lawler et al., 2003; Brocca et al., 2010; Desaphy et al., 2010), especially since prolonged skeletal muscle inactivity due to immobilization leads to chronic increases in production of ROS and oxidative damage in quiescent muscle fibres (Kondo et al., 1991). Although increases in the levels of oxidative stress markers were also reported in hibernating or aestivating animals, these increases were accompanied by increases in the expression of genes/proteins involved in oxidative defence (Grundy and Storey, 1998; Ramos-Vasconcelos et al., 2003; Hudson et al., 2006; Nowakowska et al., 2010, 2014; Young et al., 2013a, b), indicating that increased oxidative defence conferred a protective effect on the skeletal muscle. These results, together with results obtained from this study, are summarised in Tables 19 and 20.

Table 19. Comparison of changes in expression of various genes/proteins involved in oxidative defense in response to fasting-induced muscle atrophy, disuse-induced muscle atrophy (includes denervation, hindlimb suspension and unloading), torpor (includes hibernation and aestivation) and the three phases of aestivation. Decreases in expression are denoted with '-', while increases in expression are denoted with '+'. No significant changes in expression are denoted with '0'. 'N.A.' denotes no information is available.

Genes/Proteins	Fasting	Disuse	Torpor	Aestivation		
				Induction	Maintenance	Arousal
CuZnsod/ CuZnSod	-	+	+	0	+	+
Mnsod/MnSod	-	-	+	0	0	0
cat/Cat	-	-	+	+	0	+
gpx1/Gpx1	0	-	+	0	0	+
gpx4/Gpx4	0	-	+	0	+	0

Table 20. Comparison of changes in expression of oxidative stress markers in response to fasting-induced muscle atrophy, disuse-induced muscle atrophy (includes denervation, hindlimb suspension and unloading), torpor (includes hibernation and aestivation) and the three phases of aestivation. Decreases are denoted with '-', while increases are denoted with '+'. No significant changes are denoted with '0'. 'N.A.' denotes no information is available.

Oxidative stress markers	Fasting	Disuse	Torpor	Aestivation		
				Induction	Maintenance	Arousal
Total GSheq	-	-	+	0	+	+
[GSSG]/[GSH] ratio	+	+	+	+	+	0
Lipid hydroperoxides	N.A.	+	+	0	0	0
TBARS	N.A.	+	+	0	0	-
Carbonyl protein	N.A.	+	+	0	-	-

5.7.1. Induction phase

During the induction phase, *P. annectens* experiences fasting (although not severe) and incomplete muscle disuse, especially for the first 3 days (refer to section 5.4.1.). Moreover, the lungfish hyperventilates during this period, and may experience increased oxidative stress. The stable expression of CuZnSod and MnSod in the muscle of *P. annectens* during the induction phase differs from the responses reported in fasting or disuse in mammalian models (Table 19). The stable expression of Gpx1 and *gpx4*/Gpx4, although similar to responses reported in fasting, is different from the responses reported in disuse mammalian models (Table 19). These could be due to the short period of food deprivation and the incompleteness of muscle disuse, resulting in only mild oxidative stress which could be adequately handled by the other components of the oxidative defense mechanisms. Alternatively, oxidative stress during the induction phase could result from hyperventilation and a possibly increased metabolic rate (Chew et al., 2015). DeLaney et al. (1974) reported that hyperventilation occurred in *P. aethiopicus* and that the ventilation rate increased two- to five-fold during the first 30 days of aestivation before returning to the control range (2-10 hr) within 45 days. During the first 10 days of aestivation, there was an increase in the arterial P_{O_2} from the control range of 25-40 to 50-58 mmHg, which then returned to the control range (DeLaney et al., 1974). The increase in metabolic rate could be a result from the structural and functional modifications of cells and tissues in preparation for the maintenance phase of aestivation (Chew et al., 2015).

Indeed, increases in Cat protein abundance, Gr activity, [GSSG] and [GSSG]/[GSH] occurred in the muscle of *P. annectens* during the induction phase,

indicating increased physiological oxidative stress. Cat is thought to be crucial in maintaining the integrity of muscle (Stauber et al., 1977), and increase in its expression, as opposed to decreases reported in fasting and muscle disuse models, could be essential in preventing the onset of oxidative damages and avoiding subsequent muscle atrophy. Increases in [GSSG] and [GSSG]/[GSH] in the muscle of *P. annectens* during the induction phase indicate increases in peroxide and GSH consumption, respectively. Increased GSH consumption for peroxide detoxification occurs during dormancy, and is an indicator of physiological oxidative stress during the induction phase of aestivation. Furthermore, an increase in Gr activity could be a response to the increases in [GSSG] and [GSSG]/[GSH]. GR is responsible for replenishing the intracellular GSH pool by reducing GSSG to GSH and is believed to be the major regulator of the redox reaction involving GSSG and GSH (Yang et al., 2006). Indeed, [GSH] remained unchanged in the muscle of *P. annectens* during the induction phase, despite an increase in GSH consumption, indicating that the intracellular GSH pool was probably maintained by Gr.

Despite signs of increased oxidative stress in the muscle of *P. annectens* during the induction phase, there were no significant changes in the levels of oxidative damage products in the muscle of *P. annectens* as compared to the control. These results differ from the responses to disuse (Table 20) and demonstrate the robustness of the antioxidant defenses in the muscle of *P. annectens*, where antioxidant defenses are increased to deal with increased oxidative stress during the induction phase.

5.7.2. Maintenance phase

During the maintenance phase, the aestivating lungfish faces severe fasting and muscle disuse (refer to section 5.4.2.), which might lead to increased ROS production in the skeletal muscle, and result in possible atrophy. A recent study demonstrated increases in the expression of MnSOD and CAT in the skeletal muscle of hibernating squirrels (Xu et al., 2013). These increases were associated with a corresponding increase in PPARGC-1a (Xu et al., 2013). An increase in MnSOD was also reported in the skeletal muscle of ground squirrels during early torpor (Allan and Storey, 2012). In contrast, there was a stable expression of MnSod, *cat*/Cat and Ppargc-1a (section 5.4.2.) in the skeletal muscle of *P. annectens* during the maintenance phase, which differs from mammalian models of fasting or muscle disuse (Table 19). Only increases in the protein expression of CuZnSod and Gpx4, and glutathione biosynthesis, were observed in the skeletal muscle of *P. annectens* during the maintenance phase of aestivation. The stable expression of MnSod in the skeletal muscle of *P. annectens* during the maintenance phase indicated that (1) there was little superoxide generated in the muscle of *P. annectens*, or (2) another Sod could be taking over the role of MnSod in the muscle of *P. annectens*.

As SODs are the first line of defense against oxidative stress, and since there could be intermittent bursts of ROS production during aestivation (Storey, 2002), it is highly unlikely that there was little superoxide generation in the muscle of *P. annectens.* Furthermore, the mitochondria appear to be the main site of inactivity-induced ROS production in skeletal muscles (Muller et al., 2007; Kavazis et al., 2009; Min et al., 2011; Powers et al., 2011; Talbert et al., 2013). Although CuZnSOD is

classically reported to be a cytosolic enzyme (Halliwell and Gutteridge, 1989) and does not possess a mitochondrial targeting sequence, there is emerging evidence that CuZnSOD is also located in the mitochondrial inter-membrane space (Saito et al., 1989; Kawamata and Manfredi, 2010), and is possibly present at high concentration in comparison with cytosolic CuZnSOD (Jackson, 2013). It is possible that CuZnSod plays a more important role in oxidative defense than MnSod in the muscle of *P. annectens* during the maintenance phase of aestivation. CuZnSOD is imported as a catalytically inactive enzyme into the intermembrane space during mitochondrial import, and is processed by the copper chaperone for CuZnSOD (CCS) into the active enzyme, thereby becoming trapped in the mitochondria (Leitch et al., 2009; Kawamata and Manfredi, 2010). The import of CuZnSOD and CCS occurs via a disulphide relay system involving the import receptor Mia40 (Reddehase et al., 2009; Kawamata and Manfredi, 2010).

Thus, the CuZnSod of *P. annectens* could be imported into the mitochondria in a similar manner, and may be the main Sod scavenging superoxide generated in the mitochondria instead of MnSod. This could explain the significant increase in the protein abundance of CuZnSod, but not MnSod, in the muscle of *P. annectens* after 6 months of aestivation. These results corroborate reports on increased CuZnSod activity in the muscle of aestivating snails (Hermes-Lima and Storey, 1995; Salway et al., 2010) and spadefoot toads (Grundy and Storey, 1998). Superficially, the increase in expression of CuZnSod in the muscle of *P. annectens* during the maintenance phase aestivation appears to bear similarity with the mammalian muscle disuse models (Table 19). However, in the case of mammalian muscle disuse, there are

significant decreases in the expression of multiple components of the oxidative defence system but those responses were absent from the skeletal muscle of aestivating *P. annectens* (Table 19).

Increased superoxide scavenging capacity (possibly SOD activity) was also demonstrated in both iliofibularis and gastrocnemius muscles of aestivating *Cyclorana alboguttata* (Young et al., 2013b), although it is unclear which SOD is responsible for the increased superoxide scavenging capacity. A recent study reveals suppressed mitochondrial ROS production in the disused skeletal muscle of aestivating *Cyclorana alboguttata*, which might protect against potential oxidative injury, allowing the preservation of skeletal muscle structure during aestivation in preparation for arousal (Reilly et al., 2014). To confirm which Sod is responsible for scavenging mitochondrial ROS in the muscle of *P. annectens* during the maintenance phase, further studies need to be conducted to determine the localization of each of these two Sods.

Among the selenoproteins of the GPX family, GPX4 protects membranes from oxidative insult as it has a unique ability to reduce not only H_2O_2 but also hydroperoxides in complex lipids including phospholipids, cholesterol and cholesterolester hydroperoxides, even when these lipids are found inserted into biomembranes or lipoproteins (Thomas et al., 1990). The increase in the expression of *gpx4*/Gpx4 in the muscle of aestivating *P. annectens* indicates increased protection of membranes against oxidative injury. Corresponding increases in SeGpx and total Gpx activities were also observed in the muscle of aestivating *P. annectens*, and could be attributed to the increase in the expression of *gpx4*/Gpx4, but not Gpx1. The

increased Gpx activities corroborated with increased SeGpx activity observed in the sea cucumber (Wang et al., 2011) and the muscle of aestivating land snails (Nowakowska et al., 2010, 2014), and total Gpx activity observed in spadefoot toads (Grundy and Storey, 1998).

Decreases in GSH contents in sea cucumbers during the maintenance phase of aestivation were attributed to the adaptive strategy of sea cucumbers to reduce ROS production during aestivation at higher temperatures (Ji et al., 2008; Wang et al., 2011). Similar decreases in GSH concentrations were also reported in several tissues of spadefoot toads under aestivation (Grundy and Storey, 1998). In contrast, increased GSH contents were observed in the muscle of aestivating *P. annectens*, accompanied with increases in GSSG and GSSG/GSH, indicative of physiological oxidative stress. This redox imbalance (increases in GSSG and GSSG/GSH) is also observed in land snails (Hermes-Lima and Storey, 1995) and spadefoot toads (Grundy and Storey, 1998; Hermes-Lima et al., 2001) during aestivation, and indicates oxidative stress.

Increased oxidative stress is also observed in aestivating snails (*Helix aspersa*); they have increased carbonyl protein levels in foot muscle as compared to aroused active snails (Ramos-Vasconcelos et al., 2003). Furthermore, increases in lipid peroxidation are observed in the muscle of aestivating spadefoot toads (Grundy and Storey, 1998), and in the muscle of *Helix pomatia* during winter torpor, accompanied with increases in enzymatic antioxidant activities (Nowakowska et al., 2009). Carbonyl protein levels also increase in the iliofibularis muscle, but not in the gastrocnemius muscle, in striped burrowing frogs after 6 months of aestivation

(Young et al., 2013b), indicating increased oxidative stress and is consistent with greater disuse muscle atrophy in iliofibularis than gastrocnemius (Young et al., 2013a). In contrast, different from these observations (Table 20), there was a decrease in carbonyl protein levels in the muscle of *P. annectens* after 6 months of aestivation. This, together with results from the glutathione system, implies an increase in the antioxidant capacity in the skeletal muscle of *P. annectens* during the maintenance phase, thereby reducing oxidative insult and helping to prevent disuse muscle atrophy, as observed in the gastrocnemius muscle of aestivating striped burrowing frogs (Hudson et al., 2006; Young et al., 2013a, b).

5.7.3. Arousal phase

During the arousal phase of aestivation, there is resumption of locomotor but not feeding activity in *P. annectens* (refer to section 5.4.3.). Moreover, there are increases in metabolism and oxygen uptake, implying increased oxidative stress during the arousal phase. There could be increases in the expression of genes/proteins involved in oxidative defence and in the levels of oxidative stress markers in the muscle of *P. annectens* during the arousal phase.

In mammals, fasting leads to decreases in expression of almost all the genes/proteins of interest involved in oxidative defense (Table 19), but a similar phenomenon did not occur in the skeletal muscle of *P. annectens* during the arousal phase of aestivation. The stable expression of MnSod and Gpx4 in the skeletal muscle of *P. annectens* was accompanied with increases in the protein expression levels of CuZnSod, Cat and Gpx1 during the arousal phase. There was also an increase in MnSod activity despite its stable expression. These results support the proposition

that an increase in the degradation of skeletal muscle might not have occurred in *P. annectens* during this early period of arousal.

As the rate of superoxide and H_2O_2 production by the mitochondria is proportional to oxygen tension in many biological systems (Turrens et al., 1982; Cino and Del Maestro, 1989; Beckman and Ames, 1998), a rise in oxygen tension and consumption in aestivators/hibernators during arousal could result in increased production of ROS (Storey, 2002). It is expected that ROS production would increase in the muscle of *P. annectens* upon arousal due to the increase in oxygen consumption and metabolism, which must be dealt with rapidly by endogenous antioxidant defenses in order to avoid oxidative injury. Hermes-Lima and Storey (1995) measured intracellular antioxidant enzyme activities in aestivating snails and found that there was a broad-based up-regulation in various tissues. This was thought to provide protection against ischemia-reperfusion events associated with the transition from aestivation to arousal (Hermes-Lima and Zenteno-Savín, 2002). Similar results have been obtained for other terrestrial snail that undergo aestivation (Ramos-Vasconcelos and Hermes-Lima, 2003; Ramos-Vasconcelos et al., 2005; Nowakowska et al., 2009). Upregulation in antioxidant enzymes have also been reported in hibernators upon arousal. For example, there were increases in SOD and GPX activities in the interscapular brown adipose tissue of arousing hibernators (Buzadžić et al., 1990). Enhanced GPX activity occurred in the liver of arousing 13-lined ground squirrels (Buzadžić et al., 1990; Page et al., 2009), while plasma SOD and CAT activities increased sharply in the plasma of Syrian hamsters upon arousal (Ohta et al., 2006; Okamoto et al., 2006).

The increases in MnSod activity and the expression of CuZnSod and Gpx1 in the skeletal muscle of *P. annectens* during the early arousal phase corroborates studies reporting an increase in SOD activity in the muscle of frogs aroused from winter hibernation (Bagnyukova et al., 2003) and enhanced Gpx activity in the foot muscle of arousing snails (Salway et al., 2010). The increase in Cat expression in the muscle of *P. annectens* corroborates with elevated CAT in the muscle of frogs (Bagnyukova et al., 2003) upon arousal from hibernation. Furthermore, increases in total Sod and Cat activities occurred in the foot muscle of snails upon arousal (Hermes-Lima et al., 1995). Overall, results from this study indicate increased antioxidant capacity in the muscle of *P. annectens* to counter increased oxidative stress upon arousal.

The increase in anti-oxidative defense capacity in the skeletal muscle was apparently effective in preventing oxidative damages in the skeletal muscle of *P. annectens* during the early period of arousal. In fact, oxidative damage products decreased in the muscle of arousing *P. annectens*, which was similar to the decrease in TBARS in the foot muscle of apple snails upon arousal (Giraud-Billoud et al., 2013). Levels of TBARS and carbonyl proteins remained unchanged in the foot muscle of snails upon arousal (Ramos-Vasconcelos et al., 2005; Nowakowska et al., 2009). This contradicts reports of increased oxidative damages in some non-muscle organs of aestivators (Hermes-Lima and Storey, 1995; Ramos-Vasconcelos et al., 2003) and hibernators (Orr et al., 2009) during arousal. Carbonyl proteins and lipid peroxide end products in brown adipose tissue of hibernating Arctic ground squirrels were greater in late arousal than during hibernation (Orr et al., 2009). Lipid

peroxidation also increased in the hepatopancreas of land snails during the first few minutes of arousal (Hermes-Lima and Storey, 1995; Ramos-Vasconcelos et al., 2003). Furthermore, [GSSG] returned to control values upon arousal. When taken together, these results indicate that the skeletal muscle of *P. annectens* was confronted with minimal or no oxidative stress during the arousal phase of aestivation. It could be that the skeletal muscle underwent a profound suppression of ROS formation during the maintenance phase (section 5.7.2.), and this was carried over into the early arousal phase and reduced the severity of the oxidative stress associated with the ischemic-reperfusion event.

5.8. Limitations of the study

As this study only focuses on determining the transcript levels and protein abundances of various genes and proteins known to be involved in muscle atrophy, there is still a dearth of information, especially with regards to the structural and/or ultrastructural observations of the skeletal muscle of *P. annectens* during the three phases of aestivation. Furthermore, information on the presence of satellite cells is lacking, and it remains unclear if satellite cells partake in preventing muscle atrophy, especially during the maintenance phase of aestivation. However, this study provides novel insights into some of the molecular mechanisms and pathways, and provides guidance for future studies investigating the above unknowns mentioned.

6. Summary

Results from this study reveal that there are up- and down-regulation of various genes/proteins involved in muscle formation, muscle degradation and oxidative defense in the muscle of *P. annectens* during the three phases of aestivation. Hence, aestivation cannot be simply regarded as a general depression of metabolism (Ip and Chew, 2010). Aestivation instead involves a complex interplay between up- and down-regulation of diverse cellular activities and tightly-controlled subcellular organization of transcriptional and/or translational machineries to meet the challenges associated with aestivation.

During the induction phase of aestivation, there were only minor changes in the expressions of various genes/proteins involved in both muscle formation and muscle degradation, involving only *tp53* and Fbxo32 which increased and decreased, respectively, in the muscle of *P. annectens*. The lack of changes in the expressions of most genes/proteins involved in both muscle formation and muscle degradation could be due to the short period of fasting and the incompleteness of muscle disuse during this initial period of aestivation. The increase in *tp53* could be due to the cellular stress brought on by aestivation, while the decreased Fbxo32 expression might indicate decreased ubiquitination and proteolysis of muscle proteins. These results indicate that muscle degradation was likely suppressed in the muscle of *P. annectens* during the induction phase, and is contrary to the proposition that tissue reconstruction involved mobilization of proteins/amino acids from the muscle of *P. annectens* during this initial period of aestivation (Chew et al., 2015). They also denote the importance of regulating muscle degradation over regulating muscle

formation. Although there were signs of increased oxidative stress in the muscle of *P. annectens*, as indicated by increased Cat protein abundance, Gr activity, [GSSG] and [GSSG]/[GSH], there were no significant changes in the levels of oxidative damage products in the muscle of *P. annectens* as compared to the control. This could be explained by the robustness of the antioxidant defense system in the muscle of *P. annectens*, whereby antioxidant defense mechanisms were up-regulated to deal with increased oxidative stress during the induction phase to prevent oxidative injury.

During the maintenance phase of aestivation, there were only slight changes in the expression of genes/proteins involved in muscle formation, despite the aestivating lungfish undergoing severe fasting. The stable expression of Ppargc-1α, Myog and Mapk1/3 could have contributed to muscle mass preservation through maintaining a certain rate of protein synthesis. An upregulation in the protein abundance of Myod1 could also contribute to muscle mass preservation by increasing the conversion of non-muscle cells to muscle cells during the maintenance phase of aestivation. The absence of increased expressions of genes/proteins involved in muscle degradation in the muscle of *P. annectens* during the maintenance phase was unique and differed from the mammalian fasting and muscle disuse models. Preservation of skeletal muscle structure and strength in aestivating *P. annectens* probably involved a suppression of fasting- and/or disuse-induced increase in muscle degradation. Prolonged muscle disuse can lead to increased ROS production in the mitochondria and subsequent muscle atrophy. In the case of aestivating *P. annectens*, the expression of MnSod was stable, but the expression of CuZnSod increased in the skeletal muscle, suggesting that CuZnSod could be the main Sod scavenging

mitochondrial ROS and protecting the muscle from oxidative damages. The expression of *gpx4*/Gpx4 also increased in the skeletal muscle, indicating increased protection of membranes against oxidative injury. Although there were signs of increased oxidative stress in the muscle of *P. annectens* during the maintenance phase, as indicated by increased [GSSG] and [GSSG]/[GSH], there was a decrease in the levels of carbonyl proteins. Furthermore, there could be an increase in the production of glutathione. Overall, these results indicate an increase in the antioxidant capacity in the skeletal muscle of *P. annectens* during the maintenance phase of aestivation, thereby reducing oxidative insult and helping to prevent disuse muscle atrophy.

During the arousal phase of aestivation, the expression of genes/proteins involved in muscle formation remained unchanged in the muscle of *P. annectens*. However, muscle degradation was apparently suppressed during the very early phase of arousal, as indicated by decreases in the protein abundances of FoxO1, Mstn and Fbxo32 after 1 day of arousal from aestivation. Although Hdac1 expression was upregulated after 3 days of arousal, it was not accompanied by increases in the expression of other genes/proteins involved in muscle degradation or a decrease in the expression of *myod1*/Myod1. Therefore, the increase in Hdac1 expression could be a response to the increased mRNA expression of *tp53* in the muscle of *P. annectens* during this period, so as to reduce or arrest cell death. These results denote that tissue reconstruction/regeneration of certain organs during this initial arousal period was unlikely to involve the mobilization of amino acids from the skeletal muscle. However, the possibility of the skeletal muscles being mobilized for tissue reconstruction during the subsequent period of arousal before feeding cannot be

ignored and deserves further investigation in the future. Oxygen consumption is known to increase in the lungfish during the arousal phase of aestivation. Indeed, there were increases in MnSod activity and protein abundances of CuZnSod, Cat and Gpx1 in the muscle of *P. annectens*, indicating increased antioxidant defenses therein. These responses were apparently effective in protecting the skeletal muscle against oxidative insult, as the concentrations of oxidative damage products decreased in the muscle of the aroused fish. Taken together, these results indicate that the skeletal muscle of the aroused fish was confronted with minimal or no oxidative stress, and support the notion that an increase in the degradation of skeletal muscle might not have occurred in *P. annectens* during this early period of arousal.

In the future, immunohistochemical studies should be conducted to determine the localization of CuZnSod and MnSod in the muscle of *P. annectens* during the three phases of aestivation. Immunohistochemical studies should also be performed on the skeletal muscle fibres of *P. annectens* during the three phases of aestivation to determine if there was a switch of muscle fibre types during aestivation, as certain muscle fibre types are reported to be more resistant to atrophy. As a pioneer study, information obtained from this study will guide the development of future research proposals on new interventions for the prevention of disuse muscle atrophy in many clinical situations and in our ageing society. Understanding the mechanism and pathways that contribute to amelioration or prevention of disuse muscular atrophy would prove useful in developing counter-measures against skeletal muscle wasting in humans.

7. References

Abadi, A., Glover, E. I., Isfort, R. J., Raha, S., Safdar, A., Yasuda, N., Kaczor, J. J., Melov, S., Hubbard, A., Qu, X., Phillips, S. M. and Tarnopolsky, M. (2009). Limb immobilization induces a coordinate down-regulation of mitochondrial and other metabolic pathways in men and women. *PLoS One* **4(8)**, e6518. doi: 10.1371/journal.pone.0006518

Aebi, H. (1984). Catalase *in vitro*. *Methods Enzymol.* **105**, 121–126.

Ahmad, S. and Pardini, R. S. (1988). Evidence for the presence of glutathione peroxidase activity toward an organic hydroperoxide in larvae of the cabbage looper moth, *Trichoplusia ni*. *Insect Biochem.* **18(8)**, 861–866.

Ahn, N. G., Seger, R., Bratlien, R. L., Diltz, C. D., Tonks, N. K. and Krebs, E.G. (1991). Multiple components in an epidermal growth factor–stimulated protein kinase cascade. *J. Biol. Chem.* **266**, 4220–4227.

Akimoto, T., Pohnert, S. C., Li, P., Zhang, M., Gumbs, C., Rosenberg, P. B., Williams, R. S. and Yan, Z. (2005). Exercise stimulates Pgc-1α transcription in skeletal muscle through activation of the p38 MAPK pathway. *J. Biol. Chem.* **280(20)**, 19587–19593.

Alberts, B., Johnson, A., Lewis, J., Raff, M., Roberts, K. and Walter, P. (2008) *Molecular Biology of the Cell, 5th ed*. New York: Garland Science.

Allan, M. E. and Storey, K. B. (2012). Expression of NF-κB and downstream antioxidant genes in skeletal muscle of hibernating ground squirrels, *Spermophilus tridecemlineatus*. *Cell Biochem. Funct.* **30**, 166–174.

Allen, D. L. and Unterman, T. G. (2007). Regulation of myostatin expression and myoblast differentiation by FoxO and SMAD transcription factors. *Am. J. Physiol. Cell Physiol.* **292(1)**, C188–C199.

Allen, D. L. and Du, M. (2008). Comparative functional analysis of the cow and mouse myostatin genes reveals novel regulatory elements in their upstream promoter regions. *Comp. Biochem. Physiol. B Biochem. Mol. Biol.* **150(4)**, 432–439.

Allen, D. L., Bandstra, E. R., Harrison, B. C., Thorng, S., Stodieck, L. S., Kostenuik, P. J., Morony, S., Lacey, D. L., Hammond, T. G., Leinwand, L. L., Argraves, W. S., Bateman, T. A. and Barth, J. L. (2009). Effects of spaceflight on murine skeletal muscle gene expression. *J. Appl. Physiol.* **106(2)**, 582–595.

Allen, D. L., Cleary, A. S., Lindsay, S. F., Loh, A. S. and Reed, J. M. (2010). Myostatin expression is increased by food deprivation in a muscle-specific manner and contributes to muscle atrophy during prolonged food deprivation in mice. *J. Appl. Physiol.* **109(3)**, 692–701.

Almar, M., Otero, L., Santos, C. and Gallego, J. G. (1998). Liver glutathione content and glutathione-dependent enzymes of two species of freshwater fish as bioindicators of chemical pollution. *J. Env. Sci. Health B* **33(6)**, 769–783.

Alway, S. E., Lowe, D. A. and Chen, K. D. (2001). The effects of age and hindlimb suspension on the levels of expression of the myogenic regulatory factors MyoD and myogenin in rat fast and slow skeletal muscles. *Exp. Physiol.* **86(4)**, 509–517.

Amelio, D., Garofalo, F., Brunelli, E., Loong, A. M., Wong, W. P., Ip, Y. K., Tota, B., and Cerra, M. C. (2008). Differential NOS expression in freshwater and aestivating *Protopterus dolloi* (lungfish): heart vs kidney readjustments. *Nitric Oxide* **18(1)**, 1–10.

Amelio, D., Garofalo, F., Wong, W. P., Chew, S. F., Ip, Y. K., Cerra, M. C. and Tota, B. (2013). Nitric oxide synthase-dependent "on/off" switch and apoptosis in freshwater and aestivating lungfish, *Protopterus annectens*: skeletal muscle versus cardiac muscle. *Nitric Oxide* **32**, 1–12.

Amemiya, C.T., Alföldi, J., Lee, A.P., Fan, S., Philippe, H., Maccallum, I., Braasch, I., Manousaki, T., Schneider, I., Rohner, N., Organ, C., Chalopin, D., Smith, J.J., Robinson, M., Dorrington, R.A., Gerdol, M., Aken, B., Biscotti, M.A., Barucca, M., Baurain, D., Berlin, A.M., Blatch, G.L., Buonocore, F., Burmester, T., Campbell, M.S., Canapa, A., Cannon, J.P., Christoffels, A., De Moro, G., Edkins, A.L., Fan, L., Fausto, A.M., Feiner, N., Forconi, M., Gamieldien, J., Gnerre, S., Gnirke, A., Goldstone, J.V., Haerty, W., Hahn, M.E., Hesse, U., Hoffmann, S., Johnson, J., Karchner, S.I., Kuraku, S., Lara, M., Levin, J.Z., Litman, G.W., Mauceli, E., Miyake, T., Mueller, M.G., Nelson, D.R., Nitsche, A., Olmo, E., Ota, T., Pallavicini, A., Panji, S., Picone, B., Ponting, C.P., Prohaska, S.J., Przybylski, D., Saha, N.R., Ravi, V., Ribeiro, F.J., Sauka-Spengler, T., Scapigliati, G., Searle, S.M., Sharpe, T., Simakov, O., Stadler, P.F., Stegeman, J.J., Sumiyama, K., Tabbaa, D., Tafer, H., Turner-Maier, J., van Heusden, P., White, S., Williams, L., Yandell, M., Brinkmann, H., Volff, J.N., Tabin, C.J., Shubin, N., Schartl, M., Jaffe, D.B., Postlethwait, J.H., Venkatesh, B., Di Palma, F., Lander, E.S., Meyer, A. and Lindblad-Toh, K. (2013). The African coelacanth genome provides insights into tetrapod evolution. *Nature* **496**, 311–316.

Amirouche, A., Durieux, A. C., Banzet, S., Koulmann, N., Bonnefoy, R., Mouret, C., Bigard, X., Peinnequin, A. and Freyssenet, D. (2009). Down-regulation of Akt/mammalian target of rapamycin signaling pathway in response to myostatin overexpression in skeletal muscle. *Endocrinology* **150(1)**, 286–294.

Amores, A., Force, A., Yan, Y. L., Joly, L., Amemiya, C., Fritz, A., Ho, R. K., Langeland, J., Prince, V., Wang Y. L., Westerfield, M., Ekker, M. and Postlethwait, J. H. (1998). Zebrafish hox clusters and vertebrate genome evolution. *Science* **282(5394)**, 1711–1714.

Amthor, H., Otto, A., Macharia, R., McKinnell, I. and Patel, K. (2006). Myostatin imposes reversible quiescence on embryonic muscle precursors. *Dev. Dyn.* **235(3)**, 672–680.

Andres-Mateos, E., Brinkmeier, H., Burks, T. N., Mejias, R., Files, D. C., Steinberger, M., Soleimani, A., Marx, R., Simmers, J. L., Lin, B., Hedderick, E. F., Marr, T. G., Lin, B. M., Hourdé, C., Leinwand, L. A., Kuhl, D., Föller, M., Vogelsang, S., Hernandez-Diaz, I., Vaughan, D. K., Alvarez de la Rosa, D., Lang, F. and Cohn, R. D. (2013). Activation of serum/glucocorticoid-induced kinase 1 (SGK1) is important to maintain skeletal muscle homeostasis and prevent atrophy. *EMBO Mol. Med.* **5(1)**, 80–91.

Ángeles Esteban, M. (2012). An overview of the immunological defenses in fish skin. *ISRN Immunology* 2012.

Arbogast, S., Smith, J., Matuszczak, Y., Hardin, B. J., Moylan, J. S., Smith, J. D., Ware, J., Kennedy, A. R. and Reid, M. B. (2007). Bowman-Birk inhibitor concentrate prevents atrophy, weakness and oxidative stress in soleus muscle of hindlimb-unloaded mice. *J. Appl. Physiol.* **102(3)**, 956–964.

Arnold, H. H. and Winter, B. (1998). Muscle differentiation: more complexity to the network of myogenic regulators. *Curr. Opin. Genetics Dev.* **8(5)**, 539–544.

Augustyn, K. E., Merino, E. J. and Barton, J. K. (2007). A role for DNA-mediated charge transport in regulating p53: Oxidation of the DNA-bound protein from a distance. *Proc. Natl. Acad. Sci. U. S. A.* **104(48)**, 18907–18912.

Babiker, M. M. and El Hakeem, O. (1979). Changes in blood characteristics and constituents associated with aestivation in the African lungfish *Protopterus annectens* Owen. *Zoologischer Anzeiger* **202(1-2)**, 9–16.

Bagnyukova, T. V., Storey, K. B. and Lushchak, V. I. (2003). Induction of oxidative stress in *Rana ridibunda* during recovery from winter hibernation. *J. Therm. Biol*. **28(1)**, 21–28.

Bailey, R. G. (1994). Guide to the fishes of the River Nile in the Republic of the Sudan. *J. Nat. Hist.* **28(4)**, 937–970.

Bakker, W. J., Blázquez-Domingo, M., Kolbus, A., Besooyen, J., Steinlein, P., Beug, H., Coffer, P. J., Löwenberg, B., von Lindern, M. and van Dijk, T. B. (2004). FoxO3a regulates erythroid differentiation and induces BTG1, an activator of protein arginine methyl transferase 1. *J. Cell Biol.* **164(2)**, 175–184.

Ballantyne, J. S. and Frick, N. T. (2010). Lungfish metabolism. In: *The biology of lungfishes* (ed. J. M. Jorgensen and J. Joss), pp. 301–335. Science Publishers, New Hampshire.

Beckman, K. B. and Ames, B. N. (1998). The free radical theory of aging matures. *Physiol. Rev.* **78(2)**, 547–581.

Beharry, A. W., Sandesara, P. B., Roberts, B. M., Ferreira, L. F., Senf, S. M. and Judge, A. R. (2014). HDAC1 activates FoxO and is both sufficient and required for skeletal muscle atrophy. *J. Cell Sci.* **127(7)**, 1441–1453.

Belkin, D. A. (1965). Reduction of metabolic rate in response to starvation in the turtle *Sternothaerus minor*. *Copeia* **1965(3)**, 367–368.

Bemis, W. E., Burggren, W. W. and Kemp, N. E. (1987). *The Biology and Evolution of Lungfish.* Alan R. Liss, New York.

Bengal, E., Flores, O., Rangarajan, P. N., Chen, A., Weintraub, H. and Verma, I. M. (1994). Positive control mutations in the MyoD basic region fail to show cooperative DNA binding and transcriptional activation in vitro. *Proc. Natl. Acad. Sci. U. S. A.* **91(13)**, 6221–6225.

Berghella, L., De Angelis, L., Debuysscher, T., Mortazavi, A., Biressi, S., Forcales, S. V., Sirabella, D., Cossu, G. and Wold, B. J. (2008). A highly conserved molecular switch binds MSY-3 to regulate myogenin repression in postnatal muscle. *Genes Dev.* **22**, 2125–2138.

Berra, T. M. (2001). Freshwater fish distribution. San Diego: Academic Press.

Bialek, P., Morris, C. A., Parkington, J. andre, M. S., Owens, J., Yaworsky, P., Seeherman, H. and Jelinsky, S. A. (2011). Distinct protein degradation profiles are induced by different disuse models of skeletal muscle atrophy. *Physiol. Genomics* **43(19)**, 1075–1086.

Bieging, K. T., Mello, S. S. and Attardi, L. D. (2014). Unravelling mechanisms of p53-mediated tumour suppression. *Nat. Rev. Cancer* **14(5)**, 359–370.

Biolo, G., Ciocchi, B., Lebenstedt, M., Barazzoni, R., Zanetti, M., Platen, P., Heer, M. and Guarnieri, G. (2004). Short-term bed rest impairs amino acid-induced protein anabolism in humans. *J. Physiol.* **558(2)**, 381–388.

Bjerling, P., Silverstein, R. A., Thon, G., Caudy, A., Grewal, S. and Ekwall, K. (2002). Functional divergence between histone deacetylases in fission yeast by distinct cellular localization and in vivo specificity. *Mol. Cell. Biol.* **22(7)**, 2170–2181.

Blanc, M., D'Aubenton, F. and Plessis, Y. (1956). Étude de l'enkystement de *Protopterus annectens*. *Bull. Inst. Fondam*. **18A**, 843–854.

Blander, G. and Guarente, L. (2004). The Sir2 family of protein deacetylases. *Ann. Rev. Biochem.* **73(1)**, 417–435.

Bodine, S. C. (2013). Disuse-induced muscle wasting. *Int. J. Biochem. Cell Biol.* **45(10)**, 2200–2208.

Bodine, S. C., Latres, E., Baumhueter, S., Lai, V. K. M., Nunez, L., Clarke, B. A., Poueymirou, W. T., Panaro, F. J., Na, E., Dharmarajan, K., Pan, Z. Q., Valenzuela, D. M., DeChiara, T. M., Stitt, T. N., Yancopoulos, G. D. and Glass, D. J. (2001). Identification of ubiquitin ligases required for skeletal muscle atrophy. *Science* **294(5547)**, 1704–1708.

Bogoyevitch, M. A. (2006). The isoform-specific functions of the c-Jun N-terminal Kinases (JNKs): differences revealed by gene targeting. *Bioessays* **28(9)**, 923–934.

Bogoyevitch, M. A. and Court, N. W. (2004). Counting on mitogen-activated protein kinases–ERKs 3, 4, 5, 6, 7 and 8. *Cell. Signal.* **16(12)**, 1345–1354.

Bonaldo, P. and Sandri, M. (2013). Cellular and molecular mechanisms of muscle atrophy. *Dis. Model Mech.* **6(1)**, 25–39.

Booth, F. W. and Seider, M. J. (1979). Early change in skeletal muscle protein synthesis after limb immobilization of rats. *J. Appl. Phyiol.* **47**, 974–977.

Bower, N. I. and Johnston, I. A. (2010). Paralogs of Atlantic salmon myoblast determination factor genes are distinctly regulated in proliferating and differentiating myogenic cells. *Am. J. Physiol. Regul. Integr. Comp. Physiol.* **298(6)**, R1615–R1626.

Bower, N. I., de la Serrana, D. G. and Johnston, I. A. (2010). Characterisation and differential regulation of MAFbx/Atrogin-1 α and β transcripts in skeletal muscle of Atlantic salmon (*Salmo salar*). *Biochem. Biophy. Res. Commun.* **396(2)**, 265–271.

Bradford, M. M. (1976). A rapid and sensitive method for the quantitation of microgram quantities of protein utilizing the principle of protein–dye binding. *Anal. Biochem.* **72**, 248–254.

Bradner, J. E., West, N., Grachan, M. L., Greenberg, E. F., Haggarty, S. J., Warnow, T. and Mazitschek, R. (2010). Chemical phylogenetics of histone deacetylases. *Nat. Chem. Biol.* **6(3)**, 238–243.

Brault, J. J., Jespersen, J. G. and Goldberg, A. L. (2010). Peroxisome proliferator-activated receptor γ coactivator 1α or 1β overexpression inhibits muscle protein degradation, induction of ubiquitin ligases, and disuse atrophy. *J. Biol. Chem.* **285(25)**, 19460–19471.

Braun, T. P., Zhu, X., Szumowski, M., Scott, G. D., Grossberg, A. J., Levasseur, P. R., Graham, K., Khan, S., Damaraju, S., Colmers, W. F., Baracos, V. E. and Marks, D. L. (2011). Central nervous system inflammation induces muscle atrophy via activation of the hypothalamic-pituitary-adrenal axis. *J. Exp. Med.* **208(12)**, 2449–2463.

Brennan, T. J., Chakraborty, T. and Olson, E. N. (1991). Mutagenesis of the myogenin basic region identifies an ancient protein motif critical for activation of myogenesis. *Proc. Natl. Acad. Sci. U. S. A.* **88(13)**, 5675–5679.

Brien, P., Poll, M. and Boiullon, J. (1959). Ethologie de la reproduction de *Protopterus dolloi*. *Ann. Mus. R. Congo. Belge.* **71**, 3–21.

Brigelius-Flohé, R. (1999). Tissue-specific functions of individual glutathione peroxidases. *Free Radic. Biol. Med.* **27(9)**, 951–965.

Brinkmann, H., Denk, A., Zitzler, J., Joss, J. J. and Meyer, A. (2004). Complete mitochondrial genome sequences of the South American and the Australian lungfish: testing of the phylogenetic performance of mitochondrial data sets for phylogenetic problems in tetrapod relationships. *J. Mol. Evol.* **59**, 834–848.

Brocca, L., Pellegrino, M. A., Desaphy, J. F., Pierno, S., Camerino, D. C. and Bottinelli, R. (2010). Is oxidative stress a cause or consequence of disuse muscle atrophy in mice? A proteomic approach in hindlimb-unloaded mice. *Exp. Physiol.* **95(2)**, 331–350.

Brooks, N. E., Myburgh, K. H. and Storey, K. B. (2011). Myostatin levels in skeletal muscle of hibernating ground squirrels. *J. Exp. Biol.* **214(15)**, 2522–2527.

Brunet, A., Bonni, A., Zigmond, M. J., Lin, M. Z., Juo, P., Hu, L. S., Anderson, M. J., Arden, K. C., Blenis, J. and Greenberg, M. E. (1999). Akt promotes cell survival by phosphorylating and inhibiting a Forkhead transcription factor. C*ell* **96(6)**, 857–868.

Brunet, A., Park, J., Tran, H., Hu, L. S., Hemmings, B. A. and Greenberg, M. E. (2001). The protein kinase SGK mediates survival signals by phosphorylating the Forkhead transcription factor FKHRL1/FOXO3a. *Mol Cell Biol* **(21)3**, 952–965.

Brunet, A., Kanai, F., Stehn, J., Xu, J., Sarbassova, D., Frangioni, J. V., Dalal, S. N., DeCaprio, J. A., Greenberg, M. E. and Yaffe, M. B. (2002). 14-3-3 transits to the nucleus and participates in dynamic nucleocytoplasmic transport. *J. Cell Biol.* **156(5)**, 817–828.

Brunet, A., Sweeney, L. B., Sturgill, J. F., Chua, K. F., Greer, P. L., Lin, Y., Tran, H., Ross, S. E., Mostoslavsky, R., Cohen, H. Y., Hu, L. S., Cheng, H. L., Jedrychowski, M. P., Gygi, S. P., Sinclair, D. A., Alt, F. W. and Greenberg, M. E. (2004). Stress-dependent regulation of FOXO transcription factors by the SIRT1 deacetylase. *Science* **303(5666)**, 2011–2015.

Buzadžić, B., Spasić, M., Saičić, Z. S., Radojičić, R., Petrović, V. M. and Halliwell, B. (1990). Antioxidant defenses in the ground squirrel *Citellus citellus* 2. The effect of hibernation. *Free. Radic. Biol. Med*. **9(5)**, 407–413.

Cadenas, E. and Davies, K. J. (2000). Mitochondrial free radical generation, oxidative stress and aging. *Free Radic. Biol. Med.* **29(3)**, 222–230.

Cai, R., Kwon, P., Yan-Neale, Y., Sambuccetti, L., Fischer, D. and Cohen, D. (2001). Mammalian histone deacetylase 1 protein is posttranslationally modified by phosphorylation. *Biochem. Biophy. Res. Commun.* **283(2)**, 445–453.

Calnan, D. R. and Brunet, A. (2008). The FoxO code. *Oncogene* **27(16)**, 2276–2288.

Canagarajah, B. J., Khokhlatchev, A., Cobb, M. H. and Goldsmith, E. J. (1997). Activation mechanism of the MAP kinase ERK2 by dual phosphorylation. *Cell* **90**, 859–869.

Cantó, C., Gerhart-Hines, Z., Feige, J. N., Lagouge, M., Noriega, L., Milne, J. C., Elliot, P. J. Puigserver, P. and Auwerx, J. (2009). AMPK regulates energy expenditure by modulating NAD+ metabolism and SIRT1 activity. *Nature* **458(7241)**, 1056–1060.

Cardozo, T. and Pagano, M. (2004). The SCF ubiquitin ligase: insights into a molecular machine. *Nat. Rev. Mol. Cell Biol.* **5(9)**, 739–751.

Carlson, C. J., Booth, F. W. and Gordon, S. E. (1999). Skeletal muscle myostatin mRNA expression is fiber-type specific and increases during hindlimb unloading. *Am. J. Physiol*. **277**, R601–R606.

Chakraborty, M., Abrams, S. I., Camphausen, K., Liu, K., Scott, T., Coleman, C. N. and Hodge, J. W. (2003) Irradiation of tumor cells up-regulates Fas and enhances CTL lytic activity and CTL adoptive immunotherapy. *J. Immunol.* **170**, 6338–6347.

Chanoine, C., El-Attari, A., Guyot-Lenfant, M., Ouedraogo, L. and Gallien, C. L. (1994). Myosin isoforms and their subunits in the lungfish *Protopterus annectens*: changes during development and the annual cycle. *J. Exp. Zool.* **269(5)**, 413–421.

Chew, S. F., Ong, T. F., Ho, L., Tam, W. L., Loong, A. M., Hiong, K. C., Wong, W. P. and Ip, Y. K. (2003). Urea synthesis in the African lungfish *Protopterus dolloi* – hepatic carbamoyl phosphate synthetase III and glutamine synthetase are upregulated by 6 days of aerial exposure. *J. Exp. Biol.* **206(20)**, 3615–3624.

Chew, S. F., Chan, N. K., Loong, A. M., Hiong, K. C., Tam, W. L. and Ip, Y. K. (2004). Nitrogen metabolism in the African lungfish (*Protopterus dolloi*) aestivating in a mucus cocoon on land. *J. Exp. Biol.* **207(5)**, 777–786.

Chew, S. F. and Ip, Y. K. (2014). Excretory nitrogen metabolism and defence against ammonia toxicity in air-breathing fishes. *J. Fish. Biol.* **84,** 603–638.

Chew, S. F., Ching, B., Chng, Y. R., Ong, J. L. Y., Hiong, K. C., Chen, X. L. and Ip, Y. K. (2015). Aestivation in African lungfishes: physiology, biochemistry and molecular biology. In *Phylogeny, Anatomy and Physiology of Ancient Fishes*, (ed. G. Zaccone, K. Dabrowski, M. S. Hedrick, J. M. O. Fernandes and J. M. Icardo), pp 81–132, CRC Press. In press. doi:10.1201/b18798-6.

Chiacchiera, F. and Simone, C. (2009). Inhibition of p38α unveils an AMPK-FoxO3A axis linking autophagy to cancer-specific metabolism. *Autophagy* **5(7)**, 1030–1033.

Childs, S. G. (2003). Muscle wasting. *Ortho. Nurs.* **22**, 251–257.

Ching, B. (2012). *Molecular Biology of the lung and kidney of the African lungfish, Protopterus annectens, during three phases of aestivation: cystic fibrosis transmembrane conductance regulator, gulonolactone oxidase and p53*. Retrieved from: ScholarBank@NUS (Accession 35822).

Ching, B., Ong, J. L. Y., Chng, Y. R., Chen, X. L., Wong, W. P., Chew, S. F. and Ip, Y. K. (2014). L-gulono-γ-lactone oxidase expression and vitamin C synthesis in the brain and kidney of the African lungfish, *Protopterus annectens*. *FASEB J.* **28(8)**, 3506–3517.

Chinsomboon, J., Ruas, J., Gupta, R. K., Thom, R., Shoag, J., Rowe, G. C., Sawada, N., Raghuram, S. and Arany, Z. (2009). The transcriptional coactivator PGC-1α mediates exercise-induced angiogenesis in skeletal muscle. *Proc. Natl. Acad. Sci. U. S. A.* **106(50)**, 21401–21406.

Chng, Y. R., Ong, J. L. Y., Ching, B., Chen, X. L., Wong, W. P., Chew, S. F. and Ip, Y. K. (2014). Molecular characterization of *argininosuccinate synthase* and *argininosuccinate lyase* from the liver of the African lungfish *Protopterus annectens* and their mRNA expression levels in the liver, kidney, brain and skeletal muscle during aestivation. *J. Comp. Physiol. B* **184(7)**, 835–853.

Chopard, A., Lecunff, M., Danger, R., Lamirault, G., Bihouee, A., Teusan, R., Jasmin, B. J., Marini, J. F. and Leger, J. J. (2009). Large-scale mRNA analysis of female skeletal muscles during 60 days of bed rest with and without exercise or dietary protein supplementation as countermeasures. *Physiol. Genomics* **38(3)**, 291–302.

Chuderland, D., Konson, A. and Seger, R. (2008). Identification and characterization of a general nuclear translocation signal in signaling proteins. *Mol. Cell* **31**, 850–861.

Cino, M. and Del Maestro, R. F. (1989). Generation of hydrogen peroxide by brain mitochondria: the effect of reoxygenation following postdecapitative ischemia. *Arch. Biochem. Biophys.* **269(2)**, 623–638.

Clarke, B. A., Drujan, D., Willis, M. S., Murphy, L. O., Corpina, R. A., Burova, E., Rakhilin, S. V., Stitt, T. N., Patterson, C., Latres, E. and Glass, D. J. (2007). The E3 Ligase MuRF1 degrades myosin heavy chain protein in dexamethasone-treated skeletal muscle. *Cell Metab.* **6(5)**, 376–385.

Cleveland, B. M. and Evenhuis, J. P. (2010). Molecular characterization of atrogin-1/F-box protein-32 (FBXO32) and F-box protein-25 (FBXO25) in rainbow trout (*Oncorhynchus mykiss*): Expression across tissues in response to feed deprivation. *Comp. Biochem. Physiol. B: Biochem. Mol. Biol.* **157(3)**, 248–257.

Codina, M., Bian, Y. H., Gutiérrez, J. and Du, S. J. (2008). Cloning and characterization of myogenin from seabream (*Sparus aurata*) and analysis of promoter muscle specificity. *Comp. Biochem. Physiol. D Genomics Proteomics* **3(1)**, 128–139.

Cohen, S., Brault, J. J., Gygi, S. P., Glass, D. J., Valenzuela, D. M., Gartner, C., Latres, E. and Goldberg, A. L. (2009). During muscle atrophy, thick, but not thin, filament components are degraded by MuRF1-dependent ubiquitylation. *J. Cell Biol.* **185(6)**, 1083–1095.

Conant, E. B. (1973). Regeneration in the African lungfish, *Protopterus*. III. Regeneration during fasting and estivation. *Biol. Bull.* **144**, 248–261.

Conant, E. B. (1976). Urea accumulation and other effects of estivation in the African lungfish, *Protopterus*. *Virginia J. Sci.* **27**, 42.

Cooper, J. L. and Plum, F. (1987). Biochemistry and physiology of brain ammonia. *Physiol. Rev.* **67,** 440–519.

Cotton, C. J. and Harlow, H. J. (2010). Avoidance of skeletal muscle atrophy in spontaneous and facultative hibernators. *Physiol. Biochem. Zool.* **83(3)**, 551–560.

Cress, W. D. and Seto, E. (2000). Histone deacetylases, transcriptional control, and cancer. *J. Cell. Physiol.* **184(1)**, 1–16.

Csárdi, G., Franks, A., Choi, D. S., Airoldi, E. M. and Drummond, D. A. (2015). Accounting for experimental noise reveals that mRNA levels, amplified by post-transcriptional processes, largely determine steady-state protein levels in yeast. *PLoS Genet.* **11(5)**, e1005206. doi: 10.1371/journal.pgen.1005206.

Csibi, A., Leibovitch, M. P., Cornille, K., Tintignac, L. A. and Leibovitch, S. A. (2009). MAFbx/Atrogin-1 controls the activity of the initiation factor eIF3-f in skeletal muscle atrophy by targeting multiple C-terminal lysines. *J. Biol. Chem.* **284(7)**, 4413–4421.

Cuevas, B. D., Abell, A. N. and Johnson, G. L. (2007). Role of mitogen-activated protein kinase kinase kinases in signal integration. *Oncogene* **26(22)**, 3159–3171.

Cusella-De Angelis, M. G., Lyons, G., Sonnino, C., De Angelis, L., Vivarelli, E., Farmer, K., Wright, W. E., Molinaro, M., Bouchè, M. and Buckingham, M. (1992). MyoD, myogenin independent differentiation of primordial myoblasts in mouse somites. *J. Cell Biol.* **116(5)**, 1243–1255.

Da Cruz, S., Parone, P. A., Lopes, V. S., Lillo, C., McAlonis-Downes, M., Lee, S. K., Vetto, A. P., Petrosyan, S., Marsala, M., Murphy, A. N., Williams, D. S., Spiegelman, B. M. and Cleveland, D. W. (2012). Elevated PGC-1α activity sustains mitochondrial biogenesis and muscle function without extending survival in a mouse model of inherited ALS. *Cell Metab.* **15(5)**, 778–786.

Daitoku, H., Hatta, M., Matsuzaki, H., Aratani, S., Ohshima, T., Miyagishi, M., Nakajima, T. and Fukamizu, A. (2004). Silent information regulator 2 potentiates Foxo1-mediated transcription through its deacetylase activity. *Proc. Natl. Acad. Sci. U. S. A.* **101(27)**, 10042–10047.

Daitoku, H., Sakamaki, J. I. and Fukamizu, A. (2011). Regulation of FoxO transcription factors by acetylation and protein–protein interactions. *Biochim. Biophys. Acta* **1813(11)**, 1954–1960.

Dall'Olio, S., Fontanesi, L., Nanni Costa, L., Tassinari, M., Minieri, L. and Falaschini, A. (2010). Analysis of horse myostatin gene and identification of single nucleotide polymorphisms in breeds of different morphological types. *J. Biomed. Biotechnol.* ID 542945. doi:10.1155/2010/542945

Dang, C. V. and Lee, W. M. (1988). Identification of the human c-myc protein nuclear translocation signal. *Mol. Cell. Biol.* **8(10)**, 4048–4054.

Dang, K., Li, Y. Z., Gong, L. C., Xue, W., Wang, H. P., Goswami, N. and Gao, Y. F. (2016). Stable atrogin-1 (Fbxo32) and MuRF1 (Trim63) gene expression is involved in the protective mechanism in soleus muscle of hibernating Daurian ground squirrels (*Spermophilus dauricus*). *Biol. Open* **5(1)**, 62–71.

Daniel, P. M. (1977). The metabolic homeostatic role of muscle and its function as a store of protein. *Lancet* **2**, 446–448.

Daopin, S., Piez, K. A., Ogawa, Y. and Davies, D. R. (1992). Crystal structure of transforming growth factor-beta 2: an unusual fold for the superfamily. *Science* **257(5068)**, 369–373.

Davila, D., Connolly, N. M. C., Bonner, H., Weisová, P., Dussmann, H., Concannon, C. G., Huber, H. J. and Prehn, J. H. (2012). Two-step activation of FOXO3 by AMPK generates a coherent feed-forward loop determining excitotoxic cell fate. *Cell Death Differ.* **19(10)**, 1677–1688.

Davis, R. J. (1993). The mitogen-activated protein kinase signal transduction pathway. *J. Biol. Chem.* **268**, 14553–14556.

Davis, R. L., Cheng, P. F., Lassar, A. B. and Weintraub, H. (1990). The MyoD DNA binding domain contains a recognition code for muscle-specific gene activation. *Cell* **60(5)**, 733–746.

Davis, R. L. and Weintraub, H. (1992). Acquisition of myogenic specificity by replacement of three amino acid residues from MyoD into E12. *Science* **256(5059)**, 1027–1030.

d'Azzo, A., Bongiovanni, A. and Nastasi, T. (2005). E3 ubiquitin ligases as regulators of membrane protein trafficking and degradation. *Traffic* **6(6)**, 429–441.

de Almeida-Val, V. M. F., Fé, L. M. L. and de Campos, D. F. (2015). Evolutionary aspects on the comparative biology of lungfishes: Emphasis on South-American lungfish, *Lepidosiren paradoxa*. In: *Phylogeny, Anatomy and Physiology of Ancient Fishes*. (ed. G. Zaccone, K. Dabrowski, M. S. Hedrick, J. M. O. Fernandes, J. M. Icardo), pp. 38–56. CRC Press.

de Ruijter, A. J., Van Gennip, A. H., Caron, H. N., Stephan, K. E. M. P. and Van Kuilenburg, A. B. (2003). Histone deacetylases (HDACs): characterization of the classical HDAC family. *Biochem. J.* **370(3)**, 737–749.

de Sousa Abreu, R., Penalva, L. O., Marcotte, E. M. and Vogel, C. (2009). Global signatures of protein and mRNA expression levels. *Mol. Biosyst.* **5(12)**, 1512–1526.

Delalande, J. M. and Rescan, P. Y. (1999). Differential expression of two nonallelic MyoD genes in developing and adult myotomal musculature of the trout (*Oncorhynchus mykiss*). *Dev. Genes Evol.* **209(7)**, 432–437.

DeLaney, R. G., Lahiri, S. and Fishman, A. P. (1974). Aestivation of the African lungfish *Protopterus aethiopicus*: cardiovascular and respiratory functions. *J. Exp. Biol.* **61(1)**, 111–128.

Delgado-Olguín, P., Brand-Arzamendi, K., Scott, I. C., Jungblut, B., Stainier, D. Y., Bruneau, B. G. and Recillas-Targa, F. (2011). CTCF promotes muscle differentiation by modulating the activity of myogenic regulatory factors. *J. Biol. Chem.* **286(14)**, 12483–12494.

Desaphy, J. F., Pierno, S., Liantonio, A., Giannuzzi, V., Digennaro, C., Dinardo, M. M., Camerino, G. M., Ricciuti, P., Brocca, L., Pellegrino, M. A., Bottinelli, R. and Camerino, D. C. (2010). Antioxidant treatment of hindlimb-unloaded mouse counteracts fiber type transition but not atrophy of disused muscles. *Pharmacol. Res.* **61(6)**, 553–563.

Dhanasekaran, D. N., Kashef, K., Lee, C. M., Xu, H. and Reddy, E. P. (2007). Scaffold proteins of MAP-kinase modules. *Oncogene* **26(22)**, 3185–3202.

Di Simplicio, P., Rossi, R., Falcinelli, S., Ceserani, R. and Formento, M. L. (1997). Antioxidant status in various tissues of the mouse after fasting and swimming stress. *Eur. J. Appl. Physiol. Occup. Physiol.* **76(4)**, 302–307.

Didier, N., Hourdé, C., Amthor, H., Marazzi, G. and Sassoon, D. (2012). Loss of a single allele for Ku80 leads to progenitor dysfunction and accelerated aging in skeletal muscle. *EMBO Mol. Med.* **4(9)**, 910–923.

Dijkers, P. F., Medema, R. H., Lammers, J. W. J., Koenderman, L. and Coffer, P. J. (2000). Expression of the pro-apoptotic Bcl-2 family member Bim is regulated by the forkhead transcription factor FKHR-L1. *Curr. Biol.* **10(19)**, 1201–1204.

Dirks, M. L., Wall, B. T., Nilwik, R., Weerts, D. H., Verdijk, L. B. and van Loon, L. J. (2014). Skeletal muscle disuse atrophy is not attenuated by dietary protein supplementation in healthy older men. *J. Nutr.* **144(8)**, 1196–1203.

Dodd, S. L., Gagnon, B. J., Senf, S. M., Hain, B. A. and Judge, A. R. (2010). Ros-mediated activation of NF-κB and Foxo during muscle disuse. *Muscle Nerve* **41(1)**, 110–113.

Dokmanovic, M. and Marks, P. A. (2005). Prospects: histone deacetylase inhibitors. *J. Cell. Biochem.* **96(2)**, 293–304.

Duttaroy, A., Paul, A., Kundu, M. and Belton, A. (2003). A Sod2 null mutation confers severely reduced adult life span in Drosophila. *Genetics* **165(4)**, 2295–2299.

Eddy, S. F. and Storey, K. B. (2003). Differential expression of Akt, PPARγ, and PGC-1 during hibernation in bats. *Biochem. Cell Biol.* **81(4)**, 269–274.

Eddy, S. F., Morin Jr, P. and Storey, K. B. (2005a). Cloning and expression of PPARγ and PGC-1α from the hibernating ground squirrel, *Spermophilus tridecemlineatus*. *Mol. Cell. Biochem.* **269(1)**, 175–182.

Eddy, S. F., McNally, J. D. and Storey, K. B. (2005b). Up-regulation of a thioredoxin peroxidase-like protein, proliferation-associated gene, in hibernating bats. *Arch. Biochem. Biophys.* **435(1)**, 103–111.

Edmondson, D. G., Cheng, T. C., Cserjesi, P., Chakraborty, T. and Olson, E. N. (1992). Analysis of the myogenin promoter reveals an indirect pathway for positive autoregulation mediated by the muscle-specific enhancer factor MEF-2. *Mol. Cell Biol.* **12**, 3665–3677.

Edwards, M. G. Anderson, R. M., Yuan, M., Kendziorski, C. M., Weindruch, R. and Prolla, T. A. (2007). Gene expression profiling of aging reveals activation of a p53-mediated transcriptional program. *BMC Genomics*, **8(1)**, 80.

Ehrnhoefer, D. E., Skotte, N. H., Ladha, S., Nguyen, Y. T., Qiu, X., Deng, Y., Huynh, K. T., Engemann, S., Nielsen, S. M., Becanovic, K., Leavitt, B. R., Hasholt, L. and Hayden, M. R. (2013). p53 increases caspase-6 expression and activation in muscle tissue expressing mutant huntingtin. *Hum. Mol. Genet.* **23**, 717–729.

El Hakeem, O. H. (1979). A lungfish that survives over three and half years of starvation under aquatic conditions. *Zool. Anz.* **202(1-2)**, 17–19.

Enkhbayar, P., Kamiya, M., Osaki, M., Matsumoto, T. and Matsushima, N. (2004). Structural principles of leucine-rich repeat (LRR) proteins. *Proteins* **54(3)**, 394–403.

Enslen, H. and Davis, R. J. (2001). Regulation of MAP kinases by docking domains. *Biol. Cell* **93**, 5–14.

Falk, D. J., Kavazis, A. N., Whidden, M. A., Smuder, A. J., McClung, J. M., Hudson, M. B. and Powers, S. K. (2011). Mechanical ventilation-induced oxidative stress in the diaphragm: role of heme oxygenase-1. *CHEST* **139(4)**, 816–824.

Fan, M., Rhee, J., St-Pierre, J., Handschin, C., Puigserver, P., Lin, J., Jäeger, S., Erdjument-Bromage, H., Tempst, P. and Spiegelman, B. M. (2004). Suppression of mitochondrial respiration through recruitment of p160 myb binding protein to PGC-1α: modulation by p38 MAPK. *Genes Dev.* **18(3)**, 278–289.

Fedorov, V. B., Goropashnaya, A. V., Stewart, N. C., Tøien, Ø., Chang, C., Wang, H., Yan, J., Showe, L. C., Showe, M. K. and Barnes, B. M. (2014). Comparative functional genomics of adaptation to muscular disuse in hibernating mammals. *Mol. Ecol.* **23(22)**, 5524–5537.

Ferrando, A. A., Lane, H. W., Stuart, C. A., Davis-Street, J. and Wolfe, R. R. (1996). Prolonged bed rest decreases skeletal muscle and whole body protein synthesis. *Am. J. Physiol. Endocrinol. Metab.* **270(4)**, E627–E633.

Finnin, M. S., Donigian, J. R., Cohen, A., Richon, V. M., Rifkind, R. A., Marks, P. A., Breslow, R. and Pavletich, N. P. (1999). Structures of a histone deacetylase homologue bound to the TSA and SAHA inhibitors. *Nature* **401(6749)**, 188–193.

Fishman, A. P., Pack, A. I., DeLaney, R. G. and Galante, R. J. (1986). Estivation in *Protopterus*. *J. Morphol. Suppl.* **190**, 237–248.

Fishman, A. P., Galante, R. J., Winokur, A. and Pack, A. I. (1992). Estivation in the African lungfish. *Proc. Am. Philos. Soc.* **136**, 61–72.

Fitts, R. H., Metzger, J. M., Riley, D. A. and Unsworth, B. R. (1986). Models of disuse: a comparison of hindlimb suspension and immobilization. *J. Appl. Physiol.* **60(6)**, 1946–1953.

Fitts, R. H., Riley, D. R. and Widrick, J. J. (2000). Physiology of a microgravity environment invited review: microgravity and skeletal muscle. *J. Appl. Physiol.* **89(2)**, 823–839.

Fitts, R. H., Riley, D. R. and Widrick, J. J. (2001). Functional and structural adaptations of skeletal muscle to microgravity. *J. Exp. Biol.* **204(18)**, 3201–3208.

Flach, R. J. R., Qin, H., Zhang, L. and Bennett, A. M. (2011). Loss of mitogen-activated protein kinase phosphatase-1 protects from hepatic steatosis by repression of cell death-inducing DNA fragmentation factor A (DFFA)-like effector C (CIDEC)/fat-specific protein 27. *J. Biol. Chem.* **286(25)**, 22195–22202.

Flohé, L. (1989). The selenoprotein glutathione peroxidase. In *Glutathione: Chemical, Biochemical and Medical Aspects*, (ed. D. Dolphin, R. Poulso and O. Avramovic), pp. 643–731, John Wiley and Sons Inc, New York.

Flohé, L., Toppo, S., Cozza, G. and Ursini, F. (2011). A comparison of thiol peroxidase mechanisms. *Antioxid. Redox Signal.* **15(3)**, 763–780.

Foletta, V. C., White, L. J., Larsen, A. E., Léger, B. and Russell, A. P. (2011). The role and regulation of MAFbx/atrogin-1 and MuRF1 in skeletal muscle atrophy. *Pflügers Arch.* **461(3)**, 325–335.

Forey, P. L. (1986). Relationships of lungfishes. *J. Morphol.* **190(S1)**, 75–91.

Forsberg, E. C. and Bresnick, E. H. (2001). Histone acetylation beyond promoters: long-range acetylation patterns in the chromatin world. *Bioessays* **23(9)**, 820–830.

Fox, D. K., Ebert, S. M., Bongers, K. S., Dyle, M. C., Bullard, S. A., Dierdorff, J. M., Kunkel, S. D. and Adams, C. M. (2014). p53 and ATF4 mediate distinct and additive pathways to skeletal muscle atrophy during limb immobilization. *Am. J. Physiol. Endocrinol. Metab.* **307(3)**, E245–E261.

Frerichs, K. U., Smith, C. B., Brenner, M., DeGracia, D. J., Krause, G. S., Marrone, L., Dever, T. E. and Hallenbeck, J. M. (1998). Suppression of protein synthesis in brain during hibernation involves inhibition of protein initiation and elongation. *Proc. Natl. Acad. Sci. U. S. A.* **95(24)**, 14511–14516.

Fridovich, I. (1986). Superoxide dismutases. *Adv. Enzymol. Relat. Areas Mol. Biol.* **58**, 61–97.

Fridovich, I. (1995). Superoxide radical and superoxide dismutases. *Annu. Rev. Biochem.* **64**, 87–112.

Frost, R. A., Nystrom, G. J., Jefferson, L. S. and Lang, C. H. (2007). Hormone, cytokine, and nutritional regulation of sepsis-induced increases in atrogin-1 and MuRF1 in skeletal muscle. *Am. J. Physiol. Endocrinol. Metab.* **292(2)**, E501–E512.

Furuyama, T., Nakazawa, T., Nakano, I. and Mori, N. (2000). Identification of the differential distribution patterns of mRNAs and consensus binding sequences for mouse DAF-16 homologues. *Biochem. J.* **349(2)**, 629–634.

Galasinski, S. C., Resing, K. A., Goodrich, J. A. and Ahn, N. G. (2002). Phosphatase inhibition leads to histone deacetylases 1 and 2 phosphorylation and disruption of corepressor interactions. *J. Biol. Chem.* **277(22)**, 19618–19626.

Gallinari, P., Di Marco, S., Jones, P., Pallaoro, M. and Steinkühler, C. (2007). HDACs, histone deacetylation and gene transcription: from molecular biology to cancer therapeutics. *Cell Res.* **17(3)**, 195–211.

Gao, L., Cueto, M. A., Asselbergs, F. and Atadja, P. (2002). Cloning and functional characterization of HDAC11, a novel member of the human histone deacetylase family. *J. Biol. Chem.* **277(28)**, 25748–25755.

Gao, Y. F., Wang, J., Wang, H. P., Feng, B., Dang, K., Wang, Q. and Hinghofer-Szalkay, H. G. (2012). Skeletal muscle is protected from disuse in hibernating dauria ground squirrels. *Comp. Biochem. Physiol. A Mol. Integr. Physiol.* **161(3)**, 296–300.

Garofalo, F., Amelio, D., Icardo, J. M., Chew, S. F., Tota, B., Cerra, M. C. and Ip, Y. K. (2015). Signal molecule changes in the gills and lungs of the African lungfish *Protopterus annectens*, during the maintenance and arousal phases of aestivation. *Nitric Oxide* **44**, 71–80.

Geisler, H. W., Shi, H. and Gerrard, D. E. (2013). MAPK Pathway in Skeletal Muscle Diseases. *J. Vet. Sci. Anim. Husb.* **1(1)**, 1.

Geng, T., Li, P., Yin, X. and Yan, Z. (2011). PGC-1α promotes nitric oxide antioxidant defenses and inhibits FOXO signaling against cardiac cachexia in mice. *Am. J. Pathol.* **178(4)**, 1738–1748.

Gerber, A. N., Klesert, T. R., Bergstrom, D. A. and Tapscott, S. J. (1997). Two domains of MyoD mediate transcriptional activation of genes in repressive chromatin: a mechanism for lineage determination in myogenesis. *Genes Dev.* **11(4)**, 436–450.

Gerhart-Hines, Z., Rodgers, J. T., Bare, O., Lerin, C., Kim, S. H., Mostoslavsky, R., Alt, F. W., Wu, Z. and Puigserver, P. (2007). Metabolic control of muscle mitochondrial function and fatty acid oxidation through SIRT1/PGC-1α. *EMBO J.* **26(7)**, 1913–1923.

Gerwick, L., Corley-Smith, G. and Bayne, C. J. (2007). Gene transcript changes in individual rainbow trout livers following an inflammatory stimulus. *Fish. Shellfish. Immunol.* **22,** 157–171.

Giraud-Billoud, M., Vega, I. A., Tosi, M. E. R., Abud, M. A., Calderón, M. L. and Castro-Vazquez, A. (2013). Antioxidant and molecular chaperone defences during estivation and arousal in the South American apple snail Pomacea canaliculata. *J. Exp. Biol.* **216(4)**, 614–622.

Glass, D. J. (2003). Signalling pathways that mediate skeletal muscle hypertrophy and atrophy. *Nat. Cell Biol*. **5**, 87–90.

Glover, E. I., Phillips, S. M., Oates, B. R., Tang, J. E., Tarnopolsky, M. A., Selby, A., Smith, K. and Rennie, M. J. (2008). Immobilization induces anabolic resistance in human myofibrillar protein synthesis with low and high dose amino acid infusion. *J. Physiol.* **586(24)**, 6049–6061.

Goldberg, A. L., Tischler, M. E., DeMartino, G. and Griffin, G. (1980). Hormonal regulation of protein degradation and synthesis in skeletal muscle. *Fed. Proc.* **39(1)**, 31–36.

Goldspink, D. F. (1977). The influence of immobilization and stretch on protein turnover of rat skeletal muscle. *J. Physiol.* **264(1)**, 267–282.

Gomes, M. D., Lecker, S. H., Jagoe, R. T., Navon, A. and Goldberg, A. L. (2001). Atrogin-1, a muscle-specific F-box protein highly expressed during muscle atrophy. *Proc. Natl. Acad. Sci. U. S. A.* **98(25)**, 14440–14445.

Gonzalez-Cadavid, N. F., Taylor, W. E., Yarasheski, K., Sinha-Hikim, I., Ma, K., Ezzat, S., Shen, R., Lalani, R., Asa, S., Mamita, M., Nair, G., Arver, S. and Bhasin, S. (1998). Organization of the human myostatin gene and expression in healthy men and HIV-infected men with muscle wasting. *Proc. Natl. Acad. Sci. U. S. A.* **95(25)**, 14938–14943.

Graham, J. B. (1997). *Air-breathing fishes: Evolution, diversity and adaptation.* Academic Press, San Diego.

Greenwood, P. H. (1986). The natural history of African lungfishes. *J. Morphol. Suppl.* 163–179.

Greer, E. L., Oskoui, P. R., Banko, M. R., Maniar, J. M., Gygi, M. P., Gygi, S. P. and Brunet, A. (2007). The energy sensor AMP-activated protein kinase directly regulates the mammalian FOXO3 transcription factor. *J. Biol. Chem.* **282(41)**, 30107–30119.

Greer, E. L. and Brunet, A. (2008). FOXO transcription factors in ageing and cancer. *Acta Physiol.* **192(1)**, 19–28.

Gregoretti, I., Lee, Y. M. and Goodson, H. V. (2004). Molecular evolution of the histone deacetylase family: functional implications of phylogenetic analysis. *J. Mol. Biol.* **338(1)**, 17–31.

Gregory, P.T. (1982). Reptilian hibernation. In *Biology of the Reptilia*. *Physiology and Physiological Ecology*. (ed. C. Gans and F.H. Pough), vol. 13, pp 53–154. Academic Press, London.

Griffith, O. W. (1980). Determination of glutathione and glutathione disulfide using glutathione reductase and 2-vinylpyridine. *Anal. Biochem.* **106(1)**, 207–212.

Grundy, J. E. and Storey, K. B. (1998) Antioxidant defenses and lipid peroxidation damage in estivating toads, *Scaphiopus couchii*. *J. Comp. Physiol. B* **168(2)**, 132–142.

Guppy, M. and Withers, P. (1999). Metabolic depression in animals: physiological perspectives and biochemical generalizations. *Biol. Rev.* **74**, 1–40.

Gustafsson, T., Osterlund, T., Flanagan, J. N., von Waldén, F., Trappe, T. A., Linnehan, R. M. and Tesch, P. A. (2010). Effects of 3 days unloading on molecular regulators of muscle size in humans. *J. Appl. Physiol*. **109(3)**, 721–727.

Hadjipavlou, G., Matika, O., Clop, A. and Bishop, S. C. (2008). Two single nucleotide polymorphisms in the myostatin (GDF8) gene have significant association with muscle depth of commercial Charollais sheep. *Anim. Genet.* **39(4)**, 346–353.

Haidet, A. M., Rizo, L., Handy, C., Umapathi, P., Eagle, A., Shilling, C., Boue, D., Martin, P. T., Sahenk, Z, Mendell, J. R. and Kaspar, B. K. (2008). Long-term enhancement of skeletal muscle mass and strength by single gene administration of myostatin inhibitors. *Proc. Natl. Acad. Sci. U. S. A.* **105(11)**, 4318–4322.

Hailey, A. and Loveridge, J. P. (1997). Metabolic depression during dormancy in the African tortoise *Kinixys spekii*. *Can. J. Zool.* **75**, 1328–1335.

Hall, T. A. (1999). BioEdit: a user-friendly biological sequence editor and analysis program for Windows 95/98/NT. *Nucl. Acids. Symp. Ser.* **41,** 95–98.

Halliwell, B. and Gutteridge, J. M. C. (1989). *Free Radicals in Biology and Medicine* (2nd ed.). Clarendon Press, Oxford, UK.

Hallstrom, B.M. and Janke, A. (2009). Gnathostome phylogenomics utilizing lungfish EST sequences. *Mol. Biol. Evol.* **26**, 463–471.

Handschin, C., Rhee, J., Lin, J., Tarr, P. T. and Spiegelman, B. M. (2003). An autoregulatory loop controls peroxisome proliferator-activated receptor γ coactivator 1α expression in muscle. *Proc. Natl. Acad. Sci. U. S. A.* **100(12)**, 7111–7116.

Handschin, C., Kobayashi, Y. M., Chin, S., Seale, P., Campbell, K. P. and Spiegelman, B. M. (2007a). PGC-1α regulates the neuromuscular junction program and ameliorates Duchenne muscular dystrophy. *Genes Dev.* **21(7)**, 770–783.

Handschin, C., Choi, C. S., Chin, S., Kim, S., Kawamori, D., Kurpad, A. J., Neubauer, N., Hu, J., Mootha, V. K., Kim, Y. B., Kulkarni, R. N., Shulman, G. I. and Spiegelman, B. M. (2007b). Abnormal glucose homeostasis in skeletal muscle–specific PGC-1α knockout mice reveals skeletal muscle–pancreatic β cell crosstalk. *J. Clin. Invest.* **117(11)**, 3463–3474.

Hassig, C. A., Tong, J. K., Fleischer, T. C., Owa, T., Grable, P. G., Ayer, D. E. and Schreiber, S. L. (1998). A role for histone deacetylase activity in HDAC1-mediated transcriptional repression. *Proc. Natl. Acad. Sci. U. S. A.* **95(7)**, 3519–3524.

Hasty, P., Bradley, A., Morris, J. H., Edmondson, D. G., Venuti, J. M., Olson, E. N. and Klein, W. H. (1993). Muscle deficiency and neonatal death in mice with a targeted mutation in the myogenin gene. *Nature* **364(6437)**, 501–506.

Hawke, T. J. and Garry, D. J. (2001). Myogenic satellite cells: physiology to molecular biology. *J. Appl. Physiol.* **91(2)**, 534–551.

Heery, D. M., Kalkhoven, E., Hoare, S. and Parker, M. G. (1997). A signature motif in transcriptional co-activators mediates binding to nuclear receptors. *Nature* **387(6634)**, 733–736.

Heidt, A. B., Rojas, A., Harris, I. S. and Black, B. L. (2007). Determinants of myogenic specificity within MyoD are required for noncanonical E box binding. *Mol. Cell. Biol.* **27(16)**, 5910–5920.

Hermes-Lima, M. and Storey, K. (1995). Antioxidant defences and metabolic depression in a pulmonate land snail. *Am. J. Physiol.* **268**, R1386–R1393.

Hermes-Lima, M., Willmore, W. G. and Storey, K. B. (1995). Quantification of lipid peroxidation in tissue extracts based on Fe (III) xylenol orange complex formation. *Free Rad. Biol. Med.* **19**, 271–280.

Hermes-Lima, M., Storey, J. M. and Storey, K. B. (2001) Antioxidant defenses and animal adaptation to oxygen availability during environmental stress. In *Cell and molecular responses to stress, Vol 2*, (ed. K. B. Storey and J. M. Storey), pp. 263–287, Elsevier Science, Amsterdam.

Hermes-Lima, M. and Zenteno-Savín, T. (2002). Animal response to drastic changes in oxygen availability and physiological oxidative stress. *Comp. Biochem. Physiol. C Toxicol. Pharmacol.* **133(4)**, 537–556.

Hindle, A. G., Otis, J. P., Epperson, L. E., Hornberger, T. A., Goodman, C. A., Carey, H. V. and Martin, S. L. (2015). Prioritization of skeletal muscle growth for emergence from hibernation. *J. Exp. Biol.* **218(2)**, 276–284.

Hiong, K. C., Ip, Y. K., Wong, W. P. and Chew, S. F. (2013). Differential gene expression in the brain of the African lungfish, *Protopterus annectens*, after six days or six months of aestivation in air. *PLoS One* **8(8)**, e71205. doi:10.1371/journal.pone.0071205.

Hiong, K. C., Tan, X. R., Boo, M. V., Wong, W. P., Chew, S. F. and Ip, Y. K. (2015a). Aestivation induces changes in transcription and translation of coagulation factor II and fibrinogen gamma chain in the liver of the African lungfish *Protopterus annectens. J. Exp. Biol.* **218(23)**, 3717–3728.

Hiong, K. C., Ip, Y. K., Wong, W. P. and Chew, S. F. (2015b). Differential gene expression in the liver of the African lungfish, *Protopterus annectens*, after 6

months of aestivation in air or 1 day of arousal from 6 months of aestivation. *PloS One* **10(3)**, e0121224. doi: 10.1371/journal.pone.0121224.

Hitchler, M. J. and Domann, F. E. (2014). Regulation of CuZnSOD and its redox signaling potential: implications for amyotrophic lateral sclerosis. *Antioxid. Redox Signal.* **20(10)**, 1590–1598.

Hittel, D. and Storey, K. B. (2001). Differential expression of adipose-and heart-type fatty acid binding proteins in hibernating ground squirrels. *Biochim. Biophys. Acta* **1522(3)**, 238–243.

Horn, H. F. and Vousden, K. H. (2007). Coping with stress: multiple ways to activate p53. *Oncogene* **26(9)**, 1306–1316.

Hribal, M. L., Nakae, J., Kitamura, T., Shutter, J. R. and Accili, D. (2003). Regulation of insulin-like growth factor–dependent myoblast differentiation by Foxo forkhead transcription factors. *J. Cell Biol.* **162(4)**, 535–541.

Hu, P. P., Datto, M. B. and Wang, X. F. (1998). Molecular mechanisms of transforming growth factor-β signaling. *Endocr. Rev.* **19(3)**, 349–363.

Hudson, N. J. and Franklin, C. E. (2002). Maintaining muscle mass during extended disuse: aestivating frogs as a model species. *J. Exp. Biol.* **205**, 2297–2303.

Hudson, N. J., Lavidis, N. A., Choy, P. T. and Franklin, C. E. (2005). Effect of prolonged inactivity on skeletal motor nerve terminals during aestivation in the burrowing frog, *Cyclorana alboguttata*. *J. Comp. Physiol. A* **191(4)**, 373–379.

Hudson, N. J., Lehnert, S. A., Ingham, A. B., Symonds, B., Franklin, C. E. and Harper, G. S. (2006). Lessons from an estivating frog: sparing muscle protein despite starvation and disuse. *Am J Physiol.* **290**, R836–R843.

Hung, C. Y. C., Galvez, F., Ip, Y. K. and Wood, C. M. (2009). A facilitated diffusion urea transporter in the skin of the African lungfish, *Protopterus annectens*. *J. Exp. Biol.* **212**, 1202–1211.

Huss, J. M., Kopp, R. P. and Kelly, D. P. (2002). Peroxisome proliferator-activated receptor coactivator-1α (PGC-1α) coactivates the cardiac-enriched nuclear receptors estrogen-related receptor-α and -γ. Identification of novel leucine-rich interaction motif within PGC-1α. *J. Biol. Chem.* **277**, 40265–40274.

Hussain, S. N., Mofarrahi, M., Sigala, I., Kim, H. C., Vassilakopoulos, T., Maltais, F., Bellenis, I., Chaturvedi, R., Gottfried, S. B., Metrakos, P., Danialou, G., Matecki, S., Jaber, S., Petrof, B. J. and Goldberg, P. (2010). Mechanical ventilation–induced diaphragm disuse in humans triggers autophagy. *Am. J. Respir. Crit. Care Med.* **182(11)**, 1377–1386.

Icardo, J. M., Amelio, D., Garofalo, F., Colvee, E., Cerra, M. C., Wong, W. P., Tota, B. and Ip, Y. K. (2008). The structural characteristics of the heart ventricle of the African lungfish *Protopterus dolloi*: freshwater and aestivation. *J. Anat.* **213(2)**, 106–119.

Icardo, J. M., Loong, A. I., Colvee, E., Wong, W. P. and Ip, Y. K. (2012a). The alimentary canal of the African lungfish *Protopterus annectens* during aestivation and after arousal. *Anat. Rec. (Hoboken)* **295(1)**, 60–72.

Icardo, J. M., Wong, W. P., Colvee, E., Loong, A. M. and Ip, Y. K. (2012b). The spleen of the African lungfish *Protopterus annectens*: freshwater and aestivation. *Cell Tissue Res.* **350(1)**, 143–156.

Ikemoto, M., Nikawa, T., Watanabe, C., Kitano, T., Baldwin, K. M., Izumi, R., Nonaka, I., Towatari, T., Teshima, S., Rokutan, K. and Kishi, K. (2001). Space shuttle flight (STS-90) enhances degradation of rat myosin heavy chain in association with activation of ubiquitin–proteasome pathway. *FASEB J.* **15(7)**, 1279–1281.

Imae, M., Fu, Z., Yoshida, A., Noguchi, T. and Kato, H. (2003). Nutritional and hormonal factors control the gene expression of FoxOs, the mammalian homologues of DAF-16. *J. Mol. Endocrinol.* **30(2)**, 253–262.

Ip, Y. K., Yeo, P. J., Loong, A. M., Hiong, K. C., Wong, W. P. and Chew, S. F. (2005a). The interplay of increased urea synthesis and reduced ammonia production in the African lungfish *Protopterus aethiopicus* during 46 days of aestivation in a mucus cocoon. *J. Exp. Zool. A Comp. Exp. Biol.* **303(12)**, 1054–1065.

Ip, Y. K., Peh, B. K., Tam, W. L., Lee, S. L. M. and Chew. S. F. (2005b). Changes in salinity and ionic compositions act as environmental signals to induce a reduction in ammonia production in the African lungfish *Protopterus dolloi*. *J. Exp. Zool.* **303A**, 456–463.

Ip, Y. K., Peh, B. K., Tam, W. L., Wong, W. P. and Chew. S. F. (2005c). Effects of intra-peritoneal injection with NH_4Cl, urea or NH_4Cl+urea on nitrogen excretion and metabolism in the African lungfish *Protopterus dolloi*. *J. Exp. Zool.* **303A**, 272–282.

Ip, Y. K. and Chew, S. F. (2010). Nitrogen metabolism and excretion during aestivation. In *Aestivation: Molecular and Physiological Aspects, Progress in Molecular and Subcellular Biology*, (ed. C. A. Navas and J. E. Carvalho), pp. 63–93, Springer-Verlag, Heidelberg.

Ito, K., Barnes, P. J. and Adcock, I. M. (2000). Glucocorticoid receptor recruitment of histone deacetylase 2 inhibits interleukin-1β-induced histone H4 acetylation on lysines 8 and 12. *Mol. Cell. Biol.* **20(18)**, 6891–6903.

Izzi, S. A., Colantuono, B. J., Sullivan, K., Khare, P. and Meedel, T. H. (2013). Functional studies of the *Ciona intestinalis* myogenic regulatory factor reveal conserved features of chordate myogenesis. *Dev. Biol.* **376(2)**, 213–223.

Jaber, S., Petrof, B. J., Jung, B., Chanques, G., Berthet, J. P., Rabuel, C., Bouyabrine, H., Courouble, P., Koechlin-Ramonatxo, C., Sebbane, M., Similowski, T., Scheuermann, V., Mebazaa, A., Capdevila, X., Mornet, D., Mercier, J., Lacampagne, A., Philips, A. and Matecki, S. (2011). Rapidly

progressive diaphragmatic weakness and injury during mechanical ventilation in humans. *Am. J. Respir. Crit. Care Med.* **183(3)**, 364–371.

Jackman, R. W. and Kandarian, S. C. (2004). The molecular basis of skeletal muscle atrophy. *Am. J. Physiol. Cell Physiol.* **287(4)**, C834–C843.

Jackson, M. J. (2013). Interactions between reactive oxygen species generated by contractile activity and aging in skeletal muscle? *Antioxid. Redox Signal.* **19(8)**, 804–812.

Jäger, S., Handschin, C., Pierre, J. S. and Spiegelman, B. M. (2007). AMP-activated protein kinase (AMPK) action in skeletal muscle via direct phosphorylation of PGC-1α. *Proc. Natl. Acad. Sci. U. S. A.* **104(29)**, 12017–12022.

Jagoe, R. T., Lecker, S. H., Gomes, M. and Goldberg, A. L. (2002). Patterns of gene expression in atrophying skeletal muscles: response to food deprivation. *FASEB J.* **16(13)**, 1697–1712.

James, R. S., Staples, J. F., Brown, J. C. L., Tessier, S. N. and Storey, K. B. (2013). The effects of hibernation on the contractile and biochemical properties of skeletal muscles in the thirteen-lined ground squirrel, *Ictidomys tridecemlineatus*. *J. Exp. Biol.* **216**, 2587–2594.

Jang, Y. C., Perez , V. I., Song, W., Lustgarten, M. S., Salmon, A. B., Mele, J., Qi, W., Liu, Y., Liang, H., Chaudhuri, A., Ikeno, Y., Epstein, C. J., Van Remmen, H., and Richardson, A. (2009). Overexpression of Mn superoxide dismutase does not increase life span in mice. *J. Gerontol. A. Biol. Sci. Med. Sci.* **64**, 1114–1125.

Janssens, P. A. (1964). The metabolism of the aestivating African lungfish. *Comp. Biochem. Physiol.* **11**, 105–117.

Janssens, P. A. and Cohen, P. P. (1968). Biosynthesis of urea in the estivating African lungfish and in *Xenopus laevis* under conditions of water-shortage. *Comp. Biochem. Physiol.* **24**, 887–898.

Ji, M., Zhang, Q., Ye, J., Wang, X., Yang, W. and Zhu, D. (2008). Myostatin induces p300 degradation to silence cyclin D1 expression through the PI3K/PTEN/Akt pathway. *Cell. Signal.* **20(8)**, 1452–1458.

Ji, S., Losinski, R. L., Cornelius, S. G., Frank, G. R., Willis, G. M., Gerrard, D. E., Depreux, F. F. and Spurlock, M. E. (1998). Myostatin expression in porcine tissues: tissue specificity and developmental and postnatal regulation. *Am. J. Physiol.* **275(4)**, R1265–R1273.

Jin, J., Cardozo, T., Lovering, R. C., Elledge, S. J., Pagano, M. and Harper, J. W. (2004). Systematic analysis and nomenclature of mammalian F-box proteins. *Genes Dev.* **18(21)**, 2573–2580.

Johansen, K. and Lenfant, C. (1967). Respiratory function in the South American lungfish, *Lepidosiren paradoxa* (Fitz). *J. Exp. Biol.* **46(2)**, 205–218.

Johansen, K., Lomholt, J. P. and Maloiy, G. M. O. (1976). Importance of air and water breathing in relation to size of the African lungfish *Protopterus amphibius* Peters. *J. Exp. Biol.* **65**, 395–399.

Johnels, A. G. and Svensson, G. S. O. (1954). On the biology of *Protopterus annectens* (Owen). *Arkiv. Zool.* **7**, 131–158.

Johnstone, R. W. (2002). Histone-deacetylase inhibitors: novel drugs for the treatment of cancer. *Nat. Rev. Drug Discov.* **1(4)**, 287–299.

Jones, S. W., Hill, R. J., Krasney, P. A., O'Conner, B., Peirce, N. and Greenhaff, P. L. (2004). Disuse atrophy and exercise rehabilitation in humans profoundly affects the expression of genes associated with the regulation of skeletal muscle mass. *FASEB J.* **18**, 1025–1027.

Joulia, D., Bernardi, H., Garandel, V., Rabenoelina, F., Vernus, B. and Cabello, G. (2003). Mechanisms involved in the inhibition of myoblast proliferation and differentiation by myostatin. *Exp. Cell Res.* **286(2)**, 263–275.

Joulia-Ekaza, D. and Cabello, G. (2006). Myostatin regulation of muscle development: molecular basis, natural mutations, physiopathological aspects. *Exp. Cell Res.* **312(13)**, 2401–2414.

Kadosh, D. and Struhl, K. (1998). Histone deacetylase activity of Rpd3 is important for transcriptional repression in vivo. *Genes Dev.* **12(6)**, 797–805.

Kaestner, K. H., Knöchel, W. and Martínez, D. E. (2000). Unified nomenclature for the winged helix/forkhead transcription factors. *Genes Dev.* **14(2)**, 142–146.

Kambadur, R., Sharma, M., Smith, T. P. and Bass, J. J. (1997). Mutations in myostatin (GDF8) in double-muscled Belgian Blue and Piedmontese cattle. *Genome Res.* **7(9)**, 910–915.

Kamei, Y., Miura, S., Suzuki, M., Kai, Y., Mizukami, J., Taniguchi, T., Mochida, K., Hata, T., Matsuda, J., Aburatani, H., Nishino, I. and Ezaki, O. (2004). Skeletal muscle FOXO1 (FKHR) transgenic mice have less skeletal muscle mass, down-regulated Type I (slow twitch/red muscle) fiber genes and impaired glycemic control. *J. Biol. Chem.* **279(39)**, 41114–41123.

Kang, C. and Ji, L. L. (2013). Muscle immobilization and remobilization downregulates PGC-1α signaling and the mitochondrial biogenesis pathway. *J. Appl. Physiol.* **115(11)**, 1618–1625.

Kang, C., Goodman, C. A., Hornberger, T. A. and Ji, L. L. (2015). PGC-1α overexpression by *in vivo* transfection attenuates mitochondrial deterioration of skeletal muscle caused by immobilization. *FASEB J.* **29(10)**, 4092–4106.

Kao, H. Y., Downes, M., Ordentlich, P. and Evans, R. M. (2000). Isolation of a novel histone deacetylase reveals that class I and class II deacetylases promote SMRT-mediated repression. *Genes Dev.* **14(1)**, 55–66.

Karawajew, L., Rhein, P., Czerwony, G. and Ludwig, W. D. (2005). Stress-induced activation of the p53 tumor suppressor in leukemia cells and normal

lymphocytes requires mitochondrial activity and reactive oxygen species. *Blood* **105(12)**, 4767–4775.

Karwowska-Desaulniers, P., Ketko, A., Kamath, N. and Pflum, M. K. H. (2007). Histone deacetylase 1 phosphorylation at S421 and S423 is constitutive in vivo, but dispensable in vitro. *Biochem. Biophy. Res. Commun.* **361(2)**, 349–355.

Kasemset, D. and Oberley, L. W. (1984). Regulation of Mn-SOD activity in the mouse heart: Glucose effect. *Biochem. Biophys. Res. Commun.* **122**, 682–686.

Kavazis, A. N., Talbert, E. E., Smuder, A. J., Hudson, M. B., Nelson, W. B. and Powers, S. K. (2009). Mechanical ventilation induces diaphragmatic mitochondrial dysfunction and increased oxidant production. *Free Radic. Biol. Med.* **46(6)**, 842–850.

Kawamata, H. and Manfredi, G. (2010). Import, maturation and function of SOD1 and its copper chaperone CCS in the mitochondrial intermembrane space. *Antioxid. Redox Signal.* **13(9)**, 1375–1384.

Keane, T. M., Creevey, C. J., Pentony, M. M., Naughton, T. J. and McInerney, J. O. (2006). Assessment of methods for amino acid matrix selection and their use on empirical data shows that ad hoc assumptions for choice of matrix are not justified. *BMC Evol. Biol.* **6**, 29. doi: 10.1186/1471-2148-6-29.

Kelleher, A. R., Kimball, S. R., Dennis, M. D., Schilder, R. J. and Jefferson, L. S. (2013). The mTORC1 signaling repressors REDD1/2 are rapidly induced and activation of p70S6K1 by leucine is defective in skeletal muscle of an immobilized rat hindlimb. *Am. J. Physiol. Endocrinol. Metab.* **304(2)**, E229–E236.

Kemp, A. (1986). The biology of the Australian lungfish, *Neoceratodus forsteri* (Krefft 1870). *J. Morphol.* **190(S1)**, 181–198.

Kerr, T., Roalson, E. H. and Rodgers, B. D. (2005). Phylogenetic analysis of the *myostatin* gene sub-family and the differential expression of a novel member in zebrafish. *Evol. Dev.* **7(5)**, 390–400.

Kim, J. Y., Shen, S., Dietz, K., He, Y., Howell, O., Reynolds, R. and Casaccia, P. (2010). HDAC1 nuclear export induced by pathological conditions is essential for the onset of axonal damage. *Nature Neurosci.* **13(2)**, 180–189.

Kim, S. J., Roy, R. R., Kim, J. A., Zhong, H., Haddad, F., Baldwin, K. M. and Edgerton, V. R. (2008). Gene expression during inactivity-induced muscle atrophy: effects of brief bouts of a forceful contraction countermeasure. *J. Appl. Physiol.* **105(4)**, 1246–1254.

Kind, P. K. (2010). The natural history of the Australian lungfish *Neoceratodus forsteri* (Krefft, 1870). In *Biology of Lungfishes*. (ed. J. M. Jorgensen and J. Joss), pp. 61–96. Enfield, Science Publishers.

Kipreos, E. T. and Pagano, M. (2000). The F-box protein family. *Genome Biol.* **1(5)**, 3002.1–3002.7.

Kirkman, H. N. and Gaetani, G. F. (1984). Catalase: a tetrameric enzyme with four tightly bound molecules of NADPH. *Proc. Natl. Acad. Sci. U. S. A.* **81(14)**, 4343–4347.

Kitzmann, M. and Fernandez, A. (2001). Crosstalk between cell cycle regulators and the myogenic factor MyoD in skeletal myoblasts. *Cell. Mol. Life Sci.* **58(4)**, 571–579.

Knutti, D., Kressler, D. and Kralli, A. (2001). Regulation of the transcriptional coactivator PGC-1 via MAPK-sensitive interaction with a repressor. *Proc. Natl. Acad. Sci. U. S. A.* **98(17)**, 9713–9718.

Kobe, B. and Kajava, A. V. (2001). The leucine-rich repeat as a protein recognition motif. *Curr. Opin. Struct. Biol.* **11(6)**, 725–732.

Kondo, H., Miura, M. and Itokawa, Y. (1991). Oxidative stress in skeletal muscle atrophied by immobiIization. *Acta Physiol. Scand.* **142(4)**, 527–528.

Kondo H., Miura M. and Itokawa Y. (1993). Antioxidant enzyme systems in skeletal muscle atrophied by immobilization. *Pflüg. Arch.* **422**, 404–406.

Kops, G. J., Dansen, T. B., Polderman, P. E., Saarloos, I., Wirtz, K. W., Coffer, P. J., Huang, T. T., Bos, J. L., Medema, R. H. and Burgering, B. M. (2002). Forkhead transcription factor FOXO3a protects quiescent cells from oxidative stress. *Nature* **419(6904)**, 316–321.

Kosugi S., Hasebe M., Tomita M. and Yanagawa H. (2009) Systematic identification of yeast cell cycle-dependent nucleocytoplasmic shuttling proteins by prediction of composite motifs. *Proc. Natl. Acad. Sci. U. S. A.* **106**, 10171–10176.

Koulmann, N., and Bigard, A. X. (2006). Interaction between signalling pathways involved in skeletal muscle responses to endurance exercise. *Pflügers Arch.* **452(2)**, 125–139.

Krens, S. G., Spaink, H. P. and Snaar-Jagalska, B. E. (2006). Functions of the MAPK family in vertebrate-development. *FEBS Lett.* **580(21)**, 4984–4990.

Kwon, H. S., Huang, B., Unterman, T. G. and Harris, R. A. (2004). Protein kinase B-α inhibits human pyruvate dehydrogenase kinase-4 gene induction by dexamethasone through inactivation of FOXO transcription factors. *Diabetes* **53(4)**, 899–910.

Laemmli, U. K. (1970). Cleavage of structural proteins during the assembly of the head of bacteriophage T4. *Nature* **227**, 680–685.

Lagirand-Cantaloube, J., Offner, N., Csibi, A., Leibovitch, M. P., Batonnet-Pichon, S., Tintignac, L. A., Segura, C. T. and Leibovitch, S. A. (2008). The initiation factor eIF3-f is a major target for Atrogin1/MAFbx function in skeletal muscle atrophy. *EMBO J.* **27(8)**, 1266–1276.

Lagirand-Cantaloube, J., Cornille, K., Csibi, A., Batonnet-Pichon, S., Leibovitch, M. P. and Leibovitch, S. A. (2009). Inhibition of atrogin-1/MAFbx mediated

MyoD proteolysis prevents skeletal muscle atrophy *in vivo*. *PloS One* **4(3)**, e4973. doi:10.1371/journal.pone.0004973.

Lam, E. W. F., Brosens, J. J., Gomes, A. R. and Koo, C. Y. (2013). Forkhead box proteins: tuning forks for transcriptional harmony. *Nat. Rev. Cancer* **13(7)**, 482–495.

Lang, S. M., Kazi, A. A., Hong-Brown, L. and Lang, C. H. (2012). Delayed recovery of skeletal muscle mass following hindlimb immobilization in mTOR heterozygous mice. *PloS One* **7(6)**, e38910.

Langley, B., Thomas, M., Bishop, A., Sharma, M., Gilmour, S. and Kambadur, R. (2002). Myostatin inhibits myoblast differentiation by down-regulating MyoD expression. *J. Biol. Chem.* **277(51)**, 49831–49840.

Laptenko, O. and Prives, C. (2006). Transcriptional regulation by p53: one protein, many possibilities. *Cell Death Differ.* **13(6)**, 951–961.

Latres, E., Amini, A. R., Amini, A. A., Griffiths, J., Martin, F. J., Wei, Y., Lin, H. C., Yancopoulos, G. D. and Glass, D. J. (2005). Insulin-like growth factor-1 (IGF-1) inversely regulates atrophy-induced genes via the phosphatidylinositol 3-kinase/Akt/mammalian target of rapamycin (PI3K/Akt/mTOR) pathway. *J. Biol. Chem.* **280(4)**, 2737–2744.

Lawan, A., Shi, H., Gatzke, F. and Bennett, A. M. (2013). Diversity and specificity of the mitogen-activated protein kinase phosphatase-1 functions. *Cell. Mol. Life Sci.* **70(2)**, 223–237.

Lawler, J. M., Song, W. and Demaree, S. R. (2003). Hindlimb unloading increases oxidative stress and disrupts antioxidant capacity in skeletal muscle. *Free Radic. Biol. Med.* **35(1)**, 9–16.

Lecker, S. H., Solomon, V., Mitch, W. E. and Goldberg, A. L. (1999). Muscle protein breakdown and the critical role of the ubiquitin-proteasome pathway in normal and disease states. *J. Nutr.* **129(1)**, 227S–237S.

Lecker, S. H. and Goldberg, A. L. (2002). Slowing muscle atrophy: putting the brakes on protein breakdown. *J. Physiol.* **545(3)**, 729–729.

Lecker, S. H., Jagoe, R. T., Gilbert, A., Gomes, M., Baracos, V., Bailey, J., Price, S. R., Mitch, W. E. and Goldberg, A. L. (2004). Multiple types of skeletal muscle atrophy involve a common program of changes in gene expression. *FASEB J.* **18(1)**, 39–51.

Lee, K., So, H., Gwag, T., Ju, H., Lee, J. W., Yamashita, M. and Choi, I. (2010). Molecular mechanism underlying muscle mass retention in hibernating bats: role of periodic arousal *J. Cell. Physiol.* **222(2)**, 313–319.

Lee, S. J. (2004). Regulation of muscle mass by myostatin. *Annu. Rev. Cell Dev. Biol.* **20**, 61–86.

Lee, S. J. and McPherron, A. C. (2001). Regulation of myostatin activity and muscle growth. *Proc. Natl. Acad. Sci. U. S. A.* **98(16)**, 9306–9311.

Lee, S. S., Kennedy, S., Tolonen, A. C. and Ruvkun, G. (2003). DAF-16 target genes that control C. elegans life-span and metabolism. *Science 300*(5619), 644–647.

Leitch, J. M., Yick, P. J. and Culotta, V. C. (2009). The right to choose: multiple pathways for activating copper, zinc superoxide dismutase. *J. Biol. Chem.* **284(37)**, 24679–24683.

LeMoine, C. M., Lougheed, S. C. and Moyes, C. D. (2010). Modular evolution of PGC-1α in vertebrates. *J. Mol. Evol.* **70(5)**, 492–505.

Lerin, C., Rodgers, J. T., Kalume, D. E., Kim, S. H., Pandey, A. and Puigserver, P. (2006). GCN5 acetyltransferase complex controls glucose metabolism through transcriptional repression of PGC-1α. *Cell Metab.* **3(6)**, 429–438.

Levine, S., Nguyen, T., Taylor, N., Friscia, M. E., Budak, M. T., Rothenberg, P., Zhu, J., Sachdeva, R., Sonnad, S., Kaiser, L. R., Rubinstein, N. A., Powers, S. K. and Shrager, J. B. (2008). Rapid disuse atrophy of diaphragm fibers in mechanically ventilated humans. *N. Engl. J. Med.* **358(13)**, 1327–1335.

Li, J., Lin, Q., Wang, W., Wade, P. and Wong, J. (2002). Specific targeting and constitutive association of histone deacetylase complexes during transcriptional repression. *Genes Dev.* **16(6)**, 687–692.

Li, M., Liu, J. and Zhang, C. (2011). Evolutionary history of the vertebrate mitogen activated protein kinases family. *PLoS One* **6(10)**, e26999. doi:10.1371/journal.pone.0026999.

Li, X., Monks, B., Ge, Q. and Birnbaum, M. J. (2007). Akt/PKB regulates hepatic metabolism by directly inhibiting PGC-1alpha transcription coactivator. *Nature* **447(7147)**, 1012–1016.

Li, Z. B., Kollias, H. D. and Wagner, K. R. (2008). Myostatin directly regulates skeletal muscle fibrosis. *J. Biol. Chem.* **283(28)**, 19371–19378.

Lin, J., Arnold, H. B., Della-Fera, M. A., Azain, M. J., Hartzell, D. L. and Baile, C. A. (2002). Myostatin knockout in mice increases myogenesis and decreases adipogenesis. *Biochem. Biophys. Res. Commun.* **291(3)**, 701–706.

Lindholm, D., Eriksson, O., Mäkelä, J., Belluardo, N. and Korhonen, L. (2012). PGC-1α: a master gene that is hard to master. *Cell. Mol. Life Sci.* **69(15)**, 2465–2468.

Lipina, C., Kendall, H., McPherron, A. C., Taylor, P. M. and Hundal, H. S. (2010). Mechanisms involved in the enhancement of mammalian target of rapamycin signalling and hypertrophy in skeletal muscle of myostatin-deficient mice. *FEBS Lett.* **584(11)**, 2403–2408.

Liu, C. M., Yang, Z., Liu, C. W., Wang, R., Tien, P., Dale, R. and Sun, L. Q. (2007). Effect of RNA oligonucleotide targeting Foxo-1 on muscle growth in normal and cancer cachexia mice. *Cancer Gene Ther.* **14(12)**, 945–952.

Löfberg, E., Gutierrez, A., Wernerman, J., Anderstam, B., Mitch, W. E., Price, S. R., Bergström, J. and Alvestrand, A. (2002). Effects of high doses of glucocorticoids on free amino acids, ribosomes and protein turnover in human muscle. *Eur. J. Clin. Invest.* **32(5)**, 345–353.

Lohuis, T. D., Harlow, H. J., Beck, T. D. I. and Iaizzo, P. A. (2007). Hibernating bears conserve muscle strength and maintain fatigue resistance. *Physiol. Biochem. Zool.* **80(3)**, 257–269.

Loong, A. M., Hiong, K. C., Lee, S. L. M., Wong, W. P., Chew, S. F. and Ip, Y. K. (2005). Ornithine-urea cycle and urea synthesis in African lungfishes, *Protopterus aethiopicus* and *Protopterus annectens*, exposed to terrestrial conditions for 6 days. *J. Exp. Zool.* **303A**, 354–365.

Loong, A. M., Pang, C. Y., Hiong, K. C., Wong, W. P., Chew, S. F. and Ip, Y. K. (2008a). Increased urea synthesis and/or suppressed ammonia production in the African lungfish, *Protopterus annectens*, during aestivation in air or mud. *J. Comp. Physiol. B* **178(3)**, 351–363.

Loong, A. M., Ang, S. F., Wong, W. P., Porter, H. O., Bock, C., Wittig, R., Bridges, C. R., Chew, S. F. and Ip, Y. K. (2008b). Effects of hypoxia on the energy status and nitrogen metabolism of African lungfish during aestivation in a mucus cocoon. *J. Comp. Physio. B.* **178B**, 351–365.

Loong, A. M., Hiong, K. C., Wong, W. P., Chew, S. F. and Ip, Y. K. (2012a). Differential gene expression in the liver of the African lungfish, *Protopterus annectens*, after 6 days of estivation in air. *J. Comp. Physiol. B* **182(2)**, 231–245.

Loong, A. M., Chng, Y. R., Chew, S. F., Wong, W. P. and Ip, Y. K. (2012b). Molecular characterization and mRNA expression of carbamoyl phosphate synthetase III in the liver of the African lungfish, *Protopterus annectens*, during aestivation or exposure to ammonia. *J. Comp. Physiol. B* **182(3)**, 367–379.

Lowe-McConnell, R. H. (1987). *Ecological studies in tropical fish communities.* Cambridge: Cambridge University Press.

Luo, J., Su, F., Chen, D., Shiloh, A. and Gu, W. (2000). Deacetylation of p53 modulates its effect on cell growth and apoptosis. *Nature* **408(6810)**, 377–381.

Luo, Y., Jian, W., Stavreva, D., Fu, X., Hager, G., Bungert, J., Huang, S. and Qiu, Y. (2009). Trans-regulation of histone deacetylase activities through acetylation. *J. Biol. Chem.* **284(50)**, 34901–34910.

Ma, K., Mallidis, C., Bhasin, S., Mahabadi, V., Artaza, J., Gonzalez-Cadavid, N., Arias, J. and Salehian, B. (2003). Glucocorticoid-induced skeletal muscle atrophy is associated with upregulation of myostatin gene expression. *Am. J. Physiol. Endocrinol. Metab.* **285(2)**, E363–E371.

Ma, P. C., Rould, M. A., Weintraub, H. and Pabo, C. O. (1994). Crystal structure of MyoD bHLH domain-DNA complex: perspectives on DNA recognition and implications for transcriptional activation. *Cell* **77(3)**, 451–459.

MacDonald, J. A. and Storey, K. B. (2005). Mitogen-activated protein kinases and selected downstream targets display organ-specific responses in the hibernating ground squirrel. *Int. J. Biochem. Cell Biol.* **37(3)**, 679–691.

Macpherson, P. C., Wang, X. and Goldman, D. (2011). Myogenin regulates denervation-dependent muscle atrophy in mouse soleus muscle. *J. Cell. Biochem.* **112(8)**, 2149–2159.

Macqueen, D. J. and Johnston, I. A. (2006). A novel salmonid myoD gene is distinctly regulated during development and probably arose by duplication after the genome tetraploidization. *FEBS Lett*. **580(21)**, 4996–5002.

Macqueen, D. J. and Johnston, I. A. (2008). An update on MyoD evolution in teleosts and a proposed consensus nomenclature to accommodate the tetraploidization of different vertebrate genomes. *PLoS One* **3(2)**, e1567. doi: 10.1371/journal.pone.0001567.

Maier, T., Güell, M. and Serrano, L. (2009). Correlation of mRNA and protein in complex biological samples. *FEBS Lett.* **583(24)**, 3966–3973.

Maiese, K., Chong, Z. Z. and Shang, Y. C. (2008). OutFOXOing disease and disability: the therapeutic potential of targeting FoxO proteins. *Trends Mol. Med.* **14(5)**, 219–227.

Mal, A., Sturniolo, M., Schiltz, R. L., Ghosh, M. K. and Harter, M. L. (2001). A role for histone deacetylase HDAC1 in modulating the transcriptional activity of MyoD: inhibition of the myogenic program. *EMBO J.* **20(7)**, 1739–1753.

Mammucari, C., Milan, G., Romanello, V., Masiero, E., Rudolf, R., Del Piccolo, P., Burden, S. J., Di Lisi, R., Sandri, C., Zhao, J., Goldberg, A. L., Schiaffino, S. and Sandri, M. (2007). FoxO3 controls autophagy in skeletal muscle in vivo. *Cell Metab.* **6(6)**, 458–471.

Manceau, M., Gros, J., Savage, K., Thomé, V., McPherron, A., Paterson, B. and Marcelle, C. (2008). Myostatin promotes the terminal differentiation of embryonic muscle progenitors. *Genes Dev.* **22(5)**, 668–681.

Mansour, S. J., Matten, W. T., Hermann, A. S., Candia, J. M., Rong, S., Fukasawa, K., Vande Woude, G. F. and Ahn, N. G. (1994). Transformation of mammalian cells by constitutively active MAP kinase kinase. *Science* **265**, 966–970.

Mantle, B. L., Hudson, N. J., Harper, G. S., Cramp, R. L. and Franklin, C. E. (2009). Skeletal muscle atrophy occurs slowly and selectively during prolonged aestivation in *Cyclorana alboguttata* (Günther 1867). *J. Exp. Biol.* **212(22)**, 3664–3672.

Marimuthu, K., Murton, A. J. and Greenhaff, P. L. (2011). Mechanisms regulating muscle mass during disuse atrophy and rehabilitation in humans. *J. Appl. Physiol.* **110(2)**, 555–560.

Marks, P. A. and Breslow, R. (2007). Dimethyl sulfoxide to vorinostat: development of this histone deacetylase inhibitor as an anticancer drug. *Nat. Biotech.* **25(1)**, 84–90.

Marmorstein, R. (2001). Structure of histone deacetylases: insights into substrate recognition and catalysis. *Structure* **9(12)**, 1127–1133.

Marshall, C. and Schultze, H. P. (1992) Relative importance of molecular, neontological, and paleontological data in understanding the biology of the vertebrate invasion of land. *J. Mol. Evol.* **35**, 93– 101.

Martin, J. F., Li, L. and Olson, E. N. (1992). Repression of myogenin function by TGF-β1 is targeted at the basic helix-loop-helix motif and is independent of E2A products. *J. Biol. Chem.* **267(16)**, 10956–10960.

Masiero, E. and Sandri, M. (2010). Autophagy inhibition induces atrophy and myopathy in adult skeletal muscles. *Autophagy* **6(2)**, 307–309.

Massari, M. E. and Murre, C. (2000). Helix-loop-helix proteins: regulators of transcription in eukaryotic organisms. *Mol. Cell. Biol.* **20(2)**, 429–440.

Matsakas, A. and Diel, P. (2005). The growth factor myostatin, a key regulator in skeletal muscle growth and homeostasis. *Int. J. Sports Med.* **26**, 83–89.

Matsuzaki, H., Daitoku, H., Hatta, M., Aoyama, H., Yoshimochi, K. and Fukamizu, A. (2005). Acetylation of Foxo1 alters its DNA-binding ability and sensitivity to phosphorylation. *Proc. Natl. Acad. Sci. U. S. A.* **102(32)**, 11278–11283.

McClelland, G. B., Craig, P. M., Dhekney, K. and Dipardo, S. (2006). Temperature-and exercise-induced gene expression and metabolic enzyme changes in skeletal muscle of adult zebrafish (*Danio rerio*). *J. Physiol.* **577(2)**, 739–751.

McCroskery, S., Thomas, M., Maxwell, L., Sharma, M. and Kambadur, R. (2003). Myostatin negatively regulates satellite cell activation and self-renewal. *J. Cell Biol.* **162(6)**, 1135–1147.

McFarlane, C., Plummer, E., Thomas, M., Hennebry, A., Ashby, M., Ling, N., Smith, H., Sharma, M. and Kambadur, R. (2006). Myostatin induces cachexia by activating the ubiquitin proteolytic system through an NF-κB-independent, FoxO1-dependent mechanism. *J. Cell. Physiol.* **209(2)**, 501–514.

McFarlane, C., Hennebry, A., Thomas, M., Plummer, E., Ling, N., Sharma, M. and Kambadur, R. (2008). Myostatin signals through Pax7 to regulate satellite cell self-renewal. *Exp. Cell Res.* **314(2)**, 317–329.

McPherron, A. C. and Lee, S. J. (1997). Double muscling in cattle due to mutations in the myostatin gene. *Proc. Natl. Acad. Sci. U. S. A.* **94(23)**, 12457–12461.

McPherron, A. C., Lawler, A. M. and Lee, S. J. (1997). Regulation of skeletal muscle mass in mice by a new TGF-p superfamily member. *Nature* **387(6628)**, 83–90.

Meadows, E., Flynn, J. M. and Klein, W. H. (2011). Myogenin regulates exercise capacity but is dispensable for skeletal muscle regeneration in adult mdx mice. *PLoS One* **6(1)**, e16184. doi:10.1371/journal.pone.0016184.

Medema, R. H., Kops, G. J., Bos, J. L. and Burgering, B. M. (2000). AFX-like Forkhead transcription factors mediate cell-cycle regulation by Ras and PKB through p27kip1. *Nature* **404(6779)**, 782–787.

Medina, R., Wing, S. S. and Goldberg, A. L. (1995). Increase in levels of polyubiquitin and proteasome mRNA in skeletal muscle during starvation and denervation atrophy. *Biochem. J.* **307(3)**, 631–637.

Megeney, L. A. and Rudnicki, M. A. (1995). Determination versus differentiation and the MyoD family of transcription factors. *Biochem. Cell Biol.* **73**, 723–732.

Méplan, C., Richard, M. J. and Hainaut, P. (2000). Redox signalling and transition metals in the control of the p53 pathway. *Biochem. Pharmacol.* **59(1)**, 25–33.

Meyer, A. and Wilson, A.C. (1990). Origin of tetrapods inferred from their mitochondrial DNA affiliation to lungfish. *J. Mol. Evol.* **31**, 359–365.

Min, K., Smuder, A. J., Kwon, O. S., Kavazis, A. N., Szeto, H. H. and Powers, S. K. (2011). Mitochondrial-targeted antioxidants protect skeletal muscle against immobilization-induced muscle atrophy. *J. Appl. Physiol.* **111(5)**, 1459–1466.

Minucci, S. and Pelicci, P. G. (2006). Histone deacetylase inhibitors and the promise of epigenetic (and more) treatments for cancer. *Nat. Rev. Cancer* **6(1)**, 38–51.

Miura, S., Kawanaka, K., Kai, Y., Tamura, M., Goto, M., Shiuchi, T., Minokoshi, Y. and Ezaki, O. (2007). An increase in murine skeletal muscle peroxisome proliferator-activated receptor-γ coactivator-1α (PGC-1α) mRNA in response to exercise is mediated by β-adrenergic receptor activation. *Endocrinology* **148(7)**, 3441–3448.

Miyamoto, K., Araki, K. Y., Naka, K., Arai, F., Takubo, K., Yamazaki, S., Matsuoka, S., Miyamoto, T., Ito, K., Ohmura, M., Chen, C., Hosokawa, K., Nakauchi, H., Nakayama, K., Nakayama, K. I., Harada, M., Motoyama, N., Suda, T. and Hirao, A. (2007). Foxo3a is essential for maintenance of the hematopoietic stem cell pool. *Cell Stem Cell* **1(1)**, 101–112.

Mlewa, C. M., Green, J. M. and Dunbrack, R. L. (2010). The general natural history of the African lungfishes. In *The Biology of Lungfishes*. (ed. J. M. Jorgensen and J. Joss), pp. 97–127. Enfield, Science Publishers.

Molkentin, J. D., Black, B. L., Martin, J. F. and Olson, E. N. (1995). Cooperative activation of muscle gene expression by MEF2 and myogenic bHLH proteins. *Cell 83*(7), 1125–1136.

Monsalve, M., Wu, Z., Adelmant, G., Puigserver, P., Fan, M. and Spiegelman, B. M. (2000). Direct coupling of transcription and mRNA processing through the thermogenic coactivator PGC-1. *Mol. Cell* **6(2)**, 307–316.

Moresi, V., Williams, A. H., Meadows, E., Flynn, J. M., Potthoff, M. J., McAnally, J., Shelton, J. M., Backs, J., Klein, W. H., Richardson, J. A., Bassel-Duby, R. and Olson, E. N. (2010). Myogenin and class II HDACs control neurogenic muscle atrophy by inducing E3 ubiquitin ligases. *Cell* **143(1)**, 35–45.

Moresi, V., Carrer, M., Grueter, C. E., Rifki, O. F., Shelton, J. M., Richardson, J. A., Bassel-Duby, R. and Olson, E. N. (2012). Histone deacetylases 1 and 2 regulate autophagy flux and skeletal muscle homeostasis in mice. *Proc. Natl. Acad. Sci.* **109(5)**, 1649–1654.

Morey-Holton, E. R. and Globus, R. K. (2002). Hindlimb unloading model: technical aspects. *J. Appl. Physiol.* **92(4)**, 1367–1377.

Morin, P. Jr. and Storey, K. B. (2006). Evidence for a reduced transcriptional state during hibernation in ground squirrels. *Cryobiology* **53(3)**, 310–318.

Motta, M. C., Divecha, N., Lemieux, M., Kamel, C., Chen, D., Gu, W., Bultsma, Y., McBurney, M. and Guarente, L. (2004). Mammalian SIRT1 represses forkhead transcription factors. *Cell* **116(4)**, 551–563.

Mozdziak, P. E., Greaser, M. L. and Schultz, E. (1999). Myogenin, MyoD, and myosin heavy chain isoform expression following hindlimb suspension. *Aviat., Space Environ. Med.* **70(5)**, 511–516.

Muller, F. L., Song, W., Jang, Y. C., Liu, Y., Sabia, M., Richardson, A. and Van Remmen, H. (2007). Denervation-induced skeletal muscle atrophy is associated with increased mitochondrial ROS production. *Am. J. Physiol. Regul. Integr. Comp. Physiol.* **293(3)**, R1159–R1168.

Murakami, K., Kondo, T., Epstein, C. J., and Chan, P. H. (1997). Overexpression of CuZn-superoxide dismutase reduces hippocampal injury after global ischemia in transgenic mice. *Stroke* **28**, 1797–1804.

Murgia, M., Serrano, A. L., Calabria, E., Pallafacchina, G., Lømo, T. and Schiaffino, S. (2000). Ras is involved in nerve-activity-dependent regulation of muscle genes. *Nat. Cell Biol.* **2(3)**, 142–147.

Murphy, C. T., McCarroll, S. A., Bargmann, C. I., Fraser, A., Kamath, R. S., Ahringer, J., Li, H. and Kenyon, C. (2003). Genes that act downstream of DAF-16 to influence the lifespan of *Caenorhabditis elegans*. *Nature* **424(6946)**, 277–283.

Nakae, J., Kitamura, T., Kitamura, Y., Biggs, W. H., Arden, K. C. and Accili, D. (2003). The forkhead transcription factor Foxo1 regulates adipocyte differentiation. *Dev. Cell* **4(1)**, 119–129.

Nakashima, K., Yakabe, Y., Yamazaki, M. and Abe, H. (2006). Effects of fasting and refeeding on expression of atrogin-1 and Akt/FOXO signaling pathway in skeletal muscle of chicks. *Biosci. Biotech. Biochem.* **70(11)**, 2775–2778.

Nasrin, N., Ogg, S., Cahill, C. M., Biggs, W., Nui, S., Dore, J., Calvo, D., Shi, Y. Ruvkun, G. and Alexander-Bridges, M. C. (2000). DAF-16 recruits the

CREB-binding protein coactivator complex to the insulin-like growth factor binding protein 1 promoter in HepG2 cells. *Proc. Natl. Acad. Sci. U. S. A.* **97(19)**, 10412–10417.

Nelson, J. S. (2006). *Fishes of the World, 4th ed*. New York: John Wiley and Sons Inc. p. 601.

Nemoto, S. and Finkel, T. (2002). Redox regulation of forkhead proteins through a p66shc-dependent signaling pathway. *Science* **295(5564)**, 2450–2452.

Norbury, C. and Zhivotovsky, B. (2004) DNA damage-induced apoptosis. *Oncogene* **23**, 2797–2808

Nowakowska, A., Swiderska-Kolacz, G., Rogalska, J. and Caputa, M. (2009). Effect of winter torpor upon antioxidative defence in *Helix pomatia*. *Can. J. Zool.* **87(6)**, 471–479.

Nowakowska, A., Caputa, M. and Rogalska, J. (2010). Natural aestivation and antioxidant defence in *Helix pomatia*: effect of acclimation to various external conditions. *J. Mollusc. Stud.* **76(4)**, 354–359.

Nowakowska, A., Gralikowska, P., Rogalska, J., Ligaszewski, M. and Caputa, M. (2014). Effect of induced spring aestivation on antioxidant defence in *Helix aspersa* OF Müller, 1774 (Gastropoda: Pulmonata: Helicidae). *Folia Malacologica* **22(1)**, 41–48.

Oberkofler, H., Schraml, E., Krempler, F. and Patsch, W. (2003). Potentiation of liver X receptor transcriptional activity by peroxisome-proliferator-activated receptor gamma co-activator 1alpha. *Biochem. J.* **371**, 89–96.

Ohnishi, T., Takahashi, A., Wang, X., Ohnishi, K., Ohira, Y. and Nagaoka, S. (1999). Accumulation of a tumor suppressor p53 protein in rat muscle during a space flight. *Mutat. Res. Fund. Mol. Mech. Mut.* **430(2)**, 271–274.

Ohta, H., Okamoto, I., Hanaya, T., Arai, S., Ohta, T. and Fukuda, S. (2006). Enhanced antioxidant defense due to extracellular catalase activity in Syrian hamster during arousal from hibernation. *Comp. Biochem. Physiol. C Toxicol. Pharmacol.* **143(4)**, 484–491.

Ojeda, J. L., Wong, W. P., Ip, Y. K. and Icardo, J. M. (2008). Renal corpuscle of the African lungfish *Protopterus dolloi*: structural and histochemical modifications during aestivation. *Anat. Rec. (Hoboken)* **291**, 1156–1172.

Okamoto, I., Kayano, T., Hanaya, T., Arai, S., Ikeda, M. and Kurimoto, M. (2006). Up-regulation of an extracellular superoxide dismutase-like activity in hibernating hamsters subjected to oxidative stress in mid-to late arousal from torpor. *Comp. Biochem. Physiol. C Toxicol. Pharmacol.* **144(1)**, 47–56.

Olson, B. L., Hock, M. B., Ekholm-Reed, S., Wohlschlegel, J. A., Kralli, A. and Reed, S. I. (2008). SCFCdc4 acts antagonistically to the PGC-1α transcriptional coactivator by targeting it for ubiquitin-mediated proteolysis. *Genes Dev.* **22(2)**, 252–264.

Olson, E. N. (1992). Interplay between proliferation and differentiation within the myogenic lineage. *Dev. Biol.* **154(2)**, 261–272.

Ong, J. L. Y. (2010). Sequencing, phylogenetic analysis and mRNA expression of *superoxide dismutase*, *catalase* and *glutathione s-transferase* genes in the African lungfish, *Protopterus annectens*, during three phases of aestivation in normoxia.

Ong, J. L. Y. (2011). Molecular characterization and mRNA expression of six genes associated with oxidative defense in the liver and the brain of the African lungfish, *Protopterus annectens*, during aestivation.

Ong, J. L. Y., Woo, J. M., Hiong, K. C., Ching, B., Wong, W. P., Chew, S. F. and Ip, Y. K. (2015). Molecular characterization of betaine-homocysteine methyltransferase 1 from the liver and effects of aestivation on its expressions and homocysteine concentrations in the liver, kidney and muscle, of the African lungfish, *Protopterus annectens*. *Comp. Biochem. Physiol. B Biochem. Mol. Biol.* **183**, 30–41.

Ørngreen, M. C., Zacho, M., Hebert, A., Laub, M. and Vissing, J. (2003). Patients with severe muscle wasting are prone to develop hypoglycemia during fasting. *Neurology* **61(7)**, 997–1000.

Orr, A. L., Lohse, L. A., Drew, K. L. and Hermes-Lima, M. (2009). Physiological oxidative stress after arousal from hibernation in arctic ground squirrel. *Comp. Biochem. Physiol. A Mol. Integr. Physiol.* **153**, 213–221.

Otero, O. (2011). Current knowledge and new assumptions on the evolutionary history of the African lungfish, *Protopterus*, based on a review of its fossil record. *Fish Fish.* **12**, 235–255.

Paddon-Jones, D., Sheffield-Moore, M., Cree, M. G., Hewlings, S. J., Aarsland, A., Wolfe, R. R. and Ferrando, A. A. (2006). Atrophy and impaired muscle protein synthesis during prolonged inactivity and stress. *J. Clin. Endocrinol. Metab.* **91(12)**, 4836–4841.

Page, M. M., Peters, C. W., Staples, J. F. and Stuart, J. A. (2009). Intracellular antioxidant enzymes are not globally upregulated during hibernation in the major oxidative tissues of the 13-lined ground squirrel *Spermophilus tridecemlineatus*. *Comp. Biochem. Physiol. A Mol. Integr. Physiol.* **152(1)**, 115–122.

Page, M. M., Salway, K. D., Ip, Y. K., Chew, S. F., Warren, S. A., Ballantyne, J. S. and Stuart, J. A. (2010). Upregulation of intracellular antioxidant enzymes in brain and heart during estivation in the African lungfish *Protopterus dolloi*. *J. Comp. Physiol. B* **180(3)**, 361–369.

Payne, D. M., Rossomando, A. J., Martino, P., Erickson, A. K., Her, J.-H., Shabanowitz, J., Hunt, D. F., Weber, M. J. and Sturgill, T. W. (1991). Identification of the regulatory phosphorylation sites in pp42/mitogen-activated protein kinase (MAP kinase). *EMBO J.* **10**, 885–892.

Pearson, G., Robinson, F., Beers Gibson, T., Xu, B. E., Karandikar, M., Berman, K. and Cobb, M. H. (2001). Mitogen-activated protein (MAP) kinase pathways: regulation and physiological functions 1. *Endocrine Rev.* **22(2)**, 153–183.

Pérez-Schindler, J. and Handschin, C. (2013). New insights in the regulation of skeletal muscle PGC-1α by exercise and metabolic diseases. *Drug Discov. Today Dis. Models* **10(2)**, e79–e85.

Perrot, V. and Rechler, M. M. (2005). The coactivator p300 directly acetylates the forkhead transcription factor Foxo1 and stimulates Foxo1-induced transcription. *Mol. Endocrinol.* **19(9)**, 2283–2298.

Perry, S. F., Wilson, R. J. A., Straus, C., Harris, M. B. and Remmers, J. (2001). Which came first, the lung or the breath? *Comp. Biochem. Physiol. A.* **129**, 37–47.

Perry, S. F., Euverman, R., Wang, T., Loong, A. M., Chew, S. F., Ip, Y. K. and Gilmour, K. M. (2008). Control of breathing in African lungfish (*Protopterus dolloi*): A comparison of aquatic and cocooned (terrestrialized) animals. *Resp. Physiol. Neurobiol.* **160**, 8–17.

Peterson, C. C. and Stone, P. A. (2000). Physiological capacity for estivation of the Sonoran mud turtle, *Kinosternon sonoriense*. *Copeia* **2000**, 684–700.

Pflum, M. K. H., Tong, J. K., Lane, W. S. and Schreiber, S. L. (2001). Histone deacetylase 1 phosphorylation promotes enzymatic activity and complex formation. *J. Biol. Chem.* **276(50)**, 47733–47741.

Pilegaard, H., Saltin, B. and Neufer, P. D. (2003). Exercise induces transient transcriptional activation of the PGC-1α gene in human skeletal muscle. *J. Physiol.* **546(3)**, 851–858.

Planquette, P., Keith, P. and Le Bail, P. Y. (1996). Atlas des Poissons d'Eau Douce de Guyane, Tome 1. Paris: Museum National d'Histoire Naturelle. p. 429.

Pluemsampant, S., Safronova, O. S., Nakahama, K. I. and Morita, I. (2008). Protein kinase CK2 is a key activator of histone deacetylase in hypoxia-associated tumors. *Int. J. Cancer* **122(2)**, 333–341.

Poll, M. (1961). Révision systématique et raciation géographique des Protopteridae de l'Afrique centrale. *Ann. Mus. R. Afr. Centr. Sci. Zool.* **103**, 3–50.

Poll, M. and Damas. H. (1939). Poissons. In *Exploration du Parc National Albert. Mission H. Damas (1935-36). Institut des Parcs Nationaux du Congo belge, Bruxelles, Fasc*. **6**, 1–73.

Postlethwait, J. H., Yan, Y. L., Gates, M. A., Horne, S., Amores, A., Brownlie, A., Donovan, A., Egan, E. S., Force, A., Gong, Z., Goutel, C., Fritz, A., Kelsh, R., Knapik, E., Liao, E., Paw, B., Ransom, D., Singer, A, Thomson, M., Abduljabbar, T. S., Yelick, P., Beier, D., Joly, J. S., Larhammar, D., Rosa, F., Westerfield, M., Zon, L. I., Johnson, S. L. and Talbot, W. S. (1998).

Vertebrate genome evolution and the zebrafish gene map. *Nat. Genet.* **18(4)**, 345–349.

Powers, S. K., Kavazis, A. N. and DeRuisseau, K. C. (2005). Mechanisms of disuse muscle atrophy: role of oxidative stress. *Am. J. Physiol. Regul. Integr. Comp. Physiol.* **288(2)**, R337–R344.

Powers, S. K., Kavazis, A. N. and McClung, J. M. (2007). Oxidative stress and disuse muscle atrophy. *J. Appl. Physiol.* **102(6)**, 2389–2397.

Powers, S. K., Hudson, M. B., Nelson, W. B., Talbert, E. E., Min, K., Szeto, H. H., Kavazis, A. N. and Smuder, A. J. (2011). Mitochondria-targeted antioxidants protect against mechanical ventilation-induced diaphragm weakness. *Crit. Care Med.* **39(7)**, 1749–1759.

Pownall, M. E., Gustafsson, M. K. and Emerson Jr, C. P. (2002). Myogenic regulatory factors and the specification of muscle progenitors in vertebrate embryos. *Annu. Rev. Cell Dev. Biol.* **18(1)**, 747–783.

Puigserver, P., Wu, Z., Park, C. W., Graves, R., Wright, M. and Spiegelman, B. M. (1998). A cold-inducible coactivator of nuclear receptors linked to adaptive thermogenesis. *Cell* **92**, 829–839.

Puigserver, P., Adelmant, G., Wu, Z., Fan, M., Xu, J., O'Malley, B. and Spiegelman, B. M. (1999). Activation of PPARγ coactivator-1 through transcription factor docking. *Science* **286**, 1368–1371.

Puigserver, P., Rhee, J., Lin, J., Wu, Z., Yoon, J. C., Zhang, C. Y., Krauss, S., Mootha, V. K., Lowell, B. B. and Spiegelman, B. M. (2001). Cytokine stimulation of energy expenditure through p38 MAP kinase activation of PPARγ coactivator-1. *Mol. Cell* **8(5)**, 971–982.

Puigserver, P., Rhee, J., Donovan, J., Walkey, C. J., Yoon, J. C., Oriente, F., Kitamura, Y., Altomonte, J., Dong, H., Accili, D. and Spiegelman, B. M. (2003). Insulin-regulated hepatic gluconeogenesis through FOXO1–PGC-1α interaction. *Nature* **423(6939)**, 550–555.

Qiu, Y., Zhao, Y., Becker, M., John, S., Parekh, B. S., Huang, S., Hendarwanto, A., Martinez, E.D., Chen, Y., Lu, H., Adkins, N. L., Stavreva, D. A., Wiench, M., Georgel, P. T., Schiltz, R. L. and Hager, G. L. (2006). HDAC1 acetylation is linked to progressive modulation of steroid receptor-induced gene transcription. *Mol. Cell* **22(5)**, 669–679.

Ramos-Vasconcelos, G. R. and Hermes-Lima, M. (2003). Hypometabolism, antioxidant defenses and free radical metabolism in the pulmonate land snail *Helix aspersa*. *J. Exp. Biol.* **206**, 675–685.

Ramos-Vasconcelos, G. R., Cardoso, L. A. and Hermes-Lima, M. (2005). Seasonal modulation of free radical metabolism in estivating land snails *Helix aspersa*. *Comp. Biochem. Physiol. C Toxicol. Pharmacol.* **140(2)**, 165–174.

Reardon, K. A., Davis, J., Kapsa, R. M., Choong, P. and Byrne, E. (2001). Myostatin, insulin-like growth factor-1, and leukemia inhibitory factor

mRNAs are upregulated in chronic human disuse muscle atrophy. *Muscle Nerve* **24(7)**, 893–899.

Reddehase, S., Grumbt, B., Neupert, W. and Hell, K. (2009). The disulfide relay system of mitochondria is required for the biogenesis of mitochondrial Ccs1 and Sod1. *J. Mol. Biol.* **385(2)**, 331–338.

Reilly, B. D., Hickey, A. J., Cramp, R. L. and Franklin, C. E. (2014). Decreased hydrogen peroxide production and mitochondrial respiration in skeletal muscle but not cardiac muscle of the green-striped burrowing frog, a natural model of muscle disuse. *J. Exp. Biol.* **217(7)**, 1087–1093.

Rena, G., Prescott, A., Guo, S., Cohen, P. and Unterman, T. (2001). Roles of the forkhead in rhabdomyosarcoma (FKHR) phosphorylation sites in regulating 14-3-3 binding, transactivation and nuclear targetting. *Biochem. J.* **354**, 605–612.

Rena, G., Woods, Y. L., Prescott, A. R., Peggie, M., Unterman, T. G., Williams, M. R. and Cohen, P. (2002). Two novel phosphorylation sites on FKHR that are critical for its nuclear exclusion. *EMBO J.* **21(9)**, 2263–2271.

Rena, G., Bain, J., Elliott, M. and Cohen, P. (2004). D4476, a cell-permeant inhibitor of CK1, suppresses the site-specific phosphorylation and nuclear exclusion of FOXO1a. *EMBO Rep.* **5(1)**, 60–65.

Rennie, M. J., Selby, A., Atherton, P., Smith, K., Kumar, V., Glover, E. L. and Philips, S. M. (2010). Facts, noise and wishful thinking: muscle protein turnover in aging and human disuse atrophy. *Scand. J. Med. Sci. Spor.* **20(1)**, 5–9.

Rescan, P. Y. (2001). Regulation and functions of myogenic regulatory factors in lower vertebrates. *Comp. Biochem. Physiol. B Biochem. Mol. Biol.* **130**, 1–12.

Rescan, P. Y., Montfort, J., Rallière, C., Le Cam, A., Esquerré, D. and Hugot, K. (2007). Dynamic gene expression in fish muscle during recovery growth induced by a fasting-refeeding schedule. *BMC Genomics* **8(1)**, 438.

Rey, B., Halsey, L. G., Dolmazon, V., Rouanet, J. L., Roussel, D., Handrich, Y., Butler, P. J. and Duchamp, C. (2008). Long-term fasting decreases mitochondrial avian UCP-mediated oxygen consumption in hypometabolic king penguins. *Am. J. Physiol. Regul. Integr. Comp. Physiol.* **295(1)**, R92–R100.

Riley, T., Sontag, E., Chen, P. and Levine, A. (2008) Transcriptional control of human p53-regulated genes. *Nat. Rev. Mol. Cell. Biol.* **9(5)**, 402–412.

Ríos, R., Carneiro, I., Arce, V. M. and Devesa, J. (2002). Myostatin is an inhibitor of myogenic differentiation. *Am. J. Physiol. Cell Physiol.* **282(5)**, C993–C999.

Robbins, D. J. and Cobb, M. H. (1992). ERK2 autophosphorylates on a subset of peptides phosphorylated in intact cells in response to insulin and nerve growth factor: analysis by peptide mapping. *Mol. Biol. Cell* **3**, 299–308.

Robbins, D. J., Zhen, E., Owaki, H., Vanderbilt, C. A., Ebert, D., Geppert, T. D. and Cobb, M. H. (1993). Regulation and properties of extracellular signal-regulated protein kinases 1 and 2 in vitro. *J. Biol. Chem.* **268**, 5097–5106.

Rodgers, B. D. and Garikipati, D. K. (2008). Clinical, agricultural and evolutionary biology of myostatin: a comparative review. *Endocr. Rev.* **29(5)**, 513–534.

Rodgers, J. T., Lerin, C., Haas, W., Gygi, S. P., Spiegelman, B. M. and Puigserver, P. (2005). Nutrient control of glucose homeostasis through a complex of PGC-1alpha and SIRT1. *Nature* **434**, 113–118.

Rodier, F., Campisi, J. and Bhaumik, D. (2007). Two faces of p53: aging and tumor suppression. *Nucleic Acids Res.* **35(22)**, 7475–7484.

Rosato, R. R. and Grant, S. (2005). Histone deacetylase inhibitors: insights into mechanisms of lethality. *Expert Opin. Ther. Targets* **9(4)**, 809–824.

Roth, R. J., Le, A. M., Zhang, L., Kahn, M., Samuel, V. T., Shulman, G. I. and Bennett, A. M. (2009). MAPK phosphatase-1 facilitates the loss of oxidative myofibers associated with obesity in mice. *J. Clin. Invest.* **119(12)**, 3817–3829.

Rubinfeld, H., Hanoch, T. and Seger, R. (1999). Identification of a cytoplasmic-retention sequence in ERK2. *J. Biol. Chem.* **274**, 30349–30352.

Rudnicki, M. A. and Jaenisch, R. (1995). The MyoD family of transcription factors and skeletal myogenesis. *Bioessays* **17(3)**, 203–209.

Ryan, J., Llinas, A. J., White, D. A., Turner, B. M. and Sommerville, J. (1999). Maternal histone deacetylase is accumulated in the nuclei of *Xenopus* oocytes as protein complexes with potential enzyme activity. *J. Cell Sci.* **112(14)**, 2441–2452.

Sacheck, J. M., Ohtsuka, A., McLary, S. C. and Goldberg, A. L. (2004). IGF-I stimulates muscle growth by suppressing protein breakdown and expression of atrophy-related ubiquitin ligases, atrogin-1 and MuRF1. *Am. J. Physiol. Endocrinol. Metab.* **287(4)**, E591–E601.

Sacheck, J. M., Hyatt, J. P. K., Raffaello, A., Jagoe, R. T., Roy, R. R., Edgerton, V. R., Lecker, S. H. and Goldberg, A. L. (2007). Rapid disuse and denervation atrophy involve transcriptional changes similar to those of muscle wasting during systemic diseases. *FASEB J.* **21(1)**, 140–155.

Sadana, P. and Park, E. (2007). Characterization of the transactivation domain in the peroxisome-proliferator-activated receptor gamma co-activator (PGC-1). *Biochem. J.* **403**, 511–518.

Saito, T., Shinzawa, H., Togashi, H., Wakabayashi, H., Ukai, K., Takahashi, T., Ishikawa, M., Dobashi, M. and Imai, Y. (1989). Ultrastructural localization of Cu, Zn-SOD in hepatocytes of patients with various liver diseases. *Histol. Histopathol*. **4(1)**, 1–6.

Salway, K. D., Tattersall, G. J. and Stuart, J. A. (2010). Rapid upregulation of heart antioxidant enzymes during arousal from estivation in the Giant African

snail (*Achatina fulica*). *Comp. Biochem. Physiol. A Mol. Integr. Physiol.* **157(3)**, 229–236.

Sanchez, A. M., Csibi, A., Raibon, A., Cornille, K., Gay, S., Bernardi, H. and Candau, R. (2012). AMPK promotes skeletal muscle autophagy through activation of forkhead FoxO3a and interaction with Ulk1. *J. Cell Biochem.* **113(2)**, 695–710.

Sandri, M., Sandri, C., Gilbert, A., Skurk, C., Calabria, E., Picard, A., Walsh, K., Schiaffino, S., Lecker, S. H. and Goldberg, A. L. (2004). Foxo transcription factors induce the atrophy-related ubiquitin ligase atrogin-1 and cause skeletal muscle atrophy. *Cell* **117(3)**, 399–412.

Sandri, M., Lin, J., Handschin, C., Yang, W., Arany, Z. P., Lecker, S. H., Goldberg, A. L. and Spiegelman, B. M. (2006). PGC-1α protects skeletal muscle from atrophy by suppressing FoxO3 action and atrophy-specific gene transcription. *Proc. Natl. Acad. Sci. U. S. A.* **103(44)**, 16260–16265.

Sarbassov, D. D., Ali, S. M. and Sabatini, D. M. (2005). Growing roles for the mTOR pathway. *Curr. Opin. Cell Biol.* **17(6)**, 596–603.

Sartori, R., Milan, G., Patron, M., Mammucari, C., Blaauw, B., Abraham, R. and Sandri, M. (2009). Smad2 and 3 transcription factors control muscle mass in adulthood. *Am. J. Physiol. Cell Physiol.* **296(6)**, C1248–C1257.

Scarpulla, R. C. (2008). Transcriptional paradigms in mammalian mitochondrial biogenesis and function. *Physiol. Rev.* **88(2)**, 611–638.

Schlenstedt, G. (1996). Protein import into the nucleus. *FEBS Lett*. **389**, 75–79.

Schultze, H. P. (2015). Phylogenetic Introduction. In *Phylogeny, Anatomy and Physiology of Ancient Fishes*, (ed. G. Zaccone, K. Dabrowski, M. S. Hedrick, J. M. O. Fernandes, and J. M. Icardo), pp 1–18, CRC Press.

Schwarzkopf, M., Coletti, D., Sassoon, D. and Marazzi, G. (2006). Muscle cachexia is regulated by a p53–PW1/Peg3-dependent pathway. *Genes Dev.* **20(24)**, 3440–3452.

Schwarzkopf, M., Coletti, D., Marazzi, G. and Sassoon, D. (2008). Chronic p53 activity leads to skeletal muscle atrophy and muscle stem cell perturbation. *Basic Appl. Myol.* **18(5)**, 131–138.

Ścibior, D. and Czeczot, H. (2006). Catalase: structure, properties, functions. Postepy Hig. Med. Dosw. (Online). **60**, 170–180.

Seale, P., Sabourin, L. A., Girgis-Gabardo, A., Mansouri, A., Gruss, P. and Rudnicki, M. A. (2000). Pax7 is required for the specification of myogenic satellite cells. *Cell* **102(6)**, 777–786.

Seger, R., Seger, D., Lozeman, F. J., Ahn, N. G., Graves, L. M., Campbell, J. S., Ericsson, L., Harrylock, M., Jensen, A. M. and Krebs, E. G. (1992). Human T-cell mitogen-activated protein kinase kinases are related to yeast signal transduction kinases. *J. Biol. Chem.* **267**, 25628–25631.

Seidel, M. E. (1978). Terrestrial dormancy in the turtle *Kinosternon flavescens*: respiratory metabolism and dehydration. *Comp. Biochem. Physiol. A* **61**, 1–4.

Seiler, A., Schneider, M., Förster, H., Roth, S., Wirth, E. K., Culmsee, C., Plesnila, N., Kremmer, E., Rådmark, O., Wurst, W., Bornkamm, G. W., Schweizer, U. and Conrad, M. (2008). Glutathione peroxidase 4 senses and translates oxidative stress into 12/15-lipoxygenase dependent-and AIF-mediated cell death. *Cell Metab.* **8(3)**, 237–248.

Seiliez, I., Sabin, N. and Gabillard, J. C. (2011). FoxO1 is not a key transcription factor in the regulation of *myostatin* (*mstn-1a* and *mstn-1b*) gene expression in trout myotubes. *Am. J. Physiol. Regul. Integr. Comp. Physiol.* **301(1)**, R97–R104.

Senf, S. M., Dodd, S. L. and Judge, A. R. (2010). FOXO signaling is required for disuse muscle atrophy and is directly regulated by Hsp70. *Am. J. Physiol. Cell Physiol.* **298(1)**, C38–C45.

Shan, X., Chi, L., Luo, C., Qian, S., Gozal, D., and Liu, R. (2007). Manganese superoxide dismutase protects mouse cortical neurons from chronic intermittent hypoxia-mediated oxidative damage. *Neurobiol. Dis.* **28**, 206–215.

Shao, C., Liu, M., Wu, X. and Ding, F. (2007). Time-dependent expression of myostatin RNA transcript and protein in gastrocnemius muscle of mice after sciatic nerve resection. *Microsurgery* **27(5)**, 487–493.

Shao, C., Liu, Y., Ruan, H., Li, Y., Wang, H., Kohl, F., Goropashnaya, A. V., Fedorov, V. B., Zeng, R., Barnes, B. M. and Yan, J. (2010). Shotgun proteomics analysis of hibernating arctic ground squirrels. *Mol. Cell. Proteomics* **9(2)**, 313–326.

Sherr, C. J. and Roberts, J. M. (1995) Inhibitors of mammalian G1 cyclin-dependent kinases. *Genes Dev*. **9**, 1149–1163.

Shi, H., Zeng, C., Ricome, A., Hannon, K., Grant, A. and Gerrard, D. E. (2007). Extracellular signal-regulated kinase pathway is differentially involved in β-agonist-induced hypertrophy in slow and fast muscle. *Am. J. Physiol. Cell Physiol.* **292**, C1681–C1689.

Shi, H., Scheffler, J. M., Pleitner, J. M., Zeng, C., Park, S., Hannon, K. M., Grant, A. L. and Gerrard, D. E. (2008). Modulation of skeletal muscle fibre type by mitogen-activated protein kinase signaling. *FASEB J.* **22**, 2990–3000.

Shi, H., Scheffler, J. M., Zeng, C., Pleitner, J. M., Hannon, K. M., Grant, A. L. and Gerrard, D. E. (2009). Mitogen-activated protein kinase signaling is necessary for the maintenance of skeletal muscle mass. *Am. J. Physiol. Cell Physiol.* **296(5)**, C1040–C1048.

Sievert, L. M., Sievert, G. A. and Cupp, Jr. P. V. (1988). Metabolic rates of feeding and fasting juvenile midland painted turtles, *Chrysemys picta marginata*. *Comp. Biochem. Physiol. A.* **90**, 157–159.

Siu, P. M and Alway, S. E. (2005a). Id2 and p53 participate in apoptosis during unloading-induced muscle atrophy. *Am. J. Physiol. Cell Physiol.* **288(5)**, C1058–C1073.

Siu, P. M and Alway, S. E. (2005b). Mitochondria-associated apoptotic signalling in denervated rat skeletal muscle. *J. Physiol.* **565(1)**, 309–323.

Smith, H. K., Matthews, K. G., Oldham, J. M., Jeanplong, F., Falconer, S. J., Bass, J. J., Senna-Salerno, M., Bracegirdle, J. W. and McMahon, C. D. (2014). Translational signalling, atrogenic and myogenic gene expression during unloading and reloading of skeletal muscle in myostatin-deficient mice. *PLoS One* **9(4)**, e94356. doi:10.1371/journal.pone.0094356.

Smith, H. W. (1930). Metabolism of the lungfish, *Protopterus aethiopicus*. *J. Biol. Chem.* **88(1)**, 97–130.

Smith, H. W. (1931). Observations on the African lungfish, *Protopterus aethiopicus*, and on evolution from water to land environments. *Ecology* **12**, 164–181.

Smith, T. F., Gaitatzes, C., Saxena, K. and Neer, E. J. (1999). The WD repeat: a common architecture for diverse functions. *Trends Biochem. Sci.* **24(5)**, 181–185.

Songyang, Z., Lu, K. P., Kwon, Y. T., Tsai, L. H., Filhol, O., Cochet, C., Brickey, D. A., Soderling, T. R., Bartleson, C., Graves, D. J., DeMaggio, A. J., Hoekstra, M. F., Blenis, J., Hunter, T. and Cantley, L. C. (1996). A structural basis for substrate specificities of protein Ser/Thr kinases: primary sequence preference of casein kinases I and II, NIMA, phosphorylase kinase, calmodulin-dependent kinase II, CDK5 and Erk1. *Mol. Cell. Biol.* **16(11)**, 6486–6493.

Southgate, R. J., Neill, B., Prelovsek, O., El-Osta, A., Kamei, Y., Miura, S., Ezaki, O., McLoughlin, T. J., Zhang, W., Unterman, T. G. and Febbraio, M. A. (2007). FOXO1 regulates the expression of 4E-BP1 and inhibits mTOR signaling in mammalian skeletal muscle. *J. Biol. Chem.* **282(29)**, 21176–21186.

Stadtman, E. R. and Levine, R. L. (2000). Protein oxidation. *Ann. N. Y. Acad. Sci.* **899**, 191–208.

Stamatakis, A. (2014). RAxML Version 8: A tool for phylogenetic analysis and post-analysis of large phylogenies. bioinformatics. doi: 10.1093/bioinformatics/btu033.

Stauber, W. T., Bird, J. W. C. and Schottelius, B. A. (1977). Catalase: an enzymatic indicator of the degree of muscle wasting. *Exp.Neurol.* **55(2)**, 381–389.

Stefanovsky, V., Langlois, F., Gagnon-Kugler, T., Rothblum, L. I. and Moss, T. (2006). Growth factor signaling regulates elongation of RNA polymerase I transcription in mammals via UBF phosphorylation and r-chromatin remodeling. *Mol. Cell* **21(5)**, 629–639.

Steffen, J. M., Koebel, D. A., Musacchia, X. J. and Milsom, W. K. (1991). Morphometric and metabolic indices of disuse in muscles of hibernating ground squirrels. *Comp. Biochem. Physiol.* **99B**, 815–819.

Stevenson, E. J., Giresi, P. G., Koncarevic, A. and Kandarian, S. C. (2003). Global analysis of gene expression patterns during disuse atrophy in rat skeletal muscle. *J. Physiol.* **551(1)**, 33–48.

Storey, K. B. (2002). Review – Life in the slow lane: molecular mechanisms of estivation. *Comp. Biochem. Physiol. A Mol. Integr. Physiol.* **133(3)**, 733–754.

Storey, K. B. and Storey, J. M. (1990). Metabolic rate depression and biochemical adaptation in anaerobiosis, hibernation, and estivation. *Q. Rev. Biol.* **65**, 145–174.

Storey, K. B. and Storey, J. M. (2010). Metabolic regulation and gene expression during aestivation. In *Aestivation: Molecular and Physiological Aspects, Progress in Molecular and Subcellular Biology*, (ed. C. A. Navas and J. E. Carvalho), pp. 25–46, Springer-Verlag, Heidelberg.

St-Pierre, J., Drori, S., Uldry, M., Silvaggi, J. M., Rhee, J., Jäger, S., Handschin, C., Zheng, K., Lin, J., Yang, W., Simon, D. K., Bachoo, R. and Spiegelman, B. M. (2006). Suppression of reactive oxygen species and neurodegeneration by the PGC-1 transcriptional coactivators. *Cell* **127(2)**, 397–408.

Sturla, M., Paola, P., Carlo, G., Angela, M. M. and Maria, U. B. (2002). Effects of induced aestivation in *Protopterus annectens*: a histomorphological study. *J. Exp. Zool.* **292(1**), 26–31.

Sun, J. M., Chen, H. Y. and Davie, J. R. (2007). Differential distribution of unmodified and phosphorylated histone deacetylase 2 in chromatin. *J. Biol. Chem.* **282(45)**, 33227–33236.

Suryawan, A., Frank, J. W., Nguyen, H. V. and Davis, T. A. (2006). Expression of the TGF-β family of ligands is developmentally regulated in skeletal muscle of neonatal rats. *Pediatr. Res.* **59(2)**, 175–179.

Suzuki, N., Motohashi, N., Uezumi, A., Fukada, S. I., Yoshimura, T., Itoyama, Y., Aoki, M., Miyagoe-Suzuki, Y. and Takeda, S. I. (2007). NO production results in suspension-induced muscle atrophy through dislocation of neuronal NOS. *J. Clin. Invest.* **117(9)**, 2468–2476.

Symonds, B. L., James, R. S. and Franklin, C. E. (2007). Getting the jump on skeletal muscle disuse atrophy: preservation of contractile performance in aestivating *Cyclorana alboguttata* (Günther 1867). *J. Exp. Biol.* **210**, 825–835.

Tacchi, L., Bickerdike, R., Secombes, C. J., Pooley, N. J., Urquhart, K. L., Collet, B. and Martin, S. A. (2010). Ubiquitin E3 ligase atrogin-1 (Fbox-32) in Atlantic salmon (*Salmo salar*): sequence analysis, genomic structure and modulation of expression. *Comp. Biochem. Physiol. B Biochem. Mol Biol.* **157(4)**, 364–373.

Taillandier, D., Aurousseau, E., Meynial-Denis, D., Bechet, D., Ferrara, M., Cottin, P., Ducastaing, A., Bigard, X., Guezennec, C. Y., Schmid, H. P. and Attaix, D. (1996). Coordinate activation of lysosomal, Ca2+-activated and ATP-ubiquitin-dependent proteinases in the unweighted rat soleus muscle. *Biochem. J.* **316(1)**, 65–72.

Takezaki, N., Figueroa, F., Zaleska-Rutczynska, Z., Takahata, N. and Klein, J. (2004). The phylogenetic relationship of tetrapod, coelacanth and lungfish revealed by the sequences of forty-four nuclear genes. *Mol. Biol. Evol.* **21(8)**, 1512–1524.

Talbert, E. E., Smuder, A. J., Min, K., Kwon, O. S., Szeto, H. H. and Powers, S. K. (2013). Immobilization-induced activation of key proteolytic systems in skeletal muscles is prevented by a mitochondria-targeted antioxidant. *J. Appl. Physiol.* **115(4)**, 529–538.

Tanoue, T. and Nishida, E. (2003). Molecular recognitions in the MAP kinase cascades. *Cell. Signal.* **15**, 455–462.

Tanoue, T., Adachi, M., Moriguchi, T. and Nishida, E. (2000). A conserved docking motif in MAP kinases common to substrates, activators and regulators. *Nat. Cell Biol.* **2**, 110–116.

Taplick, J., Kurtev, V., Kroboth, K., Posch, M., Lechner, T. and Seiser, C. (2001). Homo-oligomerisation and nuclear localisation of mouse histone deacetylase 1. *J. Mol. Biol.* **308(1)**, 27–38.

Tapscott, S. J. (2005). The circuitry of a master switch: Myod and the regulation of skeletal muscle gene transcription. *Development* **132(12)**, 2685–2695.

Tawa, N. E. Jr, Odessey, R. and Goldberg, A. L. (1997). Inhibitors of the proteasome reduce the accelerated proteolysis in atrophying rat skeletal muscles. *J. Clin. Invest.*, **100(1)**, 197–203.

Taylor, W. E., Bhasin, S., Artaza, J., Byhower, F., Azam, M., Willard, D. H., Kull, F. C. and Gonzalez-Cadavid, N. (2001). Myostatin inhibits cell proliferation and protein synthesis in C_2C_{12} muscle cells. *Am. J. Physiol. Endocrinol. Metab.* **280(2)**, E221–E228.

Terada, S. and Tabata, I. (2004). Effects of acute bouts of running and swimming exercise on PGC-1α protein expression in rat epitrochlearis and soleus muscle. *Am. J. Physiol. Endocrinol. Metab.* **286(2)**, E208–E216.

Tessier, S. N. and Storey, K. B. (2014). To be or not to be: the regulation of mRNA fate as a survival strategy during mammalian hibernation. *Cell Stress Chaperon.* **19(6)**, 763–776.

Thomas, J. P., Geiger, P. G., Maiorino, M., Ursini, F. and Girotti, A. W. (1990). Enzymatic reduction of phospholipid and cholesterol hydroperoxides in artificial bilayers and lipoproteins. *Biochim. Biophys. Acta* **1045(3)**, 252–260.

Thomason, D. B., Biggs, R. B. and Booth, F. W. (1989). Protein metabolism and beta-myosin heavy-chain mRNA in unweighted soleus muscle. *Am. J. Physiol.* **257**, R300–R305.

Thomson, K. S. (1969). The biology of the lobe-finned fishes. *Biol. Rev.* **44(1)**, 91–154.

Tinkum, K. L., White, L. S., Marpegan, L., Herzog, E., Piwnica-Worms, D. and Piwnica-Worms, H. (2013). Forkhead box O1 (FOXO1) protein, but not p53, contributes to robust induction of p21 expression in fasted mice. *J. Biol. Chem.* **288(39)**, 27999–28008.

Tintignac, L. A., Lagirand, J., Batonnet, S., Sirri, V., Leibovitch, M. P. and Leibovitch, S. A. (2005). Degradation of MyoD mediated by the SCF (MAFbx) ubiquitin ligase. *J. Biol. Chem.* **280(4)**, 2847–2856.

Tischler, M. E. (1994). Effect of the antiglucocorticoid RU38486 on protein metabolism in unweighted soleus muscle. *Metabolism* **43(11)**, 1451–1455.

Tobimatsu, K., Noguchi, T., Hosooka, T., Sakai, M., Inagaki, K., Matsuki, Y., Hiramatsu, R. and Kasuga, M. (2009). Overexpression of the transcriptional coregulator Cited2 protects against glucocorticoid-induced atrophy of C2C12 myotubes. *Biochem. Biophys. Res. Commun.* **378(3)**, 399–403.

Tohyama, Y., Ichimiya, T., Kasama-Yoshida, H., Cao, Y., Hasegawa, M., Kojima, H., Tamai, Y. and Kurihara, T. (2000). Phylogenetic relation of lungfish indicated by the amino acid sequence of myelin DM20. *Brain Res.* **80**, 256–259.

Tomas, F. M., Munro, H. N. and Young, V. R. (1979). Effect of glucocorticoid administration on the rate of muscle protein breakdown in vivo in rats, as measured by urinary excretion of Nτ-methylhistidine. *Biochem. J.* **178(1)**, 139–146.

Toppo, S., Flohé, L., Ursini, F., Vanin, S. and Maiorino, M. (2009). Catalytic mechanisms and specificities of glutathione peroxidases: variations of a basic scheme. *Biochim. Biophys. Acta* **1790(11)**, 1486–1500.

Tothova, Z., Kollipara, R., Huntly, B. J., Lee, B. H., Castrillon, D. H., Cullen, D. E., McDowell, E. P., Lazo-Kallanian, S., Williams, I. R., Sears, C., Armstrong, S. A., Passequé, E., DePinho, R. A. and Gilliland, D. G. (2007). FoxOs are critical mediators of hematopoietic stem cell resistance to physiologic oxidative stress. *Cell* **128(2)**, 325–339.

Touhata, K., Toyohara, H., Mitani, T., Kinoshita, M., Satou, M. and Sakaguchi, M. (1995). Distribution of L-gulono-1,4-lactone oxidase among fishes. *Fisheries Sci.* **61**, 729–730.

Tran, E. J. and Wente, S. R. (2006). Dynamic nuclear pore complexes: life on the edge. *Cell* **125**, 1041–1053.

Tran, H., Brunet, A., Grenier, J. M., Datta, S. R., Fornace, A. J., DiStefano, P. S., Chiang, L. W. and Greenberg, M. E. (2002). DNA repair pathway

stimulated by the forkhead transcription factor FOXO3a through the Gadd45 protein. *Science* **296(5567)**, 530–534.

Trausch-Azar, J. S., Abed, M., Orian, A. and Schwartz, A. L. (2015). Isoform-specific SCF(Fbw7) ubiquitination mediates differential regulation of PGC-1α. *J. Cell. Physiol.* **230(4)**, 842–852.

Trendelenburg, A. U., Meyer, A., Rohner, D., Boyle, J., Hatakeyama, S. and Glass, D. J. (2009). Myostatin reduces Akt/TORC1/p70S6K signaling, inhibiting myoblast differentiation and myotube size. *Am. J. Physiol. Cell Physiol.* **296(6)**, C1258–C1270.

Trewavas, E. (1954). The presence in Africa east of the Rift Valleys of two species of Protopterus, (*P. annectens and P. amphibious*). *Ann. Mus. R. Congo. Belg (N. S) Zool.* **1**, 83–100.

Turjanski, A. G., Vaque, J. P. and Gutkind, J. S. (2007). MAP kinases and the control of nuclear events. *Oncogene* **26(22)**, 3240–3253.

Turrens, J. F., Freeman, B. A., Levitt, J. G. and Crapo, J. D. (1982). The effect of hyperoxia on superoxide production by lung submitochondrial particles. *Arch. Biochem. Biophys.* **217(2)**, 401–410.

Ultsch, G. R. (1989). Ecology and physiology of hibernation and overwintering among freshwater fishes, turtles, and snakes. *Biol. Rev.* **64**, 435–516.

van der Heide, L. P. and Smidt, M. P. (2005). Regulation of FoxO activity by CBP/p300-mediated acetylation. *Trends Biochem. Sci.* **30(2)**, 81–86.

van der Horst, A., Tertoolen, L. G., de Vries-Smits, L. M., Frye, R. A., Medema, R. H. and Burgering, B. M. (2004). FOXO4 is acetylated upon peroxide stress and deacetylated by the longevity protein hSir2SIRT1. *J. Biol. Chem.* **279(28)**, 28873–28879.

Vandromme, M., Cavadore, J. C., Bonnieu, A., Froeschle, A., Lamb, N. and Fernandez, A. (1995). Two nuclear localization signals present in the basic helix 1 domains of MyoD promote its active nuclear translocation and can function independently. *Proc. Natl. Acad. Sci. U. S. A.* **92**, 4646–4650.

Vazquez, A., Bond, E., Levine, A. and Bond, G. (2008) The genetics of the p53 pathway, apoptosis and cancer therapy. *Nat. Rev. Drug Discov.* **7(12)**, 979–987.

Vega, R. B., Huss, J. M. and Kelly, D. P. (2000). The coactivator PGC-1 cooperates with peroxisome proliferator-activated receptor α in transcriptional control of nuclear genes encoding mitochondrial fatty acid oxidation enzymes. *Mol. Cell. Biol.* **20(5)**, 1868–1876.

Velickovska, V., Lloyd, B. P., Qureshi, S. and van Breukelen, F. (2005). Proteolysis is depressed during torpor in hibernators at the level of the 20S core protease. *J. Comp. Physiol. B* **175(5)**, 329–335.

Velickovska, V. and van Breukelen, F. (2007). Ubiquitylation of proteins in livers of hibernating golden-mantled ground squirrels, *Spermophilus lateralis*. *Cryobiology* **55(3)**, 230–235.

Venuti, J. M., Morris, J. H., Vivian, J. L., Olson, E. N. and Klein, W. H. (1995). Myogenin is required for late but not early aspects of myogenesis during mouse development. *J. Cell Biol.* **128(4)**, 563–576.

Vermaak, D., Wade, P. A., Jones, P. L., Shi, Y. B. and Wolffe, A. P. (1999). Functional analysis of the SIN3-histone deacetylase RPD3-RbAp48-histone H4 Connection in the *Xenopus* oocyte. *Mol. Cell Biol.* **19(9)**, 5847–5860.

Vogel, C. and Marcotte, E. M. (2012). Insights into the regulation of protein abundance from proteomic and transcriptomic analyses. *Nat. Rev. Genet.* **13(4)**, 227–232.

Vogt, B. L. and Richie, J. P. (1993). Fasting-induced depletion of glutathione in the aging mouse. *Biochem. Pharmacol.* **46(2)**, 257–263.

Wade, P. A. (2001). Transcriptional control at regulatory checkpoints by histone deacetylases: molecular connections between cancer and chromatin. *Hum. Mol. Genet.* **10(7)**, 693–698.

Wancket, L. M., Frazier, W. J. and Liu, Y. (2012). Mitogen-activated protein kinase phosphatase (MKP)-1 in immunology, physiology, and disease. *Life Sci.* **90(7)**, 237–248.

Wang, F., Yang, H., Wang, X., Xing, K. and Gao, F. (2011). Antioxidant enzymes in sea cucumber *Apostichopus japonicus* (Selenka) during aestivation. *J. Mar. Biol. Assoc. U. K.* **91(01)**, 209–214.

Wang, F., Marshall, C. B., Yamamoto, K., Li, G. Y., Gasmi-Seabrook, G. M., Okada, H., Mak, T. W. and Ikura, M. (2012). Structures of KIX domain of CBP in complex with two FOXO3a transactivation domains reveal promiscuity and plasticity in coactivator recruitment. *Proc. Natl. Acad. Sci. U. S. A.* **109(16)**, 6078–6083.

Wang, L. C. and Lee, T. F. (1996). Torpor and hibernation in mammals: metabolic, physiological and biochemical adaptations. In *Handbook of Physiology: Environmental Physiology*, (ed. M. J. Fregley and C. M. Blatteis), pp. 507–532, Oxford University Press, New York.

Wasawo, D. P. S. (1959). A dry season burrow of *Protopterus aethiopicus*. *Heckel. Rev. Zool. Bot. Afr.* **60**, 65–70.

Watson, M. L., Baehr, L. M., Reichardt, H. M., Tuckermann, J. P., Bodine, S. C. and Furlow, J. D. (2012). A cell-autonomous role for the glucocorticoid receptor in skeletal muscle atrophy induced by systemic glucocorticoid exposure. *Am. J. Physiol. Endocrinol. Metab.* **302(10)**, E1210–E1220.

Wei, P., Pan, D., Mao, C. and Wang, Y. X. (2012). RNF34 is a cold-regulated E3 ubiquitin ligase for PGC-1α and modulates brown fat cell metabolism. *Mol. Cell. Biol.* **32(2)**, 266–275.

Weintraub, H., Tapscott, S. J., Davis, R. L., Thayer, M. J., Adam, M. A., Lassar, A. B. and Miller, A. D. (1989). Activation of muscle-specific genes in pigment, nerve, fat, liver and fibroblast cell lines by forced expression of MyoD. *Proc. Natl. Acad. Sci. U. S. A.* **86(14)**, 5434–5438.

Weintraub, H., Dwarki, V. J., Verma, I., Davis, R., Hollenberg, S., Snider, L., Lassar, A. and Tapscott, S. J. (1991). Muscle-specific transcriptional activation by MyoD. *Genes Dev.* **5(8)**, 1377–1386.

Welle, S., Brooks, A. I., Delehanty, J. M., Needler, N. and Thornton, C. A. (2003). Gene expression profile of aging in human muscle. *Physiol. Genomics* **14(2)**, 149–159.

Welle, S., Brooks, A. I., Delehanty, J. M., Needler, N., Bhatt, K., Shah, B. and Thornton, C. A. (2004). Skeletal muscle gene expression profiles in 20–29 year old and 65–71 year old women. *Exp. Gerontol.* **39(3)**, 369–377.

Welle, S., Bhatt, K. and Pinkert, C. A. (2006). Myofibrillar protein synthesis in myostatin-deficient mice. *Am. J. Physiol. Endocrinol. Metab.* **290(3)**, E409–E415.

Welle, S., Burgess, K. and Mehta, S. (2009). Stimulation of skeletal muscle myofibrillar protein synthesis, p70 S6 kinase phosphorylation, and ribosomal protein S6 phosphorylation by inhibition of myostatin in mature mice. *Am. J. Physiol. Endocrinol. Metab.* **296(3)**, E567–E572.

Wenz, T., Rossi, S. G., Rotundo, R. L., Spiegelman, B. M. and Moraes, C. T. (2009). Increased muscle PGC-1α expression protects from sarcopenia and metabolic disease during aging. *Proc. Natl. Acad. Sci. U. S. A.* **106(48)**, 20405–20410.

Whidden, M. A., McClung, J. M., Falk, D. J., Hudson, M. B., Smuder, A. J., Nelson, W. B. and Powers, S. K. (2009). Xanthine oxidase contributes to mechanical ventilation-induced diaphragmatic oxidative stress and contractile dysfunction. *J. Appl. Physiol.* **106(2)**, 385–394.

Whidden, M. A., Smuder, A. J., Wu, M., Hudson, M. B., Nelson, W. B. and Powers, S. K. (2010). Oxidative stress is required for mechanical ventilation-induced protease activation in the diaphragm. *J. Appl. Physiol.* **108(5)**, 1376–1382.

Whitmarsh, A. J. (2006). The JIP family of MAPK scaffold proteins. *Biochem. Soc. Trans.* **34(5)**, 828–832.

Wickler, S., Horwitz, B. and Kott, K. (1987). Muscle function in hibernating hamsters: a natural analog to bed rest. *J. Therm. Biol.* **12**, 163–166.

Wickler, S., Hoyt, D. and Breukelen, F. V. (1991). Disuse atrophy in the hibernating golden mantled ground squirrel, *Spermophilus lateralis*. *Am J. Physiol.* **261**, R1214–R1217.

Williams, M. D., Van Remmen, H., Conrad, C. C., Huang, T. T., Epstein, C. J. and Richardson, A. (1998). Increased oxidative damage is correlated to

altered mitochondrial function in heterozygous manganese superoxide dismutase knockout mice. *J. Biol. Chem.* **273(43)**, 28510–28515.

Wing, S. S. and Goldberg, A. L. (1993). Glucocorticoids activate the ATP-ubiquitin-dependent proteolytic system in skeletal muscle during fasting. *Am. J. Physiol. Endocrinol. Metab.* **264(4)**, E668–E676.

Wispé, J. R., Clark, J. C., Burhans, M. S., Kropp, K. E., Korfhagen, T. R. and Whitsett, J. A. (1989). Synthesis and processing of the precursor for human mangano-superoxide dismutase. *Biochim. Biophys. Acta.* **994(1)**, 30–36.

Wittwer, M., Flück, M., Hoppeler, H., Müller, S., Desplanches, D. and Billeter, R. (2002). Prolonged unloading of rat soleus muscle causes distinct adaptations of the gene profile. *FASEB J.* **16(8)**, 884–886.

Wood, C. M., Walsh, P. J., Chew, S. F. and Ip, Y. K. (2005). Greatly elevated urea excretion after air exposure appears to be carrier mediated in the slender lungfish (*Protopterus dolloi*). *Physiol. Biochem. Zool.* **78**, 893–907.

Woods, Y., Rena, G., Morrice, N., Barthel, A., Becker, W., Guo, S., Unterman, T. G. and Cohen, P. (2001). The kinase DYRK1A phosphorylates the transcription factor FKHR at Ser329 in vitro, a novel in vivo phosphorylation site. *Biochem.. J.* **355**, 597–607.

Wu, H., Kanatous, S. B., Thurmond, F. A., Gallardo, T., Isotani, E., Bassel-Duby, R. and Williams, R. S. (2002b). Regulation of mitochondrial biogenesis in skeletal muscle by CaMK. *Science* **296(5566)**, 349–352.

Wu, J. J., Roth, R. J., Anderson, E. J., Hong, E. G., Lee, M. K., Choi, C. S., Neufer, P. D., Shulman, G. I., Kim, J. K. and Bennett, A. M. (2006). Mice lacking MAP kinase phosphatase-1 have enhanced MAP kinase activity and resistance to diet-induced obesity. *Cell Metab.* **4(1)**, 61–73.

Wu, Y., Delerive, P., Chin, W. W. and Burris, T. P. (2002a). Requirement of helix 1 and the AF-2 domain of the thyroid hormone receptor for coactivation by PGC-1. *J. Biol. Chem.* **277(11)**, 8898–8905.

Xu, D., Marquis K., Pei J., Fu, S-C., Cagatay, T., Grishin N. V. and Chook, Y. M. (2014). LocNES: A computational tool for locating classical NESs in CRM1 cargo proteins. *Bioinformatics* pii: but826 [Epub ahead of print].

Xu, R., Andres-Mateos, E., Mejias, R., MacDonald, E. M., Leinwand, L. A., Merriman, D. K., Fink, R. H. and Cohn, R. D. (2013). Hibernating squirrel muscle activates the endurance exercise pathway despite prolonged immobilization. *Exp. Neurol.* **247**, 392–401.

Xu, W. S., Parmigiani, R. B. and Marks, P. A. (2007). Histone deacetylase inhibitors: molecular mechanisms of action. *Oncogene* **26(37)**, 5541–5552.

Xuan, Z. and Zhang, M. Q. (2005). From worm to human: bioinformatics approaches to identify FOXO target genes. *Mech. Ageing Dev.* **126(1)**, 209–215.

Yacoe, M. E. (1983). Maintenance of the pectoralis muscle during hibernation in the big brown bat, *Eptesicus fuscus*. *J. Comp. Physiol.* **152**, 97–104.

Yan, J., Barnes, B. M., Kohl, F. and Marr, T. G. (2008). Modulation of gene expression in hibernating arctic ground squirrels. *Physiol. Genomics* **32(2)**, 170–181.

Yang, J. Y., Zong, C. S., Xia, W., Yamaguchi, H., Ding, Q., Xie, X., Lang, J. Y., Lai, C. C., Chang, C. J., Huang, W. C., Huang, H., Kuo, H. P., Lee, D. F., Li, L. Y., Lien, H. C., Cheng, X., Chang, K. J., Hsiao, C. D., Tsai, F. J., Tsai, C. H., Sahin, A. A., Muller, W. J., Mills, G. B., Yu, D., Hortobagyi, G. N. and Hung, M. C. (2008a). ERK promotes tumorigenesis by inhibiting FOXO3a via MDM2-mediated degradation. *Nat. Cell Biol.* **10(2)**, 138–148.

Yang, M. S., Chan, H. W. and Yu, L. C. (2006) Glutathione peroxidase and glutathione reductase activities are partially responsible for determining the susceptibility of cells to oxidative stress. *Toxicology* **226**, 126–130.

Yang, S. Y., Hoy, M., Fuller, B., Sales, K. M., Seifalian, A. M. and Winslet, M. C. (2010). Pretreatment with insulin-like growth factor I protects skeletal muscle cells against oxidative damage via PI3K/Akt and ERK1/2 MAPK pathways. *Lab. Invest.* **90(3)**, 391–401.

Yang, W., Dolloff, N. G. and El-Deiry, W. S. (2008b). ERK and MDM2 prey on FOXO3a. *Nat. Cell Biol.* **10(2)**, 125–126.

Yang, W., Zhang, Y., Li, Y., Wu, Z. and Zhu, D. (2007). Myostatin induces cyclin D1 degradation to cause cell cycle arrest through a phosphatidylinositol 3-kinase/AKT/GSK-3β pathway and is antagonized by insulin-like growth factor 1. *J. Biol. Chem.* **282(6)**, 3799–3808.

Yang, Z. J. P., Broz, D. K., Noderer, W. L., Ferreira, J. P., Overton, K. W., Spencer, S. L., Meyer, Y., Tapscott, S. J., Attardi, L. D. and Wang, C. L. (2015). p53 suppresses muscle differentiation at the myogenin step in response to genotoxic stress. *Cell Death Differ.* **22(4)**, 560–573.

Yoon, J. C., Puigserver, P., Chen, G., Donovan, J., Wu, Z., Rhee, J., Adelmant, G., Stafford, J., Kahn, C. R., Granner, D. K., Newgard, C. B. and Spiegelman, B. M. (2001). Control of hepatic gluconeogenesis through the transcriptional coactivator PGC-1. *Nature* **413(6852)**, 131–138.

Youn, H. D., Kim, E. J., Roe, J. H., Hah, Y. C., and Kang, S. O. (1996). A novel nickel containing superoxide dismutase from Streptomyces spp. *Biochem. J.* **318**, 889–896.

Young, K. M., Cramp, R. L. and Franklin, C. E. (2013a). Hot and steady: elevated temperatures do not enhance muscle disuse atrophy during prolonged aestivation in the ectotherm *Cyclorana alboguttata*. *J. Morphol.* **274(2)**, 165–174.

Young, K. M., Cramp, R. L. and Franklin, C. E. (2013b). Each to their own: skeletal muscles of different function use different biochemical strategies during aestivation at high temperature. *J. Exp. Biol.* **216**, 1012–1024.

Yuryev, A., Patturajan, M., Litingtung, Y., Joshi, R. V., Gentile, C., Gebara, M. and Corden, J. L. (1996). The C-terminal domain of the largest subunit of RNA polymerase II interacts with a novel set of serine/arginine-rich proteins. *Proc. Natl. Acad. Sci. U. S. A.* **93(14)**, 6975–6980.

Zardoya, R., Cao, Y., Hasegawa, M. and Meyer, A. (1998). Searching for the closest living relative (s) of tetrapods through evolutionary analyses of mitochondrial and nuclear data. *Mol. Biol. Evol.* **15(5)**, 506–517.

Zarubin, T. and Han, J. (2005). Activation and signaling of the p38 MAP kinase pathway. *Cell Res.* **15(1)**, 11–18.

Zhang, F., Strand, A., Robbins, D., Cobb, M. H. and Goldsmith, E. J. (1994). Atomic structure of the MAP kinase ERK2 at 2.3A° resolution. *Nature* **367**, 704–711.

Zhang, Y., Ma, K., Song, S., Elam, M. B., Cook, G. A. and Park, E. A. (2004). Peroxisomal proliferator-activated receptor-γ coactivator-1α (PGC-1α) enhances the thyroid hormone induction of carnitine palmitoyltransferase I (CPT-Iα). *J. Biol. Chem.* **279**, 53963–53971.

Zhao, J., Brault, J. J., Schild, A., Cao, P., Sandri, M., Schiaffino, S., Lecker, S. H. and Goldberg, A. L. (2007). FoxO3 coordinately activates protein degradation by the autophagic/lysosomal and proteasomal pathways in atrophying muscle cells. *Cell Metab.* **6(6)**, 472–483.

Zhao, P., Iezzi, S., Carver, E., Dressman, D., Gridley, T., Sartorelli, V. and Hoffman, E. P. (2002). Slug is a novel downstream target of MyoD. Temporal profiling in muscle regeneration. *J. Biol. Chem.* **277(33)**, 30091–30101.

Zhao, X., Gan, L., Pan, H., Kan, D., Majeski, M., Adam, S. A. and Unterman, T. G. (2004). Multiple elements regulate nuclear/cytoplasmic shuttling of FOXO1: characterization of phosphorylation- and 14-3-3-dependent and –independent mechanisms. *Biochem. J.* **378**, 839–849.

Zhu, K., Chen, L., Zhao, J., Wang, H., Wang, W., Li, Z. and Wang, H. (2014). Molecular characterization and expression patterns of myogenin in compensatory growth of *Megalobrama amblycephala*. *Comp. Biochem. Physiol. B Biochem. Mol. Biol.* **170**, 10–17.

Zimmers, T. A., Davies, M. V., Koniaris, L. G., Haynes, P., Esquela, A. F., Tomkinson, K. N., McPherron, A. C., Wolfman, N. M. and Lee, S. J. (2002). Induction of cachexia in mice by systemically administered myostatin. *Science* **296(5572)**, 1486–1488.

Zlatković, J. and Filipović, D. (2011). Stress-induced alternations in CuZnSOD and MnSOD activity in cellular compartments of rat liver. *Mol. Cell. Biochem.* **357(1-2)**, 143–150.

8. Appendix

Appendix 1a. List of selected species and their accession numbers used for dendrogram analyses of PPARGC-1α/Ppargc-1α. "*" indicates the outgroup.

Species	Accession number
Callorhinchus milii Ppargc-1α isoform X1	XP_007887233.1
Chelonia mydas PPARGC-1α	XP_007058167.1
Ciona intestinalis Ppargc-1α	XP_009858764.1
Cynoglossus semilaevis Ppargc-1α	XP_008324663.1
Esox lucius Ppargc-1α	XP_012995919.1
Fundulus heteroclitus Ppargc-1α	XP_012720393.1
Harpegnathos saltator Ppargc-1α	EFN77825.1
Homo sapiens PPARGC-1α	NP_037393.1
Ictalurus punctatus Ppargc-1α	AHH38878.1
Larimichthys crocea Ppargc-1α	XP_010732114.1
Latimeria chalumnae Ppargc-1α	XP_005997925.1
Mus musculus PPARGC-1α	NP_032930.1
Oryzias latipes Ppargc-1α	XP_011485675.1
Pelodiscus sinensis PPARGC-1α isoform 1	XP_006138221.1
Pelodiscus sinensis PPARGC-1α isoform 2	XP_006138222.1
Rattus norvegicus PPARGC-1α	NP_112637.1
Squalous acanthias Ppargc-1α	ACY24363.1_1
Takifugu rubripes Ppargc-1α	XP_011605089.1
Xenopus (Silurana) tropicalis Ppargc-1α isoform 1	XP_002936759.2
Xenopus (Silurana) tropicalis Ppargc-1α isoform 2	XP_004911281.1
Hydra vulgaris Ppargc-1α*	XM_002154953.3

Appendix 1b. List of selected species and their accession numbers used for dendrogram analyses of MYOD1/Myod1 and MYOG/Myog. "*" indicates the outgroup. MDF: Myogenic determination factor; MRF: Myogenic regulatory factor.

Species	Accession number
Ameiurus catus Myog	AAS67040.1
Callorhinchus milii Myod1	XP_007885677.1
Cyprinus carpio Myod1	BAA33565.1
Cyprinus carpio Myog	BAA33564.1
Danio rerio Myod1	AAI14262.1
Danio rerio Myog	NP_571081.1
Devario aequipinnatus Myog	ABB00908.1
Epinephelus coioides Myog	ADJ95349.1
Himantura signifier Myog	KX494984
Hippoglossus hippoglossus Myod1	CAF34063.1
Hippoglossus hippoglossus Myog	CAD32316.1
Homo sapiens MYOD1	AAH64493.1
Homo sapiens MYOG	NP_002470.2
Latimeria chalumnae Myod1	XP_005990556.1
Latimeria chalumnae Myog	XP_005987662.1
Megalobrama amblycephala Myod1	AHW49178.1
Mus musculus MYOD1	AAI03620.1
Mus musculus MYOG	AAB59676.1
Oncorhynchus mykiss Myod1	Q91205.1
Oreochromis aureus Myog	ADA84044.1
Oreochromis niloticus Myog	NP_001266455.1
Paralichthys olivaceus Myog	ABO43958.1
Rattus norvegicus MYOD1	AAI27481.1
Rattus norvegicus MYOG	NP_058811.2
Salmo salar Myod1	CAD89607.1
Salmo salar Myod2	NP_001117026.1
Salmo salar Myog	NP_001117072.1
Sparus aurata Myog	ABR22022.1
Xenopus laevis Myod1A	NP_001079366.1
Xenopus laevis Myod1B	NP_001081292.1
Xenopus laevis Myog	NP_001079326.1
Xenopus (Silurana) tropicalis Myod1	NP_988972.1
Xenopus (Silurana) tropicalis Myog	NP_001016725.1
Branchiostoma belcheri MDF	AAL47678.1
Phallusia mammillata MRF*	ADP06890.1

Appendix 1c. List of selected species and their accession numbers used for dendrogram analyses of MAPK/Mapk. "*" indicates the outgroup.

Species	Accession number
Astyanax mexicanus Mapk1	XP_007229493.1
Astyanax mexicanus Mapk3	XP_007234538.1
Bos taurus MAPK1	NP_786987.1
Bos taurus MAPK3	NP_001103488.1
Callorhinchus milii Mapk1	AFP02819.1
Chrysemys picta bellii Mapk3	XP_005290239.1
Clarias batrachus Mapk3	AKC01948.1
Clupea harengus Mapk1	XP_012671405.1
Danio rerio Mapk1	NP_878308.2
Danio rerio Mapk3	NP_958915.1
Harpegnathos saltator Mapk1	XP_011148219.1
Homo sapiens MAPK1	NP_620407.1
Homo sapiens MAPK3 isoform 1	NP_002737.2
Homo sapiens MAPK3 isoform 2	NP_001035145.1
Hydra vulgaris Mapk1	CDG71148.1
Larimichthys crocea Mapk1	KKF25704.1
Larimichthys crocea Mapk3	KKF25582.1
Latimeria chalumnae Mapk1	XP_005990239.1
Maylandia zebra Mapk1	XP_004555701.1
Mus musculus MAPK1	NP_036079.1
Mus musculus MAPK3	NP_036082.1
Oreochromis niloticus Mapk1	XP_003444522.1
Poecilia formosa Mapk1	XP_007547416.1
Poecilia reticulata Mapk1	XP_008417574.1
Rattus norvegicus MAPK1	NP_446294.1
Rattus norvegicus MAPK3	NP_059043.1
Scleropages formosus Mapk3	KKX11163.1
Squalus acanthias Mapk1	KT324594.1
Stegastes partitus Mapk1	XP_008298479.1
Stegastes partitus Mapk3	XP_008303580.1
Xenopus (Silurana) tropicalis Mapk1	NP_001017127.1
Xenopus laevis Mapk1	NP_001083548.1
Hymenolepis microstoma Mapk*	CDS31779.2

Appendix 1d. List of selected species and their accession numbers used for dendrogram analyses of HDAC1/Hdac1. "*" indicates the outgroup.

Species	Accession number
Callorhinchus milii Hdac1	AFO97213.1
Cynoglossus semilaevis Hdac1	XP_008314048.1
Danio rerio Hdac1	NP_775343.1
Esox lucius Hdac1	XP_010877522.1
Homo sapiens HDAC1	NP_004955.2
Mus musculus HDAC1	NP_032254.1
Notothenia coriiceps Hdac1	XP_010770908.1
Rattus norvegicus HDAC1	NP_001020580.1
Stegastes partitus Hdac1	XP_008282430.1
Takifugu rubripes Hdac1	AAL89665.1
Xenopus (Silurana) tropicalis Hdac1	AAH90604.1
Xenopus laevis Hdac1	NP_001079396.1
Strongylocentrotus purpuratus Hdac1*	NP_999711.1

Appendix 1e. List of selected species and their accession numbers used for dendrogram analyses of FOXO/FoxO. "*" indicates the outgroup.

Species	Accession number
Danio rerio FoxO1b	AAI63020.1
Danio rerio FoxO3	NP_571160.1
Homo sapiens FOXO1	AAH21981.1
Homo sapiens FOXO3	AAH68552.1
Homo sapiens FOXO4 isoform 1	NP_005929.2
Homo sapiens FOXO4 isoform 2	NP_001164402.1
Mus musculus FOXO1	NP_062713.2
Mus musculus FOXO3	NP_062714.1
Mus musculus FOXO4	NP_061259.1
Rattus norvegicus FOXO4	NP_001100413.1
Xenopus laevis FoxO1	NP_001086417.1
Xenopus laevis FoxO3	NP_001086418.1
Xenopus laevis FoxO4	ACO24746.1
Cerapachys biroi FoxO*	XP_011336986.1

Appendix 1f. List of selected species and their accession numbers used for dendrogram analyses of MSTN/Mstn. "*" indicates the outgroup.

Species	Accession number
Catla catla Mstn	AEN75196.1
Cyprinus carpio Mstn1a	ACY01745.1
Cyprinus carpio Mstn1b	ACY01746.1
Danio rerio Mstn	AAB86693.1
Homo sapiens MSTN	ABI48513.1
Labeo fimbriatus Mstn	AEN75197.1
Latimeria chalumnae Mstn	XM_005996542.1
Mus musculus MSTN	AAI05675.1
Oncorhynchus mykiss Mstn1a	AAZ85121.1
Oncorhynchus mykiss Mstn1b	ABA42586.1
Rattus norvegicus MSTN	AAB86691.1
Salmo salar Mstn1b	CAC59700.1
Salmo salar Mstn1a	ABN72586.1
Xenopus (Silurana) tropicalis Mstn	XP_002931542.1
Nematostella vectensis Mstn*	AGL96595.1

Appendix 1g. List of selected species and their accession numbers used for dendrogram analyses of FBXO32/Fbxo32. "*" indicates the outgroup.

Species	Accession number
Astyanax mexicanus Fbxo32	XP_007250892.1
Callorhinchus milii Fbxo32	XP_007898752.1
Chelonia mydas Fbxo32	XP_007070931.1
Chrysemys picta bellii Fbxo32	XP_005288831.1
Danio rerio Fbxo32	NP_957211.1
Esox lucius Fbxo32	XP_010891067.1
Homo sapiens FBXO32 isoform 1	NP_478136.1
Larimichthys crocea Fbxo32	XP_010738325.1
Latimeria chalumnae Fbxo32	XP_006000858.1
Mus musculus FBXO32	NP_080622.1
Notothenia coriiceps Fbxo32	XP_010780879.1
Oncorhynchus mykiss Fbxo32	NP_001180255.1
Pelodiscus sinensis Fbxo32 isoform X1	XP_006137545.1
Pelodiscus sinensis Fbxo32 isoform X2	XP_006137546.1
Poecilia reticulata Fbxo32	XP_008430324.1
Rattus norvegicus FBXO32	NP_598205.1
Salmo salar Fbxo32	NP_001171956.1
Stegastes partitus Fbxo32	XP_008275201.1
Strongylocentrotus purpuratus Fbxo32*	XP_011663485.1

Appendix 2a. The nucleotide sequence and the translated amino acid sequence of *peroxisome proliferator-activated receptor gamma, coactivator 1 alpha (ppargc-1α)*/Ppargc-1a from the muscle of *Protopterus annectens*. The stop codon is indicated by an asterisk.


790 800 810 820 830 840
CCTCTGACTCCAGATTCACCAAATGATCCCAAGAGTTCCCCATTTGAAAATAAGACTATC
P L T P D S P N D P K S S P F E N K T I
850 860 870 880 890 900
GAACAAACATTGAGTGTGGAGCTCTCAGGCACTGCATGTCTAACTCCACCTACTACACCT
E Q T L S V E L S G T A C L T P P T T P
910 920 930 940 950 960
CCACACAAAGCAAGCCAGGATAATCCTTTCAAGACTTCTTTGAAGCCTGTTGAGTCATTC
P H K A S Q D N P F K T S L K P V E S F
970 980 990 1000 1010 1020
AAGTCCTCACAATCACCAGTTAAAAAAGCAACGCTTTAGTGACCCTTTGACACCTCAAGGG
K S S Q S P V K K Q R F S D P L T P Q G
1030 1040 1050 1060 1070 1080
AATTGTCCACTCAAGAAGGGCCCAGAACAAACTGAACTGTATGCACAGCTCAGCAAAACT
N C P L K K G P E Q T E L Y A Q L S K T
1090 1100 1110 1120 1130 1140
TCAGTATTAATCAATGGACCAGAGGAGAGGAAAGGGAAGCGGCCTAGTTTGCGACTATAT
S V L I N G P E E R K G K R P S L R L Y
1150 1160 1170 1180 1190 1200
GGTGACCATGACTACTGTCAAGCTGTGAATGCAAAGGCTGACATACAAATTACTGTGTCG
G D H D Y C Q A V N A K A D I Q I T V S
1210 1220 1230 1240 1250 1260
CAGGATTCACAGTACTTCAGGCAGTCAGTAGGGAAATATAATGTTTCCCATGGGCATCAA
Q D S Q Y F R Q S V G K Y N V S H G H Q
1270 1280 1290 1300 1310 1320
CTTCATCTTCATTTACCTTCTGTTCAAACAGACAGATCTGGAAAAGAAACACAGCAGCTG
L H L H L P S V Q T D R S G K E T Q Q L
1330 1340 1350 1360 1370 1380
AACAGACATCCTGACCAACTAACAAACAACAGGAAACATCTACAAGACCAGGAAATCCGT
N R H P D Q L T N N R K H L Q D Q E I R
1390 1400 1410 1420 1430 1440
GATGAACTCAATAGGCACTTTGGCCACCCAAACCAAGCTTTTTTTGATAAAAGTATAGCT
D E L N R H F G H P N Q A F F D K S I A
1450 1460 1470 1480 1490 1500
AAATTCAGTGAGTCACAAGACAATGATGCCAGTGCTAACTTTTATTCTAAACTGCCTCTG
K F S E S Q D N D A S A N F Y S K L P L
1510 1520 1530 1540 1550 1560
TGCATAAATGCAGGAATGCCTGCAAATGGTATCTTTGATGAAAGTGAGGATGATGGTGAC
C I N A G M P A N G I F D E S E D D G D
1570 1580 1590 1600 1610 1620
AAACTCCTTTATTCCTGGGATGGCGAGCAAGCAGATGTATTATTTGAAGAATGTAATTCA
K L L Y S W D G E Q A D V L F E E C N S
1630 1640 1650 1660 1670 1680
TGCTCACCTTACAGTTCTCCCCGGAGAGGATCTGTCTCACCACCCAAATCTTTATTTTTG
C S P Y S S P R R G S V S P P K S L F L
1690 1700 1710 1720 1730 1740
AAAAGAACTTGCAGAGGAAGATCTAGATCTCGGTCATTCTCCAGGCACAGATCGTGTTCT
K R T C R G R S R S R S F S R H R S C S
1750 1760 1770 1780 1790 1800
CGCTCATCATATTCTCACTCAAGATCAAGATCACCACACAGTAGATCCTCTTCAAGATCA
R S S Y S H S R S R S P H S R S S S R S


1810 1820 1830 1840 1850 1860
TGTTACTGTGACTCCGACAATCTCATAAGCAGATCCAGTACAAGCCCTTGTTCCCACTCA
C Y C D S D N L I S R S S T S P C S H S
1870 1880 1890 1900 1910 1920
CGTTCTAGATCCAGGTCACCATACAGGCACAGAACAAGGTATGACAGCTATGAGGAATAT
R S R S R S P Y R H R T R Y D S Y E E Y
1930 1940 1950 1960 1970 1980
CAGCATGAAAGGCTGAAAAGAGAGGAATATCGACGTGATTATGAGAAACGAGAATTTGAA
Q H E R L K R E E Y R R D Y E K R E F E
1990 2000 2010 2020 2030 2040
AGAGCAAAACAAAGGGAAAGACAGAAGCAAAAGGCAATTGAAGAGAGGCGTGTTATTTAC
R A K Q R E R Q K Q K A I E E R R V I Y
2050 2060 2070 2080 2090 2100
ATCGATAAACTTAGATCTGGTATAACAAGAACAGAACTCAAAACGTCGCTTTGAAGTTTTT
I D K L R S G I T R T E L K R R F E V F
2110 2120 2130 2140 2150 2160
GGTGAAATAGAAGAGTGCACTGTAAATCTGAGAGATGATGGAGACAGTTATGGATTTATA
G E I E E C T V N L R D D G D S Y G F I
2170 2180 2190 2200 2210 2220
ACTTACCGTTATACCTGTGATGCATTTGCTGCTCTTGAGAATGGATATACATTGCGCAGG
T Y R Y T C D A F A A L E N G Y T L R R
2230 2240 2250 2260 2270 2280
TCAAGCGAACCTCAGTTTGAGATGTGCTTTGGTGGACGTAAGCAGTTCTGCAAGTCTGAA
S S E P Q F E M C F G G R K Q F C K S E
2290 2300 2310 2320 2330 2340
TACACAGACTTAGATTGTAACTTGGATGACTTTGACCCAGCTTCTACCAAAAGCAAGTAT
Y T D L D C N L D D F D P A S T K S K Y
2350 2360 2370 2380 2390
GACTCCATGGATTTTGACAGCTTATTGAGAGAAGCACAGAGAAGCCTGCGCAGGTAA
D S M D F D S L L R E A Q R S L R R *

Appendix 2b. The nucleotide sequence and the translated amino acid sequence of *myogenic differentiation 1* (*myod1*)/Myod1 from the muscle of *Protopterus annectens*. The stop codon is indicated by an asterisk.

Appendix 2c. The nucleotide sequence and the translated amino acid sequence of *myogenin* (*myog*)/Myog from the muscle of *Protopterus annectens*. The stop codon is indicated by an asterisk.

Appendix 2d. The nucleotide sequence and the translated amino acid sequence of *mitogen-activated protein kinase 1* (*mapk1*)/Mapk1 from the muscle of *Protopterus annectens*. The stop codon is indicated by an asterisk.

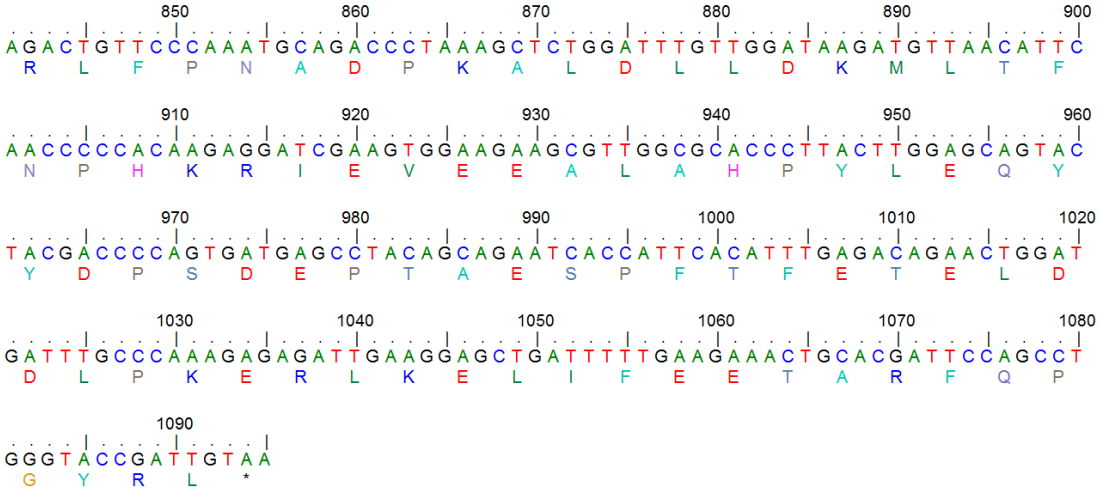
850 860 870 880 890 900
AGACTGTTCCCAAATGCAGACCCTAAAGCTCTGGATTTGTTGGATAAGATGTTAACATTC
R L F P N A D P K A L D L L D K M L T F
910 920 930 940 950 960
AACCCCCACAAGAGGATCGAAGTGGAAGAAGCGTTGGCGCACCCTTACTTGGAGCAGTAC
N P H K R I E V E E A L A H P Y L E Q Y
970 980 990 1000 1010 1020
TACGACCCCCAGTGATGAGCCTACAGCAGAAATCACCATTCACATTTGAGACAGAACTGGAT
Y D P S D E P T A E S P F T F E T E L D
1030 1040 1050 1060 1070 1080
GATTTGCCCAAAGAGAGATTGAAGGAGCTGATTTTTGAAGAAACTGCACGATTCCAGCCT
D L P K E R L K E L I F E E T A R F Q P
1090
GGGTACCGATTGTAA
G Y R L *

Appendix 2e. The nucleotide sequence and the translated amino acid sequence of *mitogen-activated protein kinase 3* (*mapk3*)/Mapk3 from the muscle of *Protopterus annectens*. The stop codon is indicated by an asterisk.

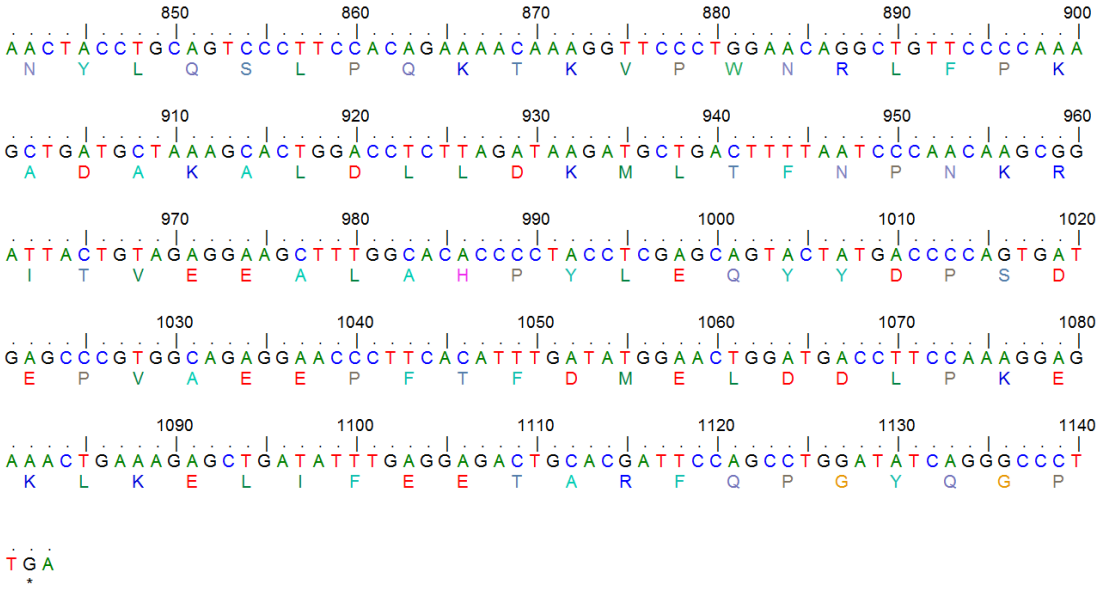
850 860 870 880 890 900
AACTACCTGCAGTCCCTTCCACAGAAAACAAAGGTTCCCTGGAACAGGCTGTTCCCCAAA
N Y L Q S L P Q K T K V P W N R L F P K
910 920 930 940 950 960
GCTGATGCTAAAGCACTGGACCTCTTAGATAAGATGCTGACTTTTAATCCCAACAAGCGG
A D A K A L D L L D K M L T F N P N K R
970 980 990 1000 1010 1020
ATTACTGTAGAGGAAGCTTTGGCACACCCCTACCTCGAGCAGTACTATGACCCCAGTGAT
I T V E E A L A H P Y L E Q Y Y D P S D
1030 1040 1050 1060 1070 1080
GAGCCCGTGGCAGAGGAACCCTTCACATTTGATATGGAACTGGATGACCTTCCAAAGGAG
E P V A E E P F T F D M E L D D L P K E
1090 1100 1110 1120 1130 1140
AAACTGAAAGAGCTGATATTTGAGGAGACTGCACGATTCCAGCCTGGATATCAGGGCCCT
K L K E L I F E E T A R F Q P G Y Q G P
TGA
*

Appendix 2f. The nucleotide sequence and the translated amino acid sequence of *histone deacetylase 1* (*hdac1*)/Hdac1 from the muscle of *Protopterus annectens*. The stop codon is indicated by an asterisk.

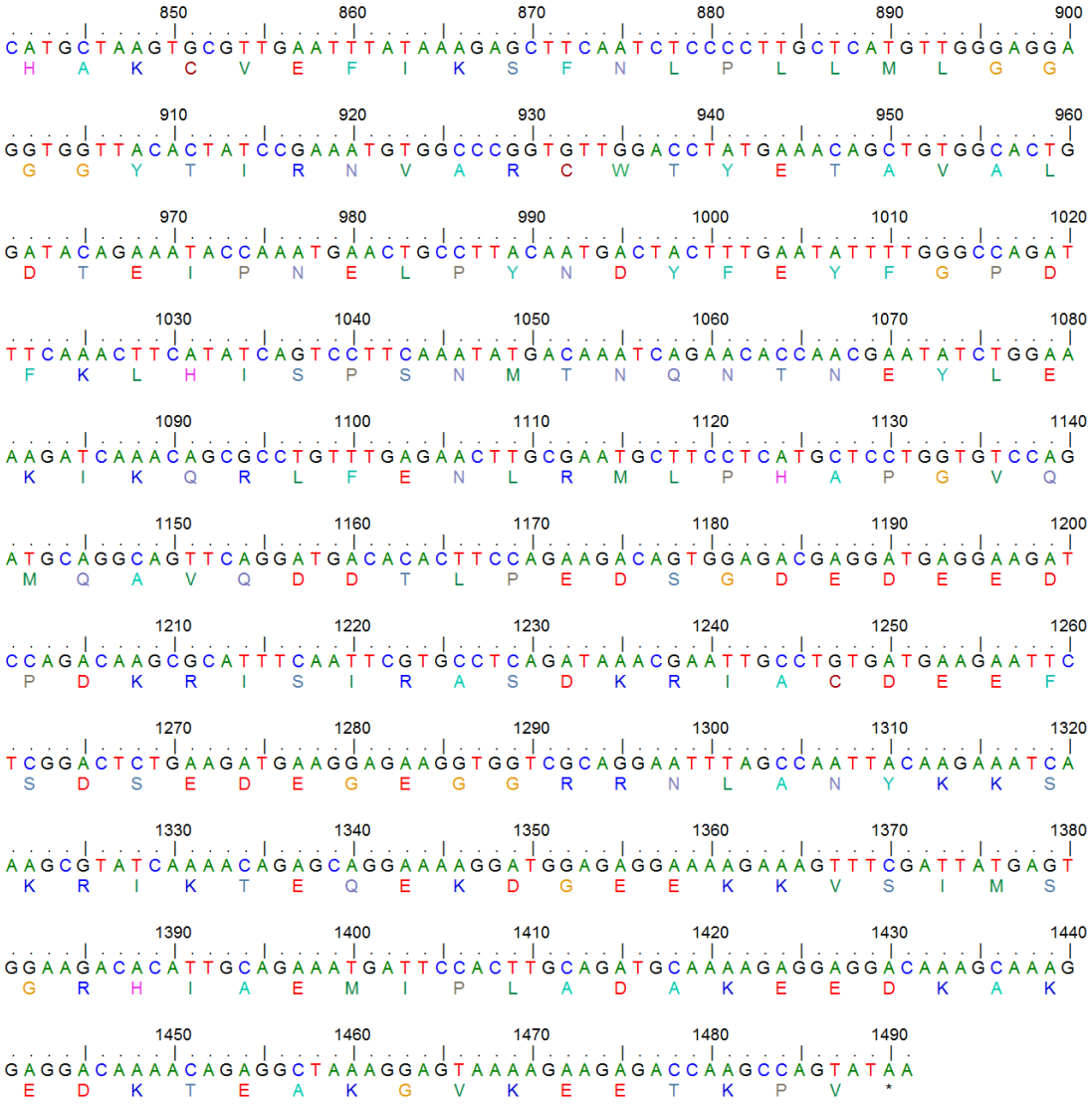
850 860 870 880 890 900
CATGCTAAGTGCGTTGAATTTATAAAGAGCTTCAATCTCCCCTTGCTCATGTTGGGAGGA
H A K C V E F I K S F N L P L L M L G G
910 920 930 940 950 960
GGTGGTTACACTATCCGAAATGTGGCCCGGTGTTGGACCTATGAAACAGCTGTGGCACTG
G G Y T I R N V A R C W T Y E T A V A L
970 980 990 1000 1010 1020
GATACAGAAATACCAAATGAACTGCCTTACAATGACTACTTTGAATATTTTGGGCCAGAT
D T E I P N E L P Y N D Y F E Y F G P D
1030 1040 1050 1060 1070 1080
TTCAAACTTCATATCAGTCCTTCAAATATGACAAATCAGAACACCAACGAATATCTGGAA
F K L H I S P S N M T N Q N T N E Y L E
1090 1100 1110 1120 1130 1140
AAGATCAAACAGCGCCTGTTTGAGAACTTGCGAATGCTTCCTCATGCTCCTGGTGTCCAG
K I K Q R L F E N L R M L P H A P G V Q
1150 1160 1170 1180 1190 1200
ATGCAGGCAGTTCAGGATGACACACTTCCAGAAGACAGTGGAGACGAGGATGAGGAAGAT
M Q A V Q D D T L P E D S G D E D E E D
1210 1220 1230 1240 1250 1260
CCAGACAAGCGCATTTCAATTCGTGCCTCAGATAAACGAATTGCCTGTGATGAAGAATTC
P D K R I S I R A S D K R I A C D E E F
1270 1280 1290 1300 1310 1320
TCGGACTCTGAAGATGAAGGAGAAGGTGGTCGCAGGAATTTAGCCAATTACAAGAAATCA
S D S E D E G E G G R R N L A N Y K K S
1330 1340 1350 1360 1370 1380
AAGCGTATCAAAACAGAGCAGGAAAAGGATGGAGAGGAAAAGAAAGTTTCGATTATGAGT
K R I K T E Q E K D G E E K K V S I M S
1390 1400 1410 1420 1430 1440
GGAAGACACATTGCAGAAATGATTCCACTTGCAGATGCAAAAGAGGAGGACAAAGCAAAG
G R H I A E M I P L A D A K E E D K A K
1450 1460 1470 1480 1490
GAGGACAAAACAGAGGCTAAAGGAGTAAAAGAAGAGACCAAGCCAGTATAA
E D K T E A K G V K E E T K P V *

Appendix 2g. The nucleotide sequence and the translated amino acid sequence of *forkhead box O1* (*foxO1*)/FoxO1 from the muscle of *Protopterus annectens*. The stop codon is indicated by an asterisk.


850 860 870 880 890 900
CAATTTTCAAAGTGGCCTGGCAGTCCTAACTCTCACAGTAATGATGACTTTGAGACCTGG
Q F S K W P G S P N S H S N D D F E T W
910 920 930 940 950 960
AACAGTTTCAGACCACGAACAAGTTCTAATGCTAGTTCAGTAGGTGTACGACTTTCCCCA
N S F R P R T S S N A S S V G V R L S P
970 980 990 1000 1010 1020
ATTATGCCAGAACAGGAGGATCTTGGAGATGGAGATGTTCATTCTCTTGTGTATACCCCG
I M P E Q E D L G D G D V H S L V Y T P
1030 1040 1050 1060 1070 1080
CAACCTAGCAAAATGACATCATTGCCAAGTCTGTCAGAAATGAGCAGTTCAGAAAATATG
Q P S K M T S L P S L S E M S S S E N M
1090 1100 1110 1120 1130 1140
GAAAATCTGTTGGATAATCTTAACTTACTTTCACCTAGTTCCTCAATGACAGTATCAACA
E N L L D N L N L L S P S S S M T V S T
1150 1160 1170 1180 1190 1200
CAGTCTTCACCTGCTTCTATGATGCAGCAAAACCCTGGATATTCATTTGCAACCCAGAAT
Q S S P A S M M Q Q N P G Y S F A T Q N
1210 1220 1230 1240 1250 1260
ACAAGCATGGGATCACAACCATCAGATTATAGGAAATTTAGCTACAATCAAACAAACATT
T S M G S Q P S D Y R K F S Y N Q T N I
1270 1280 1290 1300 1310 1320
AACTCTGTCCCTCAGATGCCTTTACAACCTCTCCAGGAATCTAAATCTGGTTATGGTTCT
N S V P Q M P L Q P L Q E S K S G Y G S
1330 1340 1350 1360 1370 1380
TTGAACCAGTTTAACTGTCCAACAGGACTCCTGAAGGAACTGTTAACTTCGGACTCACCA
L N Q F N C P T G L L K E L L T S D S P
1390 1400 1410 1420 1430 1440
CCTCAACCTGACATTTTATCACAAGTGGACACTGTGGTTTCCCAGCCTGGCAAGAGAATG
P Q P D I L S Q V D T V V S Q P G K R M
1450 1460 1470 1480 1490 1500
CCAAGCCAAAACGTGATGATAACAAGTAGCTCTGTGATGCCTCAATATCCTGTTCAACCT
P S Q N V M I T S S S V M P Q Y P V Q P
1510 1520 1530 1540 1550 1560
CCGCACAATAAAATGATAAACCCTGCAACCCCACCCTCATCAAGCACATAGCCAGCAAGCA
P H N K M I N P A T H P H Q A H S Q Q A
1570 1580 1590 1600 1610 1620
CAGTCTGTCAGTAGTCGTGCCTTAATGCACAACATGAGCACCATGTTACACAGTTCACAT
Q S V S S R A L M H N M S T M L H S S H
1630 1640 1650 1660 1670 1680
CCGAGTCGTTTATCTTCAGTGAAGATCCCTTTACAAGTGCCTGTTTCCCAGACCATGGGA
P S R L S S V K I P L Q V P V S Q T M G
1690 1700 1710 1720 1730 1740
ATGAATACCACAAGTCCTTTCCCTGGTATCAACAGTAATGGGCATGGAAGAGTGGGGTTT
M N T T S P F P G I N S N G H G R V G F
1750 1760 1770 1780 1790 1800
GTTGCTATGCACCAAGAAAAACTACCAAGTGACTTGGATGGTATGTTAATAGAACACCTG
V A M H Q E K L P S D L D G M L I E H L

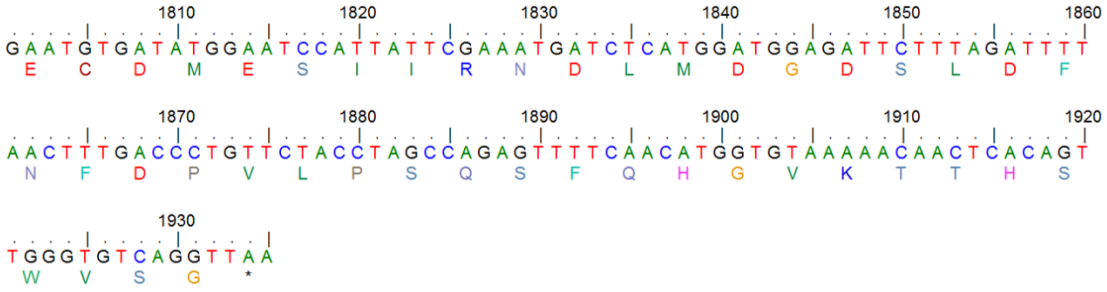
1810
1820
1830
1840
1850
1860
GAATGTGATATGGAATCCATTATTCGAAAATGATCTCATGGATGGAGATTCTTTAGATTTT
E C D M E S I I R N D L M D G D S L D F
1870
1880
1890
1900
1910
1920
AACTTTGACCCTGTTCTACCTAGCCAGAGTTTTCAACATGGTGTAAAAAACAACTCACAGT
N F D P V L P S Q S F Q H G V K T T H S
1930
TGGGTGTCAGGTTAA
W V S G *

Appendix 2h. The nucleotide sequence and the translated amino acid sequence of *forkhead box O3* (*foxO3*)/FoxO3 from the muscle of *Protopterus annectens*. The stop codon is indicated by an asterisk.


850 860 870 880 890 900
CAGCTTCTAAAATGGCCTGGCAGTCCTACTTCACGCAGCAGTGATGAGTTAGATGCATGG
Q L L K W P G S P T S R S S D E L D A W
910 920 930 940 950 960
TCAGATTTCCGCTCTCGCACTAACTCAAATGCAAGTACTATAAGTGGACGCTTGTCTCCC
S D F R S R T N S N A S T I S G R L S P
970 980 990 1000 1010 1020
ATTATAGCCAGTGCTGAGCACGATGATGTCCAGGATGATGATGATGCTGCTCCACTTTCC
I I A S A E H D D V Q D D D D A A P L S
1030 1040 1050 1060 1070 1080
CCAATGCTGTACCCTAGTCCTACCCATATGTCTCCCACTGTAAATAAACCCAGTGCTGCT
P M L Y P S P T H M S P T V N K P S A A
1090 1100 1110 1120 1130 1140
GATTTGCCCTGTATCATGGATCTGACATGCAATTTAAACTTGAAGGATGGACTTGGAAAT
D L P C I M D L T C N L N L K D G L G N
1150 1160 1170 1180 1190 1200
ACCCTCATGGATGACTTTTTAGATAATATCCATCTCCCCTCTTCCCAGCAGTCCTCTCCA
T L M D D F L D N I H L P S S Q Q S S P
1210 1220 1230 1240 1250 1260
GGAAGCCTCGTTCAAAAGAACTCAAATTTTACATACAGCTCCAAAGGCTCCAGTCTCAGT
G S L V Q K N S N F T Y S S K G S S L S
1270 1280 1290 1300 1310 1320
CCAACATCTGGTACCTTCAATAATTCCATTTTTAGTGGCTCTGCATTGACTTCCCTAAGG
P T S G T F N N S I F S G S A L T S L R
1330 1340 1350 1360 1370 1380
CAAACTCCCATGCAAACAATTCAGGAAAACAAACAGACCACCTTTTCATCCCATTATGGG
Q T P M Q T I Q E N K Q T T F S S H Y G
1390 1400 1410 1420 1430 1440
AACCAACAATTGCAGGATCTACTTACATCTGATTCTTTAAGCCACAGTGATGTACTGATG
N Q Q L Q D L L T S D S L S H S D V L M
1450 1460 1470 1480 1490 1500
ACACAGTCTGATCCATTAATGTCACAGGCCAGCACAGCAGTAGCAGTCCAGAATTCACAT
T Q S D P L M S Q A S T A V A V Q N S H
1510 1520 1530 1540 1550 1560
CGAAATTTGATGCTTCGCAGTGACCCAATGATGTCTTTTGCTGGTCAGTCAAATCAGGGA
R N L M L R S D P M M S F A G Q S N Q G
1570 1580 1590 1600 1610 1620
AATTTGTCCAATCAGAACTTACTTCATCAACAGACTCCATCACAAAGTTCTTCCCTTAAC
N L S N Q N L L H Q Q T P S Q S S S L N
1630 1640 1650 1660 1670 1680
AGTAACCGTACTAATTCCATGAACAATGCAGGCTTAAATGACTCCAACAACATGATCTCA
S N R T N S M N N A G L N D S N N M I S
1690 1700 1710 1720 1730 1740
GTGAAAAGTCAGCAGCAATCACCAAGTGGTCAATCTATGCAAATGGGACTTTCTGATTCA
V K S Q Q Q S P S G Q S M Q M G L S D S
1750 1760 1770 1780 1790 1800
TTCTCAGGCTCTTCCTTGTATTCAAATAGCATGAGCCTTCCATCTTTGGGCCAAGACAGA
F S G S S L Y S N S M S L P S L G Q D R
1810 1820 1830 1840 1850 1860
TTCCCAAGTGACCTGGACCTTGATATGTTTAATGGACCCTTGGAATGTGATGTGGAGTCC
F P S D L D L D M F N G P L E C D V E S

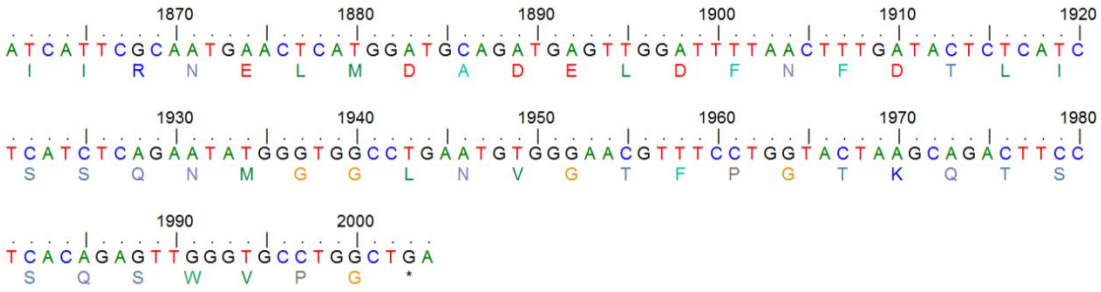
1870
1880
1890
1900
1910
1920
ATCATTCGCAATGAACTCATGGATGCAGATGAGTTGGATTTTAACTTTGATACTCTCATC
I I R N E L M D A D E L D F N F D T L I
1930
1940
1950
1960
1970
1980
TCATCTCAGAATATGGGTGGCCTGAATGTGGGAACGTTTCCTGGTACTAAGCAGACTTCC
S S Q N M G G L N V G T F P G T K Q T S
1990
2000
TCACAGAGTTGGGTGCCTGGCTGA
S Q S W V P G *

Appendix 2i. The nucleotide sequence and the translated amino acid sequence of *myostatin* (*mstn*)/Mstn from the muscle of *Protopterus annectens*. The stop codon is indicated by an asterisk.

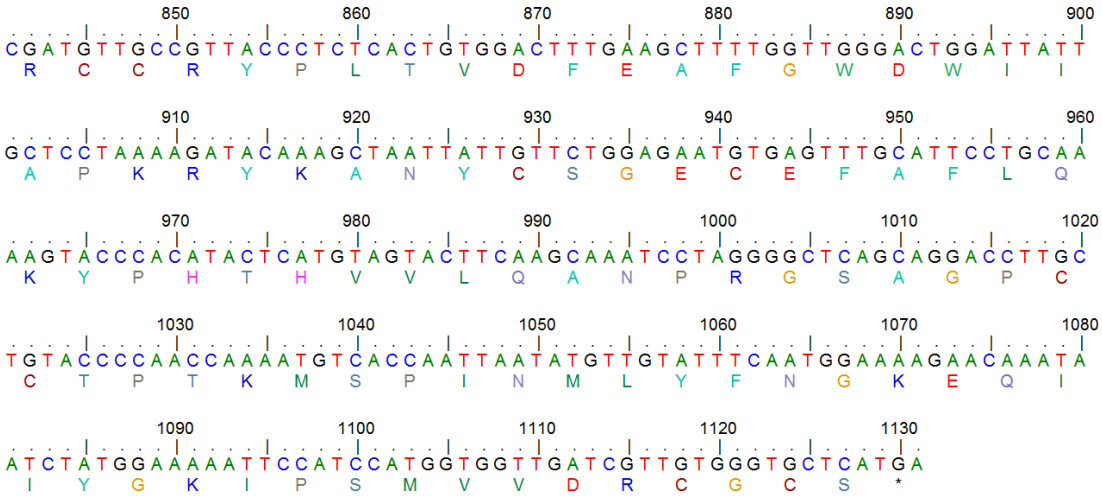
850 860 870 880 890 900
CGATGTTGCCGTTACCCTCTCACTGTGGACTTTGAAGCTTTTGGTTGGGACTGGATTATT
R C C R Y P L T V D F E A F G W D W I I
910 920 930 940 950 960
GCTCCTAAAAAGATACAAAGCTAATTATTGTTCTGGAGAAATGTGAGTTTGCATTCCTGCAA
A P K R Y K A N Y C S G E C E F A F L Q
970 980 990 1000 1010 1020
AAGTACCCACATACTCATGTAGTACTTCAAGCAAATCCTAGGGGCTCAGCAGGACCTTGC
K Y P H T H V V L Q A N P R G S A G P C
1030 1040 1050 1060 1070 1080
TGTACCCCAACCAAAATGTCACCAATTAATATGTTGTATTTCAATGGAAAAGAACAAATA
C T P T K M S P I N M L Y F N G K E Q I
1090 1100 1110 1120 1130
ATCTATGGAAAAATTCCATCCATGGTGGTTGATCGTTGTGGGTGCTCATGA
I Y G K I P S M V V D R C G C S *

Appendix 2j. The nucleotide sequence and the translated amino acid sequence of *F-box protein 32 (fbxo32)*/Fbxo32 from the muscle of *Protopterus annectens*. The stop codon is indicated by an asterisk.

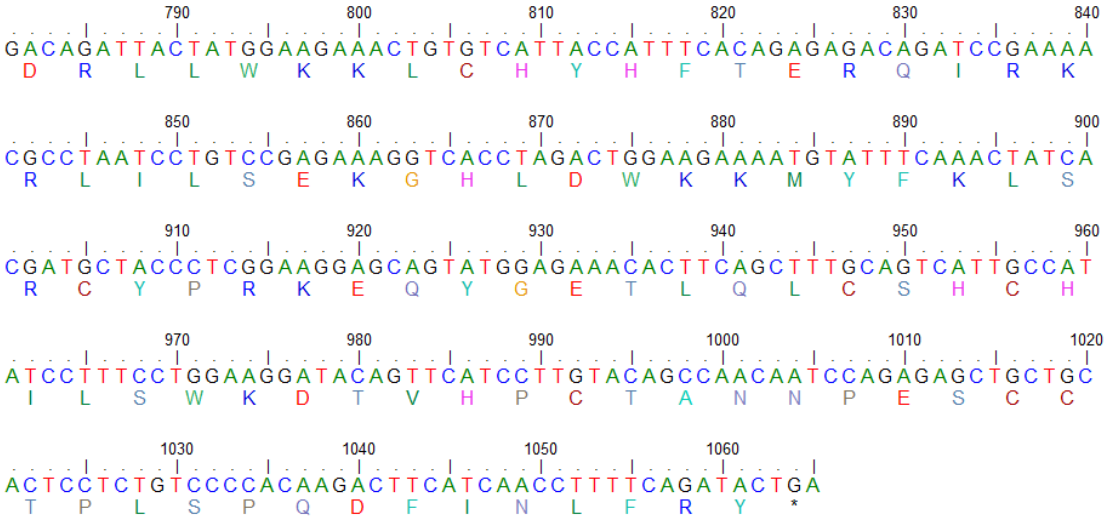
790 800 810 820 830 840
GACAGATTACTATGGAAGAAACTGTGTCATTACCATTTCACAGAGAGACAGATCCGAAAA
D R L L W K K L C H Y H F T E R Q I R K
850 860 870 880 890 900
CGCCTAATCCTGTCCGAGAAAGGTCACCTAGACTGGAAGAAAATGTATTTCAAACTATCA
R L I L S E K G H L D W K K M Y F K L S
910 920 930 940 950 960
CGATGCTACCCTCGGAAGGAGCAGTATGGAGAAACACTTCAGCTTTGCAGTCATTGCCAT
R C Y P R K E Q Y G E T L Q L C S H C H
970 980 990 1000 1010 1020
ATCCTTTCCTGGAAGGATACAGTTCATCCTTGTACAGCCAACAATCCAGAGAGCTGCTGC
I L S W K D T V H P C T A N N P E S C C
1030 1040 1050 1060
ACTCCTCTGTCCCCACAAGACTTCATCAACCTTTTCAGATACTGA
T P L S P Q D F I N L F R Y *